STRENGTH AND PERFORMANCE OF STEEL FIBER REINFORCED CONCRETE POST-TENSIONED FLAT PLATES

Joshua T. Rosenthal

Thesis submitted to the faculty of the Virginia Polytechnic Institute and State University
in partial fulfillment of the requirements for the degree of

Master of Science
In
Civil Engineering

Carin L. Roberts-Wollmann, Chair
Ioannis Koutromanos
Roberto T. Leon

June 28, 2019
Blacksburg, VA

Keywords: post-tensioned, flat plates, steel fibers, SFRC

STRENGTH AND PERFORMANCE OF STEEL FIBER REINFORCED CONCRETE POST-TENSIONED FLAT PLATES

Joshua T. Rosenthal

ABSTRACT

Load testing was performed on a one-third scale model steel fiber reinforced concrete post-tensioned flat plate. The specimen had nine 10ft x 10ft x 3in. bays along with a 2ft-6in. overhang. Distributed loading was applied with a whiffle tree loading system at each bay and overhang section. Throughout the test, crack widths, crack locations, deflections, concrete strains, and reinforcing bar strains were monitored. The post-tensioned flat plate was designed to just meet the maximum allowable stress requirements of ACI 318.

Minimal quantities of hairline cracks were observed after stressing the slab, and up through service-level loads, the cracks grew slightly in length and width. The slab behaved elastically through service-level loading. As factored-level loading was approached, the slab began to behave inelastically as indicated by both the load-deflection plots and the load-strain plots. A total ultimate load of 282psf (174psf of applied load) was reached when concrete crushing occurred. A 0.20in. wide full-length crack was observed running on the bottom surface of the slab between column lines 1 and 2, and a full-length crack was observed at column line 2 on the top surface of the slab. These two cracks were the leading contributors to the slab's failure.

The performance of the SFRC post-tensioned flat plate indicated that considerations should be made to remove requirements for negative moment reinforcement in post-tensioned flat plates when SFRC is used. Also, the requirements for positive moment reinforcement should be modified. Additionally, the SFRC post-tensioned flat plate exhibited excellent levels of ductility. More experimentation should be conducted to determine if the maximum tensile stress in ACI 318 can be increased for post-tensioned flat plates with SFRC.

STRENGTH AND PERFORMANCE OF STEEL FIBER REINFORCED CONCRETE POST-TENSIONED FLAT PLATES

Joshua T. Rosenthal

GENERAL AUDIENCE ABSTRACT

Load testing was performed on a one-third scale model steel fiber reinforced concrete (SFRC) post-tensioned flat plate. Post-tensioned flat plates are a type of concrete structural system typically used as flooring. This system typically employs high-strength steel strands, which are stretched to introduce compression into the concrete, which helps prevent the onset of cracking. The specimen had nine 10ft x 10ft x 3in. bays along with a 2ft-6in. overhang. Distributed loading was applied with a whiffle tree loading system at each bay and overhang section. The whiffle tree loading system was used to allow actuators to spread out the vertical loading on the slab. During the test, crack widths, crack locations, deflections, concrete strains, and reinforcing bar strains were monitored. The post-tensioned flat plate was designed to just meet the maximum allowable stress requirements of the governing standard, ACI 318.

Minimal quantities of hairline cracks were observed after stressing the slab, and up through service-level loads, the cracks grew slightly in length and width. As larger loads were applied, the cracks grew and the effects of these cracks on the slab were evidenced in the deflection and strain measurements. A total ultimate load of 282psf (174psf of applied load) was reached when concrete crushing occurred. A 0.20in. wide full-length crack was observed running on the bottom surface of the slab between column lines 1 and 2, and a full-length crack was observed at column line 2 on the top surface of the slab. These two cracks were a driving force in the slab's failure.

The performance of the SFRC post-tensioned flat plate indicated that considerations should be made to change the requirements for negative and positive moment reinforcement in post-tensioned flat plates when SFRC is used. Additionally, the SFRC post-tensioned flat plate exhibited great performance after significant cracking was present. More experimentation should be conducted to determine if the maximum allowable tensile stress in ACI 318 can be increased for post-tensioned flat plates with SFRC.

Acknowledgements

Most importantly, I would like to thank Dr. Roberts-Wollmann for her endless guidance throughout the project. Also, I would like to thank Dr. Leon and Dr. Koutromanos for their input and suggestions as I completed the project. Additionally, this project would not have been successful without the several hours of assistance provided by Taye Ojo, Kshitij Inerkar, and Jack Li. Kshitij Inerkar really helped get the project started with his design work on the whiffle tree and the dead load compensation, his help with building the trial slab, and his help testing the trial slab. Taye Ojo and Jack Li provided many hours of work on the first large specimen and were instrumental in ensuring that the testing ran properly. I also am greatly thankful for the assistance of Dr. Mokarem, Dennis Huffman, Brett Farmer, and Garret Blankenship who helped manufacture many parts on this project and provided insight on various designs in this project. Additionally, the support of the sponsors and oversight committee, who designed the post-tensioned flat plate and provided input, led to the success of this project.

Also, I am grateful for such a loving family and friends who supported me throughout my undergraduate and graduate years at Virginia Tech. They always supported me while I was working towards my goal of becoming a structural engineer.

Table of Contents

List of Figures

List of Tables

Chapter 1 - Introduction

1.1 Project Overview

Post-tensioned flat plates are a type of concrete structural system typically used as flooring. This system typically employs high-strength steel strands that are unbonded to the concrete. Once the concrete is placed and reaches a certain compressive strength, the tendons are stretched to induce compression into the flat plate. Since concrete cracks at relatively low amounts of tension, introducing a compression throughout the flat plate prior to introducing gravity loads prevents the formation of cracks. These types of slabs are advantageous because they reduce the need for large amounts of reinforcing bars, which are time consuming to install. Many building floor systems require beams to transfer loads to the columns, and these beams can end up being deep. However, flat plates do not require any beams or additional thickness at the columns, so they are typically very thin, leading to shorter story heights. Shorter story heights lead to a cheaper building.

ACI 318 provides several requirements for the design of post-tensioned flat plates. Chapter 8 in ACI 318-14 provides a discussion on the requirements relating to post-tensioned flat plates. In Chapter 8, requirements are given regarding the necessity and quantity of bonded reinforcement in post-tensioned flat plates. Also, the average prestress provided by the post-tensioning strands must be at least 125psi. Additional limits on the allowable stresses in post-tensioned flat plates are provided in Chapter 24 of ACI 318 (ACI, 2014).

ACI 318 provides a few different methods to design post-tensioned flat plates. Section 8.11 in ACI 318-14 provides instructions on the equivalent frame method, which is used as the primary design method in this project (ACI, 2014). In the equivalent frame method, the flat plate is divided into strips in both directions. Each strip is analyzed like a continuous beam, with a few additional guidelines. This type of analysis allows for engineers to use simple software such as RISA 2D to help design post-tensioned flat plates ("RISA-2D Demo,").

This project examines the strength and performance of steel fiber reinforced concrete post-tensioned flat plates in comparison to conventional post-tensioned flat plates. Steel fibers help control cracks, and the fibers are uniformly distributed across the

whole flat plate. Replacing conventional reinforcement with steel fibers could potentially improve cost-savings (see Chapter 2), while still providing adequate strength and performance. Two specimens in this project have steel fiber reinforced concrete, with one of these specimens (Specimen 2) having a banded-uniform tendon arrangement, while the other one (Specimen 4) will have a banded-banded tendon arrangement. Specimen 2 will be directly compared to Specimen 1, which has a banded-uniform tendon arrangement with conventional steel reinforcement. Specimen 4 will be compared to Specimen 3, which has a banded-banded tendon arrangement with conventional steel reinforcement.

This thesis is focused on the testing and results of Specimen 2. The overall project will consist of four post-tensioned flat plates. Specimen 2 has a banded-uniform tendon layout, as shown in Figure 1, and it has steel fiber reinforced concrete. In a banded-uniform tendon layout, in the uniform direction, the tendons are evenly spaced. The spacing for the uniform tendons in Specimen 2 is 2 ft. In the banded direction, groups of tendons are closely spaced in the column strip. In Specimen 2, the groups of tendons are spaced at 4 in. center-to-center in the banded direction.

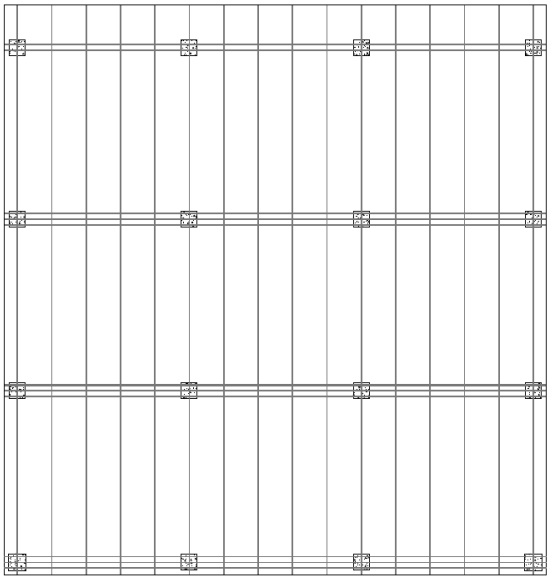

Figure 1. Banded-Uniform Tendon Layout

Specimen 1 will also have a banded-uniform tendon layout, but it will contain traditional concrete (no steel fibers). This slab will act as a control specimen to which data from Specimen 2 can be compared. This slab will adhere to all ACI 318

requirements for post-tensioned flat plates, including ultimate strength and service-level stress requirements.

Specimen 3 will have a banded-banded tendon layout, which is shown below in Figure 2. In the banded-banded tendon layout, the tendons in both directions run in the column strip of the slab. Specimen 3 will have traditional concrete (no steel fibers) and mild reinforcement, and it will be the control specimen to which Specimen 4 can be compared.

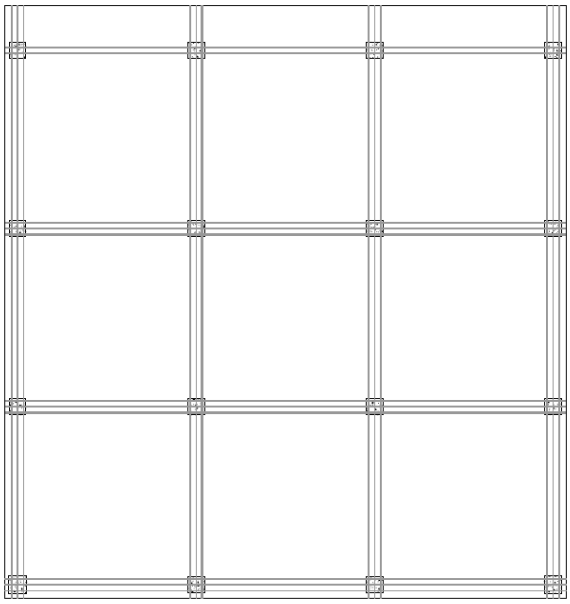

Figure 2. Banded-Banded Tendon Layout

Specimen 4 will be similar to Specimen 3 in that it will have a banded-banded tendon layout. However, Specimen 4 will have steel fiber reinforced concrete. With the addition of the steel fibers in the concrete mix, the amount of bonded reinforcement is expected to be decreased compared to Specimen 3. If strength calculations allow, all bonded reinforcement might be removed, with the exception of back-up bars at the anchorage locations for the tendons.

1.2 Project Objectives

The first objective of this project is to analyze the performance of post-tensioned flat plates with both conventional and steel fiber reinforced concrete. Using both types of concretes across the four specimens included in this overall project will allow for a direct comparison between the two types of concrete. This should allow the researchers to determine how the steel fibers impact the performance and strength of the post-tensioned

flat plates. Performance criteria includes both deflections and crack widths. The deflections of the specimens will be compared to the requirements of ACI 318 to ensure that live load deflections do not exceed l/360, where l is the span length (ACI, 2014). Also, crack widths will be compared to the requirement in Eurocode 2, which states that the crack widths should not exceed 0.50mm (0.020in.) (European Concrete Platform ASBL, 2008).

The ACI 318-14 Building Code provides many requirements for post-tensioned flat plates. However, with the addition of steel fibers into the concrete mix, some of these requirements in ACI 318 could possibly be changed, as ACI 318-14 does not provide a different set of requirements for SFRC post-tensioned flat plates.

The second objective of this project is to determine if the allowable tensile stress in steel fiber reinforced concrete post-tensioned flat plates could be increased. The footnote of Table 24.5.2.1 in ACI 318-14 states that post-tensioned flat plates be designed with uncracked concrete (Class U), with a maximum tensile stress of $6\sqrt{f'_c}$ (ACI, 2014). With the addition of steel fibers, which influence the tensile properties of concrete, this tensile stress limit could possibly be increased for SFRC post-tensioned flat plates, possibly up to $7.5\sqrt{f'_c}$.

The third objective of this project is to determine if the tensile stress limit in SFRC post-tensioned flat plates in positive moment regions that leads to the requirement of bonded reinforcement can be modified. In Table 8.6.2.3 of ACI 318-14, bonded reinforcement is required if the tensile stress in the positive moment region of a post-tensioned flat plate exceeds $2\sqrt{f'_c}$ (ACI, 2014). With the addition of steel fibers to the concrete mix, this stress limit could possibly be increased for SFRC post-tensioned flat plates, depending on the results of this investigation.

The fourth objective of this project is to determine if the requirements for the amount of bonded reinforcement in the negative moment regions of SFRC post-tensioned flat plates can be reduced. In Table 8.6.2.3 of ACI 318-14, bonded reinforcement is required at the negative moment regions with an area of $0.00075A_{cf}$, where A_{cf} is the maximum cross-sectional area of the strip passing through the column (ACI, 2014).

The final objective of this project is to investigate the performance and strength of post-tensioned flat plates with a banded-banded tendon layout, both with and without steel fibers.

At the completion of this thesis, only Specimen 2 had been tested, so no comparisons could be made to Specimen 1. All conclusions were based solely from the performance and strength of Specimen 2.

1.3 Thesis Organization

Chapter 1 discusses the project objectives and the future steps in the project. Chapter 2 provides a summary of the literature about post-tensioned flat plate research and research involving SFRC slabs. Chapter 3 provides information about the methods and procedures that were used in completing this research project, including some testing performed prior to the testing of Specimen 2. Chapter 4 provides the testing results obtained from the testing of Specimen 2, focusing on the performance of the slab at service-level loads, factored-level loads, and at the ultimate loading. Chapter 5 provides conclusions that were obtained from the testing and the results. The Appendices provide design drawings, data acquisition wiring diagrams, supporting calculations, and other relevant information.

Chapter 2 - Literature Review

2.1 Background on Prestressed Concrete and Post-Tensioned Flat Plates

Flat slabs have many advantages, as discussed by Marti et. al. First of all, these types of slabs are quicker to build compared to other slabs. Additionally, these slabs, since they do not have column capitals, have a thin overall depth. This can lead to a reduction in the story height, which reduces the overall height of structures (Marti, Ritz, & Thurlimann, 1977). Additional benefits of post-tensioned flat plates include their performance in earthquakes. According to Aalami, post-tensioned flat plates are advantageous in earthquake-prone areas because they are lightweight compared to other floor options (Aalami, 2007).

Aalami also discussed the development of prestressed concrete as a whole. He states that early prestressed concrete was mainly used in bridge projects. Although the idea of prestressed concrete was developed very early on, developments on the construction of prestressed concrete stalled out. The major roadblock was that the available steel at the time was very low strength. Thus, stressing low strength steel provided little to no prestress in the concrete after time dependent losses, so little benefit was available at the time. Development of higher strength steels allowed for prestressed concrete to be a viable option (Aalami, 2007).

Gamble and Burns provide a good overview on the development and progress made regarding prestressed concrete slabs. Prestressed concrete slabs were introduced in the middle of the twentieth century. They quickly became popular, as from 1967 to 1976, 250 million square feet of post-tensioned concrete floors were built. As for many types of structures, accurate analysis methods were developed long after the structures were constructed in the building industry. This was the case for prestressed concrete slabs, as prestressed concrete was not regulated by ACI until the ACI Building Code that was published in 1963. Early post-tensioned slabs had large amounts of prestress, which was later decreased over time for a few reasons. One issue with the large amount of prestress was that larger amounts of creep would occur in the post-tensioned flat plates. Also, with large amounts of prestress, small amounts of rebar were used in the slabs. This caused issues if extra load occurred, because cracking would occur. As a result of testing done

by Burns (described in a separate paper), ACI requirements were developed to call for minimum amounts of bonded reinforcement (Gamble & Burns, 1981).

Gamble and Burns also brought up the idea of load balancing, which was developed by T.Y. Lin and was used early on as a design tool for prestressed concrete slabs (Gamble & Burns, 1981). In Lin's paper, he discusses the concept of load balancing for designing prestressed members. This concept was best used for statically indeterminate structures. The idea of load balancing is to design the profile of the tendons to create prestressed loadings that are similar to the loadings on the beam (live loads, dead loads, etc.). If the loadings matched, or were scaled, the analysis of the prestressed member would be greatly simplified. Some important remarks by Lin included that if live loads were to be balanced by the prestressing, an examination of the live load must be performed in order to see if actual expected live load was different than the design-level live load. Also, if all the load was 100% balanced, creep would not cause any bending in the member. Lin also stated that it was very important for long prestressed members to consider the friction losses over the length of the member. A single value for the tendon force should not be used over the length of the whole member (Lin, 1963).

One of the early documents for designing post-tensioned flat plates is ACI 423 "Tentative Recommendations for Prestressed Concrete Flat Plates." This source was an extra resource to ACI 318-71, and it discussed the equivalent frame method, which is a valid method for the analysis of flat plates. This source provided limits on tension and compression stresses in the flat plate, and it also provided limits on the bearing stresses from the anchorage plates. It also provided a discussion on what percentage of tendons should run through the column strip and talks about the shear capacity of flat plates. The document provided recommendations on mild reinforcement at anchorage locations and at the columns. The document also provided some construction recommendations, including tolerances for rebar chairs used for tendons (ACI-ASCE Committee 423, 1974).

2.2 Experiments on Post-Tensioned Flat Plates

Much research has been performed on post-tensioned flat plates, especially in the 1960s through 1970s. An early paper on the testing of a post-tensioned slab was published in 1959 by Scordelis et al. They tested a specimen that was 15ft x 15ft x 3in. thick, which was split into four bays (the column spacing was 7ft in each direction). They had twelve unbonded tendons in each direction with the same draped profile. Additional reinforcement consisted of wire meshing at the columns of the specimen. The slab was designed using beam theory, which is similar to the equivalent frame method. The results from the slab indicated that beam theory is fairly accurate in predicting moments due to prestress in the slab. This slab specimen was loaded with air bags, and the pressure was monitored in these air bags in order to obtain the actual load being applied to the specimen. The slab reached an ultimate load of 362psf, when punching shear occurred at the middle column. Conclusions obtained from this testing included that the flat plate is able to carry more load after the initial cracking begins and up to the first substantial level of cracking. Thus, the cracking load was deemed to be unimportant. Another conclusion was in regards to how moments determined from the beam method should be divided up in the strip being analyzed. The authors stated that negative moments in a strip should be split up where 25 percent go to the interior strip of the slab, while 75 percent go to the column strip. For positive moments, 40 percent should go to the interior strip, while 60 percent should go to the column strip. The researchers also concluded that while the slab behaves elastically, the elastic plate theory can estimate moments in the slab with a reasonable accuracy (Scordelis, Lin, & Itaya, 1959)

Many tests were performed by Burns at the University of Texas at Austin. Burns, along with Gerber, performed experiments on both cast-in-place flat plates and lift-slab flat plates. Twelve specimens were tested. Eleven specimens had unbonded tendons, while the final specimen had grouted tendons. The specimens were 12ft x 12ft x 7in. thick with a column at the center. Each specimen had six tendons in each direction, with an average prestress of 250psi. These specimens were meant to represent the interior column of a building with 24ft x 24ft bays. The researchers varied the amount of reinforcement in the specimens. The specimens were loaded on four sides. The cast-in-

place specimens had a shear failure circular surface at the top of the flat plate. Flexure also contributed to the failure of the specimen. For the lift-slab specimens, the failure mechanism started near the lifting collar below the flat plate. It was noted that reinforcement and tendons running through the columns prevented a complete collapse of the specimen. Welded wire outperformed other typical reinforcing bars. However, the w-shaped shear reinforcement that was in one of the specimens, performed the best. Reinforcement added ductility to the specimens. Also, the specimen with the bonded tendons had a higher post-failure load capacity than a similar slab without any reinforcement (Gerber & Burns, 1971).

In another set of experiments, one of Burns' students, Hemakom, produced a dissertation regarding the testing of two post-tensioned flat plates, each with nine panels (Hemakom, 1975). This dissertation was extremely helpful in developing the test setup that is described in this thesis. Additionally, two journal articles were published based on the procedures and results presented in Hemakom's dissertation.

The first journal article published by Burns and Hemakom regarded a one-third scale model test. Each bay for the test specimen was 10ft x 10ft x 2.75in. thick. The specimen also had two 2.5ft overhangs. Sixty-eight tendons ran in each direction (70% of the tendons were near the columns), with an average prestress force of 325psi. Additionally, reinforcing bars were included at the columns. Due to the scaled down nature of the test, concrete bricks were used to compensate for the self-weight reduction caused by the scaling. A whiffle tree loading system was provided under each bay and overhang in order to simulate a distributed load on the slab. Varying bays were loaded throughout the testing procedure at different magnitudes of load (service load, factored loads, ultimate load). The slab behaved inelastically at 90psf of live load (provided by the whiffle tree), and many cracks appeared at the interior columns at the factored loading. Testing was also done to see what would happen if the load in certain tendons were removed. When this happened, some additional cracking was observed, but no major issues occurred (N. H. Burns & Hemakom, 1977).

Punching shear eventually occurred at a load of 205psf. The researchers noted that flexural failure signs were present prior to the punching shear failure. Forces in the tendons, measured by load cells on the tendons, did not significantly increase until the

load was near the slab's failure load. The specimen's capacity exceeded the factored design loads. Also, the ACI equation for tendon ultimate stress was an overestimation. Additionally, the researchers concluded that adequate shear strength was provided in the test, and that larger prestress values improve the shear strength of the slab. Finally, the testing showed that the equivalent frame method of analysis can be used to find the average moment in the locations of the slab with the highest stresses. However, the method ends up being less conservative at exterior columns (N. H. Burns & Hemakom, 1977).

The second test performed by Burns and Hemakom was a one-half scale model. The specimen bays were still 10ft x 10ft x 2.75 in. thick. The specimen had an average prestress of 135psi, which was lower than the ACI 423 suggestion of 150psi. This tendon force was designed to balance approximately 70 percent of the slab's dead load, and the tendons were in a banded-uniform tendon arrangement. Mild reinforcement was also in the slab at the column locations. The same whiffle tree system was used to load the slab, and various load patterns and magnitudes were used during the testing. At high levels of applied load, the tendon stresses began to become larger. The testing showed that the flat-plate remained elastic at service loads. Similar to the previous test, flexural failures were evident before punching shear occurred. Thus, the slab could be considered ductile. The researchers believed that the bonded reinforcement at the column locations improved the flat plate's performance. Additionally, the yield lines indicated that the uniform direction was weaker than the banded direction. Finally, the elastic plate theory was deemed to accurately estimate the moments in the flat plate (Ned H. Burns & Hemakom, 1985).

Burns also directed in another study, this time working with Kosut and Winter. In this study, four-bay specimens were tested. Each bay was 10ft x 10ft x 2.75in. thick, and the average prestress ranged from 173 to 184psi. Stirrups and bonded reinforcement were provided in variable amounts at the columns. Similarly to the previous tests done by Burns, dead load compensation blocks and a whiffle tree were used to provide loads. Nine load cases on the slab consisted of distributed loading, while four load cases examined shear strength by using concentrated loads near the columns. Throughout the testing, there was no cracking at service-level loads, but cracking began shortly after in

the negative moment regions at the interior column. At the factored load level, cracking was present near some of the other columns, and the tendon force had not significantly changed. Cracks began to appear at the bottom surface of the flat plate shortly before the flat plate reached its ultimate load. Punching shear eventually occurred in the specimen. The researchers noted that bonded reinforcement was instrumental in crack control. Also, the researchers concluded that the shear strength requirements were met by the slab, and stirrups did not improve the shear capacity. The authors proposed new equations for the ultimate tendon stress, as the tendon forces in the experiment were 10 to 16 percent smaller than the ACI estimates for ultimate stress (Kosut, Burns, & Winter, 1985).

A paper written by Kim and Lee in 2016 describes some testing performed on post-tensioned flat plates, which examined the various arrangement of tendons. Three types of slabs were examined: non-prestressed flat plate, a flat plate with tendons in one direction, and a flat plate with tendons in two orthogonal directions. Each specimen was 9ft-10in. x 9ft-10in. x 10in thick (300cm x 300cm x 25cm), and the specimens had supports on each of their four sides. For the post-tensioned flat plates, tendons were uniformly spaced. Load was applied to the center of each specimen with an applied area of 388in^2 (2500cm^2). The researchers limited the amount of reinforcement for flexural purposes, in the hopes of avoiding punching shear failures. Compared to the regular flat plate, slabs with post-tensioning had lower deflections for given loads, higher capacities, and lower strains in the steel. Additionally, the cracks in the post-tensioned plates were less concentrated, and the post-tensioned plates were stiffer once cracks began to form. Compared to the plate with two directions of post-tensioning, the plate with one-direction of strands had more cracks, and the cracks were much wider. However, both types of post-tensioned slabs experienced similar deflections and ultimate loads (Kim & Lee, 2016).

Additional tests were conducted by researchers on punching shear and on the slab-column connections in post-tensioned flat plates. Burns also wrote a paper with Stephen Smith in 1974 about some tests that were performed on the slab-column connection of post-tensioned flat plates. This test was performed prior to his other nine-bay post-tensioned flat plate tests. The researchers tested three specimens that were 9ft x

9ft x 2.75in. thick with a column in the center of the specimen. Strands ran in both directions, with the majority of the strands concentrated in the column strip. The average prestress in the specimens was 325psi, which was a large amount of prestress. The three specimens had varying amounts of mild reinforcement. During testing, all three specimens behaved similarly in the elastic region. Once cracking occurred, the specimens with mild reinforcement showed higher stiffnesses compared to the specimen without any mild reinforcement. Bonded reinforcement allowed the specimen to reach a larger ultimate load, and it allowed for narrower cracks. With no bonded reinforcement, there were fewer cracks in the slab, but the cracks were very wide. Punching shear was the ultimate mode of failure, but there were signs of flexural failure throughout the testing. The specimens did not collapse due to punching shear because of the reinforcement (when present) and the tendons that ran directly through the columns. One important piece mentioned by the authors was that the initial cracking that was noted was caused by stress concentrations in the slab. These initial cracks did not have a major impact on the slab's overall behavior. The researchers stated that the ACI estimates for the shear strength and flexural strength of the slab were lower than the actual shear strength and flexural strength of the slab (Smith & Burns, 1974).

A group of researchers published a paper in 2007 discussing punching shear in post-tensioned slabs in regards to building code requirements and actual experiments that had been performed. The three codes that were examined included ACI, FIP, and the Eurocode. The three codes were then compared to previous testing. The paper delves into testing performed by one of the authors, Ricardo Silva. Silva tested sixteen post-tensioned specimens that were 6ft-7in. x 6ft-7in. x 5in thick (2m x 2m x 125mm). The specimens were supported at their four edges, and were loaded at the center with different sized areas. Punching shear was the controlling failure mode. Earlier cracking would appear when less prestress was in the slab and when the load was applied on a smaller area. The tendon forces increased the most when the specimens had smaller prestress and when the load was applied on a bigger area. Also, the tendons near the center of the specimen (at the column) experienced the largest tendon force increase. Some data from other tests was included in the overall analysis of punching shear in post-tensioned flat plates. The researchers concluded that ACI 318 was the most conservative method

compared to the methods found in the other two building codes. The authors also discuss some problems with each of the building code's estimations for punching shear. For example, tests showed that ACI 318 became less conservative when the slab thickness-to-column size decreased (Silva, Regan, & Melo, 2007).

Two researchers wrote about additional testing done on post-tensioned concrete flat slabs after punching shear had occurred. Ramos and Lucio had 2.3m x 2.3m x10cm post-tensioned slabs with applied loads at the middle of the slab and supports at the slab edge (eight total support points). Each specimen had four tendons in each direction, except for one slab, which had no tendons. The tendons all had the same drape, but the layout of the tendons was varied. The slabs also contained mild reinforcement. For the specimens with tendons running through the column, larger deflections could be reached, and for a given deflection, a higher load could be achieved. The specimens with tendons running through the column performed better than the Eurocode's estimates, while the other slabs reached 96 percent of their predicted capacities. For the slab with no tendons, after punching, the slab could only be reloaded up to 64 percent of its original punching shear load. This was similar for slabs with tendons only running around the column. For the slabs with tendons running through the column, the slabs could be reloaded over 17 percent higher than its original punching shear load (Ramos & Lucio, 2008). This set of tests demonstrated the importance of tendons running through the column in order to provide ductility to the post-tensioned flat plate.

As shown in the above tests, and as stated by Marti et al., one advantage of adding prestressing to the concrete is that it improves the punching shear capacity of the slab. Punching shear is a major concern in flat plates, especially because it is a brittle failure (Marti et al., 1977). Brittle failures should be avoided at all costs because they occur with little warning, which is inherently dangerous to a building's occupants.

2.3 Introduction to Steel Fiber Reinforced Concrete

One of the purposes of this project is to examine the impact that steel fibers have on post-tensioned flat plates. Steel fibers have deformations in order to create a good bond between the fibers and the concrete mixture (Brandt, 2008). Steel fibers provide many benefits including that they provide shrinkage and crack control (Destrée, 2001). Larger fibers are better at controlling wider cracks. Fibers control the spreading of cracks

in the concrete and control the thickness of these cracks. When steel fibers are used in concrete, more cracks typically appear, but the widths of these cracks are much smaller (Brandt, 2008). Steel fibers also reduce costs, and they lead to more efficient casting operations (Destrée, 2001). Destrée also mentions a sixteen story building that had SFRC slabs that was built one floor per week, thus demonstrating the time savings of using SFRC slabs (Destrée, 2009). Also, the design time for SFRC slabs is much quicker, since drawings showing reinforcement details are not necessary. SFRC also has better toughness and durability when compared to traditional concrete. Additionally, SFRC slabs work well with non-traditional floor geometries (American Concrete Institute, 2015).

The earliest fiber reinforcement was created around 3500 years ago, when plant fibers and horse hair were used to reinforce masonry blocks (Brandt, 2008). Beginning in 1993, slabs began to be constructed with steel fiber reinforced concrete (Destrée, 2001). As of 2009, 65 buildings had been built with SFRC slabs that contained essentially no reinforcing bars except for integrity reinforcement (connecting the columns in a grid). Destrée gave three examples of this type of building in his article that was published in *Concrete Engineering International*. The examples provided by Destrée include a mall in Latvia, and sixteen story building in Estonia, and an office building in Spain. Most SFRC mixes used in construction have around 70 to 100 kg/m^3 of fibers, and the concrete mix typically does not require vibration during the casting operation (Destrée, 2009). In some concrete, lower fiber contents are used because of the cost of fibers, and when large amounts of fibers are used, the spread of the fibers in the concrete becomes challenging (Brandt, 2008).

The stress-strain curves for concrete, steel, and SFRC are provided in Figures 3, 4, and 5, respectively. Concrete performs much better in compression as compared to tension. Steel shows a large amount of ductility after yielding, as its ultimate strain is much higher than its yield strain. As shown in Figure 5, SFRC exhibits a good amount of ductility after cracking, unlike plain concrete.

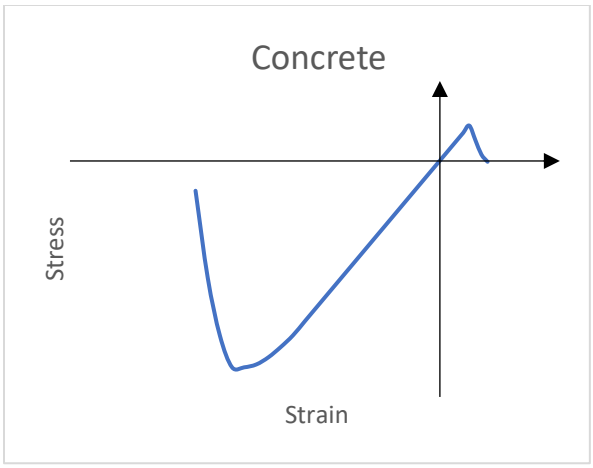

Figure 3. Concrete Stress-Strain Curve (Hind, Ozakca, & Ekmekyapar, 2016)

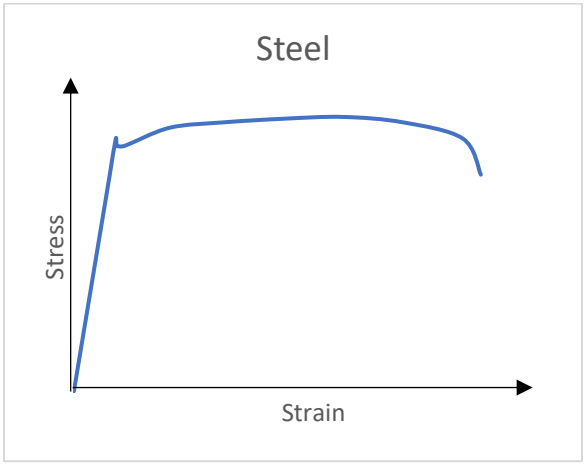

Figure 4. Steel Stress-Strain Curve

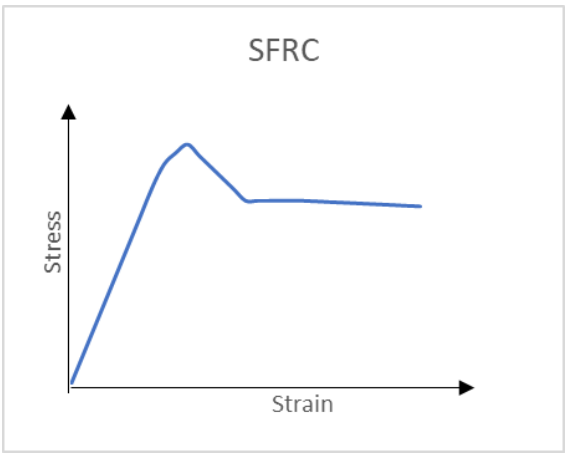

Figure 5. SFRC Stress-Strain Curve (Lok & Xiao, 1999), (Jensen & Overli, 2015)

Many researchers have worked on modelling the behavior of steel fiber reinforced concrete in various structures. Lok and Xiao tried to predict whether SFRC would strengthen or soften post-cracking based on various variables including the tensile strength of the concrete, the fiber dosage, and the bond-aspect ratio. In their paper, they also derived equations for determining the cracking stress, ultimate stress, and ultimate moment for steel fiber reinforced concrete, and they checked the validity of these equations with prior research data. However, these equations that they derived were too complex, so they provided simpler relationships involving bond aspect ratio, fiber dosage, fiber orientation, and the ultimate tensile strength of the SFRC. The individual relationships between the various inputs were used to develop an equation for the ultimate tensile strength of a steel fiber reinforced concrete mixture (Lok & Xiao, 1999).

Barros and Figueiras investigated the relationships for moment-curvature and for stress-strain that could be implemented in finite element modeling. They performed uniaxial compression tests to look at the stress-strain relationship of the SFRC and then developed models to represent this behavior. They also performed three-point bending tests with notched beams in order to develop a model that involved the fracture energy of the SFRC notched beam. Barros and Figueiras worked on flexural modeling, which took into account the tension-softening and the tension-stiffening properties of SFRC. They developed this model from tests that they had performed on SFRC. To check the validity of their models, the researchers tested slab strips that had various dosages of steel fibers. In their experimental research, Barros and Figueiras found that slabs with higher dosages of fibers had smaller spacing between cracks, but the capacities were higher than the slabs with lower dosages of steel fibers (Barros & Figueiras, 1999).

Salehian and Barros performed additional modeling on SFRC. In their paper, they talked about the layout and distribution of the steel fibers in concrete. They also examined the stress-strain relationships in both compression and tension for the SFRC. Additional consideration was given to the relationship between the flexural residual strength of the SFRC and the quantity of fibers observed at a given crack location. These considerations were used in the development a model that could represent the behavior of an SFRC slab. The authors' model was compared to finite element results in order to show that the model was valid. Additional investigations with the modelling examined

the impact of fiber segregation in the concrete on the relationships between various properties of the SFRC slabs. This paper also provided a thorough discussion on the yield line theory for SFRC elevated slabs (Salehian & Barros, 2017).

Research performed by Salehian, Barros, and Taheri examined SFRC slabs that were 2ft x 2ft x 4in. thick (60cm x 60cm x 10cm). They were supported on their edges and loaded at their center. Two different volume dosages were used: 2.8lb/ft^3 and 3.7lb/ft^3 (45kg/m^3 and 60kg/m^3). The specimens experienced flexural failures. The researchers stated that more energy was absorbed during concrete cracking for the mix with the higher fiber dosage than for the mix with the lower dosage. This observation was made from the results of one of the tensile tests performed on the SFRC mixes. The researchers then modeled both square SFRC slabs and round SFRC slabs. For the square slabs, the researchers used the simplified cracking patterns that were observed in the actual testing to help develop the models. For the circular slabs, the researchers compared their model to data from previous experiments. They found that their square SFRC model was more accurate, likely because the data used for the circular model was obtained using different methods (Salehian, Barros, & Taheri, 2014).

2.4 Physical Research on SFRC Slabs

Amir Khanlou et al. performed investigations on composite slabs with steel fiber reinforced concrete. The researchers varied fiber quantities in their composite slabs, which had two 9ft-10in. spans (3m). The fiber dosages ranged from 1.25lb/ft^3 to 3.7lb/ft^3 (20kg/m^3 to 60kg/m^3). A few of the slabs had mesh reinforcement, as well. Part of the research was focused on the shrinkage of the concrete, and the results showed that the steel fibers and mesh had similar effects on the shrinkage. Also, larger amounts of fibers (3.7lb/ft^3, or 60kg/m^3) had some improvement in controlling shrinkage as compared to smaller dosages of fibers. Another part of the test included applying gravity loads to the composite slab specimens. Slabs with fibers could withstand slightly higher maximum gravity loads when compared to the control test (a slab with no reinforcement). Also, the measured crack widths in the slab became much smaller when the fiber ratio was at 3.7lb/ft^3 (60kg/m^3). However, there was not much improvement for the lower dosages of fibers (Khanlou et al., 2016). This testing was instrumental in showing how fiber dosage can impact crack widths and shrinkage in SFRC slabs.

Ackermann and Schnell performed additional research on SFRC composite slabs. They examined both single-span and two-span slabs. Their tests indicated in the two-span slabs, a significant amount of moment redistribution could occur. In the single-span tests, the moment-rotation results showed that as rotations continued to increase, there was no sudden decrease in moments. This shows that steel fiber reinforced concrete is a very ductile material (Ackermann & Schnell, 2008).

McMahon and Birely performed tests on SFRC one-way slabs with varying thicknesses and amounts of bonded reinforcement. These specimens were actually modeled after bridge decks. The specimens were 8ft long and 18in. wide, and they were simply supported and loaded at two points. Some slabs had reinforcing bars at a height of h/2, which the researchers were hoping could allow for a single mat of reinforcement in a bridge deck, depending on the test results. The SFRC had a fiber dosage of 0.5% density by volume. The researchers noted that the inclusion of steel fibers in the concrete mix reduced the slump. Many cracks formed during testing, but the failure-related cracks continued to grow, while other cracks would stabilize as more load was added. In SFRC slabs with less reinforcement, fewer cracks formed, but the failure crack initiated at a smaller deflection. Concrete crushing was less severe when less reinforcement was used. When the reinforcing bars were at the mid-depth of the slab, wider, but fewer cracks were observed. The wider cracks occurred at smaller deflections, when compared to the slabs with a bottom mat of reinforcement. The slab stiffness after cracking was smaller for the slabs with the steel at mid-depth. When more steel was present, the stiffness of the slab after cracking was higher. Based on the study, the authors concluded that for strength considerations, SFRC slabs could have a span distance around 1 to 4ft longer than conventional concrete slabs (McMahon & Birely, 2018).

Michels et al. discussed testing on slabs that had no mild reinforcement. The specimens had 6.24lb/ft^3 (100kg/m^3) of steel fibers, and the researchers ensured that the fibers were evenly distributed in the specimens by not vibrating the concrete during the casting operation. The octagon specimens had varying thicknesses, and some specimens even had slab openings near the column face. The specimens were loaded at eight points near the edge of the specimen. Although the researchers were hoping to induce a punching shear failure, the failure was primarily in bending. During the testing, the

researchers observed yield lines, which indicated ductility in the SFRC slabs. The thicker slabs had more capacity and a higher elastic load. The slabs with cutouts caused the capacity of the slab to be decreased. The authors also examined the fiber orientation at the location of the yield lines. The researchers used this information to develop an equation relating the orientation factor for the fibers to the thickness of the slab. They found that fiber orientation affected the residual tensile strengths of the SFRC mix (Michels, Waldmann, Maas, & Zurbes, 2012).

Jensen and Overli from the Norwegian University of Science and Technology performed research on post-tensioned flat slabs with steel fiber reinforced concrete. They performed an experiment on a post-tensioned flat plate with a banded-uniform layout. This was a four-bay flat plate, with a wall support on one side. There were no reinforcing bars in the longitudinal direction, and 1.87lb/ft^3 (30kg/m^3) of steel fibers were used in the concrete mixture. To load the SFRC slab, water was placed on the slab. A flexural failure in the slab was observed after significant displacements in the slab. The moment distribution that was evident in the testing indicated the ductile nature of steel fiber reinforced concrete. A model was then created for the post-tensioned flat plate. To obtain the tensile properties of the SFRC for the model, beams were extruded from the specimen for tensile testing. The created model was used to examine the moment redistribution behavior of a flat plate. The model had agreement with the load-deflection plots from the actual experiment. The authors concluded that steel fibers in concrete slabs instead of typical bonded reinforcement has the potential to be beneficial (Jensen & Overli, 2015).

Salehian and Barros performed tests on elevated slabs with self-compacting concrete. Self-compacting concrete was used to prevent larger quantities of fibers from settling to the bottom of the slab. A one-quarter scale model test was performed. The slab had six bays, and it was 3in. (7.5cm) thick. Each bay was 3ft-3in. x 3ft-11in. (1m x 1.2m). Three different methods, including direct tension tests and three-point notched beam bending tests, were used to analyze the tensile behavior of the SFRC. In the first part of the test, cement bags were used to load two of the bays at the loads corresponding to the serviceability requirements. No cracks were present on the loaded bays, when the gravity load was 752psf (36kN/m^2). Deflections were measured for up to 500 hours, and

the data showed that the deflections decreased over time, until after 10 days, in which the deflections became stable. In the second part of the test, an actuator was placed at the middle of one of the untested bays. A load was applied with an area of 7.9in. x 7.9in (200mm x 200mm). The reaction columns were confined to prevent premature failure at the column. Cracking began at 9.67kips (43kN) (at the bottom of the slab) and at 14.4kips (64kN) (at the top of the slab). Circular cracking was present at the top of the slab, while cracks eminated from the loading location in an outward direction on the bottom of the slab. The researchers noted that when the two main cracks became wider, the other cracks became smaller. The tests showed that the system was ductile, as the deflection at failure was 3.6 times the deflection when the ultimate force was reached. The researchers also worked on a model to match the data obtained in the physical testing (Salehian & Barros, 2015).

Blanco et al. examined both plastic and steel fibers in concrete. The authors reviewed previous tests done by some of the authors of the paper. In these previous tests, slabs, which were 7.9in. (20cm) thick, were supported at the sides of the specimens and were loaded at the middle. The tests were created to allow for bending failure to occur before any potential punching shear. The fiber dosage for plastic fiber reinforced concrete specimens were 0.56lb/ft^3 (9kg/m^3), while the dosage for the SFRC was 2.50lb/ft^3 (40kg/m^3). It should be noted that each mix had the same number of fibers, even though the fiber densities were different. Beam bending tests indicated that the residual flexural tensile strength for SFRC was larger than the PFRC. The testing of the slab specimens showed that SFRC specimens had more minor cracks than the PFRC specimens, because wider cracks were needed to prompt a fiber response in PFRC. The SFRC slabs held more load, but the load decreased quickly after the peak in the load-deflection plots. For the PFRC slabs, in the load-deflection plots, there was a plateau at the peak load. This was because the plastic fibers have a lower modulus of elasticity. The authors also performed some modelling, and they provided some suggestions to change the Model Code 2010 stress-strain curves in order to match the curves that were obtained during testing (Blanco, Pujadas, Fuente, Cavalaro, & Aguado, 2016).

Parmentier et al. performed testing on SFRC flat slabs with no additional reinforcement. The specimen had nine bays. Each bay was 19ft-8in. x 19ft-8in. x 7.9in.

thick (6m x 6m x 20cm) with circular columns. The fiber dosage was 4.37lb/ft^3 (70kg/m^3). There was some cracking observed after the formwork was removed, but the researchers deemed that the cracks did not significantly impact the deflections that were measured in later testing of the specimen. In the first part of testing, the serviceability requirements of the structure were tested. Two of corner bays were loaded with a water tank. New cracking was observed when 63psf (3kN/m^2) load was applied. A bottom crack was observed running through the center of the two loaded bays. The researchers kept the applied load on the slab for approximately one full day, and they continued measuring deflections during that time period. Deflections continued to increase after the load was applied. Once the load was released, the deflections decreased, but they did not return to zero. To test the ultimate capacity of the slab, a single point load was applied at the center of the slab at three different bays. The largest load could be applied at the center bay because of redistribution. At the center bay, deflections were 1.57in. (40mm) (span length over 150) for a load of 73.7kips (328kN). Cracking occurred in both directions at the bottom of the slab. At the top of the slab, cracks formed a circle around the four surrounding columns. The largest measured crack in the testing was 8.5mm wide. Yield line theory was used to determine the capacity of the slab, and the determined capacity matched the slab's actual performance when flexural beams that were cut from the specimen were tested (Parmentier, Van Itterbeeck, & Skowron, 2014).

Destrée mentioned two tests that were performed on slabs that only had SFRC. These slabs were built in Bissen and Tallin, each with nine bays. Point loads were applied at the middle of bays until failure occurred in the slabs. Ultimate loads reached up to 135kips (600kN), which was 7.5 times the service load. This indicates the ductility of the SFRC flat plates (Destrée, 2009). ACI 544.6R-15 discussed these tests in more detail. Both specimens had similar testing procedures. In the first set of tests, water tanks were used to apply distributed loads for service level load testing, and no cracks were formed in either specimen. The next set of testing used point loads applied to the center of a few bays to reach the slab's ultimate load. The specimen in Bissen had spans that were 20ft x 20ft, and the slab was 8in. thick. The only reinforcement that was present was reinforcing bars that ran from column to column, as required by ACI. The fiber dosage in the specimen was 6.24lb/ft^3 (100kg/m^3). At the top of the slab, there was

cracking at the center of the bay, and yield lines extended the full length of the slab in each direction, running through the center of the middle bay. At the bottom of the slab, a circular crack was present around the entire middle bay. The Tallin specimen was similar to the Bissen specimen, except its spans were 16.5ft x 16.5ft, and its thickness was 7in. (American Concrete Institute, 2015).

Fall et al. wanted to research the redistribution abilities of steel fiber reinforced concrete slabs, because not much research existed in that area. They tested three types of octagon-shaped specimens that were 3.1in. (8cm) thick. One type of specimen had conventional reinforcement with typical concrete. A second type of specimen had steel fiber reinforced concrete with the same reinforcement layout. The third type of specimen had steel fiber reinforced concrete, with no mild reinforcement. For the two types of specimens with reinforcement, a strong and weak direction were created by unevenly distributing the reinforcement. The specimens were all loaded at the center, and the reactions were obtained from strain gauges at the roller supports. When steel fibers were included in the mix, the researchers observed that the cracks were thinner, but a higher quantity of cracks were found. Ductility was increased for the specimens with SFRC and reinforcing bars, when compared to the specimens with reinforcing bars and traditional concrete. Also, the specimens with SFRC and reinforcing bars had higher capacities, which was attributed to the redistribution that was provided by the inclusion of the steel fibers. The weak direction reaction still became larger once initial cracks were observed, which showed redistribution in the specimen with rebar and SFRC (Fall, Rempling, & Lundgren, 2013).

A second paper was written about the same experiments, and it provided more information about the results of these experiments. In this paper, the authors stated that the weak direction supports had a sixty percent higher load and the strong direction supports had a thirteen percent higher load for the specimens with SFRC and reinforcement when compared to the specimens with only reinforcement and typical concrete. The authors concluded that redistribution could be considered for SFRC slabs with conventional reinforcement when designing these types of slabs. The authors also provided an in-depth analysis of the slab with yield line theory (Fall, Shu, Rempling, Lundgren, & Zandi, 2014).

2.5 Research on Punching Shear in SFRC

Tan and Paramasivam performed research on single-bay specimens to examine punching shear in SFRC slabs. They varied the span-to-depth ratio, thickness of slab, concrete strength, fiber density, and the area of the applied load. The slabs were loaded at the center of the specimen, and the slabs were supported near their perimeter. Cracking began at the center of the specimen, and as more cracking occurred, the reinforcing bars in the slab began to yield. Punching shear occurred at a distance of 4.5 times the effective slab thickness from the edge of the applied load (which acted as a column). The authors found that span-to-depth ratio had little impact on the slab performance. Also, they found that higher fiber density leads to higher ductility, higher capacity, and higher cracking and yielding loads. Increasing the thickness of the slabs has a similar impact on the slab's performance. Although not definitive, higher compressive strength of concrete could have similar effects on the specimen's performance. Increasing the size of the applied load allowed for more capacity, but the ductility was not affected. The authors also compared the experimental data to punching shear equations in previous research and in building codes, and most of the equations were found to be unconservative (Tan & Paramasivam, 1994).

In another series of tests, Abdel-Rahman et al. wanted to investigate the inclusion of steel fibers to see how they affect punching shear, which is a major concern for flat plates. In these tests, the fiber dosage varied. The researchers also limited the fibers to certain distances from the edge of the column faces. Additionally, the researchers included some unbalanced loads on some of the specimens in order to examine the impact of unbalanced moments on the performance of the specimens. The specimens had a column at the middle of the slab and were reinforced with the same quantity of reinforcing bars. Fiber volumes ranged from 0.5 to 1.5% volume ratios. The researchers found that ductility was improved as the fiber contents increased. The inclusion of fibers also moved the punching shear area further from the edge of the column. The steel fibers also reduced the deflections because of the improved stiffness associated with their inclusion in the concrete mix. The capacity of the slabs increased when higher dosages of fibers were included in the mix design. The researchers then ran a finite element model and compared the results to the experimental results and found good agreement

with the crack patterns, failure mode, and ultimate load (Abdel-Rahman, Hassan, & Soliman, 2018).

Nguyen-Minh et al. performed additional research on the punching shear behavior of SFRC flat plates. Their specimens had mild reinforcement, and they varied the length and width of the specimens. For each size of slab, one specimen had conventional concrete, and three specimens had SFRC. Slabs with conventional concrete had less ductile failures, and the crack widths for the SFRC slabs were smaller. The crack widths were between 41 and 90 percent thinner for the SFRC slabs. Similar to what was found in other SFRC research, the SFRC slabs had higher stiffnesses. The capacities of the slabs increased as the fiber dosages in the slabs increased, which was in line with previously mentioned research. The researchers examined some existing models and equations, and they concluded that there was too much variability in the data. One reason the that the authors provided for why this variability occurs was that the fact that reinforcing bars do not always yield when punching shear occurs. Also, the models did not consider the exact geometry of the fibers (Nguyen-Minh, Rovnak, Tran-Quoc, & Nguyen-Kim, 2011).

Gouveia et al. performed punching shear tests on SFRC flat plates. They varied the fiber dosage, and they used plasticizer in some concrete mixes. The plasticizer was used to provide higher slump, as the fibers caused reductions in the slump. The specimens were 4.9in. (12.5cm) thick, and a load was applied at the center of the slab, with the edges of the slab restrained. Both plasticizers and fibers allowed the slabs to have higher stiffnesses and increased the capacities of the slabs. When the dosage of fibers increased, higher loads and deflections could be reached. Punching shear occurred, with the top edge of the failure located approximately double the thickness away from the edge of the column. The angle of the punching shear was lower for the slab without fibers than the slab with fibers. The authors compared the experimental results to some models that were presented by other researchers. Overall, the models were deemed to be sufficient, although some were not conservative (Gouveia, Fernandes, Faria, Ramos, & Lucio, 2014).

2.6 Summary of Literature Review

As shown in this literature review, much research has been done on post-tensioned flat plates, both investigating the flexural behavior of the flat plates and the punching shear capacity of the flat plates. Additionally, steel fiber reinforced concrete has been a popular research area in recent years. Many flat plates with SFRC have been investigated. However, the existing gap in the research is SFRC post-tensioned flat plates. This current project hopes to address the lack of research in this area by testing a scale-model of a post-tensioned flat plate with steel fiber reinforced concrete.

Chapter 3 - Methods

3.1 Introduction

In this project, a 33ft-3in. x 31ft-6in. x 3in. post-tensioned flat plate was constructed and loaded to determine the performance of a steel fiber reinforced concrete post-tensioned flat plate (referred to as Specimen 2). To determine the properties of the post-tensioning strands for this test and to test the design of the loading system, a 10ft-8in. x 10ft-8in. x 4in. conventionally reinforced concrete slab was constructed before the construction of the post-tensioned flat plate. This section will provide the details of the design, construction, and testing for these two specimens.

3.2 Trial Slab

The 10ft-8in. x 10ft-8in. x 4in. trial slab was constructed with the purpose of testing the design of the whiffle tree and formwork, in addition to obtaining preliminary data on the friction and wobble coefficients for the strands to be used in Specimen 2. Additionally, the trial slab served as a practice run for the construction of Specimen 2, in order to identify and correct any unforeseen problems.

3.2.1 Construction of the Trial Slab

Formwork was designed using the NDS Specification (American Wood Council, 2014). Plywood sheets were attached to and supported by 2x4 wood beams. The 2x4 beams were supported by double 2x6 whalers which acted as girders. These whalers were then supported by 4x4 posts. To allow for the forms to be removed prior to testing the slab, the whalers were supported on Simpson Strong-Tie JP44 jacks, which could be lowered a few inches to allow for the plywood panels to be slid out under the concrete. The Simpson Strong-Tie JP 44 jack is shown in Figure 6. Additionally, the plywood was covered with a thin plastic sheet, which acted as a bond breaker between the plywood and the concrete.

Figure 6. Simpson Strong Tie JP44 Jack

The trial slab contained traditional reinforcement along with two post-tensioned strands. The mild reinforcement was tied to slab bolsters to provide the correct amount of concrete cover. The reinforcement drawings are provided in Appendix A.

The four columns sat on swivel heads to allow for rotation at the base of the columns. The columns were precast prior to the placement of the slab. The columns were placed in the openings provided in the slab's formwork. Then, any gaps between the forms and the columns were sealed with duct tape.

The strands were tied to modified slab bolsters. The modified slab bolsters were hammered to the correct height to achieve the correct strand profile. One strand had a linear profile, as it ran through the center of the slab (2 in. from the bottom of the slab to the tendon's center). The second strand had a parabolic profile, meant to mimic the draped tendons that would be in Specimen 2. This profile is shown in Figure 7. Similar to the requirements provided for Specimen 2, the supports for the tendons were spaced at 15in. center-to-center. Also, the tendon exited the slab at the slab's center, and the draped tendon's lowest point was at approximately 0.51in. from the bottom of the slab. An L/12 reverse parabola was also used, meaning that a concave down parabola extended a distance SpanLength/12 from the column line before switching concavity.

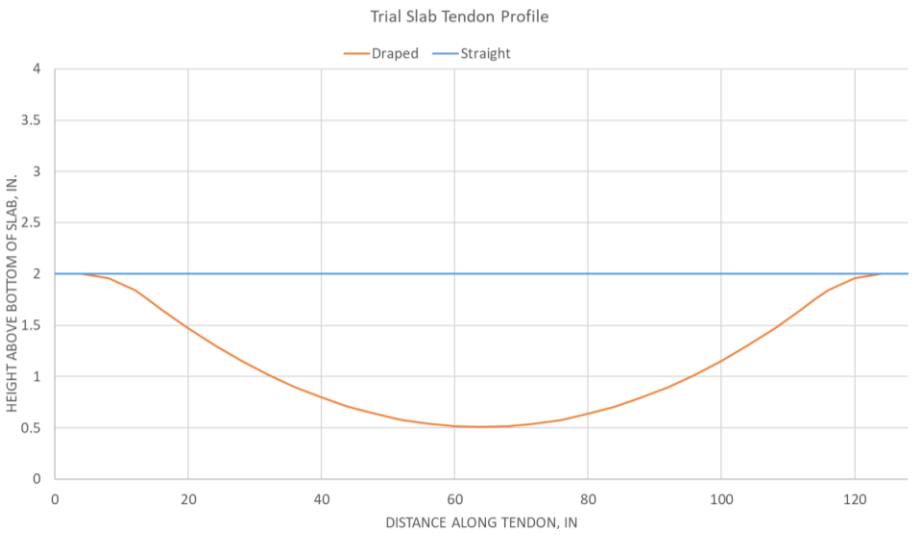

Figure 7. Trial Slab Tendon Profiles

The loading system for the trial slab was suspended beneath the slab. Sixteen point loads were applied to the slab. At these sixteen points, PVC pipes were positioned with wood dowels to form blockouts in the concrete. When the concrete was placed, many of these blockouts tipped over or were completely displaced. The design of these blockouts was changed for the construction of Specimen 2.

3.2.2 Stressing Operation

To determine the friction and wobble coefficients, each strand in the trial slab was stressed and the force was released through several trials. The following sections discuss the procedures for the stressing operation and the results from the operation.

3.2.2.1 Stressing Procedure

The stressing operation setup is shown in Figure 8. This setup was used for both the straight tendon and the draped tendon. Load cells were calibrated prior to the operation and loads were measured with a strain indicator instrument along with a switch-and-balance box (to support measuring multiple load cells at a time).

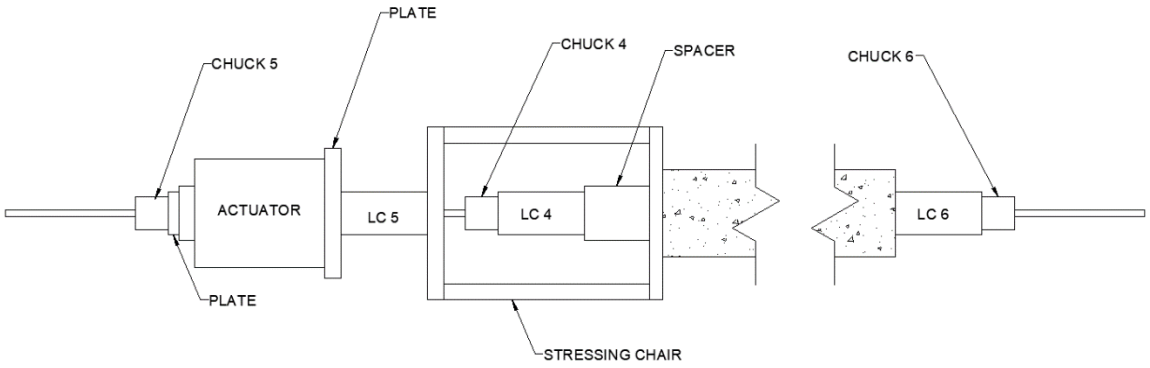

Figure 8. Stressing Operation Overview

The wedges were pushed forward into the chuck body for both Chuck 5 and Chuck 6. Also, some space was left between the actuator and the plate next to Chuck 5 (to ensure that the strand could eventually be fully de-tensioned). Some initial load (approximately 100lbs) was added with the actuator and a check was done to esnure that all components were concentric with the tendon. The wedge seating distance for Chuck 5 and Chuck 6 was measured and recorded (see Figure 9), and the load in LC 5 and LC6 was also recorded. Additionally, the piston elongation was measured and recorded (see Figure 9). The actuator load was increased in approximately 2000lb increments up to 10,000lbs. At each increment, the two wedge seating distances (Chucks 5 and 6), the load in LC 5 and 6, and the piston elongation was measured and recorded.

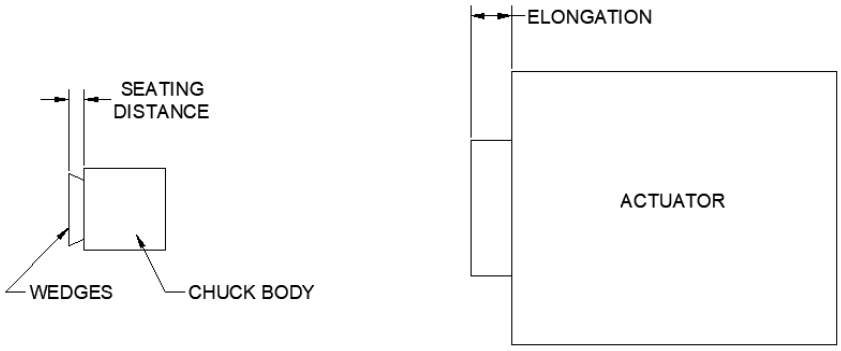

Figure 9. Wedge Seating Distance and Piston Elongation Measurements

To determine seating losses, the next step was to tap in the wedges for Chuck 4. The wedge seating was measured and recorded for this chuck, and the piston was fully retracted. Loads at LC6 and LC4 were recorded, along with the wedge seating for Chuck 4.

The strand was de-tensioned by adding approximately 10,000lbs of load to the actuator and hammering the wedges out of Chuck 4. With the wedges removed from Chuck 4, the load was released from the actuator. At this point, there was zero load in the strand, and the strand could be cut to retrieve the load cells, stressing chair, plates, spacer, and actuator from the strand. This overall procedure was repeated approximately five times for each strand.

3.2.2.2 Results from Stressing Operation

Throughout the operation, the elongation of the strand was compared to the load cell readings to ensure that there was agreement between the two measurements. The straight strand provided the wobble coefficient, since it had no curvature. The wobble coefficient was calculated to be 0.0009/ft. After determining the wobble coefficient, the friction coefficient could be determined after stressing the draped strand. It was determined to be 0.12. Additionally, seating loss based on the experimental data was estimated to be approximately 0.12in. These parameters were used for designing Specimen 2. A summary of the data is provided in Appendix I.

3.2.3 Design and Construction of the Whiffle Tree

An initial design for the whiffle tree was developed early in the project. The initial design had several steel members resting above the slab to distribute one point load at the actuator into sixteen point loads which would be applied to the slab. This compression whiffle tree was not used or built due to the uncertainties regarding its stability. It was replaced by a tension whiffle tree, similar to what had been used in other research projects.

The whiffle tree consisted of four levels of steel hung from the slab by ½in. diameter eyebolts. The baseplate on the surface of the slab is a 6x6x3/8in. steel plate. The top levels of steel below the slab were HSS members. A double channel was hung below the HSS members, and the final layer of steel was a W8x40 beam. The 25 ton single-action actuator was suspended from a W14x99 beam lying across the lab's high floor beams. The actuator applied its load to the center of the W8x40 steel member. The steel members were connected together with an assembly of anchor shackles and master links. A side view of the trial slab's whiffle tree is provided in Figure 10, and the top view of the setup is shown in Figure 11. The member sizes and anchor shackle details for

the final whiffle tree are provided in Section 3.3.9. Some larger, more conservative, steel sections were used for the HSS members (due to availability constraints). Heights of the steel members were the same as the final design to ensure that the layout would fit under Specimen 2.

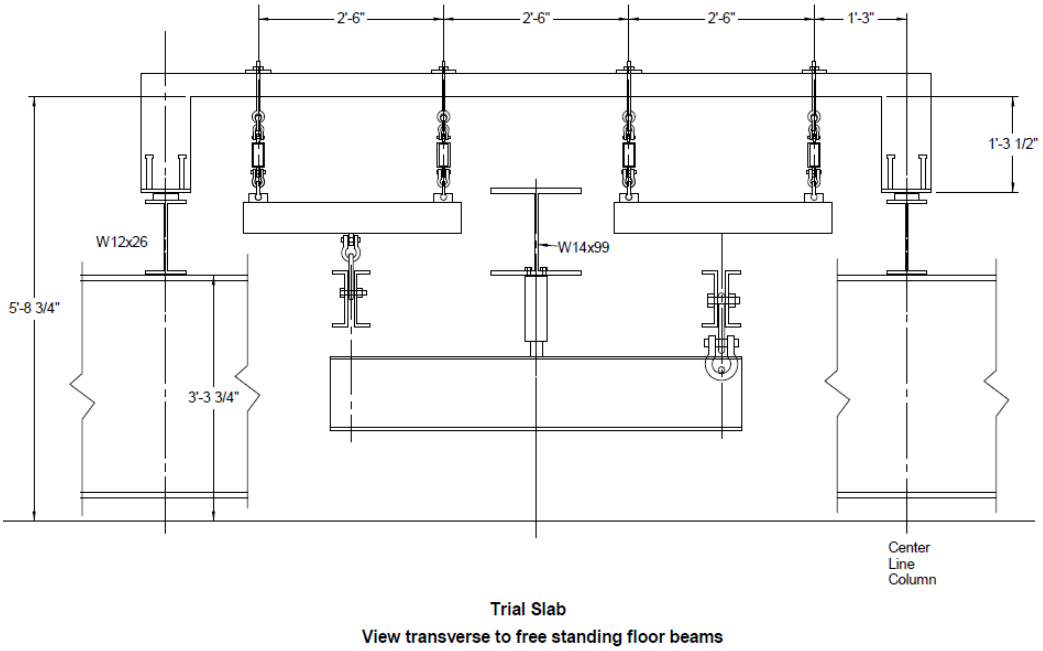

Figure 10. Side View of Trial Slab Whiffle Tree

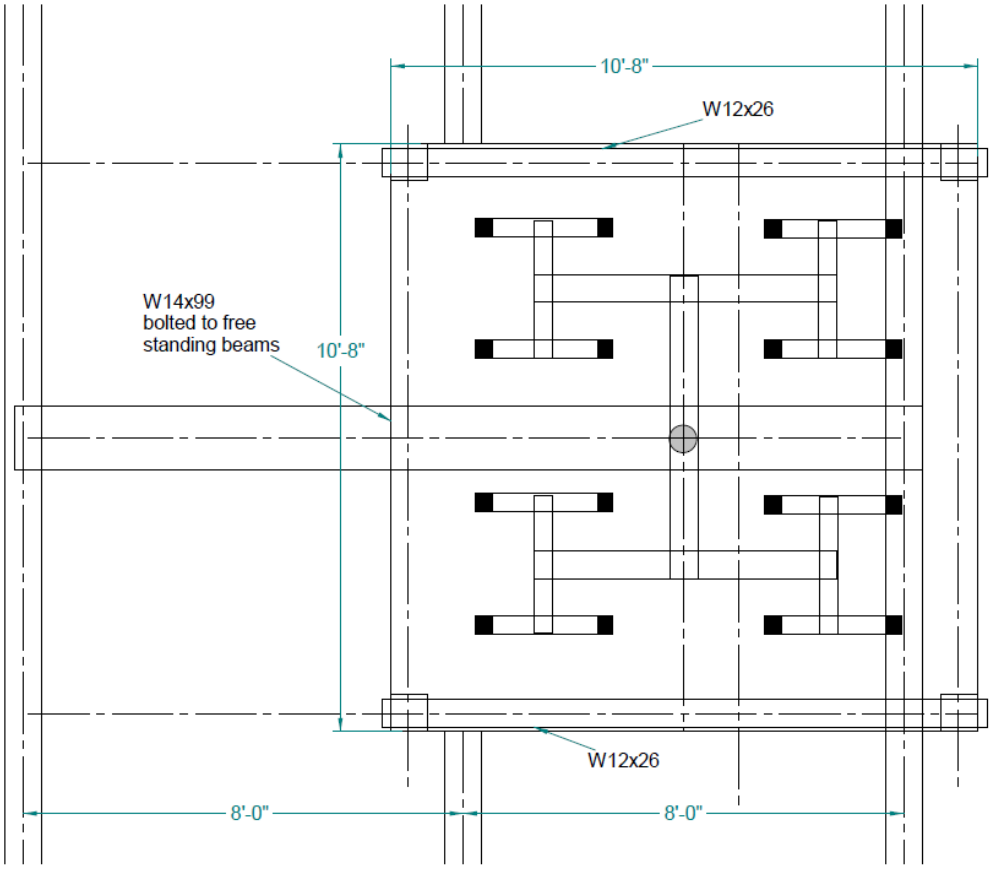

Figure 11. Top View of Trial Slab Whiffle Tree

3.2.4 Testing of the Whiffle Tree

To validate the assumption that the whiffle tree could be used to represent uniform loading on an elevated slab, testing was performed. The results of the tests needed to show that the load was divided evenly between the sixteen eyebolts. The first set of testing required the eyebolts to be instrumented with strain gauges. The second set of testing used BDI strain gauges on the top members of the whiffle tree. The procedures and results of this testing is discussed below.

3.2.4.1 Strain Gauges on Eyebolts

Small strain gauges were applied to the eyebolts on the smooth surface just above the eye of the bolt. Special care was made to ensure that the gages were protected from impacts. Each of the sixteen eyebolts were loaded into the MTS Insight machine in the lab to determine a relationship between load and strain. A CR9000 data acquisition system was used to collect the data for this test. The calibration set up is shown in Figure

12. Each strain gauge had a calibration value that could be applied to the strain to obtain a load after the test had been completed.

Figure 12. Eyebolt Calibration Setup

The test setup also had a load cell under the actuator to monitor the total load applied to the slab. Testing was performed, increasing the actuator load 1 kip at a time (10psf). The resulting eyebolt loads are shown in Figure 13.

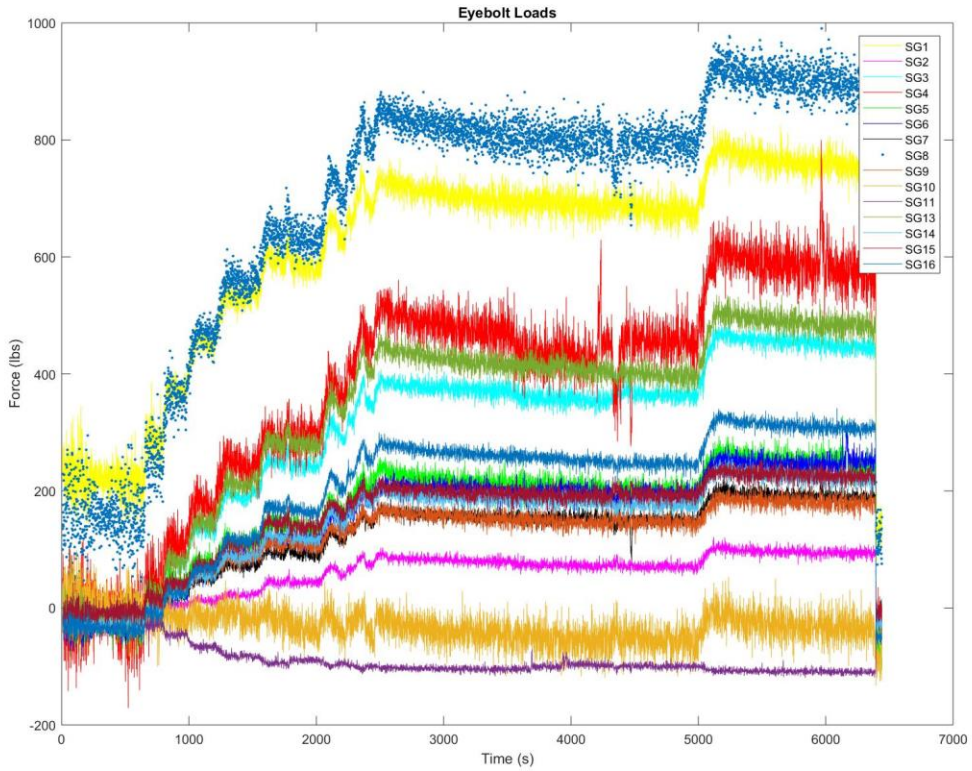

Figure 13. Eyebolt Loads from Strain Gauge Readings

Some strain gauges were not functional, as they showed decreases in load as load was added to the slab. Also, the total load from the strain gauges (only fifteen were monitored) was much different than the reading from the load cell (see Figure 14). It was unclear from the testing if the load was being equally distributed between the sixteen eyebolts, as the calibrations for the strain gauges had some issues. Some strain readings were incorrect possibly due to bending induced in the eyebolts. When the concrete was placed, many of the blockouts for the eyebolts tilted over. This introduced some rotational restraint on the eyebolts when they were installed, which could have led to bending stresses in the eyebolts.

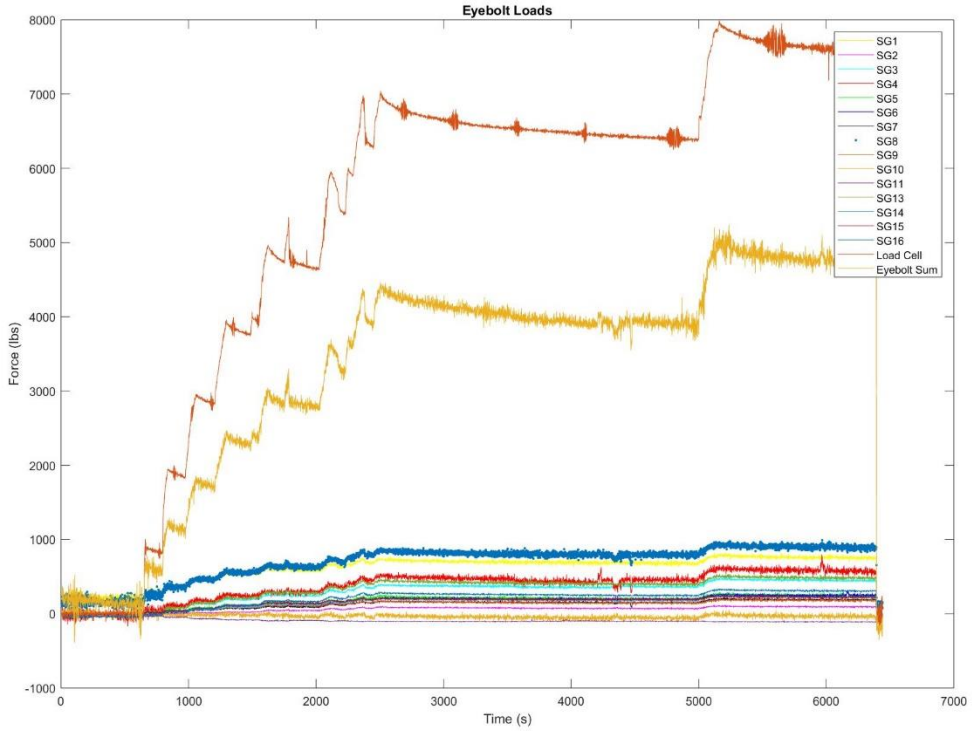

Figure 14. Load Cell and Eyebolt Loads

3.2.4.2 BDI Strain Gauges on HSS 4x2 Members

To bypass some of the issues that the traditional strain gauges were causing, BDI strain gauges were applied to the HSS 4x2 members. These strain gauges were applied at the center of the top surface of the HSS members. A similar testing procedure was performed. Total load was monitored with the load cell under the actuator. A string potentiometer was used to monitor deflection at the center of the slab. The deflection and actuator load data were collected on the CR9000 system. Additionally, dial gauges were placed at the corner of the southwest column and at both ends of the W8x40 (the lowest member on the whiffle tree). The dial gauge at the column was used to ensure that the column was not moving outward at an unsafe rate. The dial gauges at the W8x40 were used to ensure that the beam would not need to be braced. Readings from the W8x40 dial gauges showed that the beam would not need to be braced in subsequent testing. Column movement began to be concerning at higher loads, so the columns were restrained together with load ties wrapped around the bases of the four columns.

10psf (1 kip at the actuator) load increments were applied to the slab. Testing was stopped when only deflection (no load increase) was applied to the slab. BDI readings were monitored, and the strains were converted to loads. The eight BDI readings, converted to loads, were plotted in Figure 15. Bending stress were calculated using the steel's modulus of elasticity and the recorded strains. Loads were calculated by finding the bending moment corresponding to the calculated stresses.

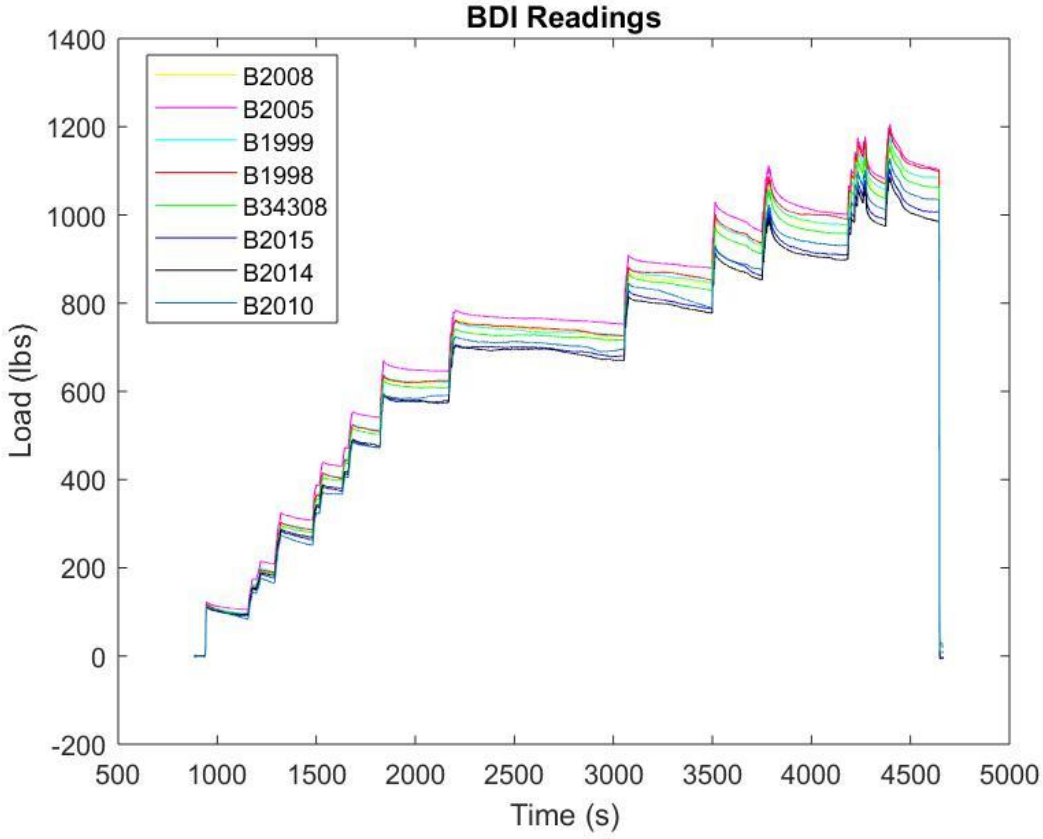

Figure 15. Loads from BDI Readings

The standard deviation of the loads calculated from the BDI gauges was approximately 45lbs at the trial slab's ultimate load (around 100psf of applied load). The range of loads calculated from the BDI gauges was approximately 120lbs at the ultimate load. From the testing with the BDI readings, it was concluded that the whiffle tree would indeed evenly distribute the single load at the actuator to sixteen individual point loads on the slab. Additionally, no bracing would be required at the bottom level of the whiffle tree (the W8x40 beam).

3.3 Specimen 2

Specimen 2 represents a one-third scale model of a 99ft x 94ft x 9in. prototype post-tensioned flat plate with a banded-uniform tendon arrangement. This section discusses the design, construction, and testing procedure of this specimen.

3.3.1 Design of Specimen 2

Specimen 2 is a 33ft x 31ft-6in. x 3in. steel fiber reinforced concrete post-tensioned flat plate. It has 11in, x 11in. columns at the interior and overhang, and 12in. x 12in. columns at the two exterior corner locations. The columns have a height of 13.5in. to the bottom of the flat plate. Dimensions comparing the scale-model (Specimen 2) to the prototype slab are provided in Table 1. For more information, Jack Li performed calculations and an analysis showing the similitude between a one-third scale model and a prototype post-tensioned flat plate (Li, 2019).

Table 1. Specimen 2 and Prototype Flat Plate Dimensions

	Specimen 2	**Prototype**
Slab Dimensions	33ft x 31ft-6in.	99ft x 94ft-6in.
Thickness	3in.	9in.
Overhang Length	2ft-6in.	7ft-5in.
Bay Size	10ft x 10ft	30ft x 30ft
Interior Column Size	11in. x 11in.	33in. x 33in.
Exterior Column Size	12in. x 12in.	36in. x 36in.
Column Height	1ft-3in.	10ft
Tendon Size	5/16in. Dia.	1/2in. Dia.
Mild Reinforcement	D5 bar (0.252in. Dia.)	#4 bar (0.5in. Dia.)
Max. Aggregate Size	0.375in.	1.125in.

Specimen 2 has a banded-uniform tendon arrangement. Tendons in the uniform direction (the tendons run in the long direction of the slab) are spaced at a 2ft spacing. There are sixteen tendons in the uniform direction. There are seventeen tendons in the banded direction. Four run through the columns closest to the overhang. Three run through the columns at the other exterior edge. The two interior column lines each have five banded tendons. The design drawings, as designed by the oversight committee, for Specimen 2 are provided in Appendix B. The only change to the design drawings were that the three banded tendons at the exterior edge of the slab were not grouped together. Additionally, the reinforcement drawings are voided, since the original design drawings were developed for a conventionally reinforced post-tensioned flat plate (Specimen 1).

Also, 3.5in. x 2.5in. x 0.5in. anchor plates were provided at the ends of the slab for the tendons. These plates were attached to the side forms with caulk.

3.3.2 Pedestal and Column Construction

To ensure that there would be enough space beneath the post-tensioned flat plate for the loading system, the slab needed to have a height of approximately 5ft-9.5in. to the bottom surface of the slab. A pedestal was designed to elevate the slab. Pedestals were anchored to the strong-floor beams in the lab. These strong-floor beams were spaced at 8ft center-to-center, so the exterior pedestals were 3ft from the center of the nearest floor beam, and the middle pedestals were 1ft from the center of the nearest floor beam (see Figure 16). Steel plates, 5/8in. thick, were used at the base of the pedestal, and four shear studs were welded to the plate to anchor the concrete to the plate. A 20in. x 20in. x 48.875in. pedestal was cast on top of the steel plate at each of the sixteen column locations. The next step was to mark the exact center of the columns on each of the pedestals. This ensured that the columns would end up in the correct location (at a 10ft spacing).

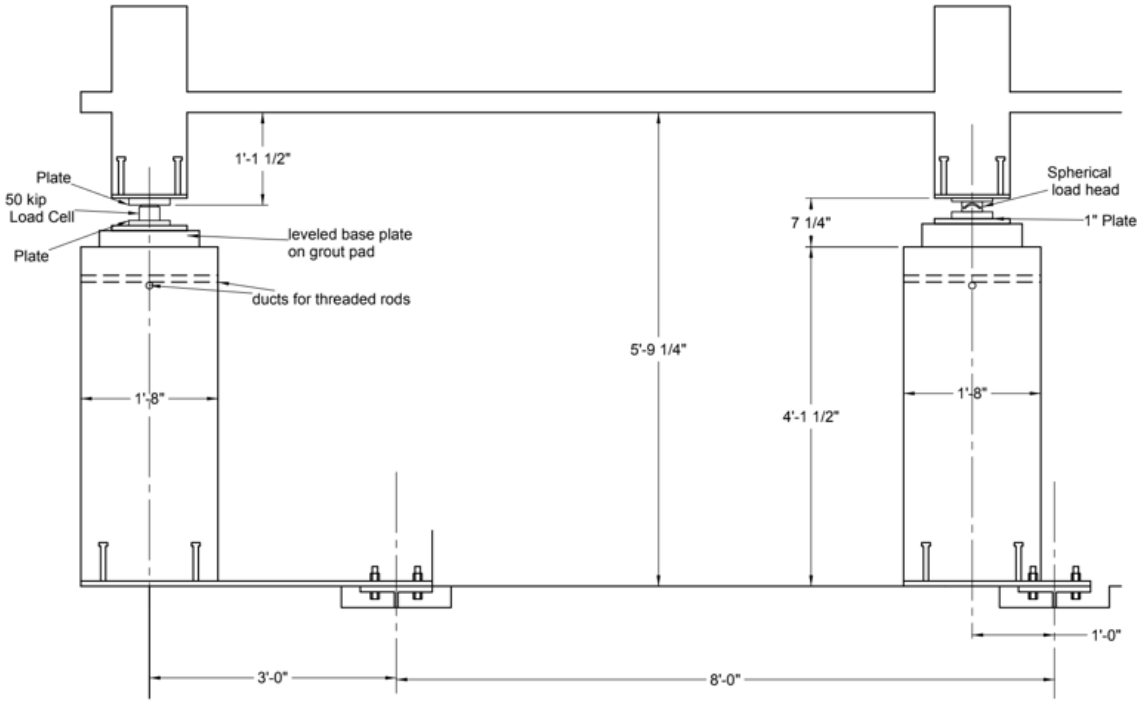

Figure 16. Pedestal Positioning on Strong Floor

The plan for the pedestal/column assembly is shown in Figure 17. There were two different pedestals assemblies. Pedestals that supported columns with load cells

required a different thickness for the grout pad compared to the grout pad thickness for pedestals with swivel heads. A steel plate assembly supported either the load cell or the swivel head. The steel plate assembly was held on small diameter steel rods with two nuts. The plate assembly was raised and lowered by twisting the bottom set of nuts. A small level was used to ensure that the top of the plate was level, and a laser level was used to obtain the correct elevation of the assembly. Small side forms were placed on top of the pedestal, centered around the plate assembly, and grout was placed in two separate mixes. Grout strengths exceeded a 5000psi compressive strength. Also, the plates immediately above and below the swivel heads had circles milled out to provide a small amount of lateral restraint for the load cells and swivel heads.

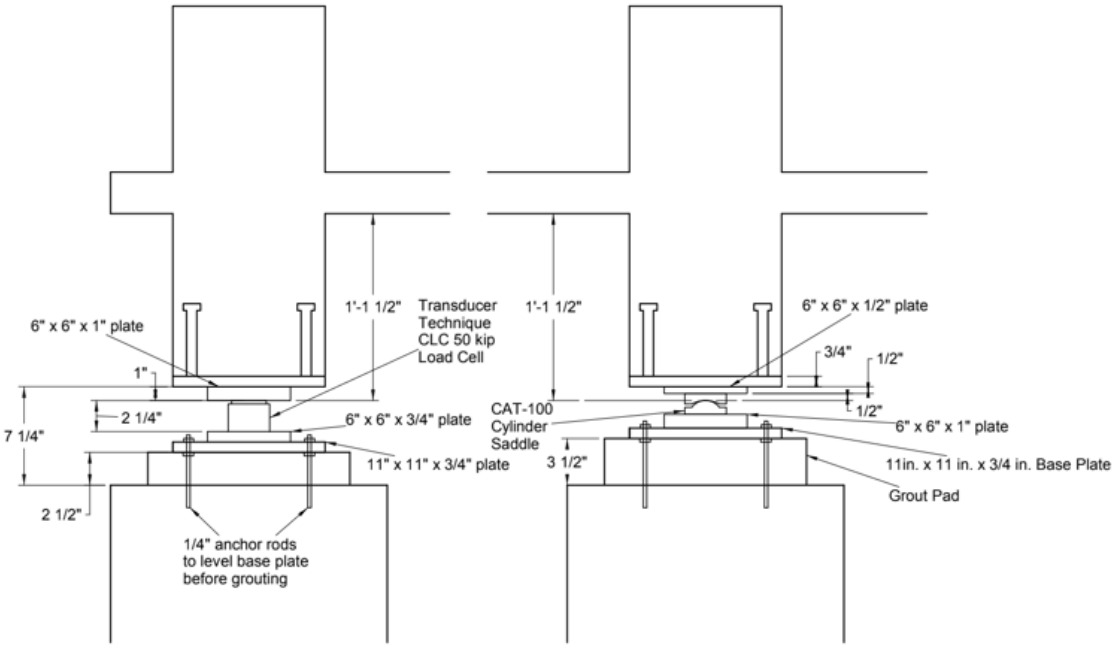

Figure 17. Pedestal and Column Assembly Details

To ensure that the columns had a pin support at their base, a swivel head (Enerpac CAT-100 cylinder saddle) was used at eight column locations. The locations of these load cells is provided in Section 3.3.6 in this thesis. The other eight columns had a Transducer Techniques® CLC-50k load cell beneath them. The 50 kip load cell had a slightly domed top, which allowed the column to rotate at the base. The 1ft-3in. column height (1ft-1.5in. to the bottom of the slab) was measured from the center of the slab to the point of rotation. From dimensional analysis of column stiffnesses, a one-third scale model column would have 1/27 the stiffness of a prototype column. Accounting for this

and the difference in column connection conditions (fixed columns above and below the slab for the prototype, and a pinned column below the slab for the scale model specimen), the required column height for the scale model was calculated to be 1ft-3in. This was measured from the pin support to the center of the slab. The point of rotation (where the pin support was located) for the columns supported by load cells was the top of the load cell. The point of rotation for the columns supported by swivel heads was at the center of the swivel head.

The pedestals were placed four at a time in approximately two week increments. There was an issue with the first batch of concrete regarding the water content, so this concrete was not used for Specimen 2's stub columns. Concrete from the next three pedestal placements were used for the sixteen columns in Specimen 2. This was done to have a test run of the concrete mix to ensure that the mix design for the flat plate would reach the desired compressive strength of 5000psi. Table 2 provides the strengths of the concrete used in some of the columns. Concrete placed on 7/19/18 and 8/2/18 had aggregate that exceeded the maximum size required for Specimen 2.

Table 2. Concrete Strengths for Columns

Placement Date	28-day Strength (psi)	Water : Cement Ratio
7/19/18	5480	0.507
8/2/18	5390	0.490
8/17/18	4260	0.527

3.3.3 Scaffolding Design and Construction

The scaffolding design and formwork was similar to the design of the formwork for the trial slab. Plywood panels were supported by 2x4's. Double 2x6 whalers acted as girders, which supported the 2x4's. 4x4 posts with Simpson Strong-Tie JP44 jacks at the top were placed under the whalers. A small gap, approximately 1/4in., was provided around each column to allow for easy removal of the forms after the concrete had cured. Some 4x4 posts were braced in each direction with lateral cross bracing, to allow for the scaffolding to be sturdy when work was being done on top of the formwork. A photo of the scaffolding at an early stage is provided in Figure 18. Additionally, design drawings for the scaffolding are provided in Appendix C. Side forms were constructed with a 3in. tall piece of plywood, and these were placed along the edge of the slab.

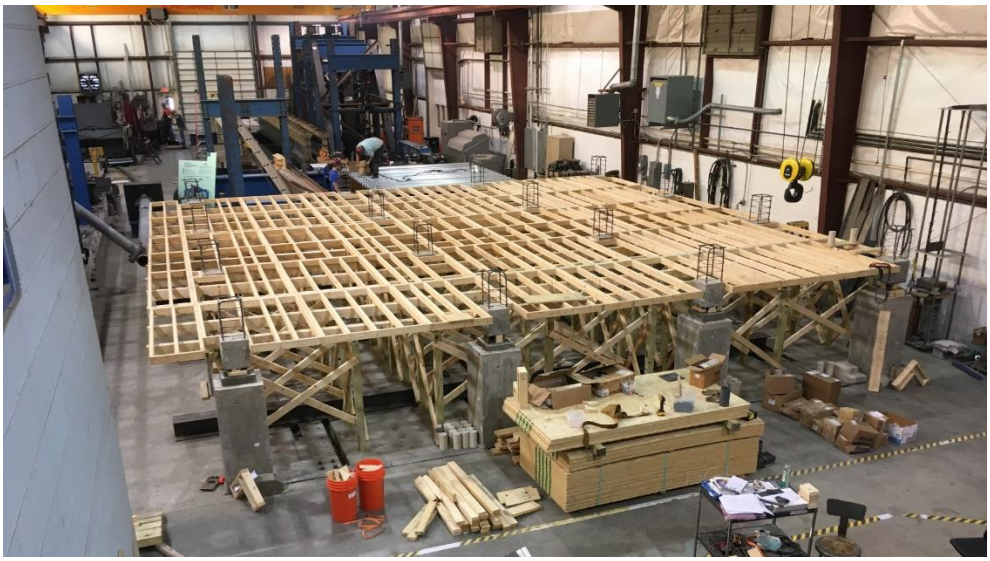

Figure 18. Scaffolding at Early Stage

Once the scaffolding was almost complete, the columns were dropped into place. The scaffolding was raised to the approximate final height by twisting the nut on the JP44 jacks. A laser level was used to fine-tune the levelling of the formwork surface. The slab elevation was estimated to be within ±3/8 inch of the goal elevation. Prior to the concrete being placed, levels were used to ensure that the columns were vertical. Wood shims were temporarily placed in the forms on the side of the columns to ensure that the columns would remain vertical throughout the placement of the concrete. If any columns extended above the formwork, they were chiseled at the edges to prevent premature failure due to punching shear. Any gaps between the columns and forms were covered in duct tape to prevent any concrete from seeping out from the formwork.

Some whiffle tree components (see Section 3.3.9) were designed to run through the slab. To successfully blockout the concrete during the placement operation, a 3/4in. PVC pipe was bolted down to the forms (see Figure 19). This ensured that the pipe would not move out of place when people walked on the formwork.

Figure 19. Whiffle Tree Blockout

3.3.4 Layout of Tendons and Reinforcement

The slab chair locations for each tendon (or set of banded tendons) were marked on the formwork with a marker. Care was taken to ensure proper cover for the reinforcement and tendons, so some spacing for the D5 bars was modified. After all marks were drawn onto the forms, the formwork was covered with a thin plastic sheet to act as a bond breaker between the concrete and plywood.

Slab chairs were used to support the uniform tendons. These chairs were hammered to the correct height. When the slab chairs were placed on the forms, they were nailed down so that they would not move when people were walking on the formwork. For the banded direction tendons, D5 bars were typically strung between two slab chairs (see Figure 20) to support the tendons. In some cases, to achieve the correct elevation for the tendons, a combination of D5 bars, 5/16in. threaded rod, and/or 3/8in. threaded rod were used to manufacture a chair or bolster.

Figure 20. Banded Tendon Slab Chair Examples

Back-up bars (as required by ACI 318 Section 25.9) for the anchor plates at the edge of the slab were provided and were attached directly to the tendons (one above and one below the tendons) (ACI, 2014). They extended across two tendons for the uniform tendons. The rebar extended at least 4in. past the centerline of the tendons. For the banded tendons, they extended approximately 4in. past the centerline of the edge tendon for each grouping of tendons.

3.3.5 Placement of Concrete

Contractors were hired to assist in the placement of the concrete. A 3in. mark was provided on each of the interior columns to help the contractors finish the concrete thickness at the correct height.

Two trucks brought concrete to the lab, and a crane and bucket were used to transport the concrete from the truck to the formwork. Each truck carried approximately 6yd^3 of the mixture. There were 7lb/yd^3 of steel fibers in the mix. It was ensured that the maximum aggregate size was not exceeded for both truckloads of concrete. The concrete mixture designs are provided in Tables 3 and 4. 6in. x 12in. cylinders were made for modulus of elasticity tests, compressive strength tests, and for creep testing. Also, shrinkage prisms were made along with flexural beams (six for each truck). 4in. x 8in.

cylinders were made so that the compressive strength could be monitored prior to the stressing operation and before the load testing. Compressive strengths at 28-days are provided in Table 5. A total of twelve flexural beams, six from each truck, were sent to TEC Services for flexural testing using ASTM C1609 and EN14651 guidelines (ASTM International, 2019), (CEN, 2005). A summary of the results from these tests is provided in Appendix G (TEC Services, 2019a), (TEC Services, 2019b).

Table 3. Truck 1 Concrete Mixture

Truck 1 Mixture	
Material	**Quantity (lbs)**
Type I/II Cement	714
Natural Sand	1285
Crushed Limestone (#9)	1571
Water	371
Fibers (Bekaert RC-80/30-BP)	84
Other Properties:	
Slump (in.)	6.50
Air Content (%)	3.1

Table 4. Truck 2 Concrete Mixture

Truck 2 Mixture	
Material	**Quantity (lbs)**
Type I/II Cement	714
Natural Sand	1285
Crushed Limestone (#9)	1571
Water	371
Fibers (Bekaert RC-80/30-BP)	84
Other Properties:	
Slump (in.)	7.00
Air Content (%)	3.4

Table 5. Specimen 2 Concrete Strengths

	28-day Strength (psi)
Truck 1	7770
Truck 2	7440
Average for Slab	7610

For adequate development length, the column reinforcement extended through the top surface of the slab. To place concrete for the top portion of the columns, small forms

were set in place and attached to the slab with caulk to prevent uplift. A 5000psi design concrete was used for the top sections of the columns. More information on the concrete mixture is provided in Appendix G.

3.3.6 Instrumentation Plan

To monitor and collect data during the experiment, two data acquisition systems were used. A CR5000 from Campbell Scientific was used for some of the long-term measurements. A CR9000 was used to collect data during the actual loading of Specimen 2.

The CR5000 was connected to the eight load cells located under the columns, the four load cells permanently measuring tendon forces, and six vibrating wire gauges. Figure 21 shows how the vibrating wire gauges were attached to the formwork. Two slab bolsters (set to the correct height with a hammer) were attached to the formwork with nails, and four zip-ties connected the gauge to the slab bolsters. Figure 22 shows the location and labels for the load cells and vibrating wire gauges. Unfortunately, the vibrating wire gauges did not record useful data due to their sensitivity and small allowable range of measurements. Twelve string potentiometers were later added to the CR5000 because it provided clearer readings.

Figure 21. Vibrating Wire Gauge Assembly

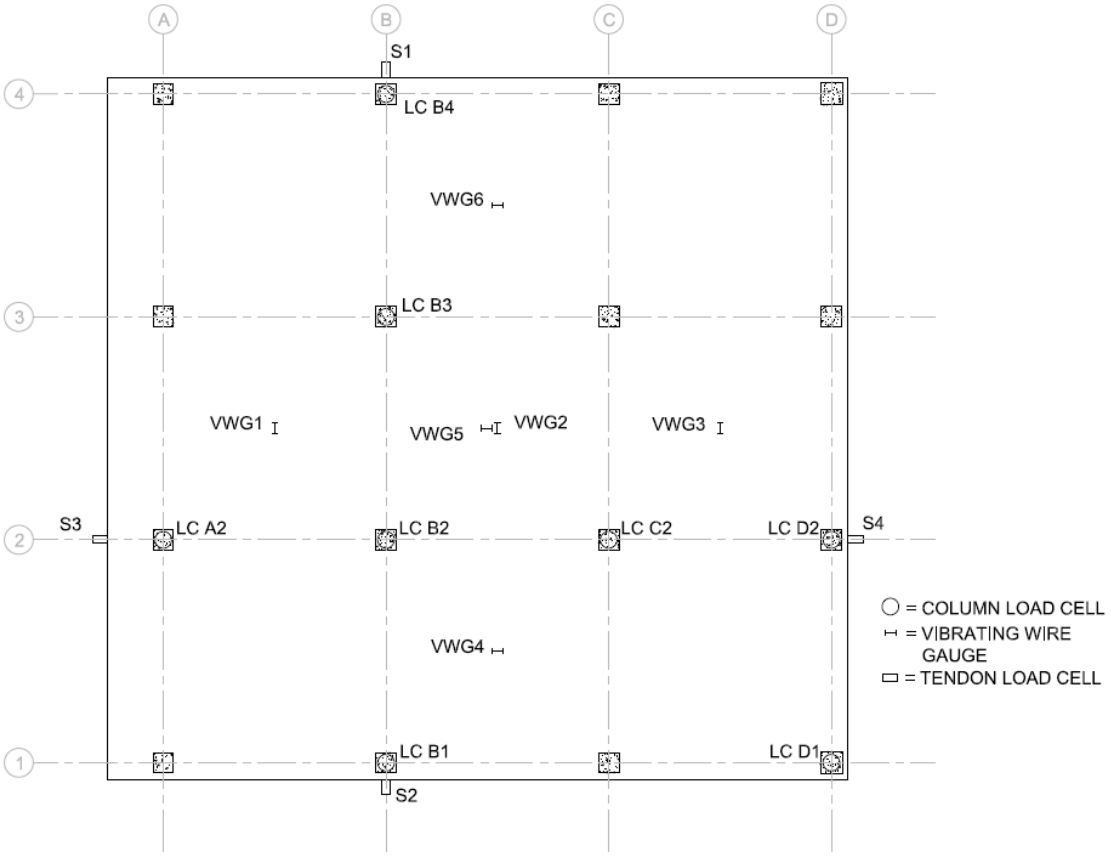

Figure 22. Vibrating Wire Gauge and Load Cell Layout

Twelve foil strain gauges, two pressure transducers, and three LVDTs were connected to the CR9000. The locations and labels for each foil strain gauge are provided in Figure 23. The twelve strain gauges were placed near the face of the columns (on the top mat of reinforcement). These two columns were the only columns to have top mat reinforcement in Specimen 2. The lead wires to the strain gauges were routed to the nearest column in preparation for the placement of concrete. Once the concrete was cast, the lead wires were routed to the data acquisition system. The position of each foil strain gauge is provided below in Table 6. Nine wire-pots were used to measure mid-span deflections at the nine 10ft x 10ft bays. The three other wire-pots were used to measure deflections at the center of the overhang bays. The locations for the wire-pots are provided in Figure 24. A calibration was performed with both pressure transducers to determine the force in the 25-ton actuators. One pressure transducer was in the hydraulic system that applied load to the three overhang bays. The other pressure transducer was in the system that applied load to the nine standard bays. The pressure

transducers allowed for real-time monitoring of the loads applied to the slab through the whiffle tree. LVDTs were used to measure the deflection of the portal frame (see Section 3.3.9), which the wirepots were attached to.

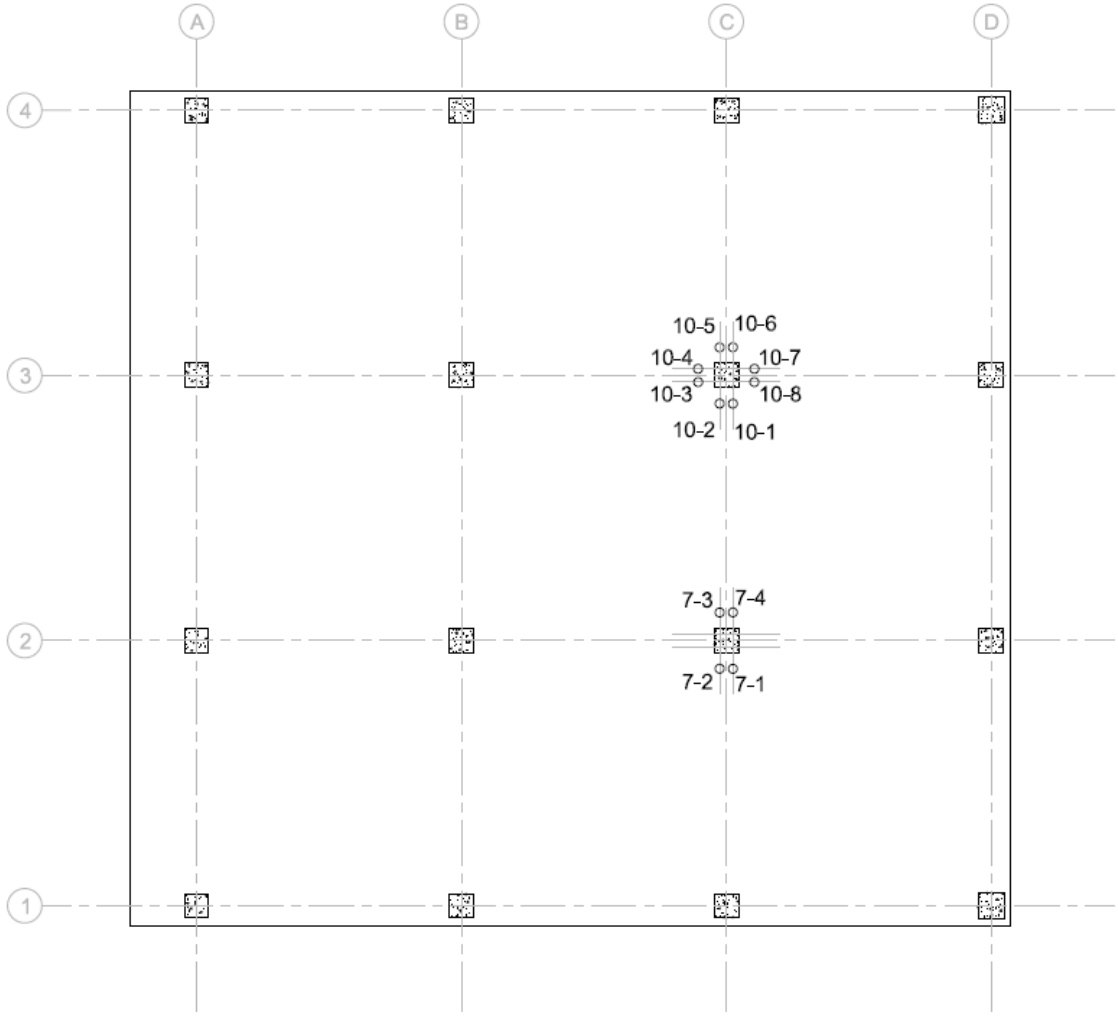

Figure 23. Foil Strain Gauge Layout

Table 6. Foil Strain Gauge Locations

Gauge ID	Elevation of Rebar (in.)	Approximate Distance from Column Face (in.)	Distance from Tendon Centerline (in.)
7-1	2.125	2.5	2.250
7-2	2.0625	3.25	3.125
7-3	2.500	3.125	2.875
7-4	2.3125	3.75	2.375
10-1	2.250	5.25	2.625
10-2	2.250	5.75	2.875
10-3	2.1875	4.625	3.375
10-4	2.3125	4.625	3.000
10-5	2.375	5.125	2.500
10-6	2.3125	5.25	2.500
10-7	2.250	4.375	3.125
10-8	2.1875	4.5	2.875

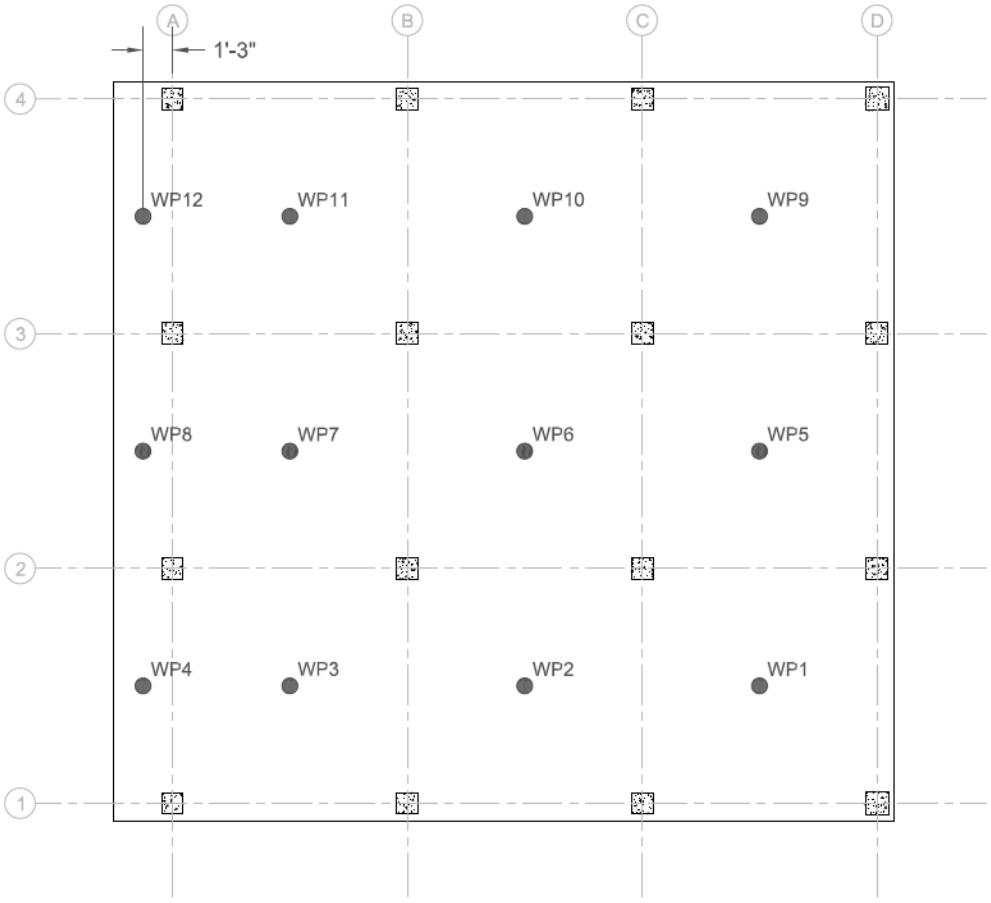

Figure 24. Wirepot Layout

Wiring diagrams for both the CR5000 and the CR9000 are provided in Appendix D. Additionally, the program code for both data acquisition systems is also provided in Appendix D.

The Bridge Diagnostic Inc. strain gauges were attached to the top of the slab at the time of stressing and form removal. These strain gauges were then removed to cast the top portions of the stub columns. Prior to load testing the slab, the same 19 strain gauges were attached to the top of the slab, and they are shown in Figure 25. These strain gauges were concentric to the faces of the columns, where the highest strains in the slab were expected.

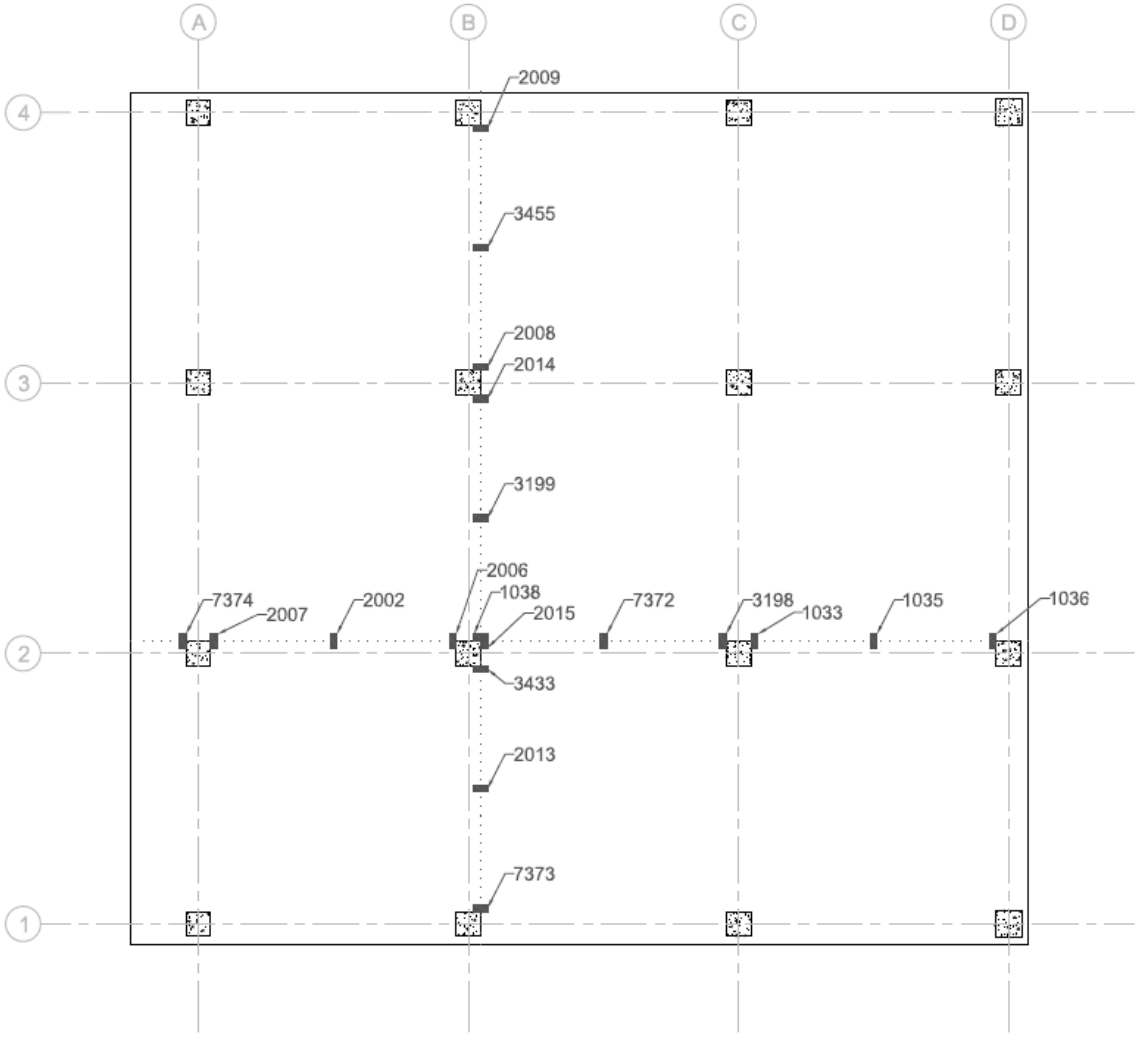

Figure 25. BDI Layout at Top Surface

Thirteen BDI strain gauges were also attached to the bottom surface of the slab. They were located in the midspan of the slab in both directions. The layout and

identifiers for these strain gauges are shown in Figure 26. All BDI strain gauges were connected wirelessly for data collection.

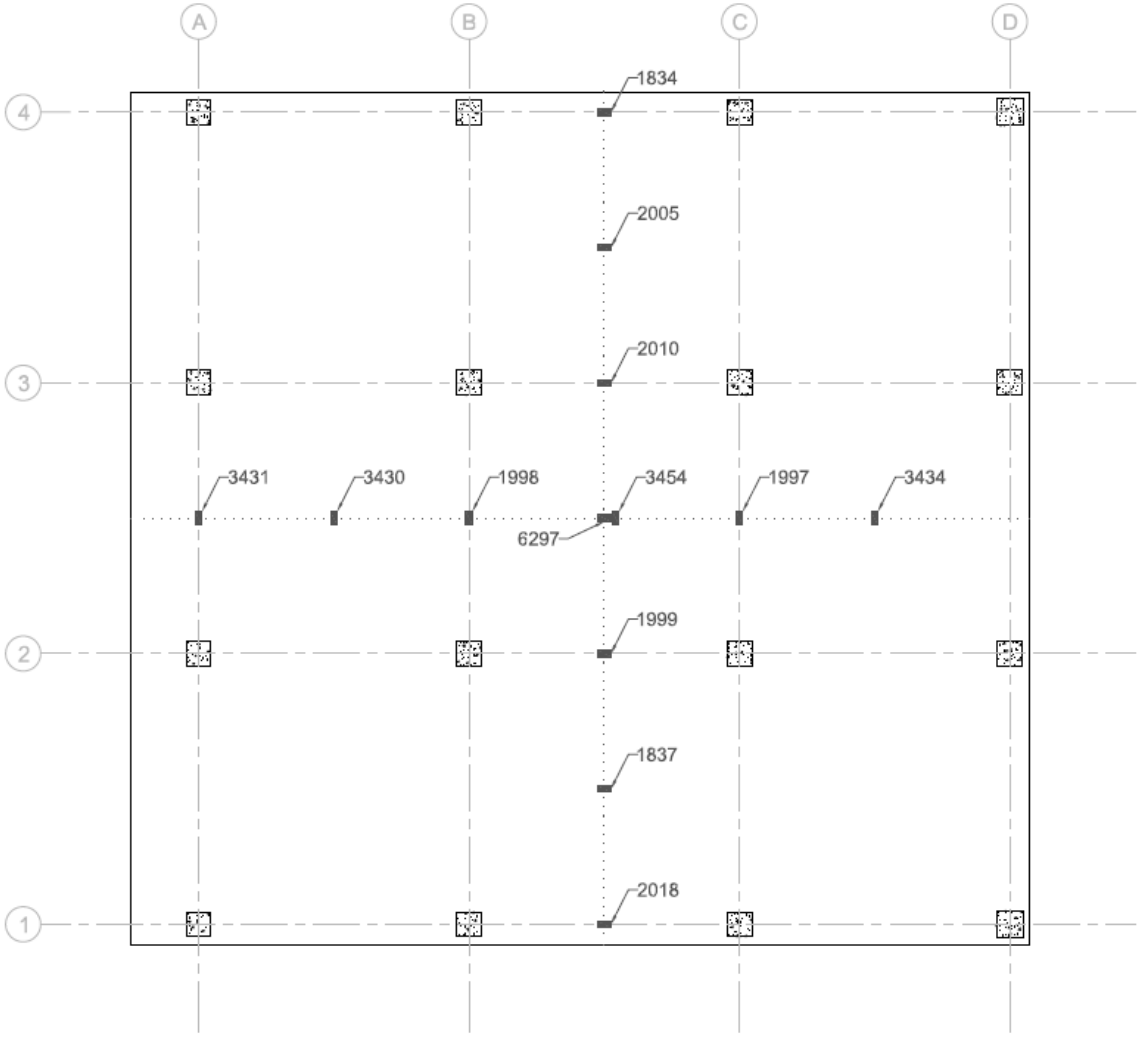

Figure 26. BDI Layout at Bottom Surface

3.3.7 Dead Load Compensation

Specimen 2 was a one-third scale model of the prototype flat plate. The prototype slab had a 9in. thickness, while Specimen 2 had a 3in. thickness. Six inches of concrete needed to be compensated for Specimen 2 to have the same loading as the prototype specimen. The whiffle tree was estimated to provide approximately 10.5psf of dead load compensation. The remaining 62psf of required dead load compensation was reached using masonry blocks. Solid masonry blocks were placed on the slab's surface to account for this loading. The blocks were placed on the flat plate once the concrete had obtained a firm set. The blocks were distributed in a manner that would mimic a

uniformly distributed load, while avoiding the whiffle tree. For the standard 10ft x 10ft bays, 12in. x 12in. x 8in. nominal solid masonry blocks were used. These blocks weighed approximately 80 pounds each. Figure 27 shows the layout of the blocks for the typical bays. Seventy-seven blocks were used on the standard 10ft x10ft bays.

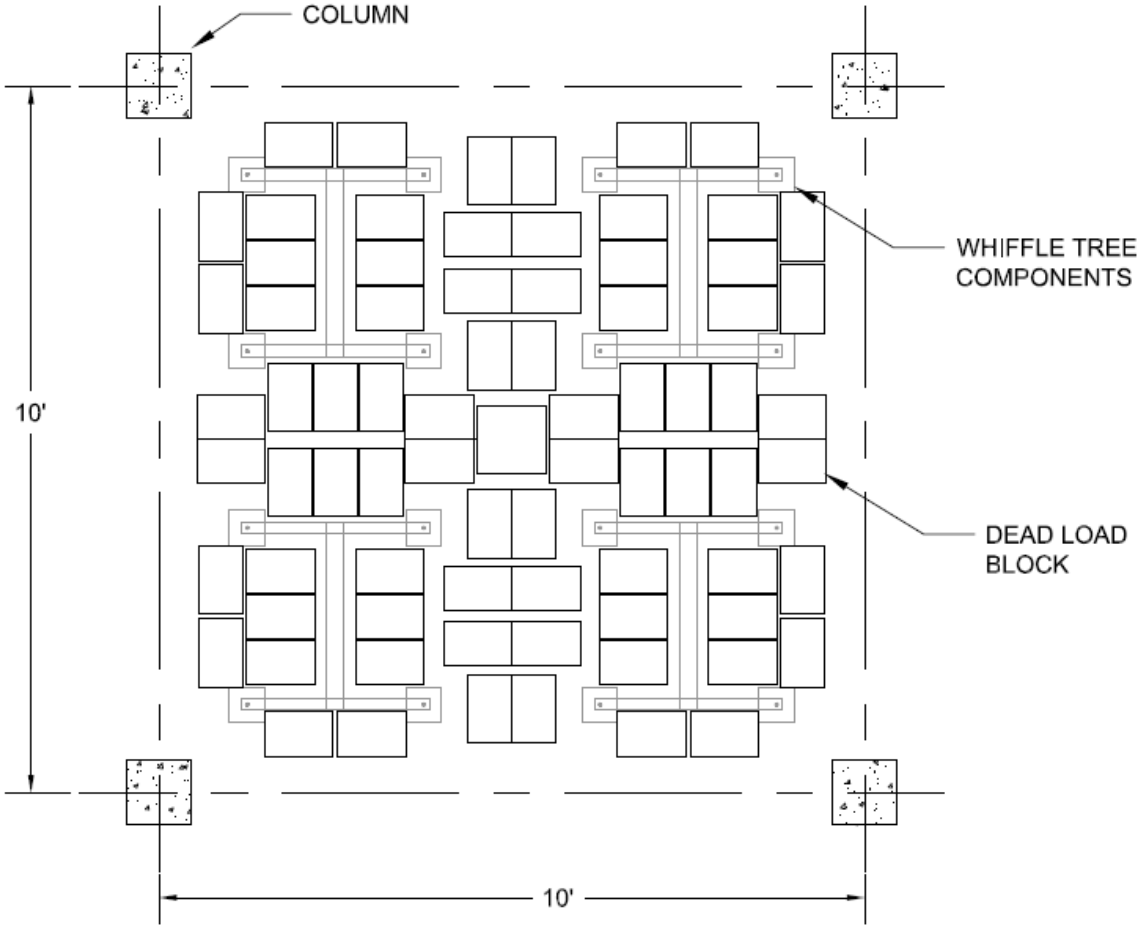

Figure 27. Dead Load Compensation Blocks Layout for Standard Bay

For the overhang bays, the whiffle tree provided approximately 12.25 psf of the dead load compensation. The remaining 60.25psf of dead load compensation was obtained with solid masonry blocks. A total of 25 16in. x 8in. x 8in. (nominal) blocks were used on each of the overhang bays. These blocks weighed approximately 60 pounds each. The layout of the blocks on the overhang bays is shown below in Figure 28.

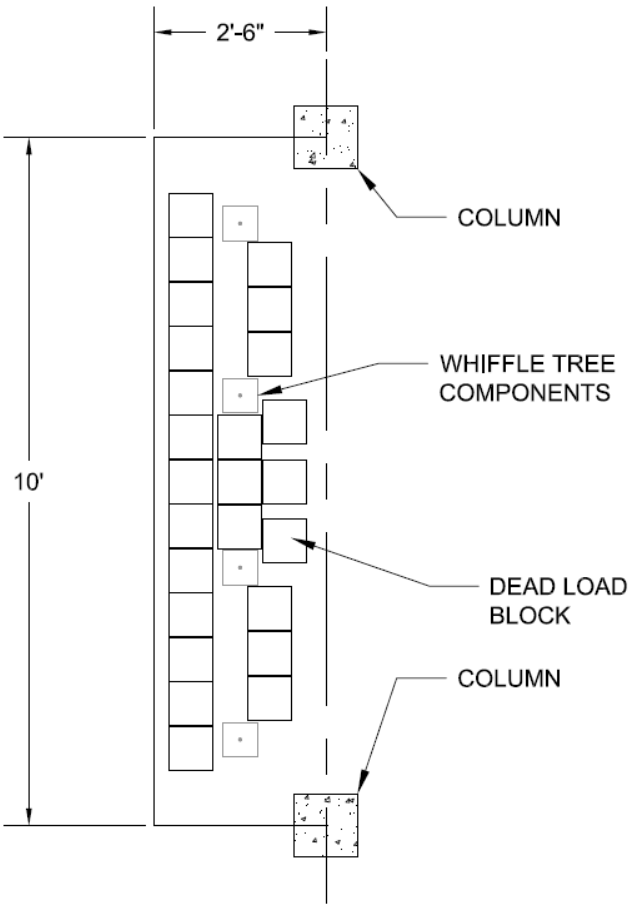

Figure 28. Dead Load Compensation Blocks Layout for Overhang Bay

When designing the layout of the dead load compensation blocks, it was determined that as long as the masonry blocks were distributed relatively evenly across the bay, the resulting moments on the slab would resemble a uniformly distributed load (Inerkar, 2018). Care was also taken to avoid covering potential crack locations. From research included in the literature review, it was determined that cracking on top of the slab in the negative moment regions would likely occur either through the centerlines of the columns or across the slab at the column faces (Hemakom, 1975), (Kosut et al., 1985), (Scordelis et al., 1959). Thus, blocks were mostly restricted from areas between adjacent columns, so that critical cracks forming yield lines could be observed during the testing of Specimen 2.

3.3.8 Stressing Operation

Prior to stressing the tendons, the dead load compensation blocks were placed as described in the previous section. The design requirements allowed for the tendons to be

stressed after the concrete achieved a compressive strength of 3000psi. Actual stressing began once the concrete had a strength of 6750 psi.

A stressing chair was designed and built for Specimen 2. Its design is shown in Figure 29. The stressing chair had small compression members so that it could fit in between the strands in the banded direction. Spanning all five tendons would have required the flexural member (the HSS 3x2.5x1/4in.) to be much larger due to a higher bending moment.

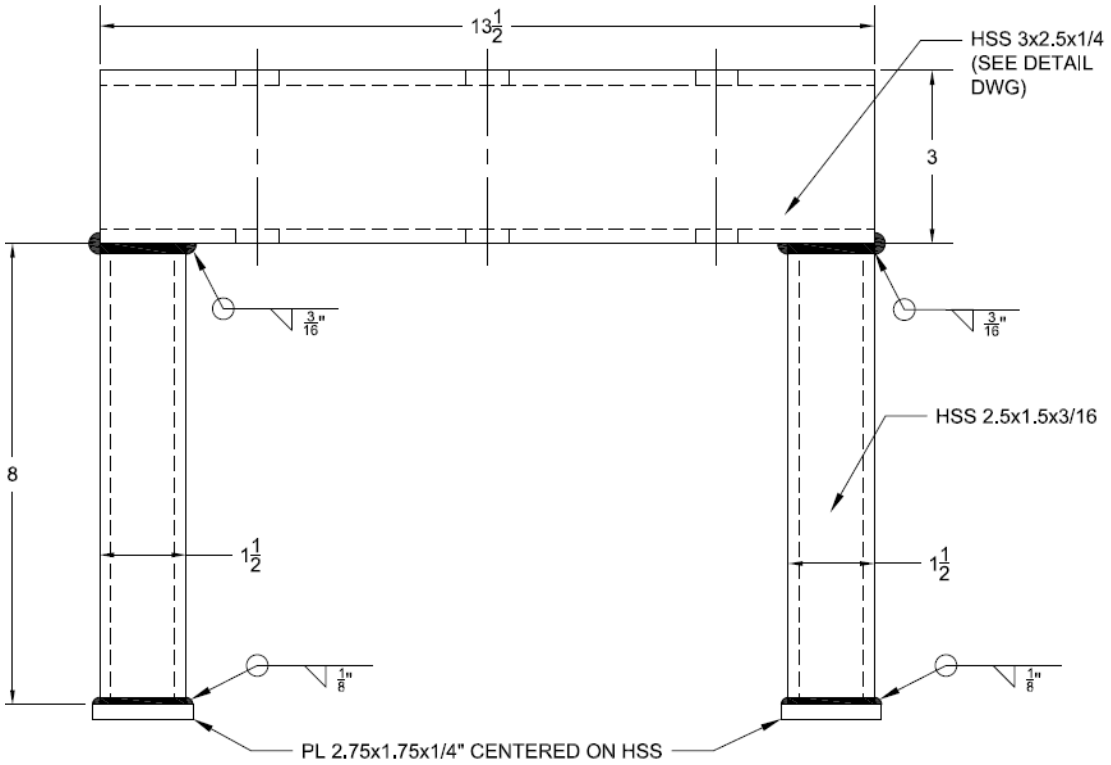

Figure 29. Stressing Chair

The jacking force for the banded tendons was 10.79 kips, while the jacking force for the uniform tendons was 10.90 kips. The jacking force was monitored with a centerhole load cell, shown in Figure 30. This load cell was connected to a P-3500 Strain Indicator (by Vishay Measurements Group) and had been previously calibrated to establish the correlation between the reading and the actual load. Elongations were also measured to double check the load measurements provided by the strain indicator instrument.

Figure 30. Load Cell for Stressing Operation

There were two different stressing setups, depending on if the tendon would have two permanent load cells. Both setups are shown in Figure 31.

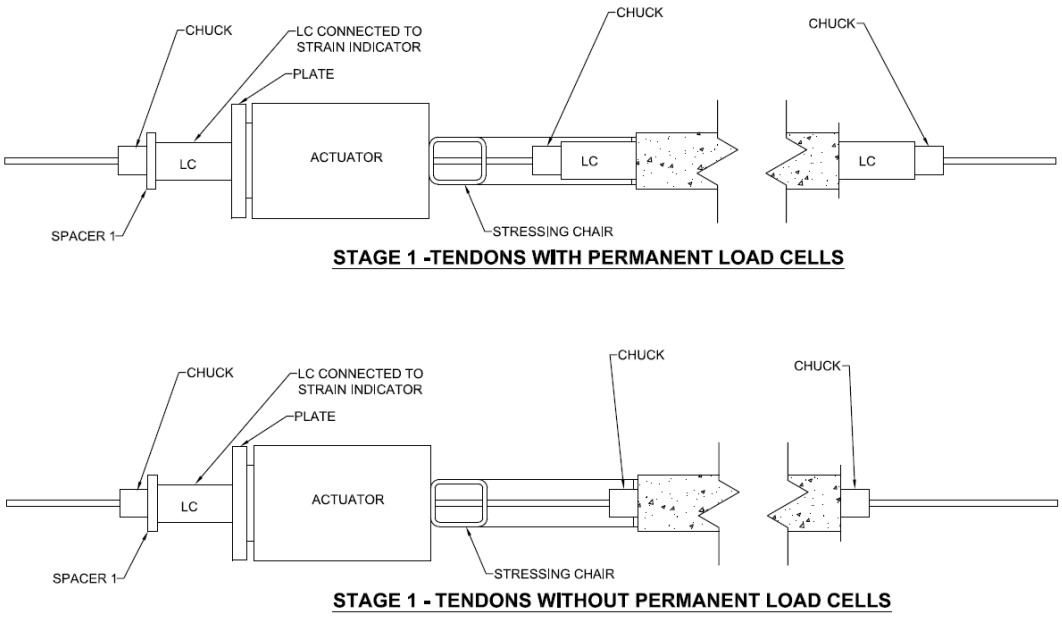

Figure 31. Stage 1 of the Stressing Operation for Specimen 2

To prepare for the stressing operation, the wedges in the chuck on the dead end of the slab were pushed into the chuck body as far as possible. Then the wedges in the chuck on the live end near the actuator were pushed in as far as possible. The load cell was balanced on the strain indicator instrument, and some initial load (approximately 1.5kips) was added to the system with the actuator to stiffen up the stressing assembly. As load was added, it was ensured that the actuator and load cell were concentric with the tendon. Once the initial load was added to the system, the wedges for the chuck body located within the stressing chair were pushed into the chuck body. The force in actuator was released. This procedure was performed to accommodate for the short stroke of the actuator.

The next stage of stressing the tendon began by adding a spacer between the plate and the load cell near the actuator. This new spacer, Spacer 2, is shown in Figure 32. Approximately 1.5 kips of load was applied by the actuator, and care was taken to ensure all of the stressing components remained concentric to the tendon.

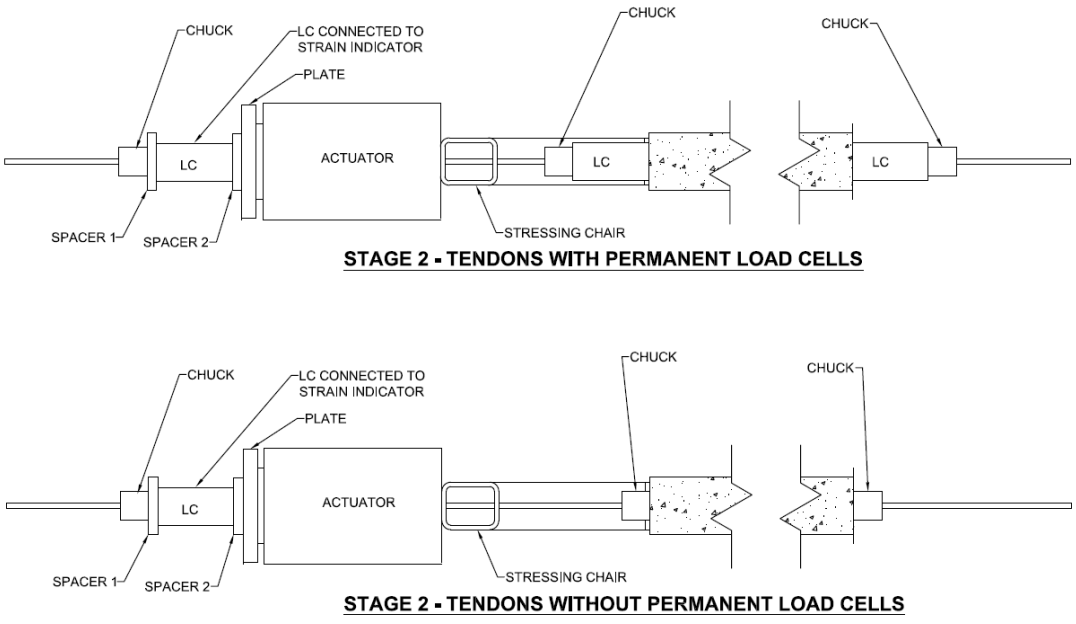

Figure 32. Stage 2 of the Stressing Operation for Specimen 2

The wedge seating distance for the dead-end wedge and the jacking wedge were measured and recorded, along with the readings for the load cell located at the actuator. Additionally, the piston extension was also recorded. These measurements are shown in Figure 33.

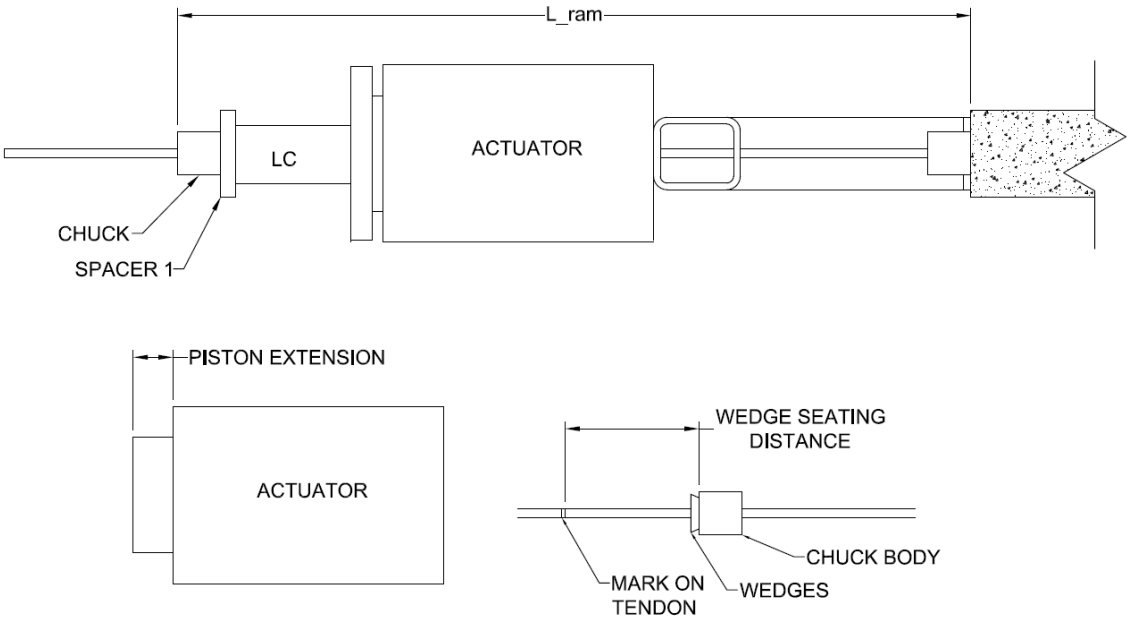

Figure 33. Stressing Elongation Measurements

Then, the load was increased to approximately 5 kips, and the piston extension and wedge seating distances for the dead-end wedge and the jacking wedge were recorded. The same procedure was used to increase the load to 8 kips.

Then, the load was increased to the final required load for each tendon. This was calculated considering the expected friction, wobble, and seating losses for the tendons. For the banded tendons, the actuator load was required to reach 10.79 kips. For the uniform tendons, the actuator load was taken to 10.90 kips. The piston extension and the wedge seating distances for the dead-end wedge and jacking wedge were recorded. The final actuator load was also recorded, and the predicted elongations were compared to the actual elongations.

The wedges were pushed into the live-end chuck that was located within the stressing chair. Then, the piston was retracted so that the load cell near the actuator showed a load of approximately 1 kip. Then, the piston extension was measured, which was used to calculate the actual seating losses for the tendon. Additionally, the seating loss was measured with a ruler. Then, all of the load was released from the system, and the next tendon was stressed.

All measurements for the loads, wedge seating distances, and piston extension were placed in a stressing spreadsheet. The stressing sheets, which were filled out for each tendon, are provided in Appendix E.

After the tendons in Specimen 2 were stressed, the forms were removed from beneath the flat plate to allow for the placement of the whiffle tree.

3.3.9 Whiffle Tree Design and Construction

A whiffle tree loading system was used on Specimen 2 to mimic a uniformly distributed load on the flat plate. Each individual bay, including the overhang bays, had a single actuator attached to a portal frame, which is shown in Figure 34. Twelve 25-ton single-action actuators were available in the lab and were used. The whiffle tree actuator is shown in Figure 35. The actuators had two threaded holes. Two bolts were used to attach the actuator to the bottom flange of the W6x15 of the portal frame. The lowest level of each whiffle tree ran under the portal frame and the attached actuator. The portal frames were attached to steel sections running across the lab's strong floor. The layout of the floor beams is shown in Figure 36.

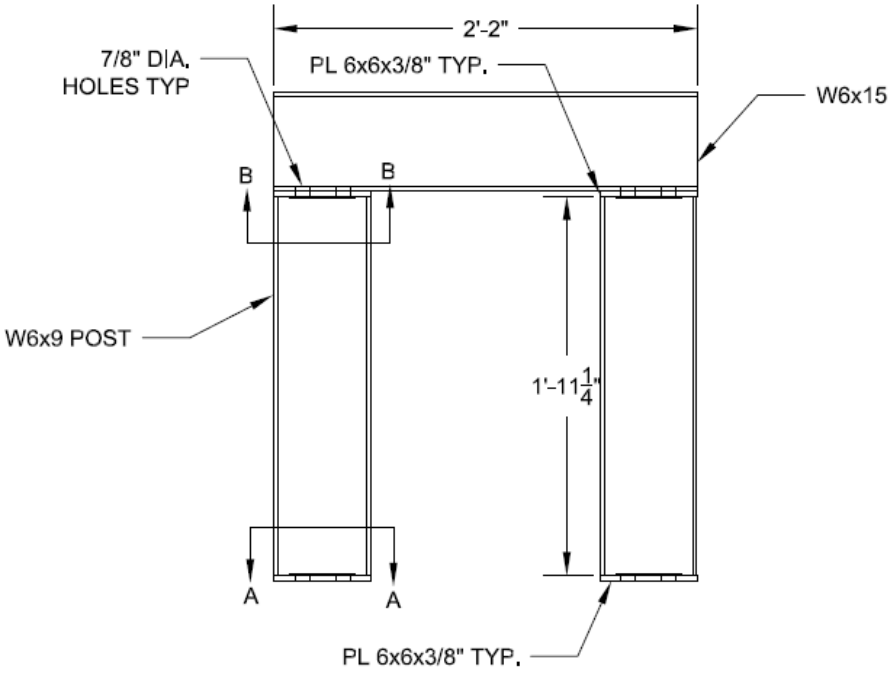

Figure 34. Portal Frame Design

Figure 35. Whiffle Tree Actuator

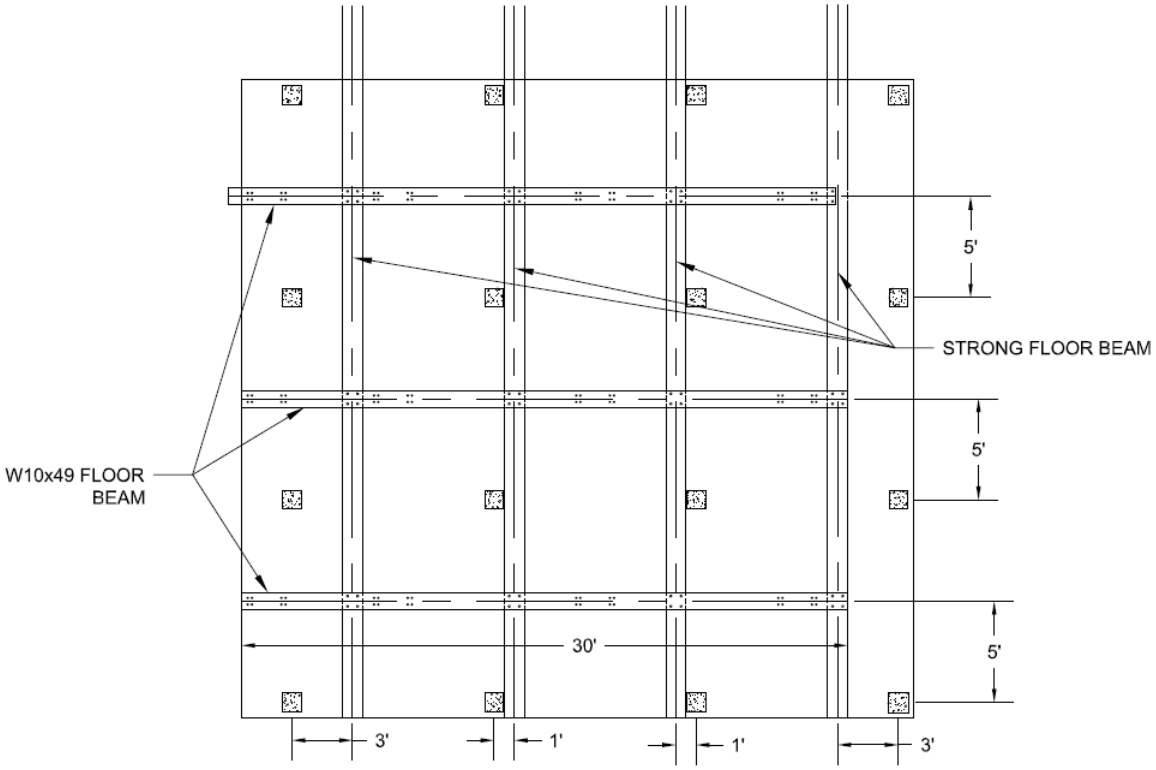

Figure 36. Steel Floor Beam Layout

At each standard 10ft x 10ft bay, a single actuator would be used along with the whiffle tree to apply sixteen even point loads to the bay. The whiffle tree design is shown in Figure 37.

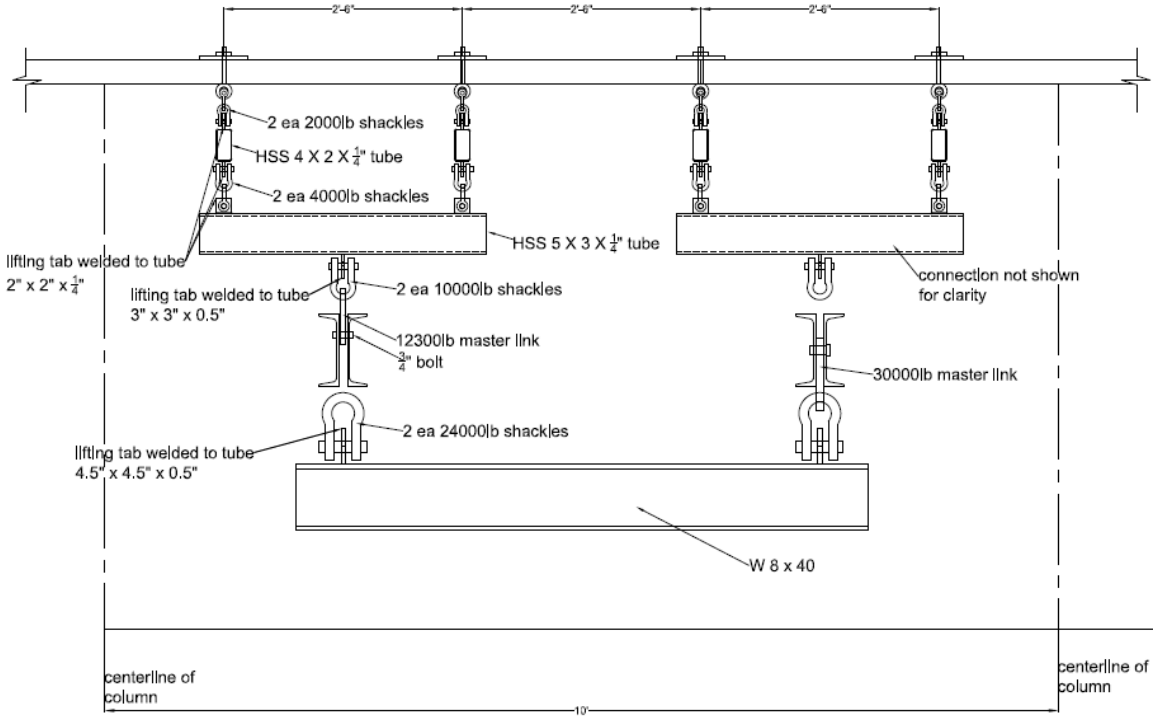

Figure 37. Standard Tension Whiffle Tree

For the standard whiffle tree, the lowest level consisted of a single W8x40 beam. 24,000lb-capacity shackles and 30000lb master links connected the W8x40 beam to the double channel sections. The double channel sections were then connected to the HSS 5x3x1/4in. sections with 10000lb shackles and 12300lb master links. The HSS 5x3x1/4in. sections were connected to the top level of the whiffle tree, the HSS 4x2x1/4in., with 4000lb-capacity shackles. To connect the whiffle tree to the flat plate, eyebolts ran through the flat plate and were connected to the HSS 4x2x1/4in. sections with 2000lb-capacity shackles. 6x6x3/8in. bearing plates were provided on the top of the flat plate at each eyebolt location.

Near column D4 (see Figure 22 for column designation), a reaction block from another project extended under Specimen 2. To avoid the reaction block, the whiffle tree design at this bay was redesigned and is shown in Figure 38. The two highest levels of the whiffle tree were moved above the flat plate and became a compression whiffle tree.

The double channel section moved above the reaction block but remained below the flat plate. Threaded rods were used to connect the W8x40 to the double channel sections. Similarly, threaded rods were used to connect the double channel sections to the HSS 5x3x1/4 sections. Three additional plates were welded to the double channels to allow for the connection of the threaded rods. At the compression whiffle tree, bearing pads were used to allow for rotation of the steel sections. Also, small angles (L2x2) were tack welded to the HSS 4x2x1/4 and to the bearing plates (6in. x 6in. x 3/8in.). These angles were included in the design of the compression whiffle tree to laterally brace the components to prevent any instability.

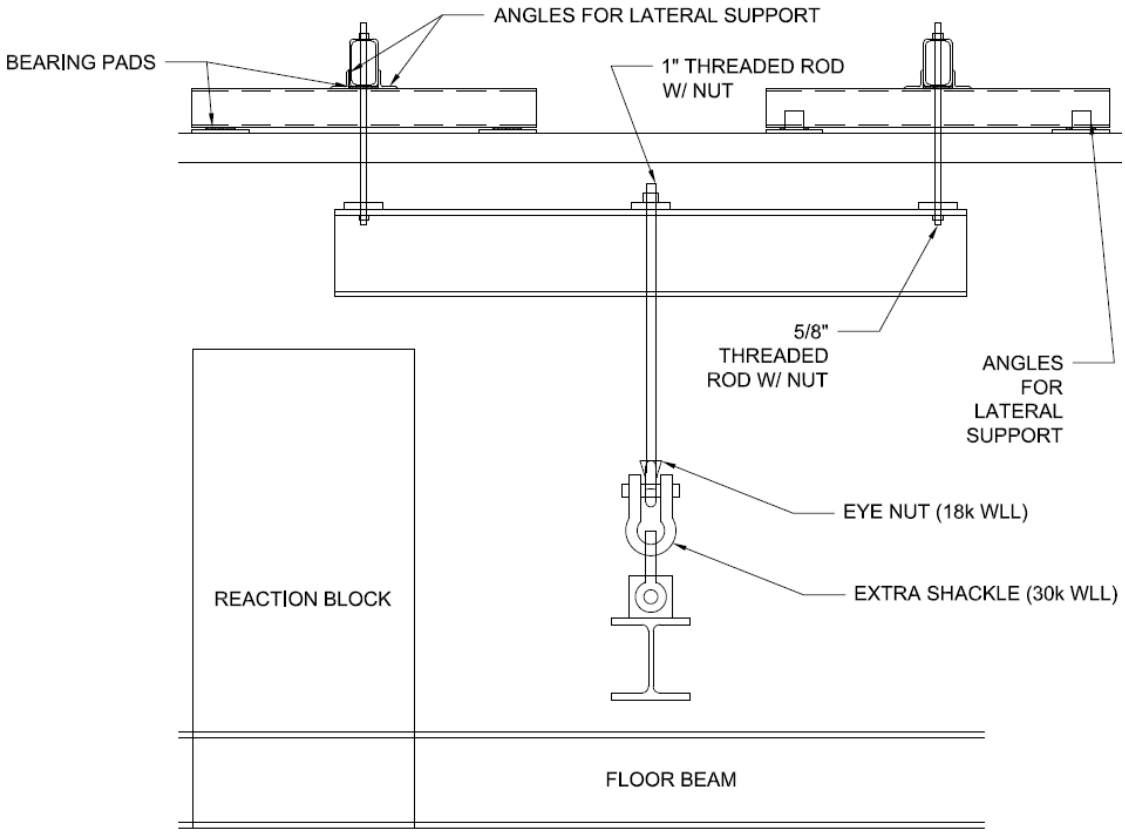

Figure 38. Reaction Block Whiffle Tree

At each of the overhang bays, a single actuator was paired with a whiffle tree to put four point loads on the overhang. The design of this whiffle tree is shown in Figure 39. A W8x40 was located under the actuator, and threaded rods connected the W8x40 to two HSS 4x2x1/4 sections under the flat plate. Eyebolts allowed the steel sections to hang from the flat plate, and the standard steel bearing plate (6in. x 6in. x 3/8in.) sat on top of the flat plate.

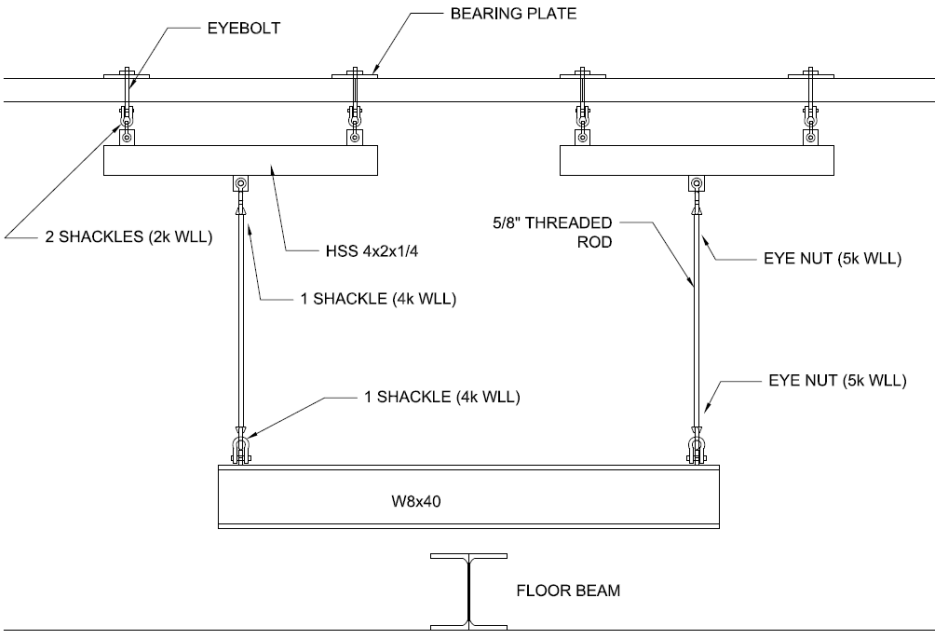

Figure 39. Overhang Whiffle Tree

3.3.10 Testing Procedure

Testing began in the afternoon on May 9, 2019. Increments of 5psf were applied to Specimen 2, with a minimum of five minutes in between each loading increment. The maximum applied load on May 9th reached 15psf. Cracks were marked on the slab, and the characteristic and average crack width for each crack was recorded at each load increment. At the end of the workday, the pressure was fully released from the actuators.

On May 10, 2019, the instruments began recording data with no applied load on the slab, and 5psf of load was applied to the slab. Then, load was applied in 10psf increments until the applied service load of approximately 74psf was reached. Then, the slab was completely unloaded. After this, load was applied in 20psf increments, until an applied load of 60psf was reached. The next applied load was 70psf, followed by 75psf and 80psf. The slab was then unloaded, and the program for the data acquisition system was modified, since it was unable to display actuator loads that were greater than 7999lbs. Once the program was fixed, loads were applied in 20psf increments, until 80psf of applied load was reached. The next loading step was 85psf of applied load. The slab was then unloaded at the end of the day.

Testing restarted on May 15, 2019 with a few changes. One leaking actuator was replaced with a newly calibrated actuator. Also, the wirepots were switched to the CR5000 data acquisition system and were recalibrated. Load was applied in 20psf increments up to 80psf. Then 85psf was applied to the slab, and then the slab was completely unloaded. Load was again applied in 20psf increments up to 80psf. Then, load was applied in 5psf increments until 110psf of applied load was reached. The slab was then unloaded for a second time. The slab was then loaded in 20psf increments up to 100psf. Then, a 110psf applied load was reached. At this point, load was applied in 5psf increments until 155psf of applied load was reached. After this, deflections began to increase significantly, so deflections were monitored carefully, and an additional 5psf was applied to the slab. After 160psf of applied load, another 5psf of applied load was added to the slab. Then, three increments of load were applied, until approximately 170psf of load was reached. Then, the slab was completely unloaded.

On May 16, 2019, load was applied in 20psf increments until 60psf of applied load was reached. At this point, one of the actuators began leaking, so the slab was unloaded, and the leaky actuator was switched out with a previously calibrated actuator. Then, load was applied in 20psf increments, until 160psf of applied load was reached. Since the applied load dropped while waiting to apply more load, the next load step involved bring the applied load back to 160psf. Then 165psf of applied load was reached. After this, load was applied in small increments, while monitoring the deflections. The final applied load that was reached was 175psf. At this point, the deflections were larger than 2in., and failure seemed imminent. For safety concerns, the slab was unloaded. Post-loading observations showed that concrete crushing occurred on the top of the slab. A plot of the load history through the four days of testing is provided in Figure 40.

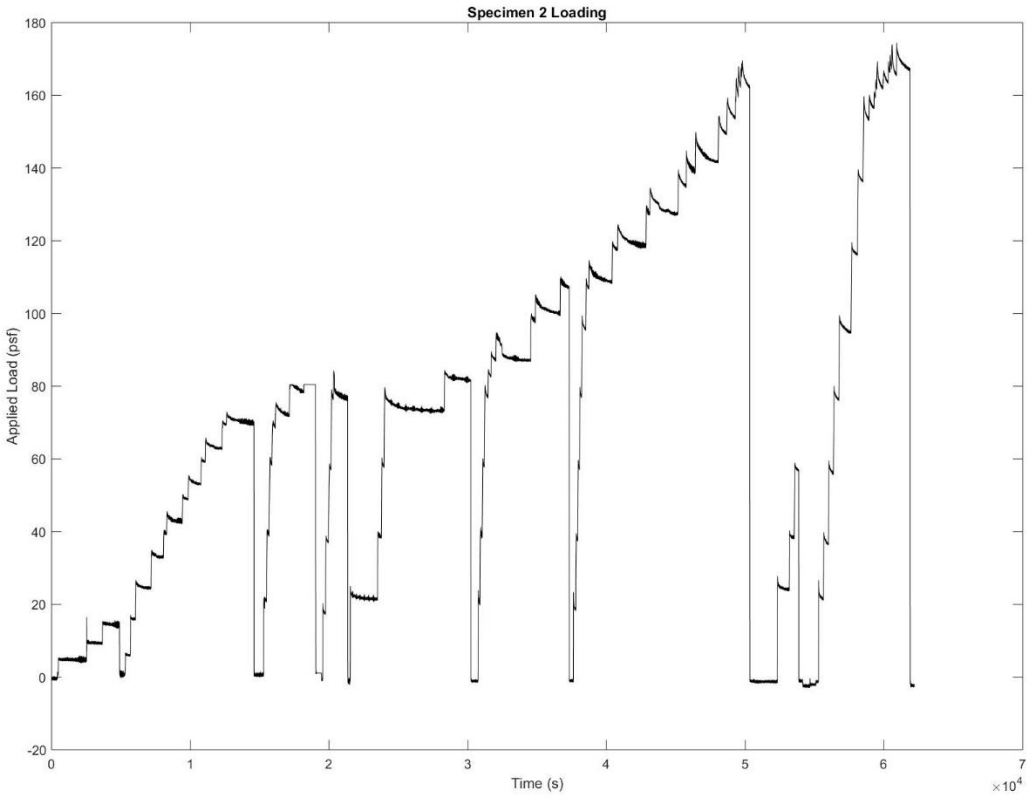

Figure 40. Load History

Chapter 4 - Results

4.1 Stressing Results

Tendon stressing was completed on April 16, 2019. The stressing sheets, which are provided in Appendix E were computed using friction and wobble coefficients determined from the trial slab testing. The friction coefficient was 0.12, and the wobble coefficient was 0.0009/ft.

4.1.1 Average Tendon Force

The average measured tendon elongation was 5.4 percent lower than the expected elongations. The likely cause for this issue was a larger amount of friction for the tendons in Specimen 2. The trial slab tendons likely had a smaller coefficient of friction, potentially due to differences in installing the tendons. To determine a corrected coefficient of friction for the tendons, for each tendon, the friction coefficient was changed so that the expected elongation was equal to the actual elongation at the end of stressing the tendon. The wobble coefficient was held at the same value from the trial slab testing. This procedure was completed for the thirty-three tendons. Some tendons had incorrect wedge seating measurements, so these tendons were excluded from the friction coefficient analysis. An average friction coefficient was taken for the tendons with correct wedge seating measurements, and the new friction measurement was determined to be 0.378.

The average jacking force for the uniform tendons was 10.92 kips, and the average jacking force for the banded tendons was 10.72 kips. Measured seating losses were between 1/16 and 3/32 inches for tendons in both directions. Using the average jacking forces, average measured seating losses, and the corrected average friction coefficient for all of the tendons in each direction, the average tendon force for each direction was calculated. The tendon forces plotted across the length of the slab are provided in Figures 41 and 42. These plots represent an average condition for each direction of tendons – not forces present on an individual tendon.

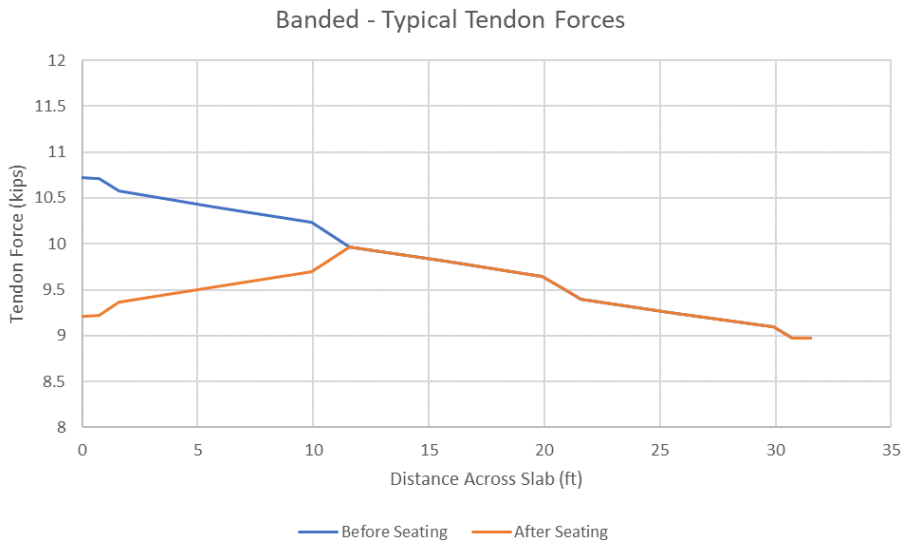

Figure 41. Typical Banded Tendon Forces at Stressing

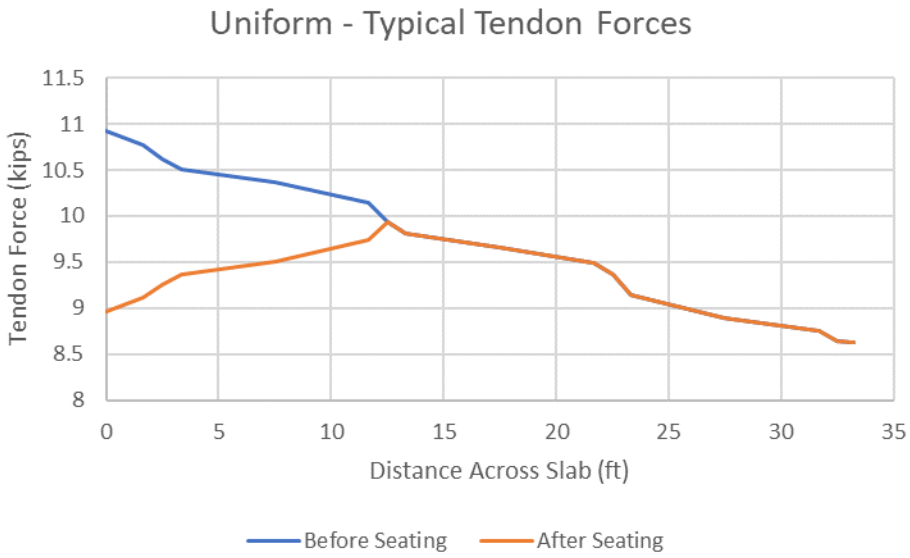

Figure 42. Typical Uniform Tendon Forces at Stressing

The average banded tendon force at the time of stressing was calculated to be 9.50kip, and the averaged uniform tendon force was 9.34kip. The assumed design tendon force for both directions was originally 10kip before time-dependent prestress losses.

4.1.2. Stresses and Strains After Stressing

BDI strain gauges were used to monitor strains in two directions along two critical column lines (column lines 2 and B). The BDI strain gauges were located in a line across the slab that was in line with the column faces where the highest expected

strains were expected to occur at the top of the slab once vertical loads were applied to the slab. The recorded strains for the BDI gauges along column line 2 after stressing are provided in Figure 43. This cross section is looking toward gridline 1. The strains for column line B are provided in Figure 44. This cross section of the slab is looking toward the overhang. In both graphs, the expected strains due to the prestress axial forces into the slab are shown.

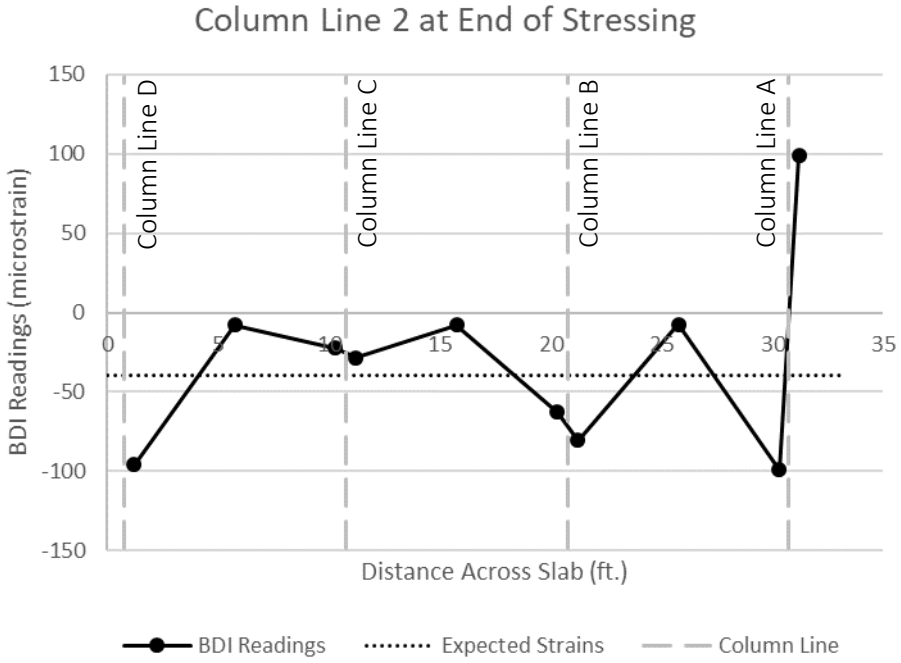

Figure 43. Strains Along Column Line 2 at End of Stressing

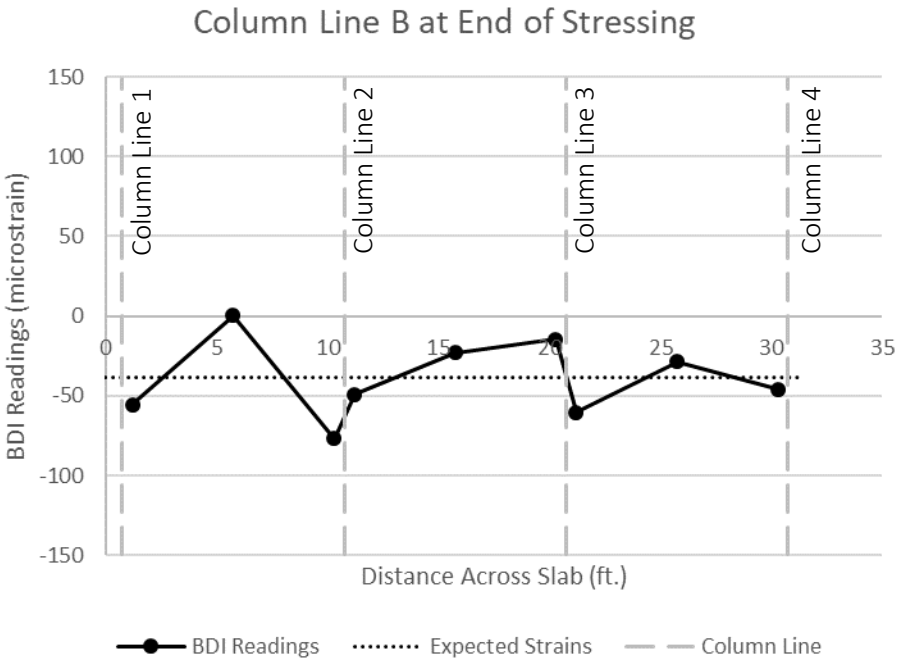

Figure 44. Strains Along Column Line B at End of Stressing

The strains in the midspan regions for both cross sections are higher than the anticipated strains due to pure axial force. This is potentially due to strains caused from bending, as the prestress force in the draped tendons will provide uniform vertical loading for each parabolic drape.

4.1.3 Stresses and Strains After Form Removal

The specimen loading at the time of stressing is provided in Table 7. These loads are slightly different than the design loads, since the concrete self-weight and the weight of the dead load blocks and whiffle tree were slightly different than their predicted values.

Table 7. Specimen 2 Loads at Stressing

Concrete Self Weight	
Concrete Density (pcf)	143
Concrete Self-Wt (psf)	35.7
Dead Load Compensation	
Large Block Weight (lbs)	80.9
Overhang Block Weight (lbs)	59.3
Average Dead Load Block Load (psf)	62.1
Whiffle Tree	
Overhang Whiffle Tree Weight (lbs)	310
Standard Whiffle Tree Weight (lbs)	1060
Average Whiffle Tree Load (psf)	10.7
Sum	
Total Load (psf)	109

The analysis performed by Jack Li assumed a friction coefficient of 0.12 (Li, 2019). Using the corrected friction coefficient, the actual concrete compressive strength, and the actual loads on the flat plate, the worst-case slab strip was re-analyzed to confirm that the slab was in conformance with ACI 318's stress requirements. The maximum tensile stress was calculated to be $2.15\sqrt{f'ci}$, which was less than the maximum allowable tensile stress of $3\sqrt{f'ci}$ (ACI, 2014). The term, $f'ci$, was the average compressive strength of the concrete that was tested at the time of stressing (see Appendix G). The uniform interior strip was the controlling analysis strip for the flat plate at the stressing stage. A plot of its stresses as a function of the square root of the average concrete compressive strength at the time of stressing is provided in Figure 45. This figure was created by using the equivalent frame method. The stresses shown on the plot are analytical, not experimental.

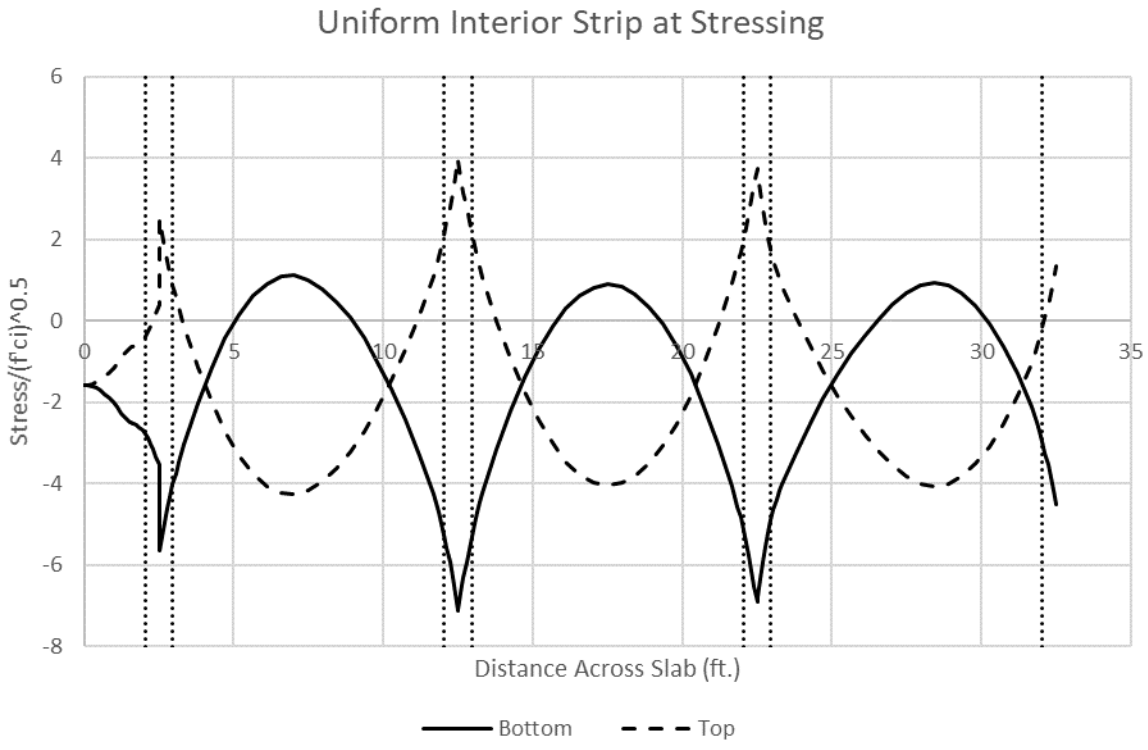

Figure 45. Stresses for Uniform Interior Strip at Stressing

The recorded strains for the BDI gauges along column line 2 of the slab after stressing and form removal are provided in Figure 46. This cross section is looking toward column line 1. The strains along column line B are provided in Figure 47. This cross section of the slab is looking toward the overhang. In both graphs, the expected strains, using the stresses obtained from the equivalent frame method and the concrete's modulus of elasticity are shown as well. At this point of strain recording, the whiffle tree for Specimen 2 was not installed, so the equivalent frame method analysis shown in these two figures did not include the whiffle tree self-weight.

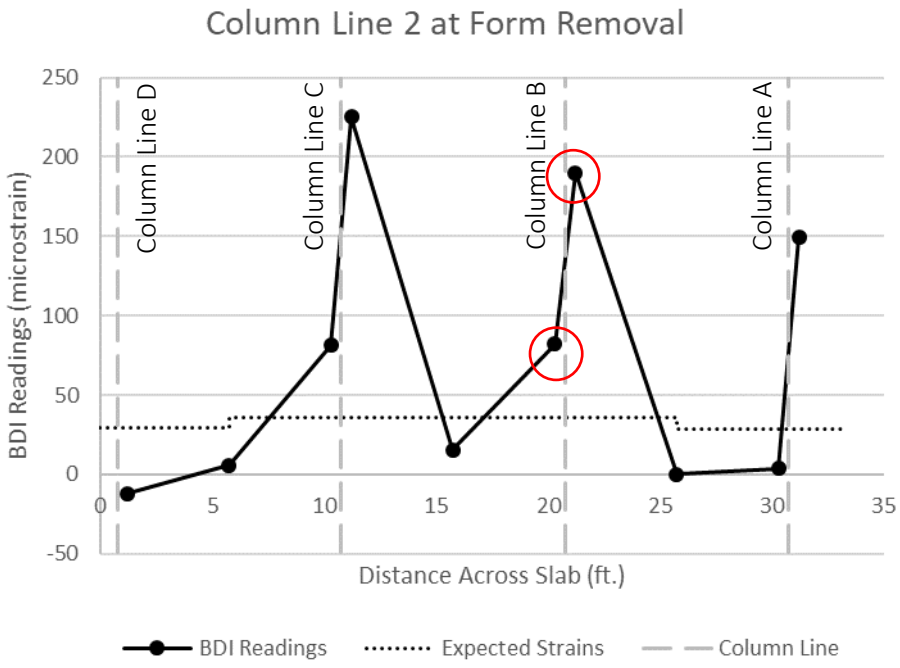

Figure 46. Strains Along Column Line 2 at Form Removal

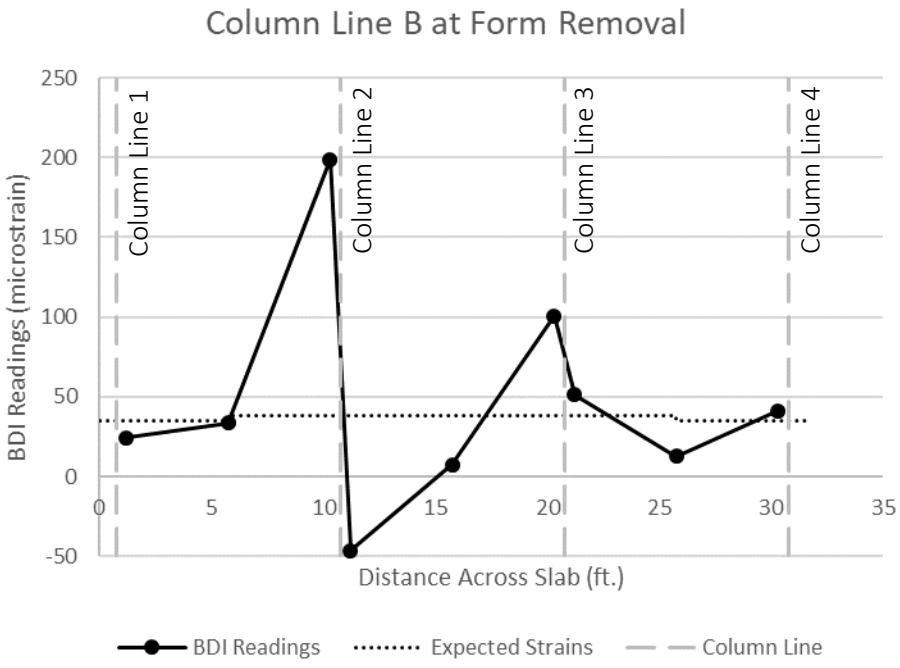

Figure 47. Strains Along Column Line B at Form Removal

The two circled readings in Figure 46 were at BDI strain gauges where cracks were observed running across the strain gauge. At these two locations, the recorded strain exceeded the expected strain, which would be expected. As can be seen in both Figure 46 and Figure 47, the recorded strains in the midspan were lower than the expected strains. At the column faces, the strains were mostly similar to or exceeded the expected strains from the equivalent frame method analysis.

4.1.4. Cracking After Stressing

As discussed in the previous section, two BDI strain gauges bridged cracks that appeared during the stressing and form removal operation. Cracks were observed at the four interior columns immediately after all of the tendons were stressed and the formwork's double 2x6s were lowered. At this point, the plywood panels were still attached to Specimen 2. Upon the complete removal of the formwork, some of the cracks grew in length. Also, a new small crack was observed at column B4. All crack widths at this point were hairline in nature (less than 0.005in., or 0.13mm). Column B2 had four observed cracks. Columns B3 and C3 each had three observed cracks. Column C2 only had two observed cracks at this point. A map of the cracks on the top surface of the post-tensioned flat plate is provided in Figure 48.

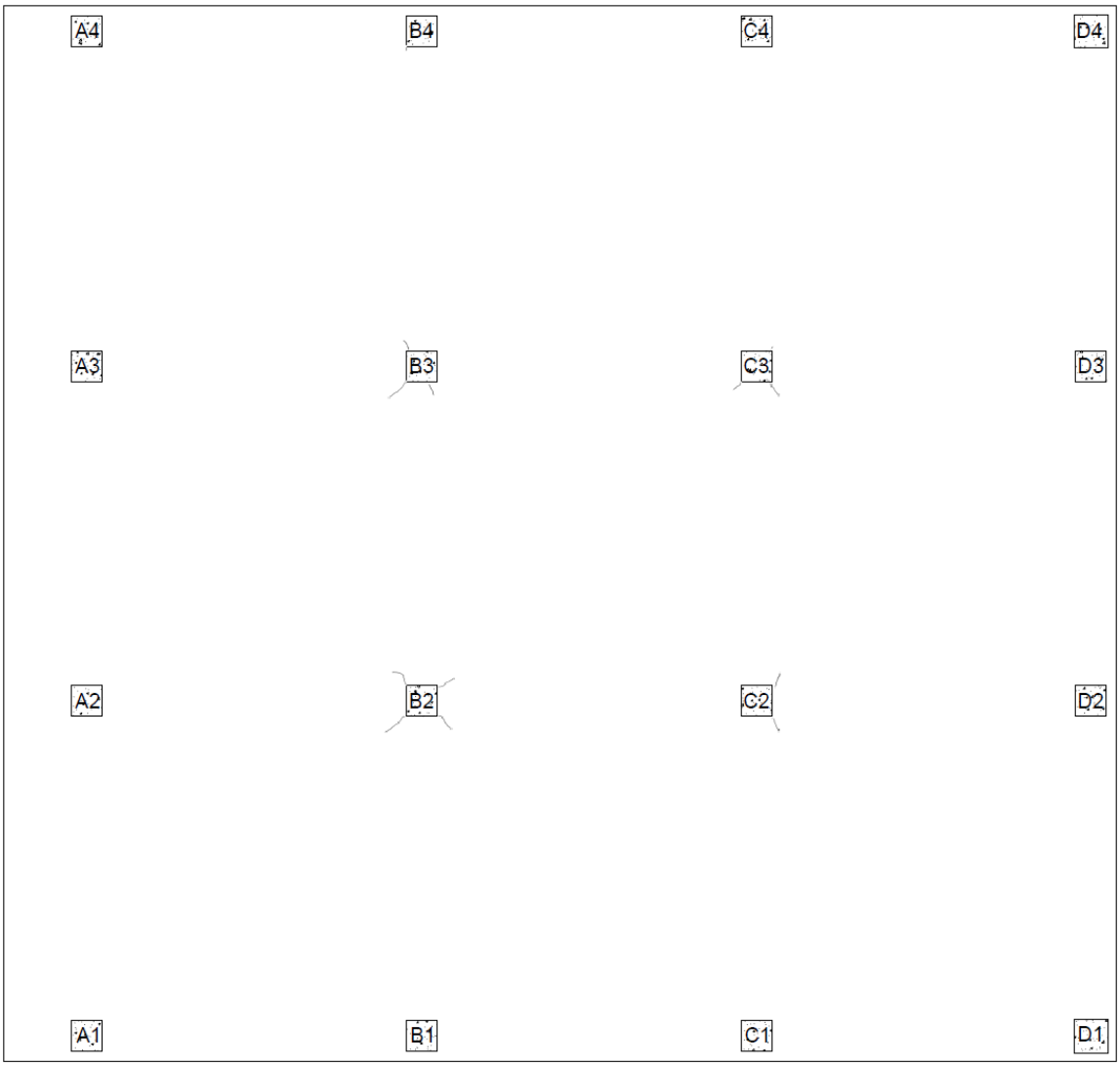

Figure 48. Cracking After Stressing and Form Removal

4.1.5. Deflections After Stressing

For convenience in recording deflection measurements, each 10ft x 10ft bay and overhang bay was assigned a label, which is shown in Figure 49.

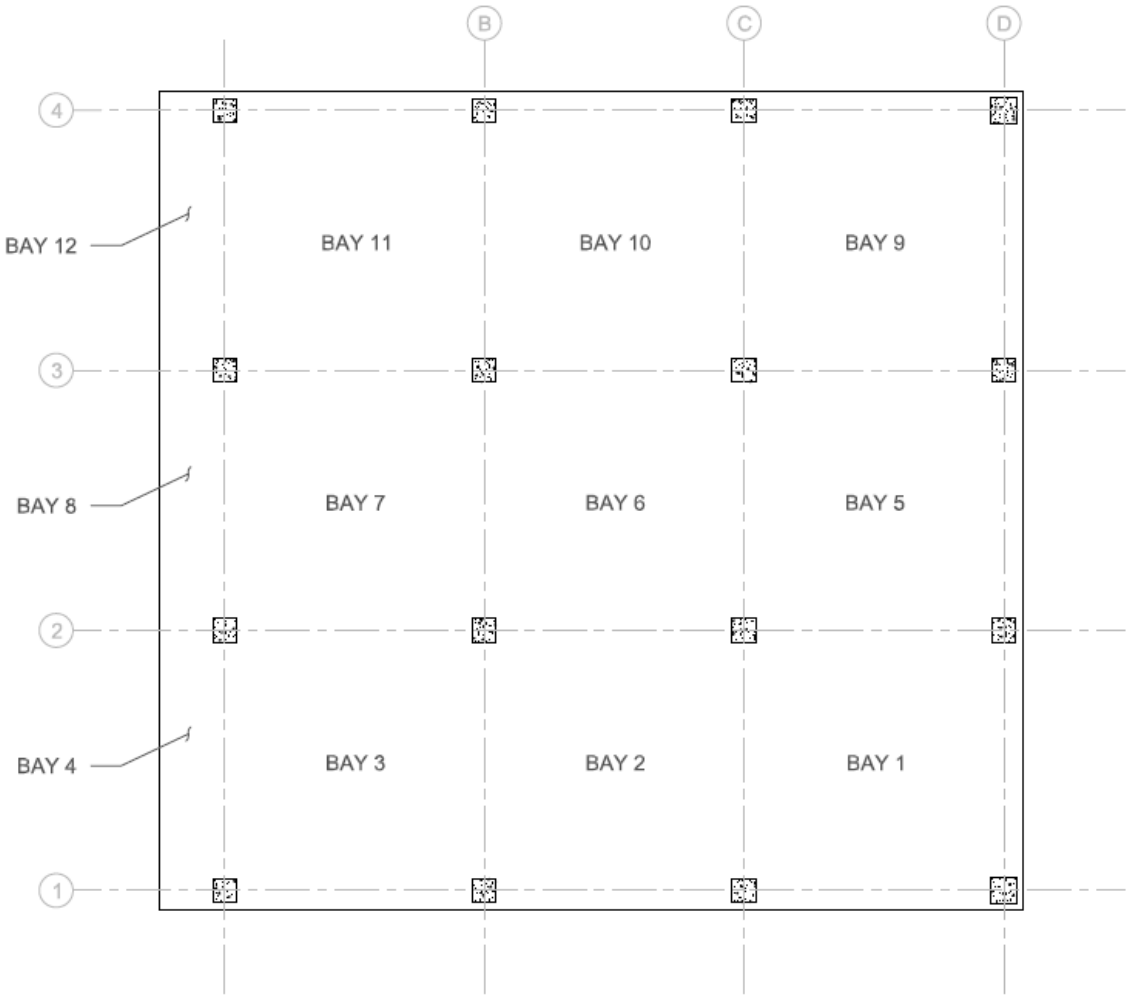

Figure 49. Grid and Bay Layout

The initial deflections were measured using a laser level mounted to a nearby steel column. Using a ruler that was placed at marked locations on Specimen 2, the deflection could be recorded at important times prior to the load testing of the slab. The laser level was used because the scaffolding and forms located below the slab prevented the use of wire potentiometers. At zero deflection, the dead load compensation blocks were in place and the slab had been stressed, but the slab was still fully supported by the shoring. The deflections were recorded after the formwork was lowered approximately two inches. Deflections were again recorded after the plywood formwork panels were detached and removed from Specimen 2. The initial deflection measurements are provided in Table 8.

Table 8. Initial Deflections Before Load Testing

Bay Number	Deflections After Forms Lowered (in.)	Deflections After Plywood Removed (in.)
Bay 1	1/8	1/8
Bay 2	1/16	1/16
Bay 3	1/8	1/8
Bay 4	1/16	1/16
Bay 5	1/8	1/8
Bay 6	1/8	1/8
Bay 7	1/8	1/8
Bay 8	0	0
Bay 9	3/16	3/16
Bay 10	1/8	1/8
Bay 11	3/16	3/16
Bay 12	0	0

4.2 Load Testing Results

4.2.1 Average Tendon Force

The four tendon load cells on Specimen 2's tendons were used after the stressing operation to determine long-term prestress losses. Figure 50 shows the decrease in tendon forces until the slab was load tested (please refer to Figure 19 for the load cell locations). The banded tendons experienced a 0.70kip loss, and the uniform tendons experienced a 0.67kip loss. The average banded tendon force at load testing was calculated to be 8.80kip, while the averaged uniform tendon force was calculated to be 8.67kip. The average prestress in the banded direction was 122psi, while the average prestress in the uniform direction was 120psi. Both values are below ACI minimums for prestressing, which requires an average prestress of 125psi (ACI, 2014).

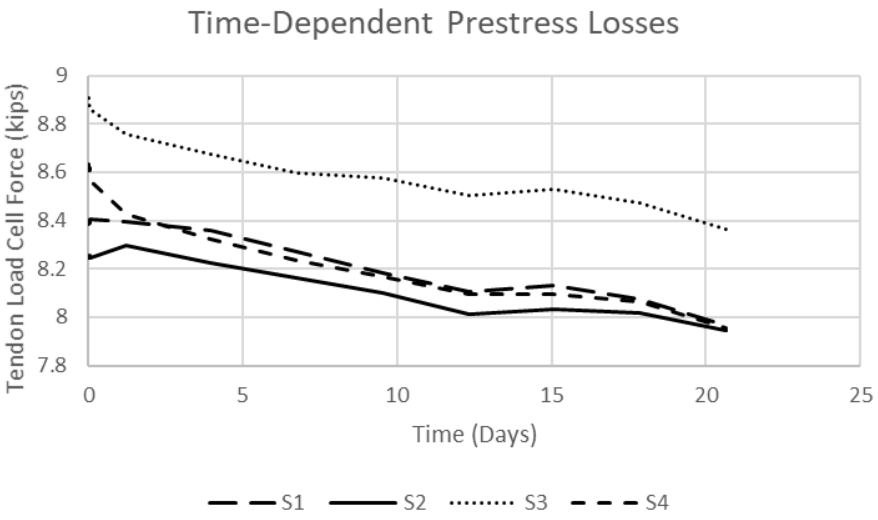

Figure 50. Time-Dependent Prestress Losses

The original design loads are included in Table 9. The equivalent frame method was used to determine if the slab with its as-built conditions (actual concrete strength and actual tendon forces) was compliant with ACI maximum allowable tensile stress limits. The uniform interior slab strip experienced the highest stresses. The stresses for this slab strip are shown in Figure 51. The largest tensile stress subject to the ACI limits occurred at the interior column's face, and it was less than $6\sqrt{f'c}$. The term, $f'c$, was the average compressive strength of the concrete that was tested at the time of load testing (see Appendix G). Thus, Specimen 2 met the maximum tensile stress limits prescribed by ACI 318 (ACI, 2014).

Table 9. Original Design Loads

Original Design Loads	
Self Weight (psf)	37.5
DL Compensation (psf)	72.5
SDL (psf)	20
Live Load - Reduced (psf)	24
Total (psf)	154

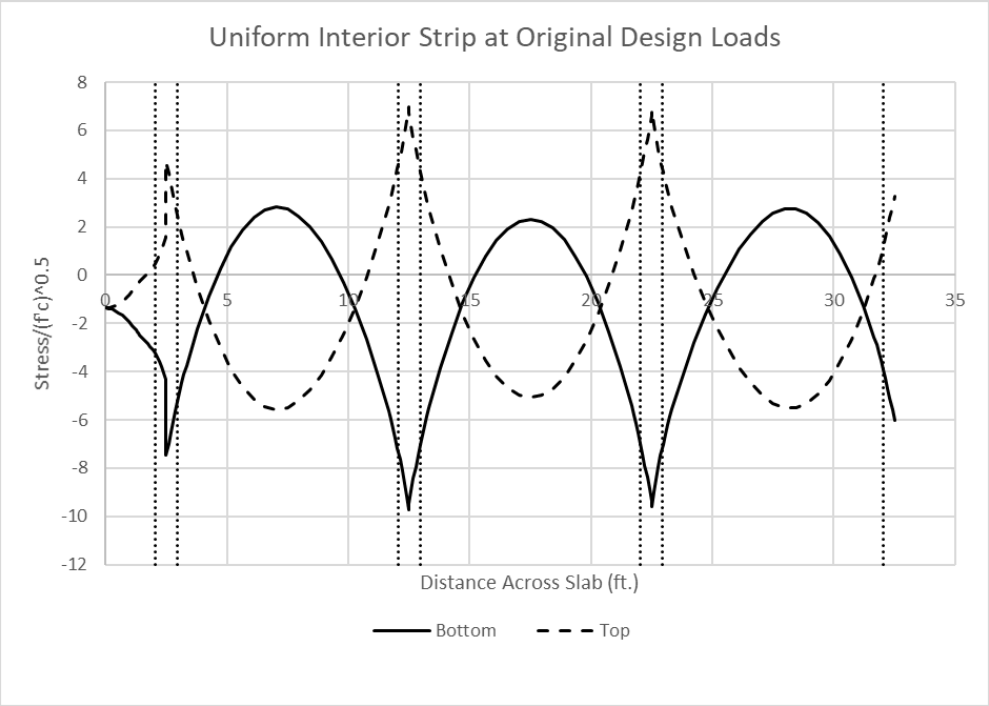

Figure 51. Uniform Interior Slab Strip at Original Design Loads

4.2.2 Performance Up to and At Service Level Loads

Due to higher than expected concrete strengths and lower tendon forces, the original design loads were adjusted to reflect the new conditions. The live load was increased to 52.8psf so that the maximum tensile stress in the equivalent frame method would be equal to $6\sqrt{f'c}$, which would represent a minimally designed post-tensioned flat plate (ACI, 2014). The updated service loads along with the required applied load to reach the service-level loading are shown in Table 10.

Table 10. Updated Service Loads

Updated Service Loads	
Self-Weight (psf)	35.1
DL Compensation (psf)	72.8
SDL (psf)	20.0
Live Load - Reduced (psf)	52.8
Total (psf)	181
Total Specimen Self Weight (psf)	108
Required Applied Load (psf)	72.8

The controlling slab strip at service was the banded interior strip. The stresses at service for the banded interior strip are shown in Figure 52. The tensile stresses are the

largest at the top surface of the slab at the interior column faces, which are indicated with the dotted lines. The analyses of the other strips at service are provided in Appendix F.

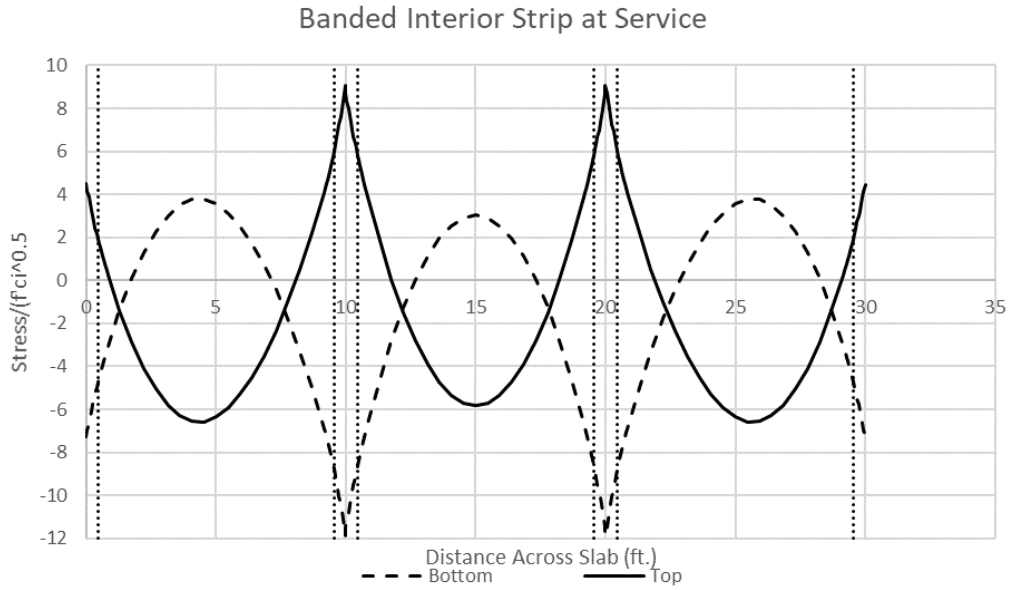

Figure 52. Banded Interior Strip at Service Loads

Loading the slab to service-level loads began on the second day of load testing. When load was applied to the slab, the load-deflection behavior of the slab was monitored in real-time. Figure 53 provides the load-deflection plot for Bays 1-4. Figure 54 provides the load-deflection plot for Bays 5-8, and Figure 55 provides the load-deflection plot for Bays 9-12.

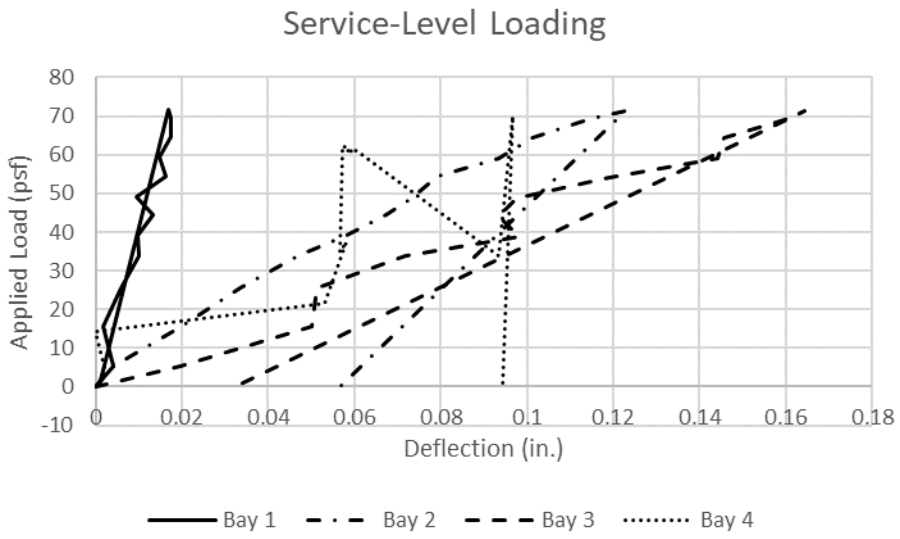

Figure 53. Load-Deflection at Service-Level Part 1

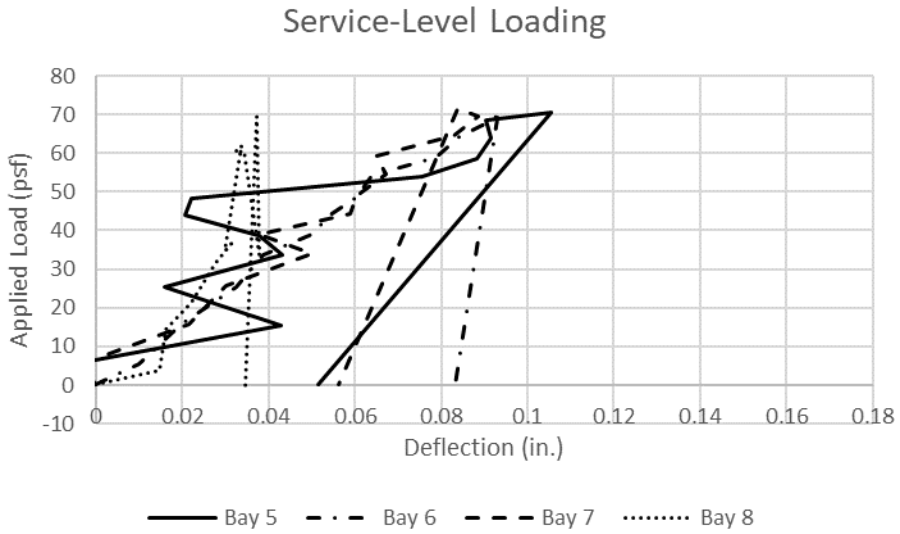

Figure 54. Load-Deflection at Service-Level Part 2

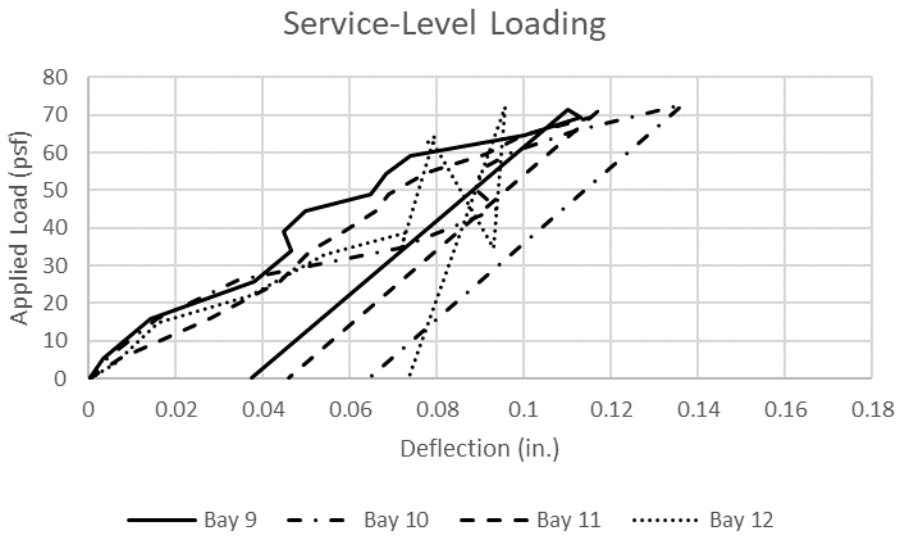

Figure 55. Load-Deflection at Service-Level Part 3

Each load-deflection plot had the same axis scaling to allow for comparison between the three sections of the slab, each running in the uniform tendon direction. The deflections in the middle section of the slab (Bays 5-8) were lower than the deflections for the two outer sections of the slab. The interior bays had more bending restraint on the edges of the bays due to the presence of surrounding bays. Thus, these bays are stiffer, leading to lower deflections.

The deflections recorded at this point were measured with the CR9000 data acquisition system, which gave fluctuating deflection readings (readings experienced fluctuations up to 0.02in.). To account for the fluctuations in readings, an average reading over seven seconds was taken to reduce the effects of the fluctuations. Many of the bays in the load-deflection plots seem to indicate a possible reduction in stiffness around after 60psf of applied load.

ACI 318 gives a deflection limit for live load deflection at L/360, which is equal to 0.33in. for the main bays (ACI, 2014). As can be seen in Figures 53 to 55, no bay deflection exceeded this limit. The overhangs cannot have deflections greater than 0.083in. Bay 4 and Bay 12 have larger deflections than 0.083 at service-level loads, but the service-level loads also include deflections due to superimposed dead loads. At the service-level stage, the superimposed dead loads account for approximately 26 percent of the applied load. The live loads only account for 74 percent of the applied load. When

the largest overhang deflection, at Bay 4, is proportionally adjusted, the deflection due to live loads became 0.073in., which is less than the maximum allowable deflection.

The BDI strain gauges provided strains at both the top surface of the slab and at the bottom surface of the slab. The strain gauges were zeroed just before applied loads were added, so the strains only represent strains that were caused by applied loading. The top surface strains along column line B looking towards the overhang are provided below in Figure 56.

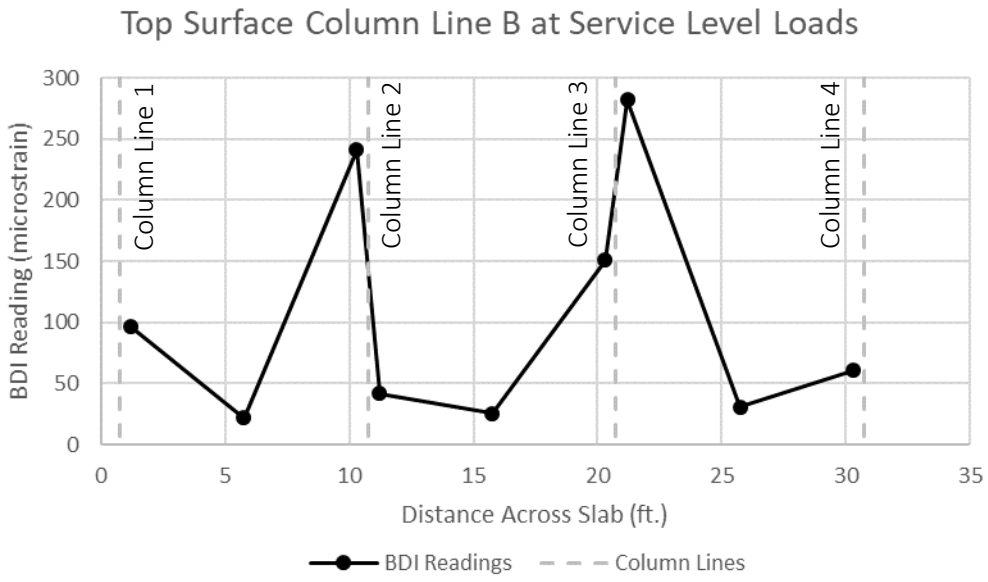

Figure 56. Top Surface Column Line B BDI Readings at Service

The top surface strains along column line 2 looking towards gridline 1 are provided below in Figure 57.

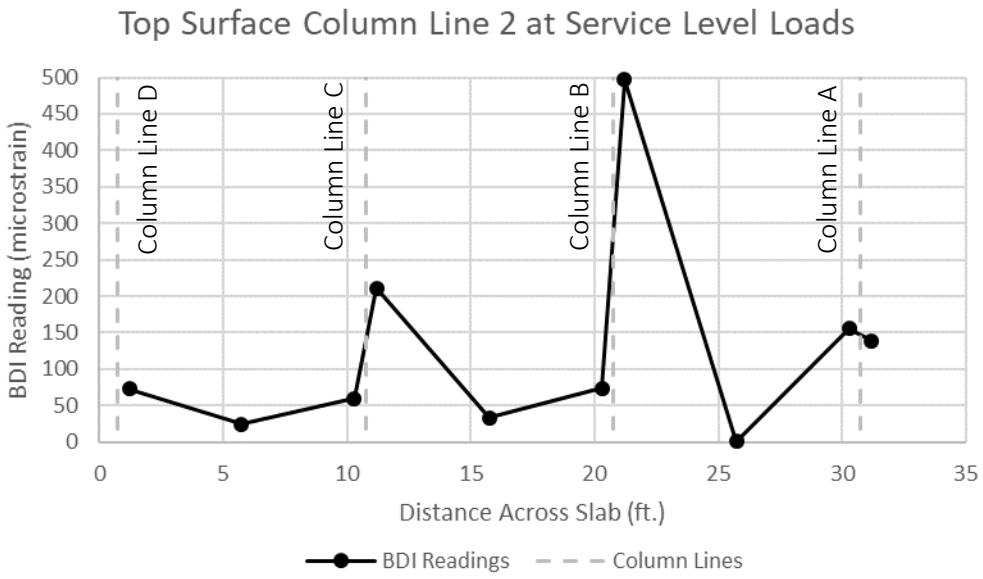

Figure 57. Top Surface Column Line 2 BDI Readings at Service

Strain gauges on the bottom surface of the slab were provided in sections across the slab positioned at the midspan of the specimen. The bottom surface strains banded direction looking towards the overhang are provided below in Figure 58.

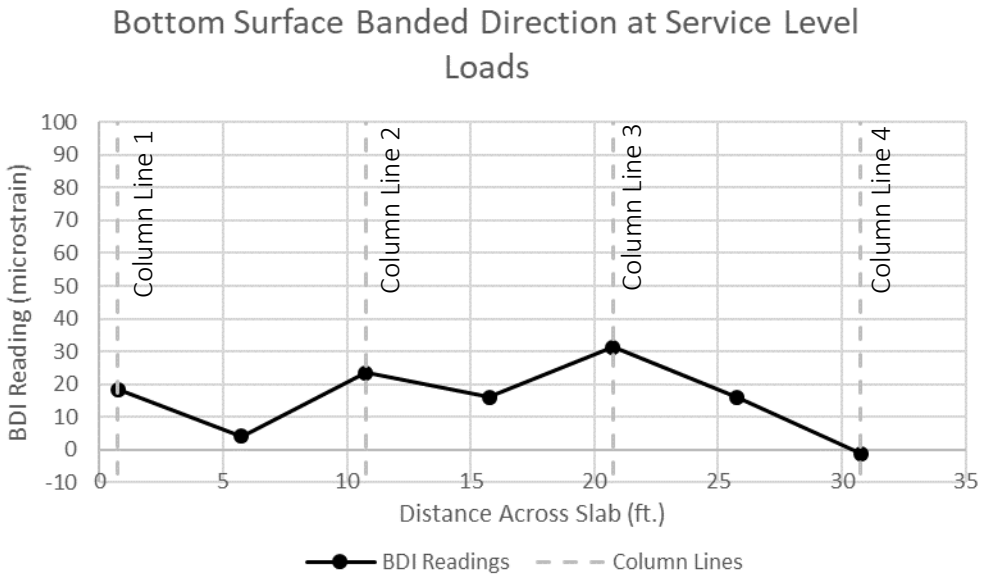

Figure 58. Bottom Surface Banded Direction BDI Readings at Service

The bottom surface strains in the uniform tendon direction looking towards the overhang are provided below in Figure 59.

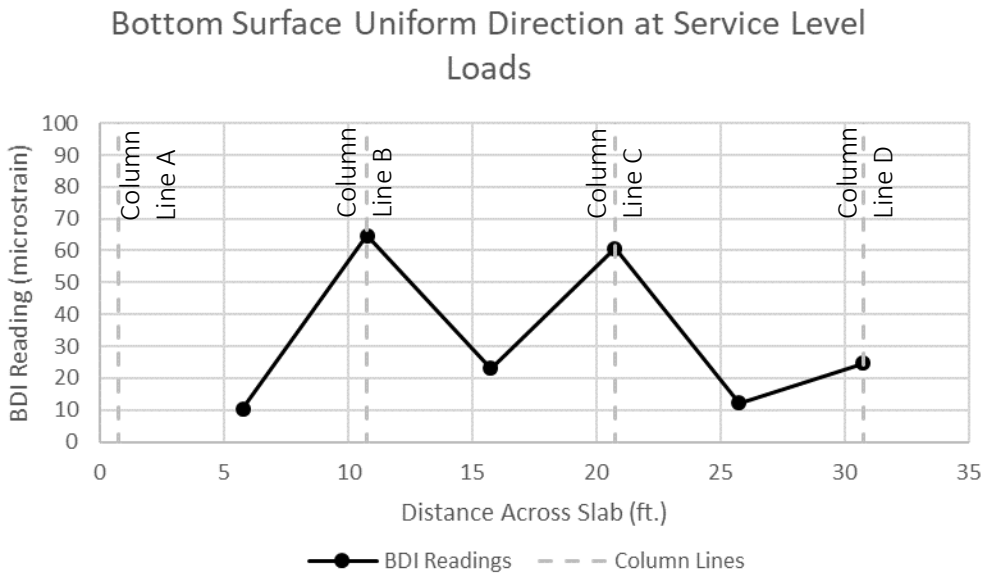

Figure 59. Bottom Surface Uniform Direction BDI Readings at Service

For each of the four cross sections of BDI strain gauges, the strains are typically lower in the mid-span locations than for the strains located at or near the column lines. This is similar to what was seen for the top surface cross sections after stressing when the formwork was lowered.

At approximately every 10psf of applied load, cracks on the specimen were marked and measured. Figure 60 shows the location of all the cracks that were observed at the service-level loading condition. The only cracks that were observed were located on the top of the slab near the columns. The cracking mainly occurred at the interior columns, where the anticipated tensile stresses were the highest. There was no indication of yield lines beginning to form.

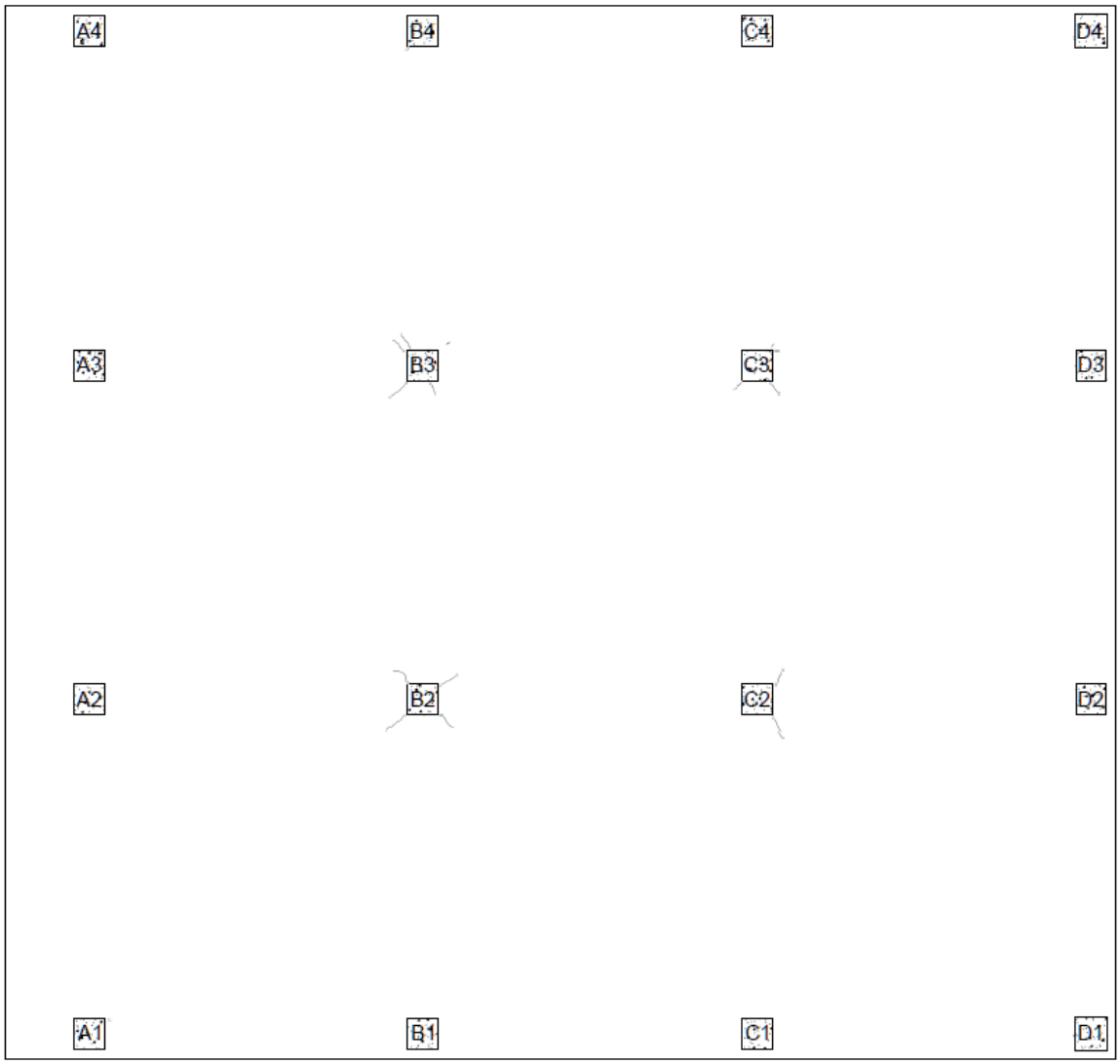

Figure 60. Crack Map at Service-Level Loads

The mean crack width and characteristic crack width for the widest crack at each column is shown in Table 11 for a service-level loading. When a crack formed, the mean crack width was the average width of the crack along its length. The mean crack width was measured at the same spot in subsequent measurements. The characteristic crack width corresponded to the crack width that was wider than approximately 90 percent of the remainder of the crack. The characteristic crack width was also measured in the same spot in subsequent measurements. All crack widths were measured with a crack width measurement card, with the smallest increment on the card of 0.10mm (crack widths were initially measured in mm). The widest crack that was observed was at column B-2, and its characteristic crack width was 0.011in. (0.28mm).

Table 11. Crack Widths at Service-Level Loads

Column	Characteristic Crack Width (in. (mm))	Mean Crack Width of Same Crack (mm)
B-2	0.011 (0.28)	0.009 (0.24)
B-3	0.008 (0.20)	0.005 (0.13)
B-4	0.004 (0.10)	0.004 (0.10)
C-2	0.008 (0.20)	0.006 (0.15)
C-3	0.004 (0.10)	0.004 (0.10)

4.2.3 Performance at Factored Loads

The factored loading for Specimen 2 was determined from the updated service-level loads. The total factored loading was 238psf, or 130.1psf of applied whiffle tree load. The controlling load combination was 1.2D + 1.6L, using the updated design loads. This load was reached on the third day of testing. The slab was unloaded five times prior to reaching the factored loads.

The load-deflection plots for each bay are shown in Figures 57-59. Figure 57 contains the load-deflection plots for Bays 1-4. Figure 58 contains the load-deflection plots for Bays 5-8, and Figure 59 contains the load-deflection plots for Bays 9-12. The axes of each plot were kept the same to allow for a more convenient comparison between the sections of the slab.

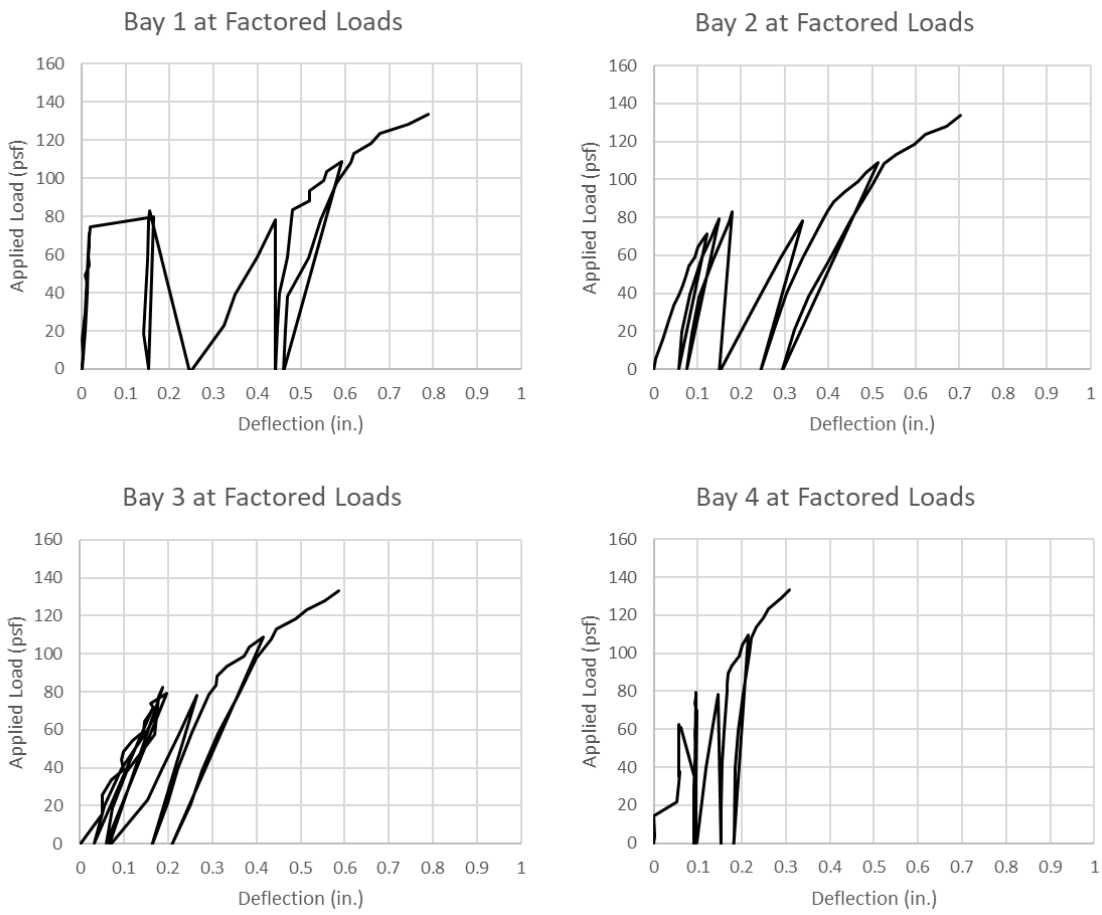

Figure 61. Load-Deflection at Factored Loads Part 1

Figure 61 shows a reduction of stiffness near 90 or 95psf of applied load, when the slope of the load-deflection plot begins to reduce. This behavior is less evident in the overhang bay of this exterior slab section, but Bays 1-3 show a more prominent reduction in stiffness around this point. At this point of loading, Bay 1 has the largest deflection throughout the slab, with a deflection of approximately 0.79 in.

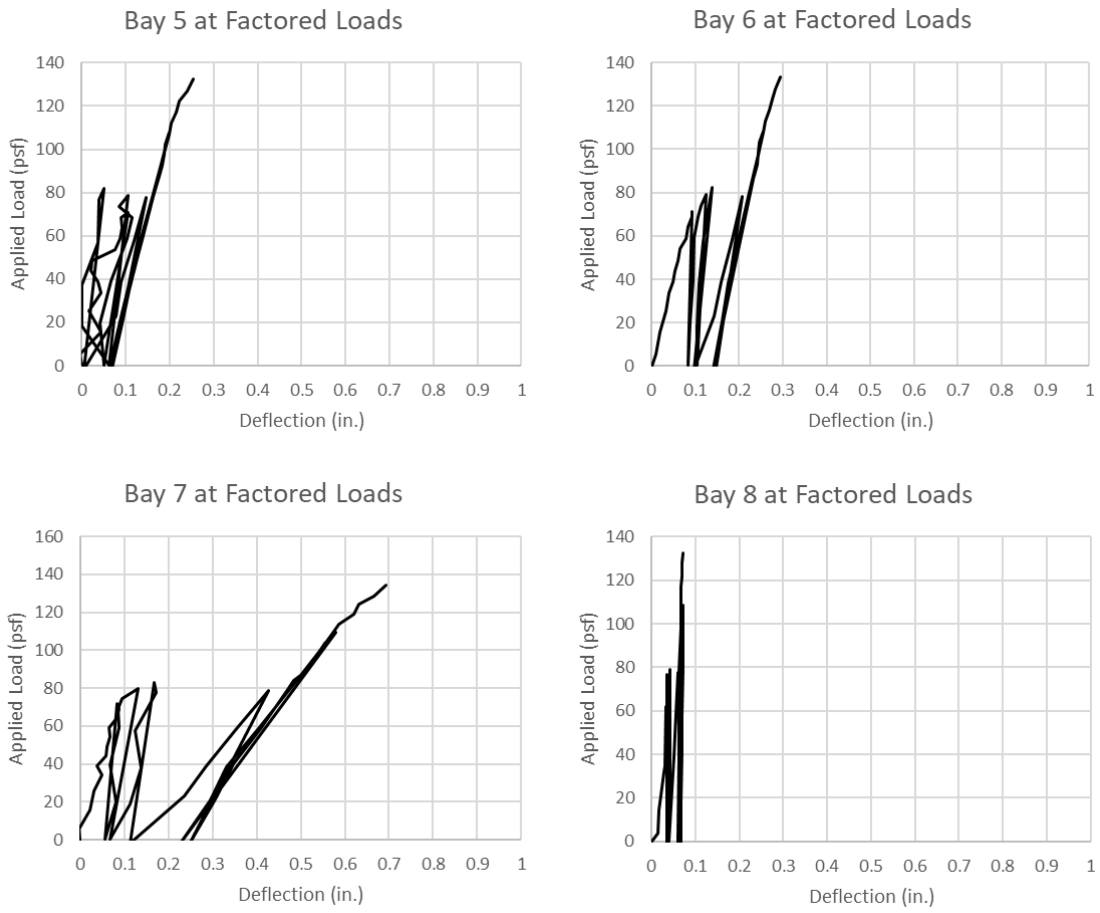

Figure 62. Load-Deflection at Factored Loads Part 2

For the interior section of the slab (Bays 5-8), the deflections are mostly smaller than the deflections in the exterior sections of the slab. Figure 62 does not show much loss of stiffness in the slab for the interior bays, but Bays 5 and 6 have a slight reduction in stiffness when approximately 120psf of load was applied to Specimen 2.

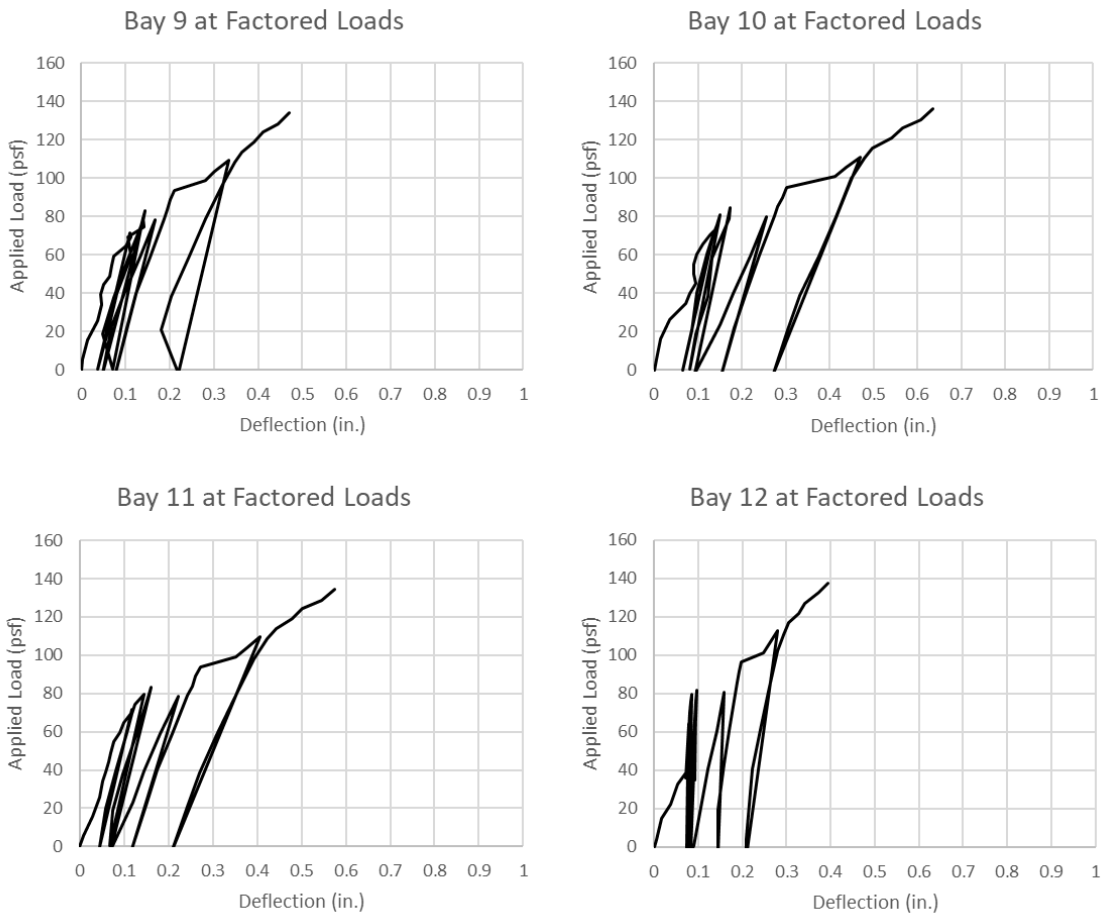

Figure 63. Load-Deflection at Factored Loads Part 3

Figure 62 shows the exterior section of the slab having a reduction in stiffness around 90 to 95psf of applied load. This is like the behavior of the other exterior section shown in Figure 61. Even the overhang shows signs of cracked behavior.

On the third day of testing, when the applied load on Specimen 2 reached 80psf, the beginning of a yield line was noticed at the bottom surface of the slab between column lines 1 and 2. At this point, no obvious yield lines were observed on the top surface of the slab, with the exception for two cracks at column C2 running outward in the uniform tendon direction.

At 95psf of applied load, the beginning of a potential yield line was observed at the bottom surface of the slab between column lines 3 and 4. The beginnings of the potential top surface yield line became a little more defined, although it was still only present near column C2. At 105psf of applied load, both bottom surface cracks stretched across the full length of the slab.

At 125psf of applied load, the cracks on the top of the slab continued to grow in length at column C2 running in the uniform tendon direction. Also, a crack running from column B2 to C2 was observed. Some cracks along column line 3 at the top surface of the slab were also observed running in the uniform tendon direction, potentially forming a yield line.

The next set of crack measurements and observations was at 135psf of applied load, slightly after factored loads were reached. The crack patterns at 135psf of applied load are shown in Figure 64 and Figure 65 at this point during the load testing. At this point, there still were not any cracks at the columns along column line D. No cracks at the top of the slab extended across the full length of the slab.

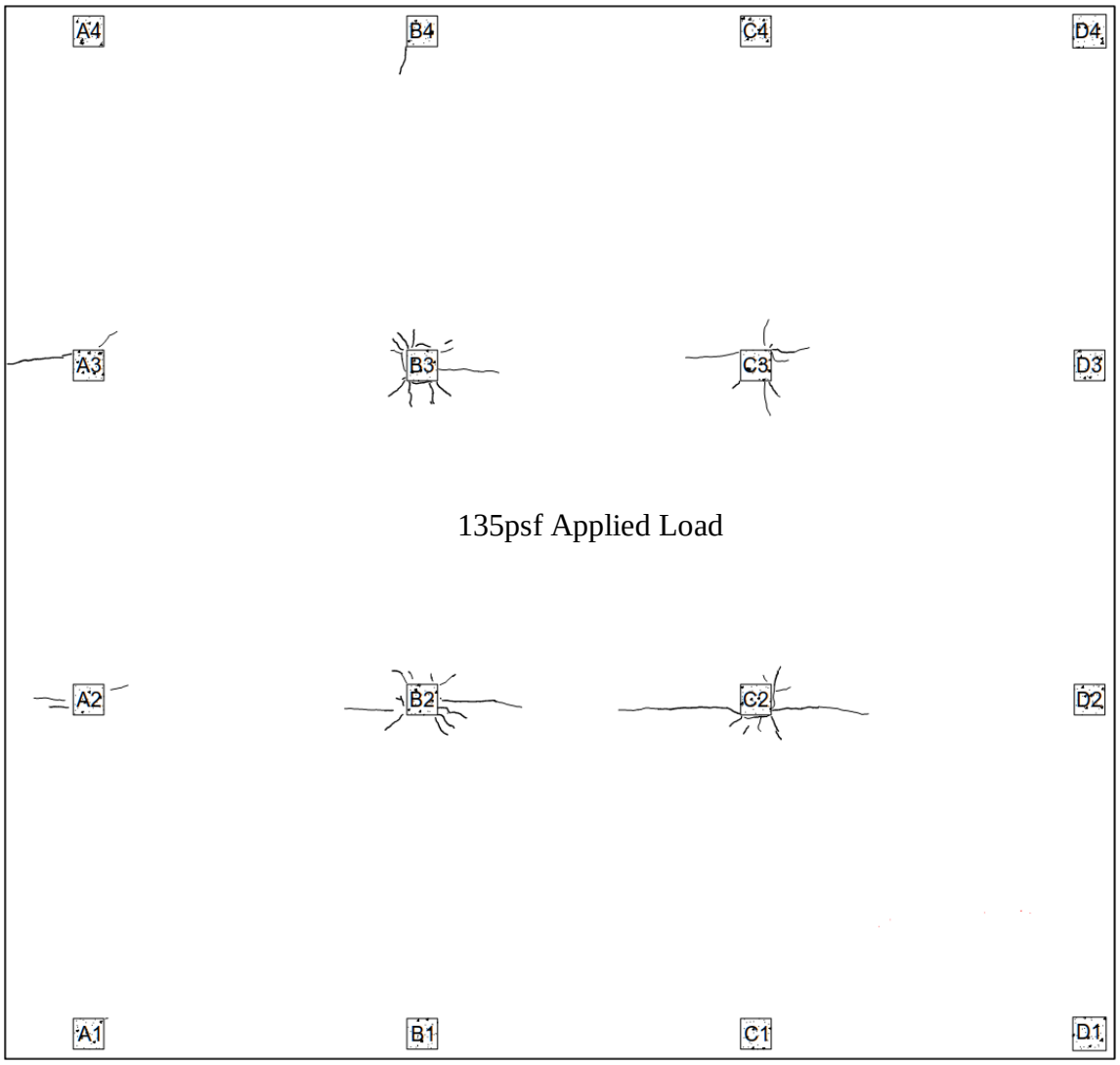

Figure 64. Top Surface Crack Map After Factored Loads

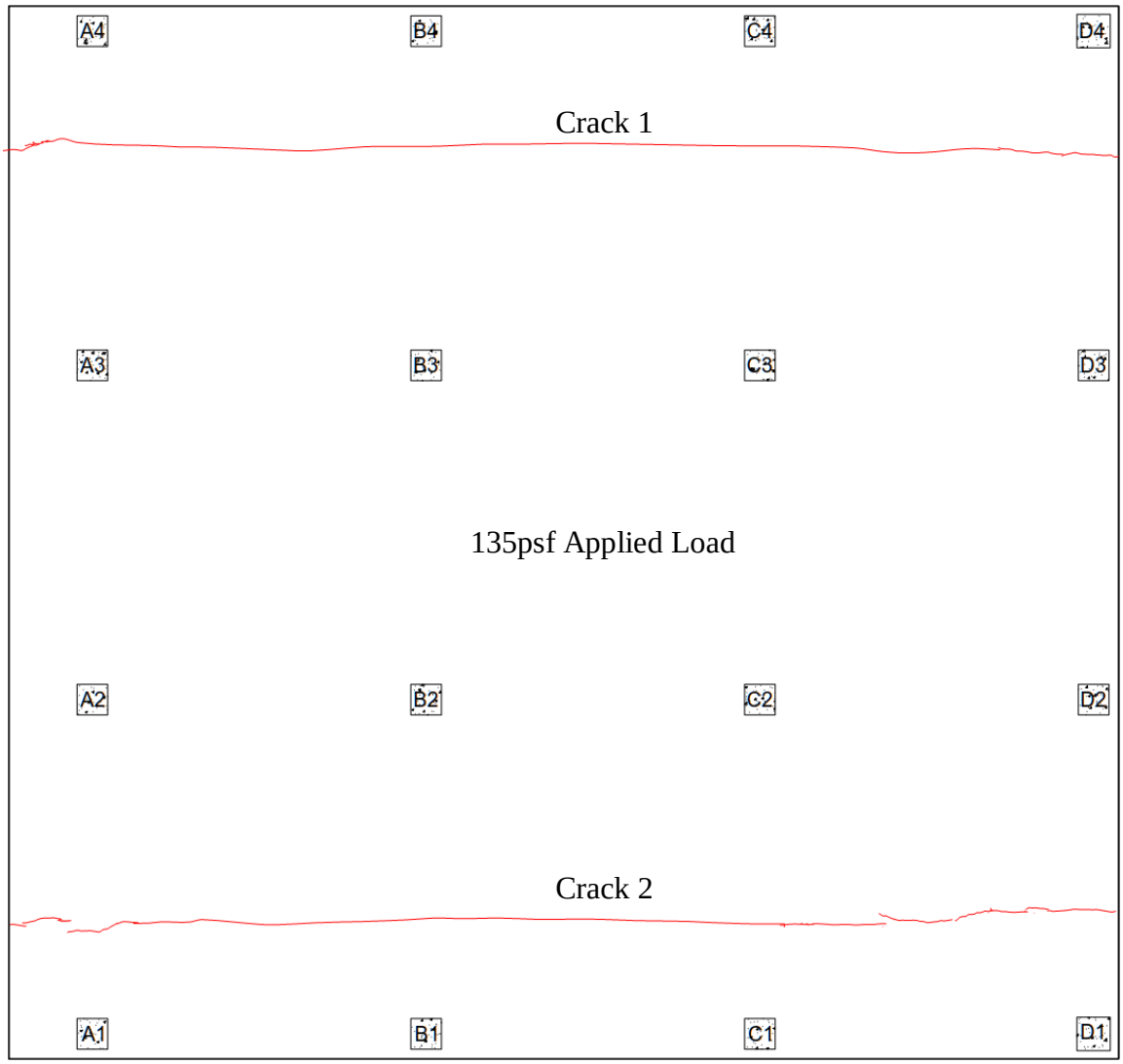

Figure 65. Bottom Surface Crack Map After Factored Loads

Before factored loads were reached, for safety reasons, only the widest cracks on the top surface of Specimen 2 were measured. The widest crack on the top surface was at the corner of column B2. The growth of this crack as the applied load was increased is shown in Table 12.

Table 12. Cracks Measurements at Column B2 up to Factored Loads

Applied Load (psf)	Characteristic Crack Width (in. (mm))	Mean Crack Width (in. (mm))
80	0.012 (0.30)	0.012 (0.30)
85	0.013 (0.34)	0.012 (0.30)
95	0.015 (0.38)	0.013 (0.34)
105	0.016 (0.40)	0.014 (0.36)
115	0.017 (0.42)	0.016 (0.40)
125	0.018 (0.46)	0.017 (0.42)
135	0.020 (0.50)	0.017 (0.44)

Table 13 provides the crack measurements for the bottom surface cracks up to the factored loads.

Table 13. Bottom Surface Crack Measurements up to Factored Loads

Applied Load (psf)	Crack 1		Crack 2	
	Characteristic Crack Width (mm)	Mean Crack Width (mm)	Characteristic Crack Width (mm)	Mean Crack Width (mm)
80	0.020 (0.50)	0.012 (0.30)	N/A	N/A
85	0.020 (0.50)	0.012 (0.30)	<0.004 (<0.10)	<0.004 (<0.10)
95	0.024 (0.60)	0.016 (0.40)	0.009 (0.22)	0.008 (0.20)
105	0.028 (0.70)	0.020 (0.50)	0.016 (0.40)	0.012 (0.30)
115	0.031 (0.80)	0.024 (0.60)	0.020 (0.50)	0.016 (0.40)
125	0.035 (0.90)	0.028 (0.70)	0.028 (0.70)	0.024 (0.60)
135	0.043 (1.1)	0.035 (0.90)	0.035 (0.90)	0.028 (0.70)

Eurocode 2 sets a limit for crack width to be no more than 0.020in. (0.5mm) since a crack of this magnitude will not close when the load is removed from the structure (European Concrete Platform ASBL, 2008). The bottom surface Crack 1's characteristic

crack width was 0.020in. at 80psf, and the top surface's widest crack was 0.020in. wide at 135psf of applied load.

Strains were monitored in the upper reinforcement in Specimen 2 at columns C-2 and C-3. These strain gauges were located near the column faces. The load-strain plots are shown below in Figures 66-68.

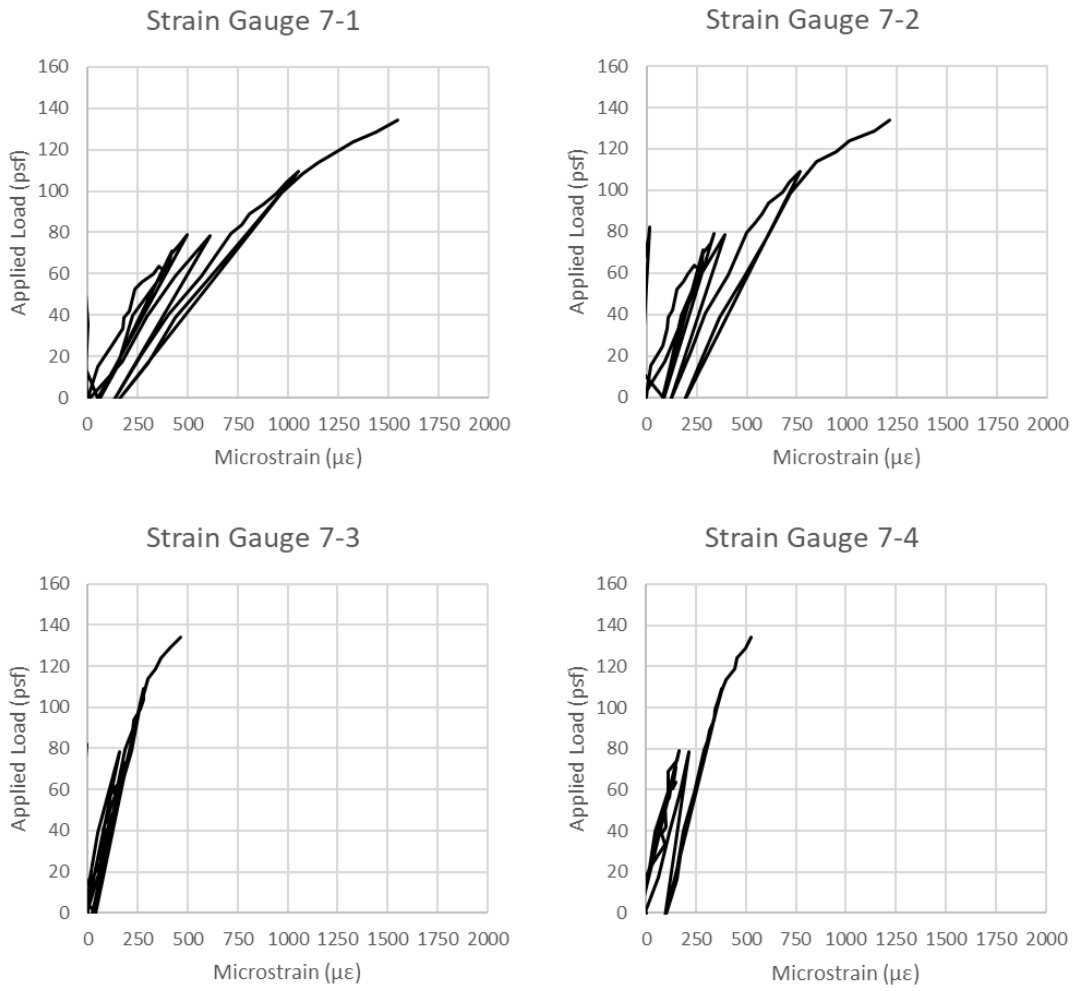

Figure 66. Factored Load Strains at Top Reinforcement at Column C-2

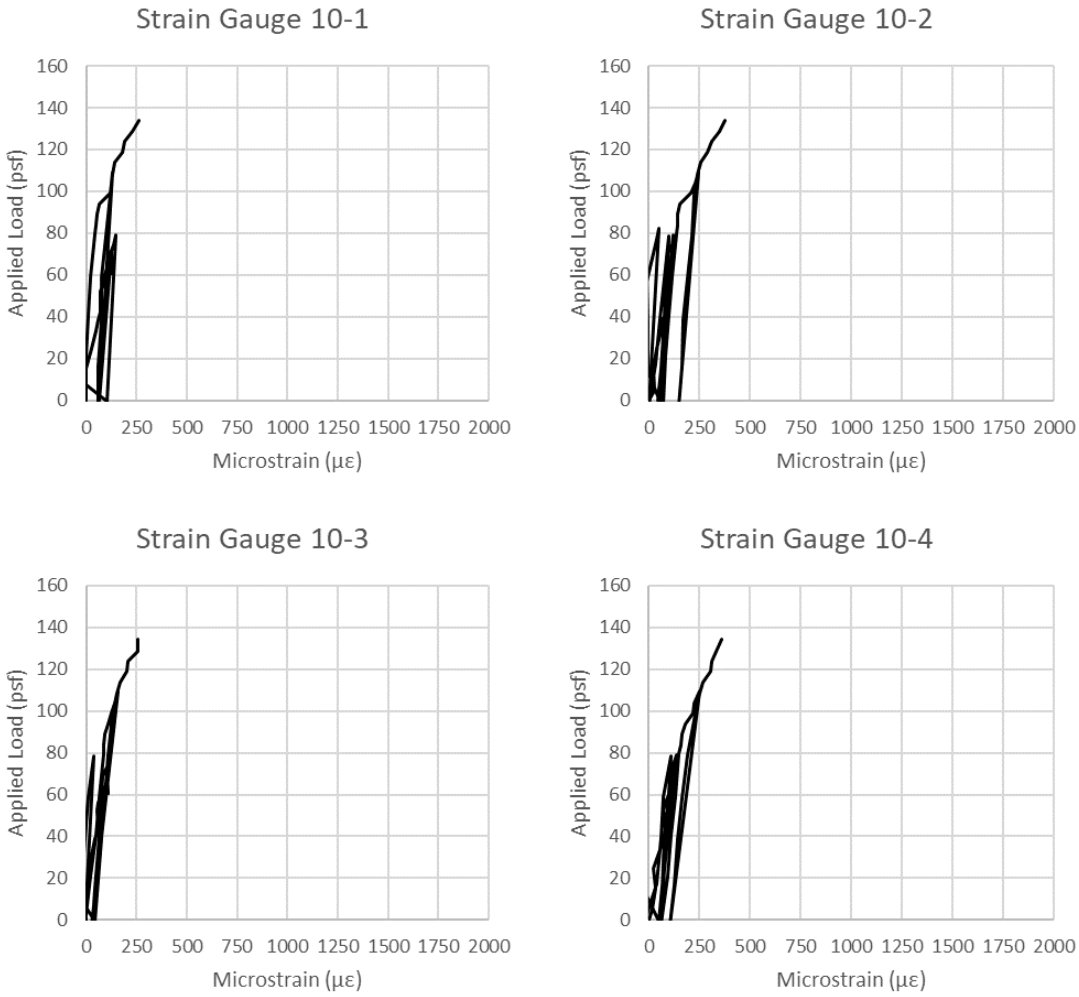

Figure 67. Factored Load Strains at Top Reinforcement at Column C-3 (Part 1)

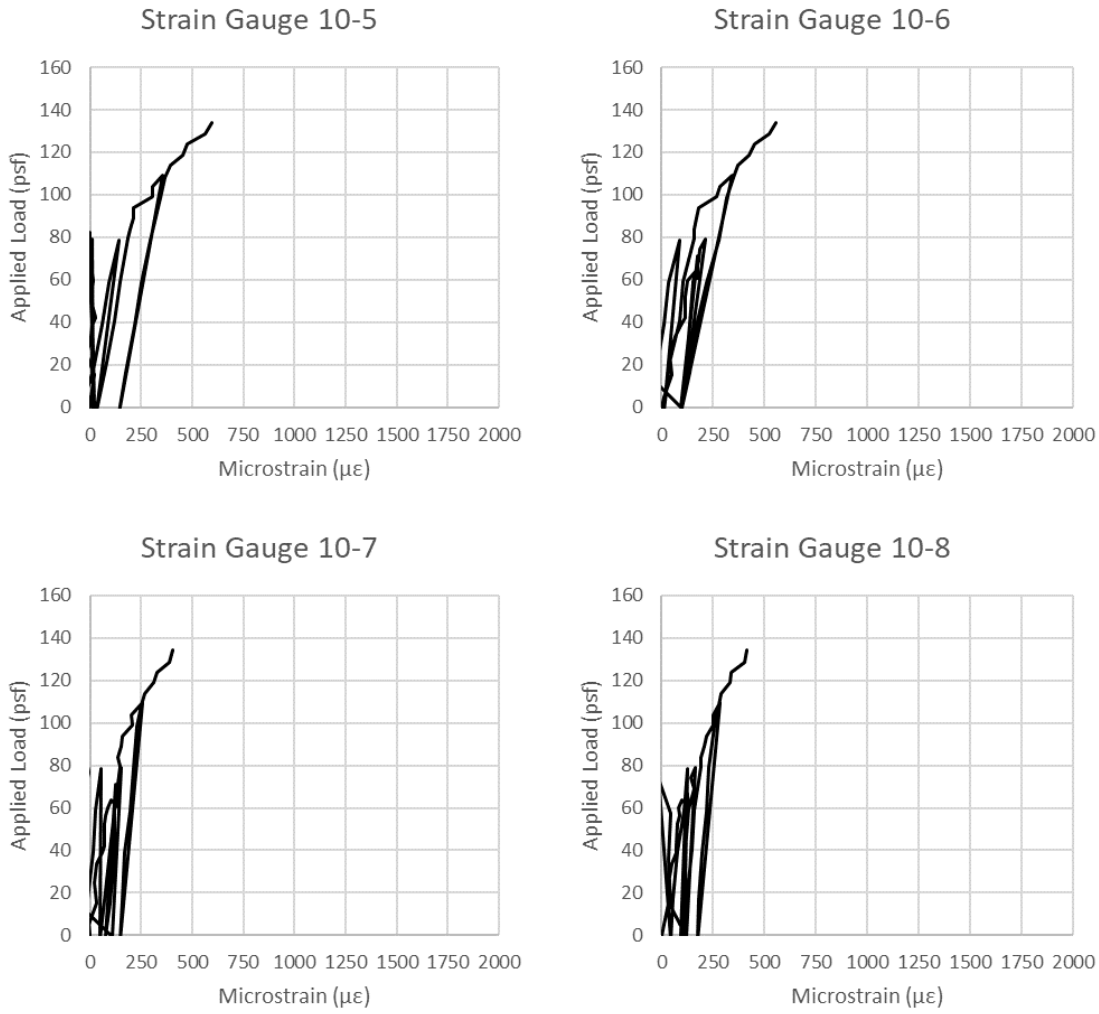

Figure 68. Factored Load Strains at Top Reinforcement at Column C-3 (Part 2)

The strain gauges up to service loads mainly remained linear. At approximately 95psf, the slope of the plots for all of the strain gauges reduced, indicating cracked behavior in the post-tensioned flat plate. The strain gauges at Column C-2 on the reinforcement extending towards Column C-1 began showing larger strains after 95psf. This area of the slab was likely behaving inelastically at this point. There was a large crack between column lines 1 and 2 that was leading to large deflections near this crack. The large deflections led to the significantly higher strains in strain gauge 7-1 and 7-2.

4.2.4 Performance at Ultimate Loads

Overall, Specimen 2 experienced eight loading and unloading cycles throughout the final three days of testing. The ultimate load that was reached was 174psf of applied load, for a total slab load, including self-weight, of 282 psf. The testing was stopped at

this point due to safety concerns. There was a possibility that the swivel heads or the load cells could be propelled out from under the columns since the columns at the exterior of the slab began experiencing large rotations, even though they were restrained by threaded rods running across the length of the slab.

The load-deflection plots for the final three days of testing up to the final unloading of Specimen 2 are provided in Figures 69 to 71.

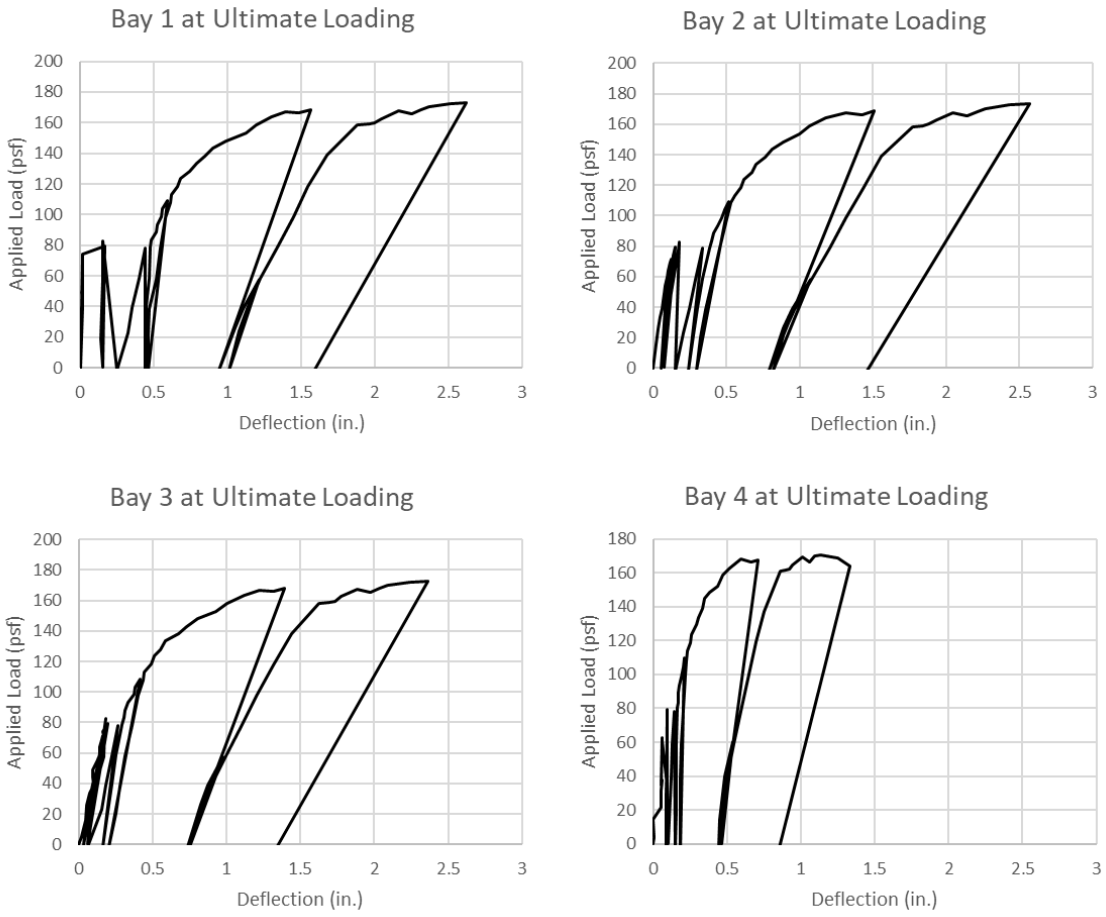

Figure 69. Load-Deflection at Ultimate Loading Part 1

Figure 69 shows a continual reduction in stiffness as more load is applied for each of the four bays in the exterior section of the slab. Residual deflections range from approximately 0.8 in. to 1.6 in. at Bay 1. The peak deflection at ultimate loading was approximately 2.6 in. located at the center of Bay 1.

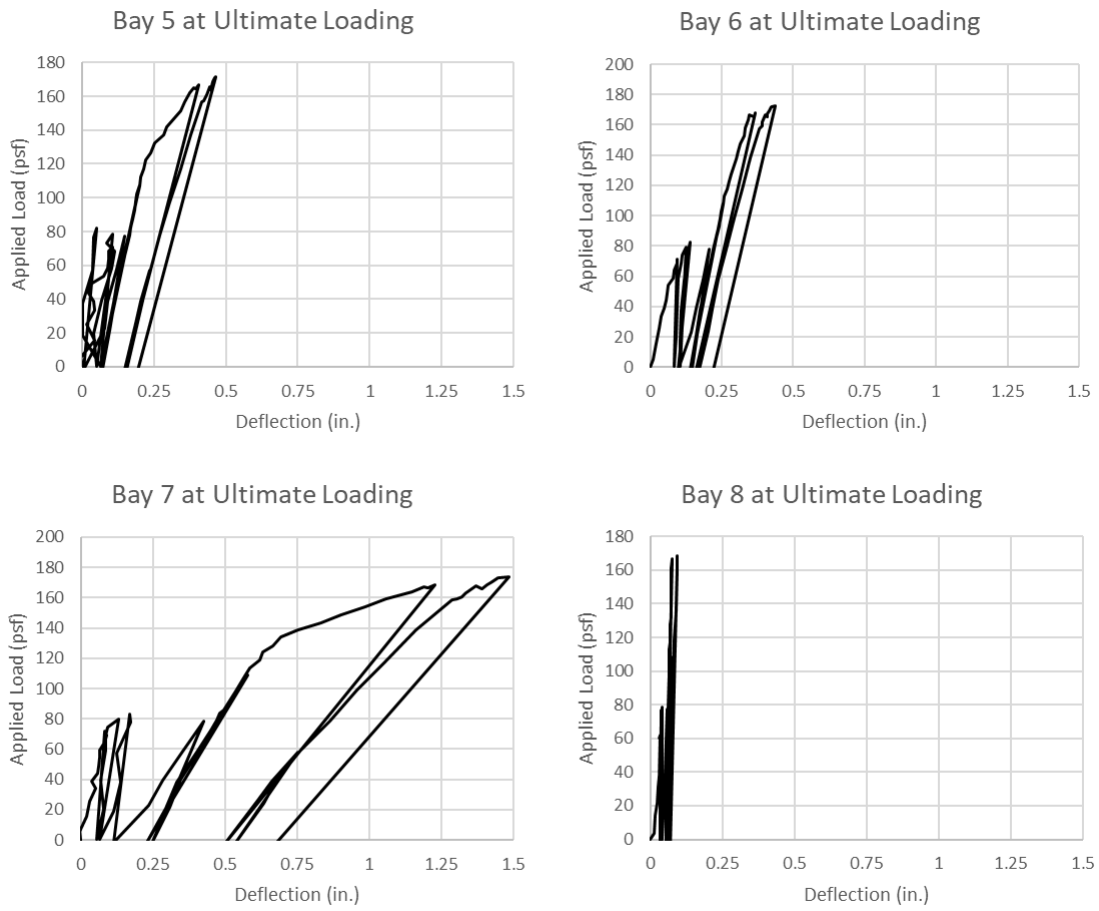

Figure 70. Load-Deflection at Ultimate Loading Part 2

Figure 70 shows much stiffer behavior for the interior slab section than compared to the behavior in Bays 1 to 4. The overhang shows almost no reduction in stiffness throughout the load testing, while Bay 7 shows the most stiffness reduction for this section of the slab. The peak deflection for this middle section of the slab was just under 1.5 in. However, most of the deflections in this section reached no more than 0.5 inches.

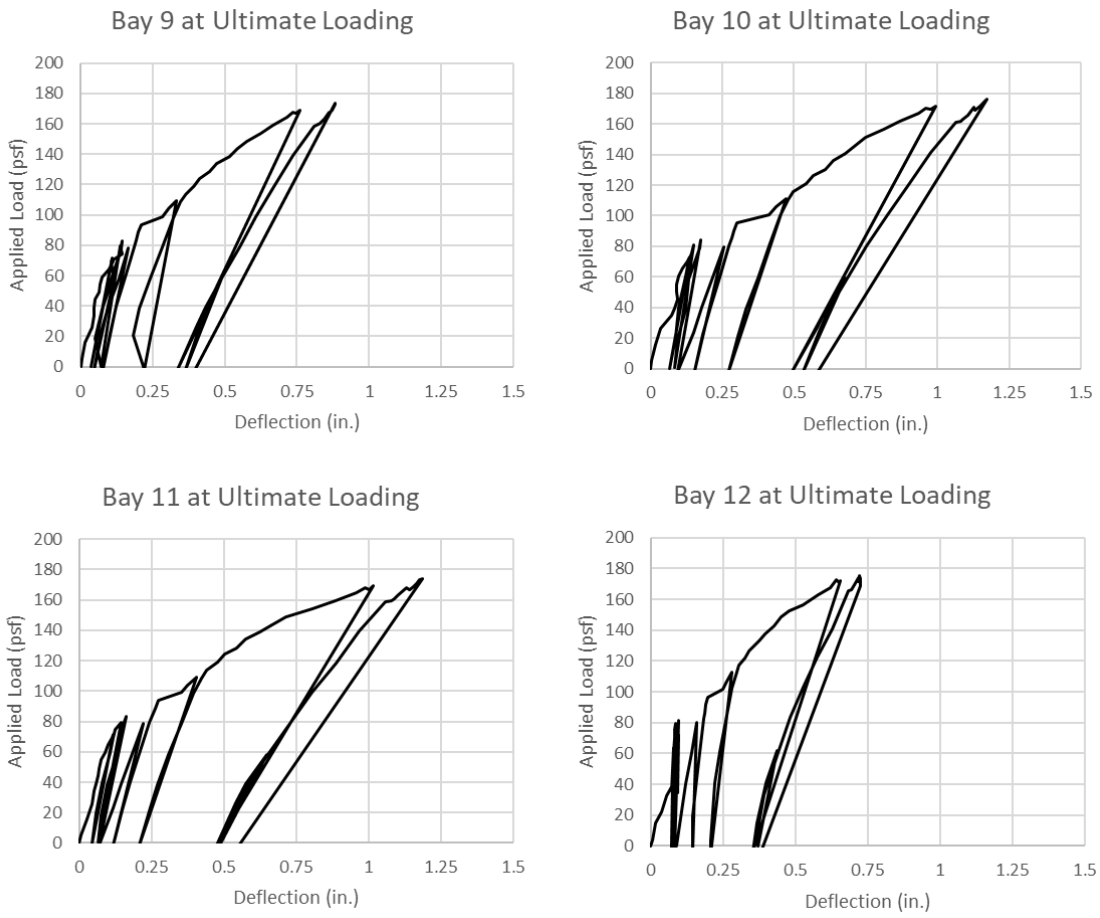

Figure 71. Load-Deflection at Ultimate Loading Part 3

Figure 71 shows larger deflections than Figure 66, but smaller deflections than the bays in Figure 69. The reduction in slab stiffness is evident in Bays 9-12, but it is significantly less than the reduction that was present in Bays 1-4.

Cracking was marked and measured on Specimen 2 when the applied loads were low enough that safety was not a concern, and a final set of crack marking was performed after the slab had been unloaded. The final crack mapping for the top surface of the slab is shown in Figure 72. The set of cracking at column line 2 extended across the whole length of the slab. The set of cracking at column line 3 extended approximately three-quarters of the length of the slab.

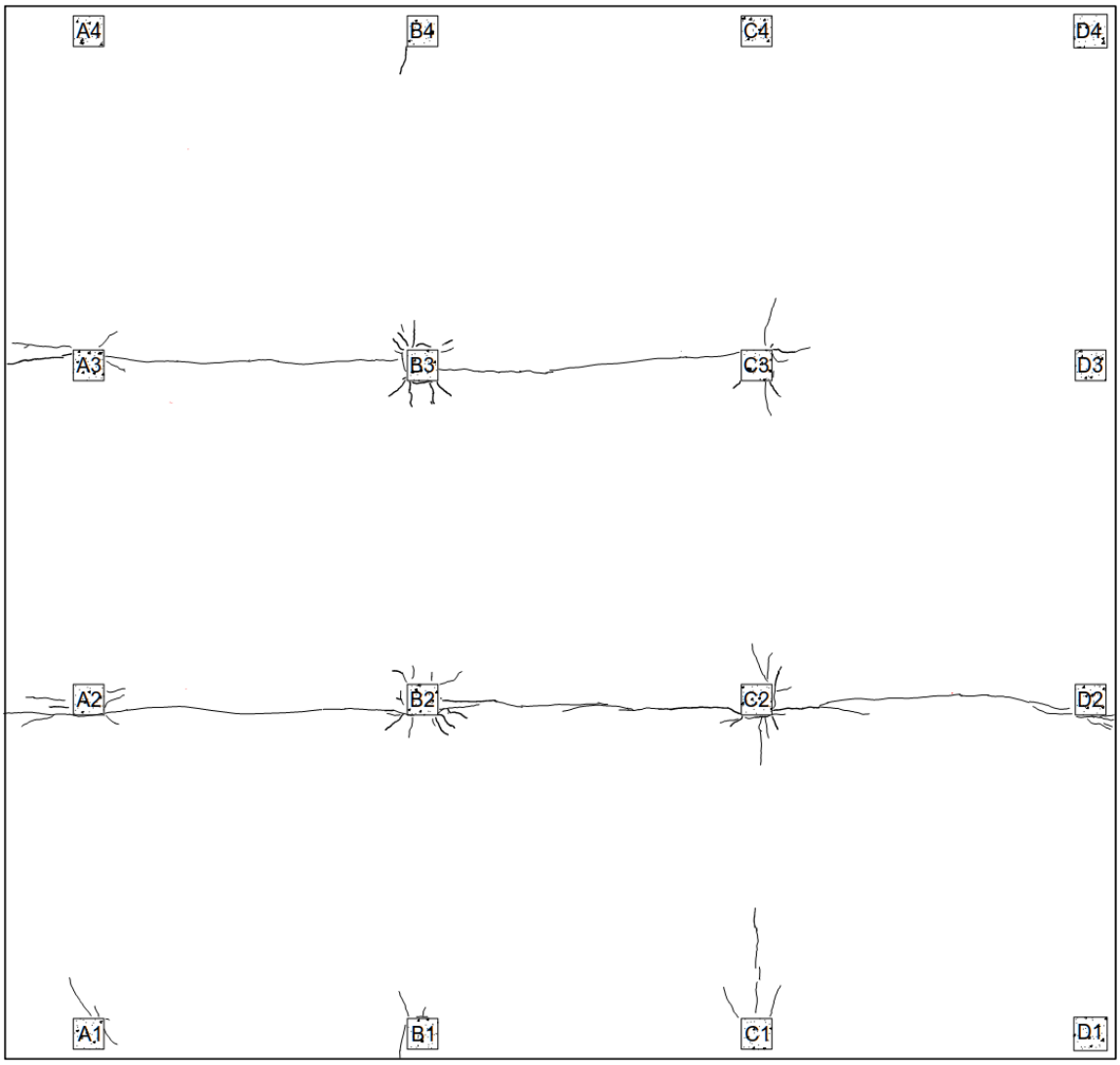

Figure 72. Top Surface Crack Map After Specimen 2 Failure

The final crack mapping for the bottom surface of the slab is shown in Figure 73. The yield line formed at Crack 1 in conjunction with the top surface crack running along column line 2. Two banded tendon direction cracks at the bottom surface of the slab were observed prior to reaching the ultimate loads. These two cracks did not extend through the full length of the slab, and they were much thinner than the other two bottom surface cracks.

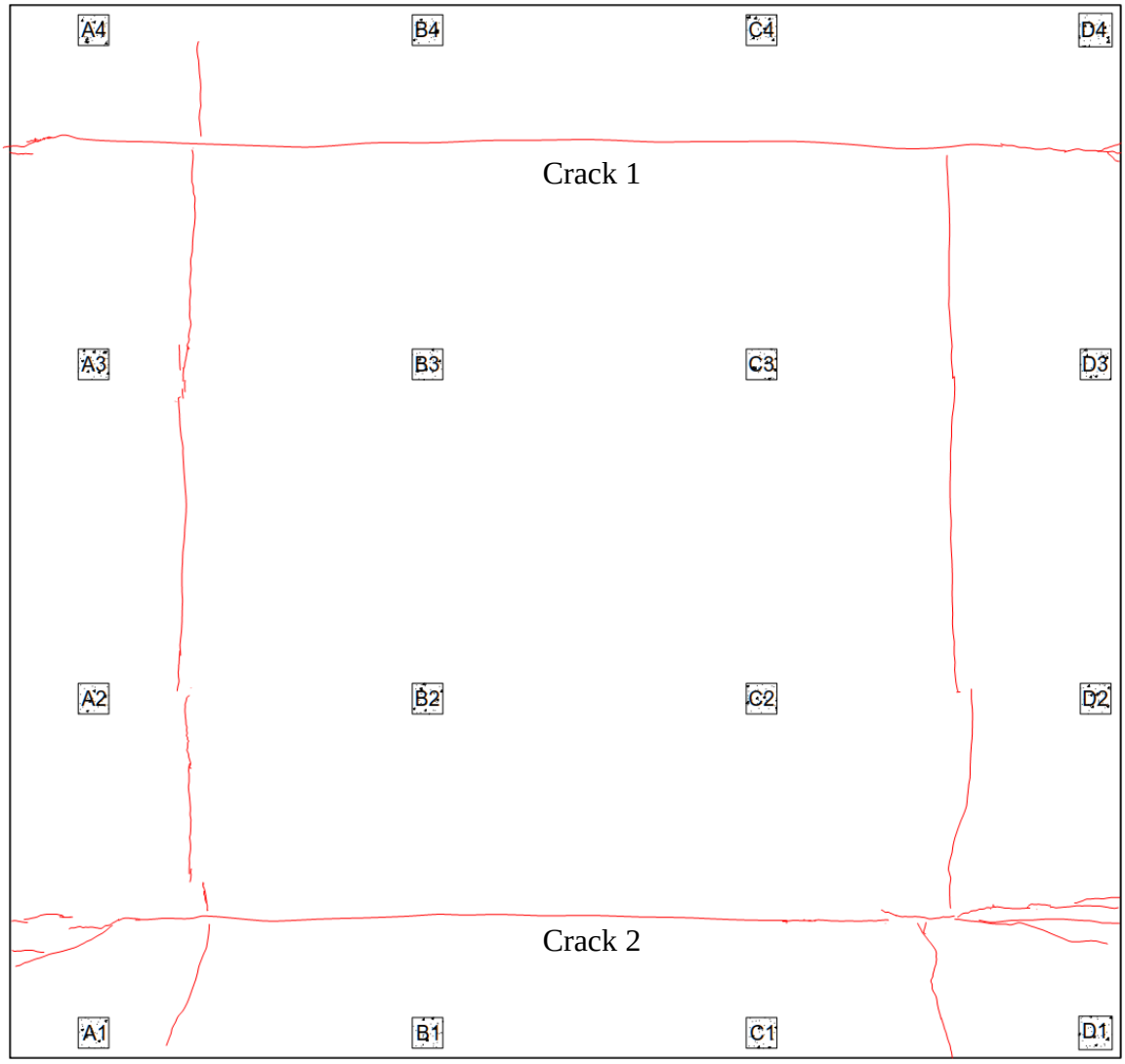

Figure 73. Bottom Surface Crack Map After Specimen 2 Failure

When the ultimate load was reached, Crack 1 was measured at the bottom of the slab in Bay 1, where it could be reached by hand without walking under the slab. The crack width was determined to be approximately 0.20in. (5.0mm) wide at the location, which is shown below in Figure 74.

Figure 74. Crack Width Measurement at Bottom Crack

The final failure mode of the slab was concrete crushing due to flexure. The concrete crushing was observed after several concrete cracking/crushing noises were heard just before ultimate loads were reached. After the slab was unloaded, the crushing was visually observed on the top surface of the slab over the bottom Crack 1 at column line B, running parallel to Crack 1. The crushing was observed to be at least 2.5ft long before it was obscured by the whiffle tree plates and the dead load compensation blocks. A picture of the concrete crushing is provided in Figure 75.

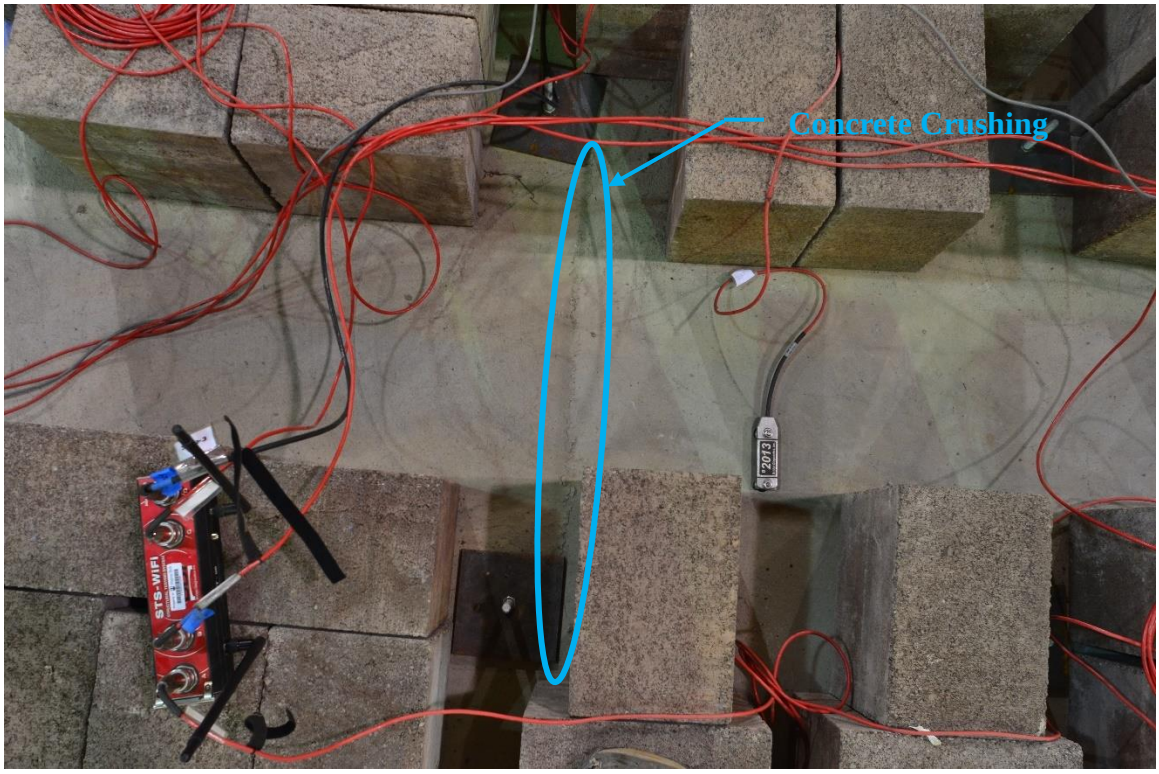

Figure 75. Concrete Crushing

The load-strain plots for the top reinforcement in the slab up to ultimate loading are shown in Figures 76 to 78. The horizontal axis is not scaled the same for each of the figures due large differences in strains that were measured at the various locations.

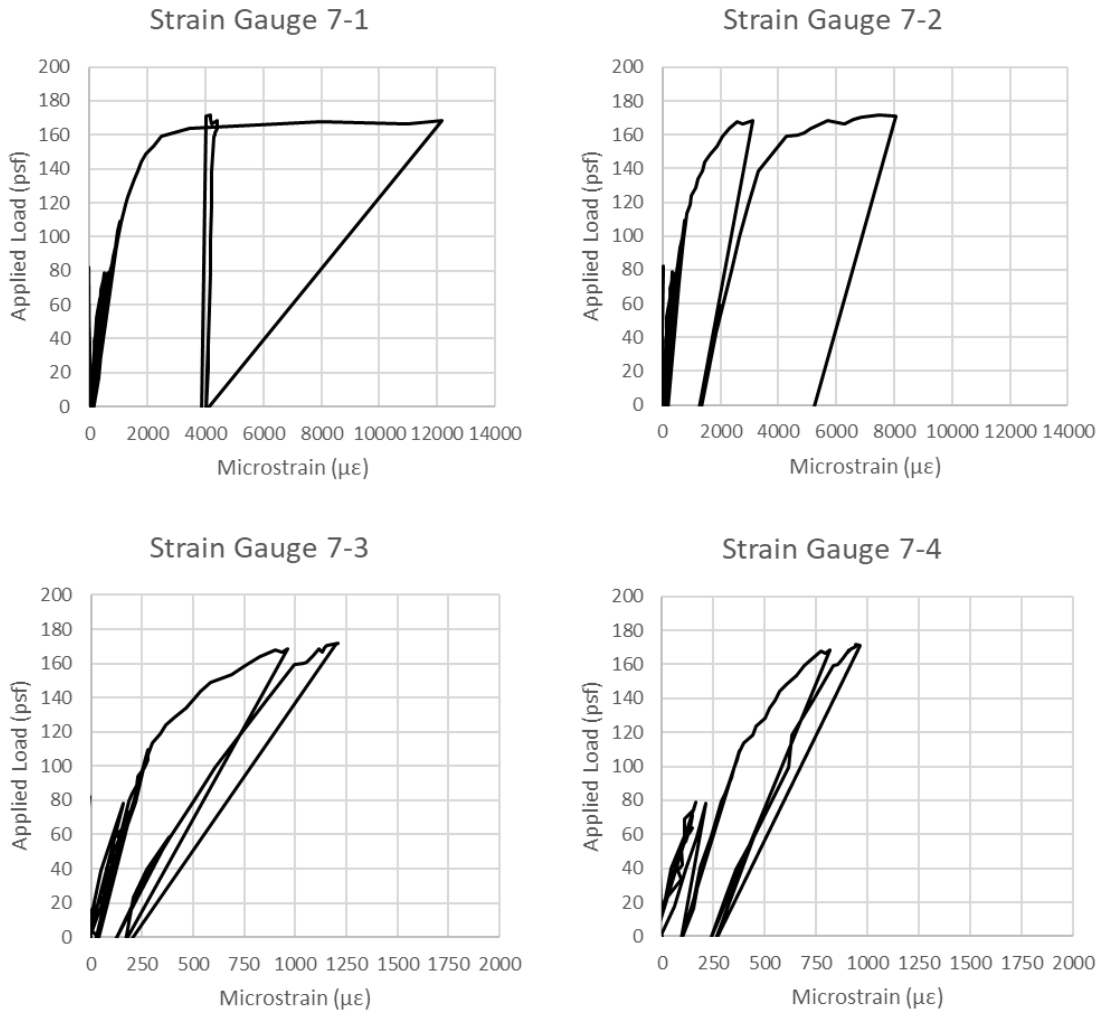

Figure 76. Ultimate Load Strains at Top Reinforcement at Column C-2

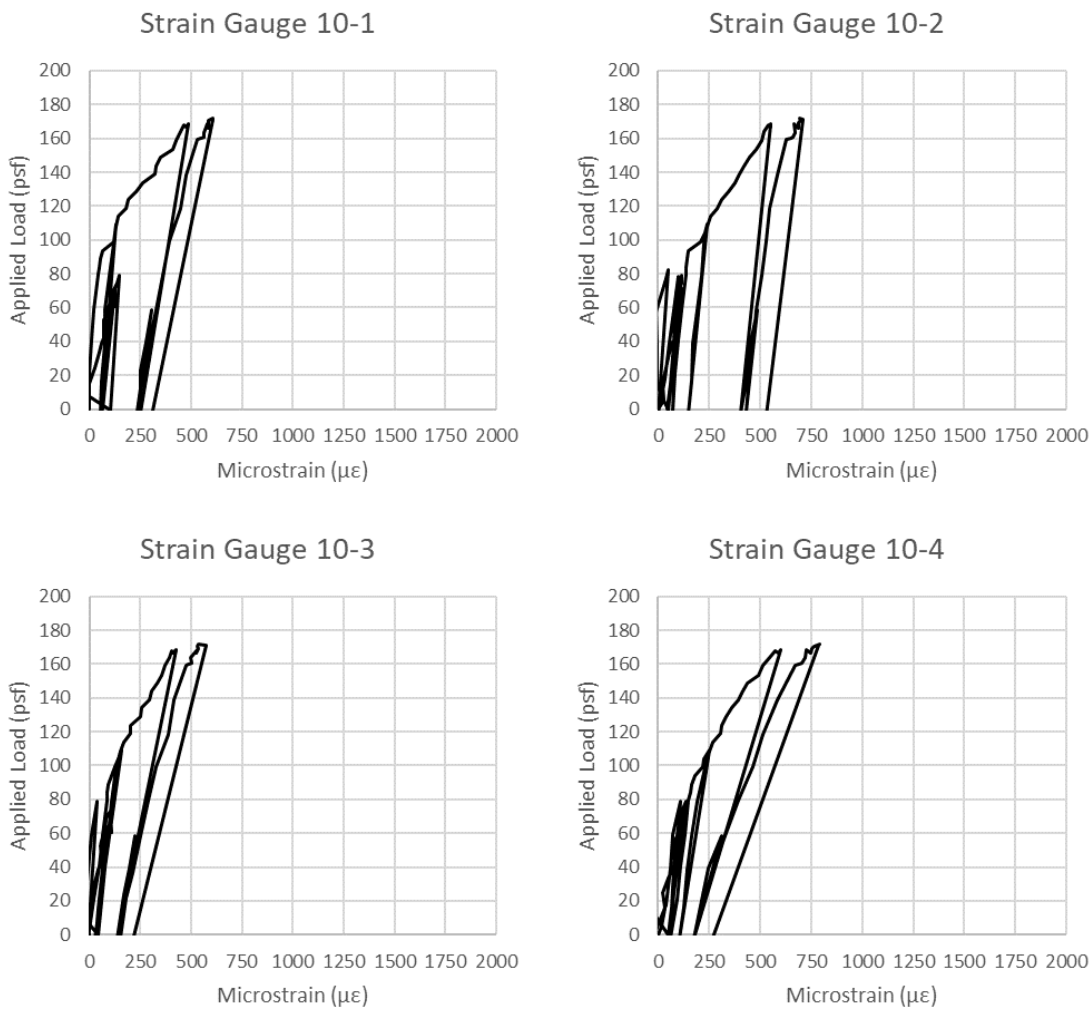

Figure 77. Ultimate Load Strains at Top Reinforcement at Column C-3 (Part 1)

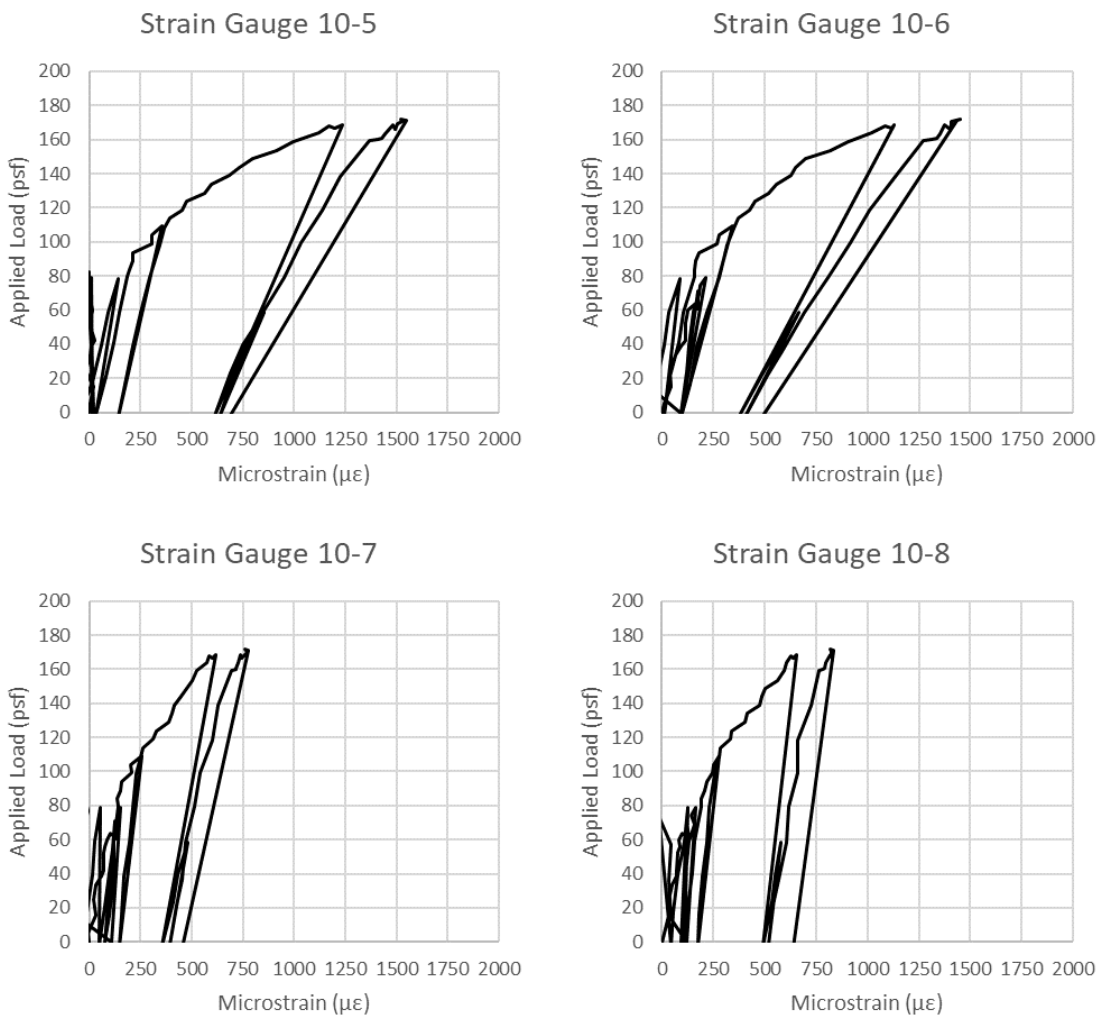

Figure 78. Ultimate Load Strains at Top Reinforcement at Column C-3 (Part 2)

Figure 76 shows that the strains on the reinforcement located at column C2 near the bottom crack experienced large strains as the applied load on the slab was increased. The strains at the other columns were much lower, probably since the main location of slab failure was located between column lines 1 and 2, which was nearest to strain gauges 7-1 and 7-2. However, all of the strain gauges show some nonlinearity, and all of the instrumented reinforcement has some residual tensile strains after the slab was unloaded.

Throughout the loading of Specimen 2, the load cells on two of the specimen's tendons were monitored. Two load cells were located on a banded tendon, and two were located on a uniform tendon. The loads were converted to stresses given the tendons' cross-section area of $0.058 in^2$. The tendon stress increase for the banded tendon as the

slab was loaded is provided in Figure 79, while the stress increase for the uniform tendon is shown in Figure 80.

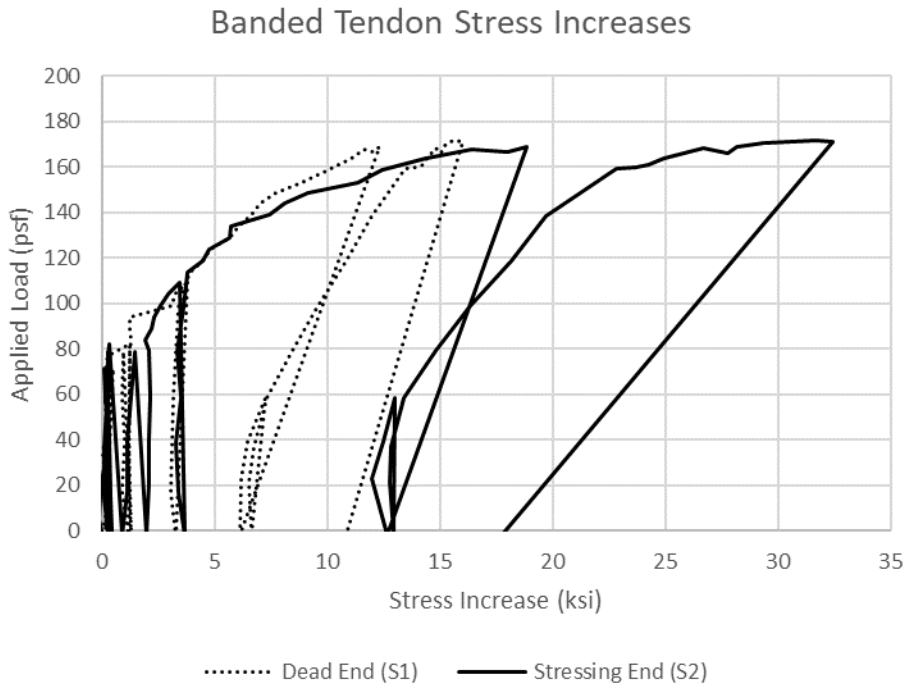

Figure 79. Stress Increases for Banded Tendon

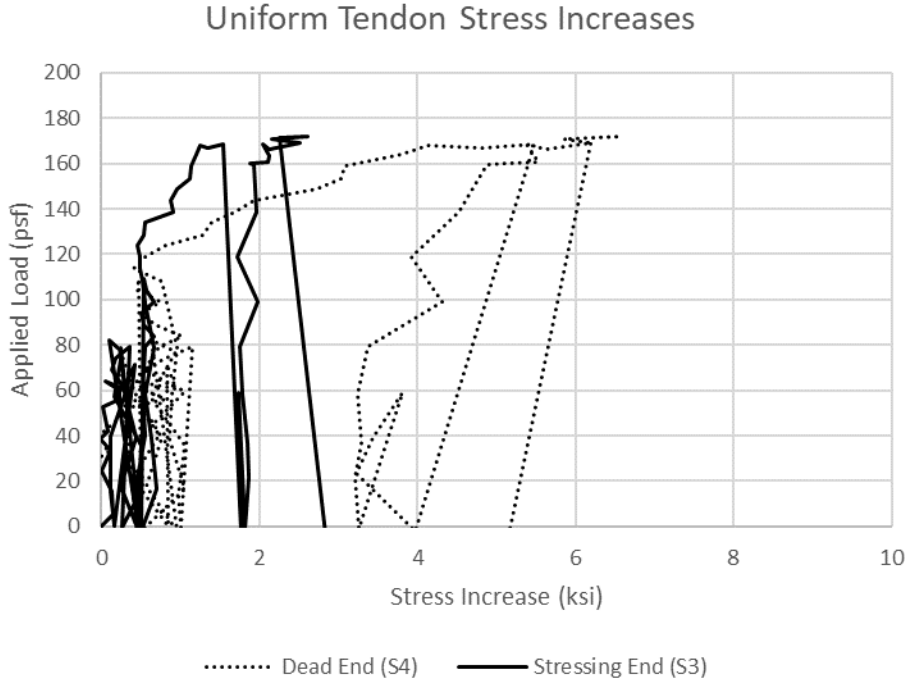

Figure 80. Stress Increases for Uniform Tendon

As can be seen in Figures 79 and 80, the banded tendons experienced significantly higher stress increases. Table 14 provides the final stress increases for the two instrumented tendons at ultimate loading conditions.

Table 14. Stress Increases for Tendons at Ultimate Loading

Tendon	Dead End (ksi)	Stressing End (ksi)	Average (ksi)
Banded	16.0	32.5	24.3
Uniform	6.2	2.3	4.3

For both tendons, ACI 318 predicts stress increases of 60ksi for the tendons. This value was obtained from Table 20.3.24.1 regarding the tendon stresses to be used in determining the flexural strength of a prestressed member with unbonded tendons (ACI, 2014). The actual stress increases are significantly lower than ACI's prediction. The banded tendon's stress increase is much larger than the uniform tendon's stress increase due to the wide cracks forming at the bottom of the slab running perpendicular to the banded tendon. These wide cracks cause the banded tendon to be elongated, leading to a large increase in tendon stress.

Column loads were monitored in the slab with the use of eight 50-kip load cells. Column line 2 and column line B were instrumented with load cells. The load cell measurements at given applied loads are shown in Figures 81 and 82. The loads for the load cell at column D1 are shown in Figure 83.

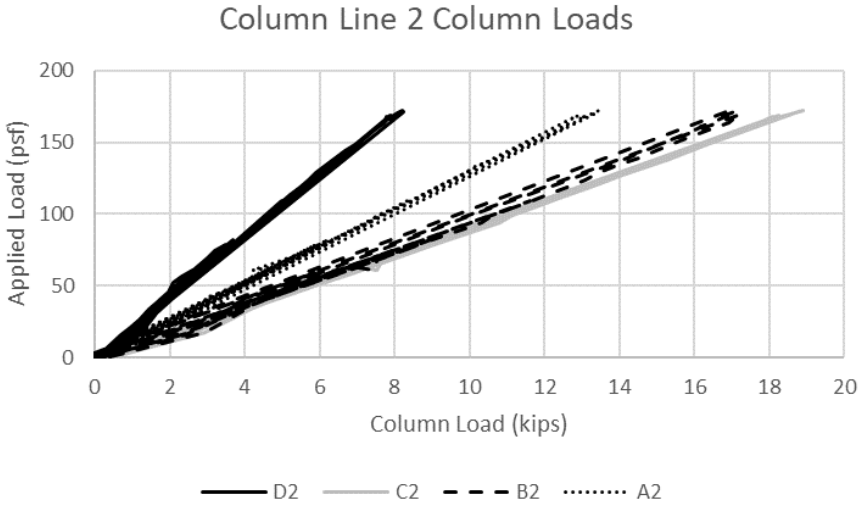

Figure 81. Column Load Cell Readings Along Column Line 2

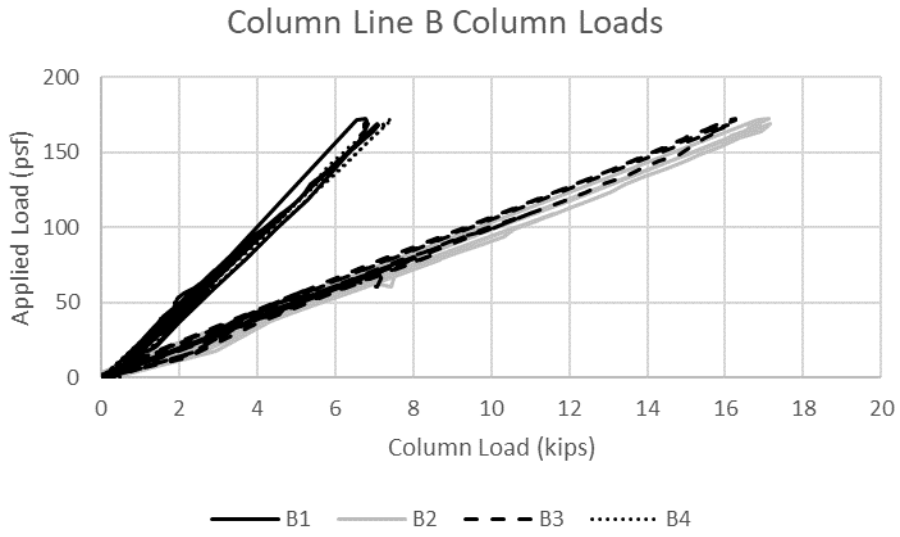

Figure 82. Column Load Cell Readings Along Column Line B

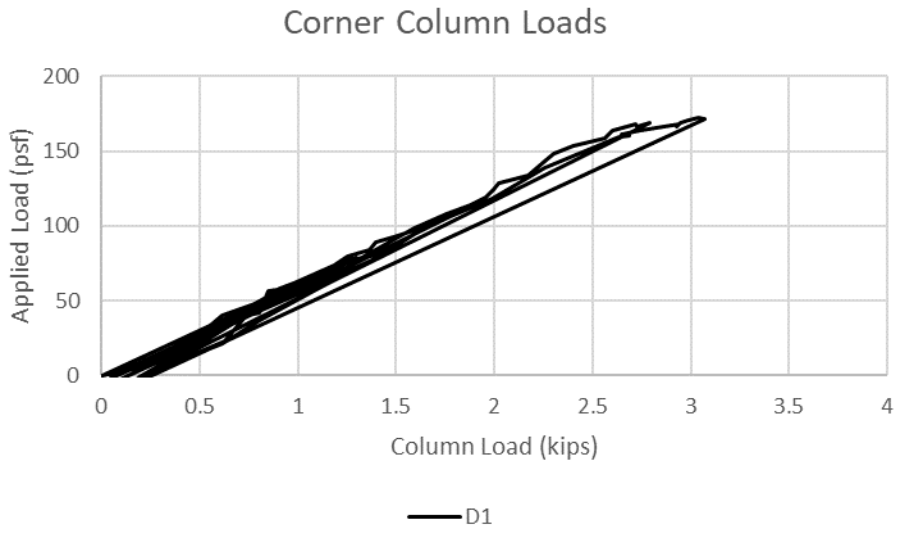

Figure 83. Column Load Cell Readings at Corner Column

The plots of the column load cells were linear throughout most of the loading of Specimen 2. This indicated that there was not much redistribution of loading during the majority of the testing. However, as can be seen for some of the load cells, and especially in load cell D1, towards the end of testing (above 160psf), the slope of the plot decreases slightly. This could possibly be caused by load redistribution in the slab.

Chapter 5 - Conclusions

5.1 Slab Ductility

The slab was assumed to behave inelastically mainly starting around 95psf of applied load, as indicated by several of the load-deflection plots and the load-strain plots. To determine the deflection ductility coefficient for the SFRC post-tensioned flat plate, the final slab deflections at ultimate loading were divided by the deflections at the start of inelasticity. The deflection ductility coefficient and the deflections at the elastic limit and at ultimate loading are provided below in Table 15.

Table 15. Deflections and Ductility

Bay	Deflection at Elastic Limit (in.)	Deflection at Ultimate Loading (in.)	Ductility Coefficient
Bay 1	0.520	2.621	5.04
Bay 2	0.437	2.567	5.88
Bay 3	0.333	2.366	7.11
Bay 4	0.179	1.329	7.43
Bay 5	0.182	0.464	2.54
Bay 6	0.241	0.437	1.81
Bay 7	0.528	1.485	2.81
Bay 8	0.072	0.092	1.28
Bay 9	0.210	0.881	4.20
Bay 10	0.301	1.174	3.90
Bay 11	0.272	1.187	4.36
Bay 12	0.197	0.726	3.69
		Average:	4.17

The average ductility coefficient was 4.17 for the specimen. However, Bays 1 through 4 have an average ductility coefficient of 6.37. This section of the flat plate was where the final failure occurred. The ductility was much higher in the area of failure.

In addition to noticing the ductility of the specimen through deflection measurements, there was plenty of warning of impending failure in the slab prior to the ultimate loading and concrete crushing. Figure 84 shows the large deflections that were observed by the researchers during the load testing.

Figure 84. Deflections Near Columns D1 and D2

Prior to the ultimate loading of the slab and before the bending failure occurred, the researchers noted that they could feel the large deflections while walking on the specimen when marking crack locations. The ability of the slab to deflect significantly enough to provide warning of impending failure highlights the ductility of the SFRC post-tensioned flat plate structural system.

The final failure of the slab was due to large amounts of bending, and it was not a brittle failure. Signs of impending failure were shown by cracks extending across the length of the slab that became especially wide at the bottom surface of the slab. These cracks would be alarming to a building's occupants, which would allow for the prevention of life-safety issues.

5.2 Effects of Removing Negative Moment Reinforcement

Although ACI 318 requires a given amount of negative moment reinforcement in post-tensioned flat plates, only two columns, C2 and C3, had negative moment reinforcement (ACI, 2014). These columns each had four D5 bars. An analysis of the crack widths at each of the columns indicates that the interior columns with no negative moment reinforcement had slightly larger characteristic crack widths when compared to

the cracks at columns C2 and C3 when service-level loads were applied to the slab. Additionally, there were larger quantities of cracks at the interior columns on column line B than at columns C2 and C3 at service-level loads. At factored loading, columns B2 and B3 had more negative moment cracks when compared to columns C2 and C3. The inclusion of negative moment reinforcement at columns C2 and C3 might have helped with crack propagation and widening.

The yield lines that began to form in Specimen 2 consisted of a bottom surface crack between column lines 1 and 2 and a top surface crack running along column line 2. The formation of the top surface crack at column line 2 did not seem to be impacted by the presence of negative moment reinforcement at column C2. The crack running in the uniform tendon direction propagated quicker at column C2 than at column B2.

5.3 Effects of Removing Positive Moment Reinforcement

Specimen 2 experienced concrete crushing between columns B1 and B2 on the top surface of the slab after an applied load of 174psf. This applied load exceeded the factored loadings by 44psf, indicating adequate strength. Despite having no positive moment bonded reinforcement, the slab's strength was higher than expected. Predictions of the slab's strength are provided in Appendix I and were calculated using yield line analysis.

Cracking at the bottom surface of the slab began much later than the formation of cracking on the top surface of the slab, where there were higher negative moments near the columns. No cracking was present at the bottom surface of the slab during service-level loading. At service level loading, the highest positive moment stress was $4.07\sqrt{f'c}$ (see Appendix F for the equivalent frame method analysis at service-level loads). Thus, positive moment reinforcement in steel fiber reinforced concrete post-tensioned flat plates is not necessary if the tensile stresses do not exceed $4\sqrt{f'c}$ in these regions.

5.4 Maximum Tensile Stress Limits

As mentioned previously, ACI 318 states that the maximum allowable tensile stress in prestressed two-way slabs is $6\sqrt{f'_c}$. These slabs are required to be designed as Class U, which assumes uncracked concrete behavior (ACI, 2014). At 80psf of applied load on the slab, a crack extended on the bottom surface across multiple bays. The equivalent frame method was used to analyze the banded interior strip, which is the

controlling strip. A plot of the stresses as a function of $\sqrt{f'_c}$ is provided below in Figure 85.

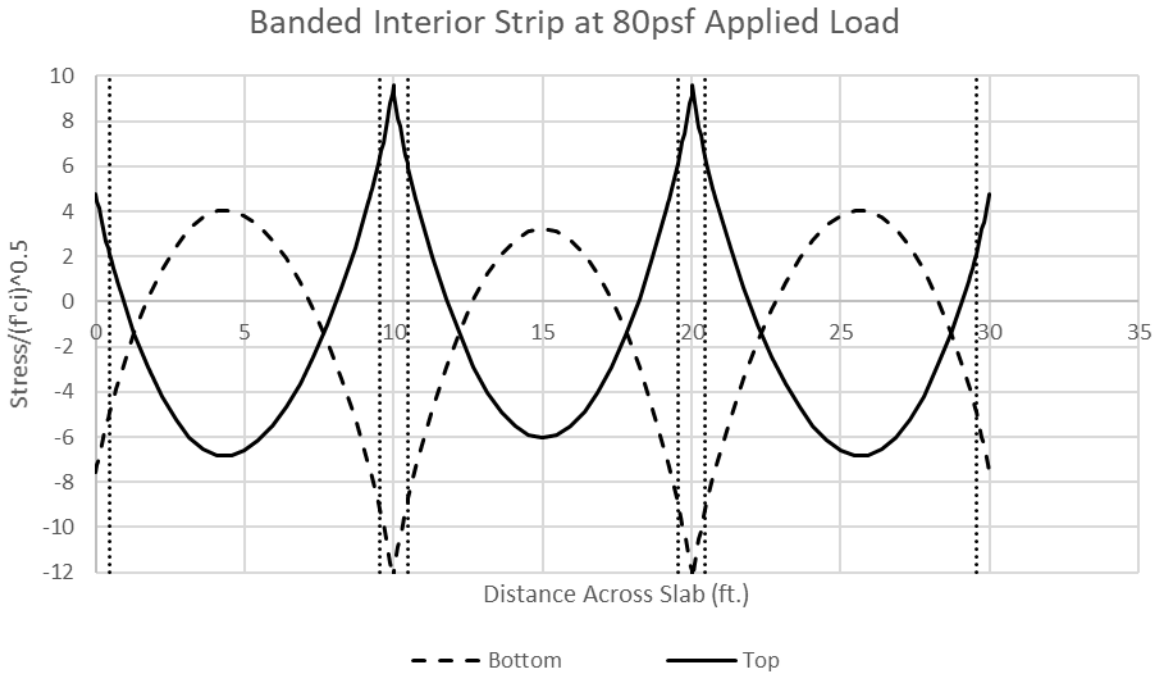

Figure 85. Banded Interior Strip at 80psf Applied Load

The highest stress was determined to be $6.39\sqrt{f'_c}$, which was slightly higher than the ACI limit. This stress occurred at the column face of the interior columns. Although the stress was higher than the ACI limit, the stress was marginally higher. Thus, unless there is more testing performed on SFRC post-tensioned flat plates showing improved performances at stresses above the ACI limit, the stress limits in ACI 318 should not be modified for SFRC post-tensioned flat plates.

5.5 Recommendations

The performance of the SFRC post-tensioned flat plate indicates the high amounts of ductility that can be provided by this structural system. To help control cracking at service-level loads, negative moment reinforcement can be provided, but it is not crucial for allowing the slab to reach its required strength or meet deflection limits. Positive moment reinforcement is not necessary to meet deflection limits or reach required

strengths. Including positive moment reinforcement could delay the onset of bottom surface cracking, but the SFRC post-tensioned flat plate performed well without the reinforcement. Since the highest stresses at service-level loadings during the testing of Spceimen 2 only reached $4.07\sqrt{f'c}$, it is only safe to assume that positive moment reinforcement should not be required if the stresses in the positive moment region are less than $4.\sqrt{f'c}$. The ACI maximum allowable tensile stresses should not be increased for SFRC post-tensioned flat plates due to the cracking behavior of the slab at stresses just above the allowable limits prescribed by ACI 318.

Although the testing of the SFRC post-tensioned flat plate provided promising results in terms of reduced amounts of reinforcement in the positive and negative moment regions, it is recommended that changes should not be made to ACI 318 until Specimen 1 is tested. The testing of Specimen 1 will allow for a more definitive analysis of the contribution of steel fibers to the performance of the scale-model post-tensioned flat plate.

References

423, A.-A. C. (1974). *Tentative Recommendations for Prestressed Concrete Flat Plates*. Retrieved from

Aalami, B. O. (2007). Critical Milestones in Development of Post-Tensioned Buildings. *Concrete International, 29*(10), 52-56.

Abdel-Rahman, A. M., Hassan, N. Z., & Soliman, A. M. (2018). Punching Shear Behavior of Reinforced Concrete Slabs Using Steel Fibers in the Mix. *Hosing and Building National Research Center, 14*(December 2018), 272-281.

ACI. (2014). Building Code Requirements for Structural Concrete (ACI 318-14). In: American Concrete Institute.

Ackermann, F. P., & Schnell, J. (2008). Steel Fibre Reinforced Continuous Composite Slabs. In *Composite Construction in Steel and Concrete VI* (pp. 125-137).

ASBL, E. C. P. (2008). *Eurcode 2 Commentary*. Brussels, Belgium: European Concrete Platform ASBL.

Barros, J. A. O., & Figueiras, J. A. (1999). Flexural Behavior of SFRC: Testing and Modeling. *Journal of Materials in Civil Engineering, 11*(4), 331-339. doi:doi:10.1061/(ASCE)0899-1561(1999)11:4(331)

Blanco, A., Pujadas, P., Fuente, A. D. l., Cavalaro, S. H. P., & Aguado, A. (2016). Influence of the Type of Fiber on the Structural Response and Design of FRC Slabs. *Journal of Structural Engineering, 142*(9), 04016054-04016051 - 04016054-04016011. doi:doi:10.1061/(ASCE)ST.1943-541X.0001515

Brandt, A. M. (2008). Fibre Reinforced Cement-Based (FRC) Composites After Over 40 Years of Development in Building and Civil Engineering. *Composite Structures, 86*(November 2008), 3-9.

Burns, N. H., & Hemakom, R. (1977). Test of Scale Model of Post-Tensioned Flat Plate. *Journal of the Structural Division, 103*(ST6), 1237-1255.

Burns, N. H., & Hemakom, R. (1985). Test of Post‐Tensioned Flat Plate with Banded Tendons. *Journal of Structural Engineering, 111*(9), 1899-1915. doi:doi:10.1061/(ASCE)0733-9445(1985)111:9(1899)

CEN. (2005). Test Method for Metallic Fibered Concrete - Measuring the Flexural Tensile Strength (Limit of Proportionality (LOP), residual). In. Brussels: European Committee for Standardization.

Council, A. W. (2014). National Design Specification for Wood Construction with Commentary. In.

Destrée, X. (2001). Steel Fibre Reinforcement for Suspended Slabs. *Concrete, 35*(8), 58-59.

Destrée, X. (2009). Steel-Fibre-Only Reinforced Concrete in Free Suspended Elevated Slabs. *Concrete Engineering International, Spring 2009*, 47-49.

Fall, D., Rempling, R., & Lundgren, K. (2013). Experiments on Fibre Reinforced Concrete Two-Way Slabs. *Fibre Concrete, 2013*.

Fall, D., Shu, J., Rempling, R., Lundgren, K., & Zandi, K. (2014). Two-Way Slabs: Experimental Investigation of Load Redistributions in Steel Fibre Reinforced Concrete. *Engineering Structures, 80*(2014), 61–74. doi:10.1016/j.engstruct.2014.08.033

Gamble, W. L., & Burns, N. H. (1981). Reinforced and Prestressed Concrete Slabs. *SP-072: Significant Developments in Engineering Practice and Research, 72*(6), 149-162.

Gerber, L. L., & Burns, N. H. (1971). Ultimate Strength Tests of Post-Tensioned Flat Plates. *PCI Journal, November-December 1971*, 40-58.

Gouveia, N. D., Fernandes, N. A. G., Faria, D. M. V., Ramos, A. M. P., & Lucio, V. J. G. (2014). SFRC Flat Slabs Punching Behaviour - Experimental Research. *Composites: Part B, 63*(July 2014), 161-171.

Hemakom, R. (1975). *Strength and Behavior of Post-Tensioned Flat Plates with Unbonded Tendons.* (Ph.D.), The University of Texas at Austin,

Hind, M. K., Ozakca, M., & Ekmekyapar, T. (2016). A Review on Nonlinear Finite Element Analysis of Reinforced Concrete Beams Retrofitted with Fiber Reinforced Polymers. *Journal of Advanced Research in Applied Mechanics, 22*(1), 13-48.

Inerkar, K. A. (2018). *Design of Loading System and Preliminary Analysis of One-Third Test Scale Model of a Post-Tensioned Flat Plate*. Virginia Tech.

Institute, A. C. (2015). *ACI 544.6R-15; Report on Design and Construction of Steel Fiber-Reinforced Concrete Elevated Slabs*. Retrieved from

International, A. (2019). ASTM C1609 / C1609M-19, Standard Test Method for Flexural Performance of Fiber-Reinforced Concrete (Using Beam With Third-Point Loading). In. West Conshohocken, PA: ASTM International.

Jensen, S. M. F., & Overli, J. A. (2015). Steel Fibres as Reinforcement in Post-Tensioned Flat Slabs. *Civil Engineering and Architecture, 3*(5), 89-98.

Khanlou, A., MacRae, G., Scott, A., Hicks, S., Clifton, C., Leon, R., & Gholamhoseini, A. (2016). Composite Slab Crack Widths Considering Shrinkage and Gravity Loading. In *Composite Construction in Steel and Concrete VII* (pp. 754-762).

Kim, M. S., & Lee, Y. H. (2016). Flexural Behavior of Posttensioned Flat Plates Depending on Tendon Layout. *Advances in Materials Science & Engineering*, 1-11. doi:10.1155/2016/2651435

Kosut, G. M., Burns, N. H., & Winter, C. V. (1985). Test of Four-Panel Post-Tensioned Flat Plate. *Journal of Structural Engineering, 111*(9), 1916-1929. doi:doi:10.1061/(ASCE)0733-9445(1985)111:9(1916)

Li, J. (2019). *Equivalent Frame Analysis of 1/3rd Scale Model of a Post-Tensioned Flat Plate and Comparison of the Model and the Full-Scale Prototype*. Retrieved from Blacksburg, VA:

Lin, T. Y. (1963). Load-Balancing Method for Design and Analysis of Prestressed Concrete Structures. *ACI Journal Proceedings, 60*(6), 719-742.

Lok, T. S., & Xiao, J. R. (1999). Flexural Strength Assessment of Steel Fiber Reinforced Concrete. *Journal of Materials in Civil Engineering, 11*(3), 188-196. doi:doi:10.1061/(ASCE)0899-1561(1999)11:3(188)

Marti, P., Ritz, P., & Thurlimann, B. (Eds.). (1977). *Prestressed Concrete Flat Slabs*: Springer Basel AG.

McMahon, J. A., & Birely, A. C. (2018). Service Performance of Steel Fiber Reinforced Concrete (SFRC) Slabs. *Engineering Structures, 168*(August 2018), 58-68.

Michels, J., Waldmann, D., Maas, S., & Zurbes, A. (2012). Steel Fibers as Only Reinforcement for Flat Slab Construction - Experimental Investigation and Design. *Construction and Building Materials, 26*(January 2012), 145-155.

Nguyen-Minh, L., Rovnak, M., Tran-Quoc, T., & Nguyen-Kim, K. (2011). Punching Shear Resistance of Steel Fiber Reinforced Concrete Flat Slabs. *Procedia Engineering, 14*(2011), 1830-1837.

Parmentier, B., Van Itterbeeck, P., & Skowron, A. (2014). *The flexural behaviour of SFRC flat slabs: the Limelette full-scale experiments for supporting design model codes*. Paper presented at the FRC 2014 Joint ACI-fib International Workshop.

Ramos, A. P., & Lucio, V. J. G. (2008). Post-Punching Behavior of Prestressed Concrete Flat Slabs. *Magazine of Concrete Research, 60*(4), 245-251.

. RISA-2D Demo. RISA Tech, Inc.

Salehian, H., & Barros, J. A. O. (2015). Assessment of the Performance of Steel Fibre Reinforced Self-Compacting Concrete in Elevated Slabs. *Cement and Concrete Composites, 55*, 268-280. doi:https://doi.org/10.1016/j.cemconcomp.2014.09.016

Salehian, H., & Barros, J. A. O. (2017). Prediction of the Load Carrying Capacity of Elevated Steel Fibre Reinforced Concrete Slabs. *Composite Structures, 170*(June 2017), 169-191.

Salehian, H., Barros, J. A. O., & Taheri, M. (2014). Evaluation of the Influence of Post-Cracking Response of Steel Fibre Reinforced Concrete (SFRC) on Load Carrying Capacity of SFRC Panels. *Construction and Building Materials, 73*(December 2014), 289-304.

Scordelis, A. C., Lin, T. Y., & Itaya, R. (1959). Behavior of a Continuous Slab Prestressed in Two Directions. *ACI Journal Proceedings, 56*(12), 441-460.

Services, T. (2019a). *Verification Mix - Truck #1 - SEL-19-001*. Retrieved from

Services, T. (2019b). *Verification Mix - Truck #2 - SEL-19-001*. Retrieved from

Silva, R. J. C., Regan, P. E., & Melo, G. S. S. A. (2007). Punching of Post-Tensioned Slabs - Tests and Codes. *ACI Structural Journal, 104*(2), 123-128.

Smith, S. W., & Burns, N. H. (1974). Post-Tensioned Flat Plate to Column Connection Behavior. *PCI Journal, May-June 1974*, 74-91.

Tan, K. H., & Paramasivam, P. (1994). Punching Shear Strength of Steel Fiber Reinforced Concrete Slabs. *Journal of Materials in Civil Engineering, 6*(2), 240-253. doi:doi:10.1061/(ASCE)0899-1561(1994)6:2(240)

Appendix A – Trial Slab Design Drawings

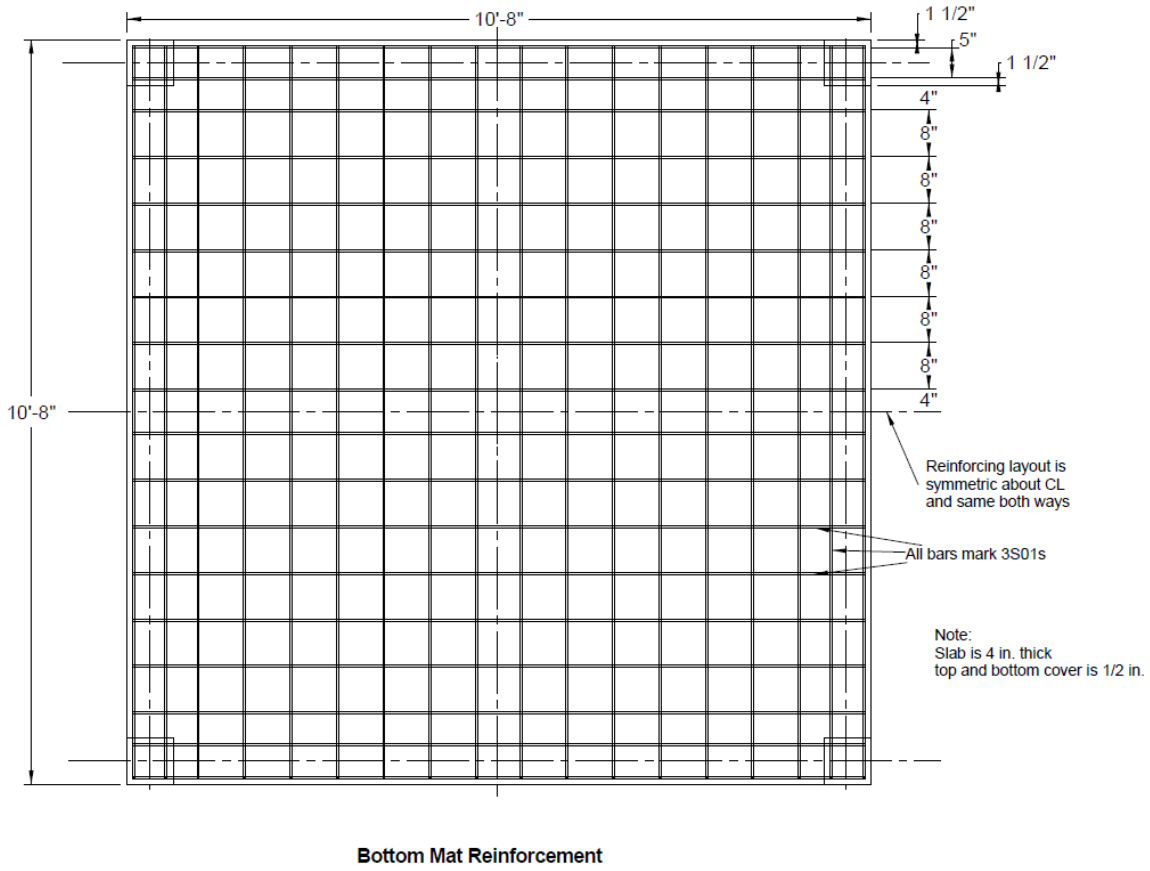

Figure A.1. Trial Slab Bottom Mat Reinforcement

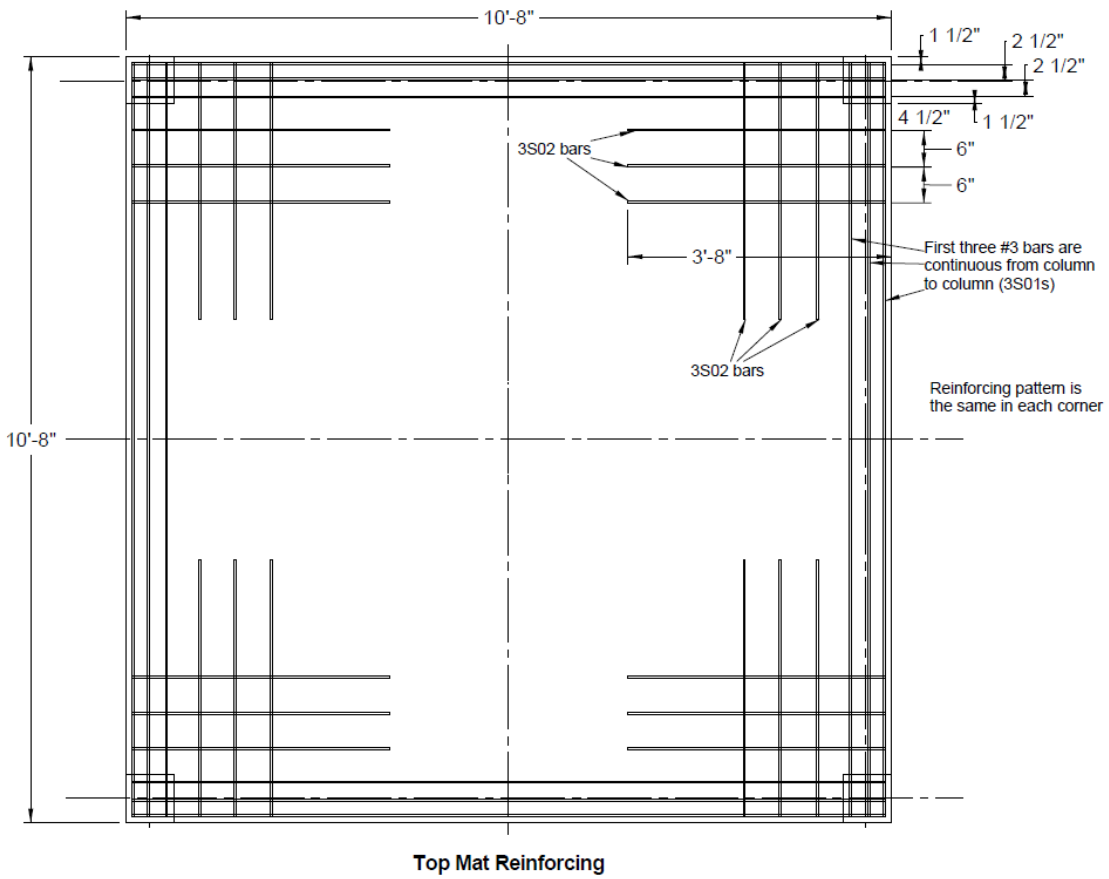

Figure A.2. Trial Slab Top Mat Reinforcement

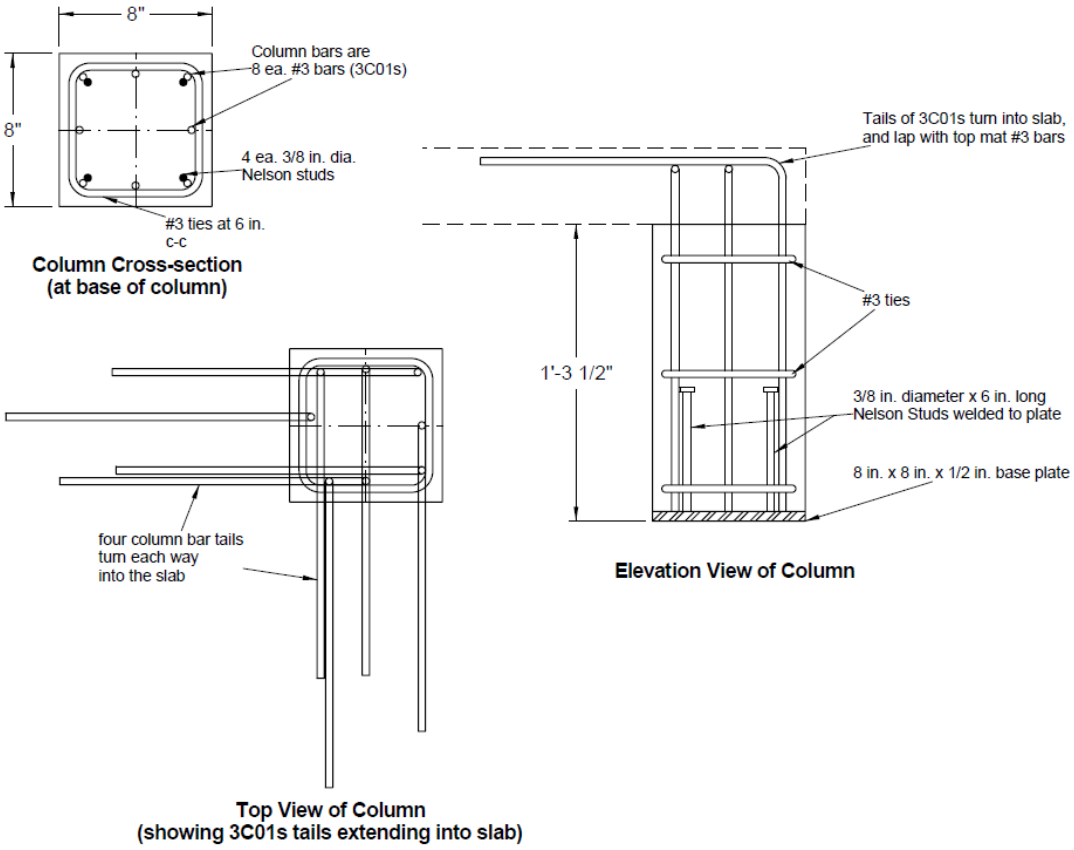

Figure A.3. Trial Slab Column Reinforcement

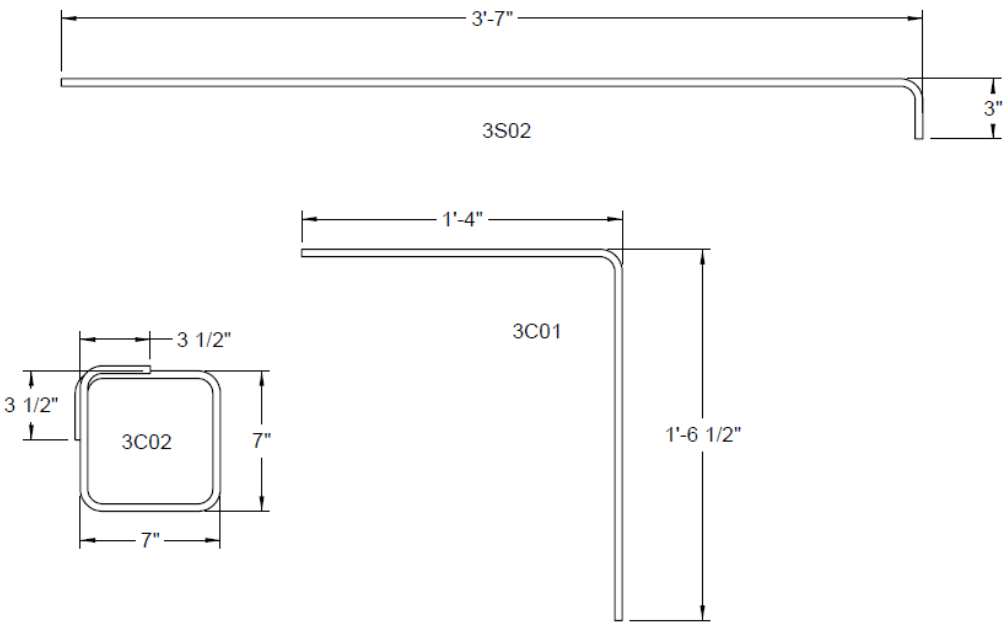

Bar Mark	Bar Size	ST or Bent	Number	Length	wt/ft	total wt	
3S01	#3	Straight	50	10'-6"	0.376	197.4	lbs
3S02	#3	Bent	24	3'-10"	0.376	34.6	lbs
3C01	#3	Bent	32	2'-10.5"	0.376	34.6	lbs
3C02	#3	Bent	12	2'-11"	0.376	13.2	lbs
					SUM	279.7	lbs

Figure A.4. Trial Slab Reinforcement Details

Appendix B – Specimen 2 Design Drawings

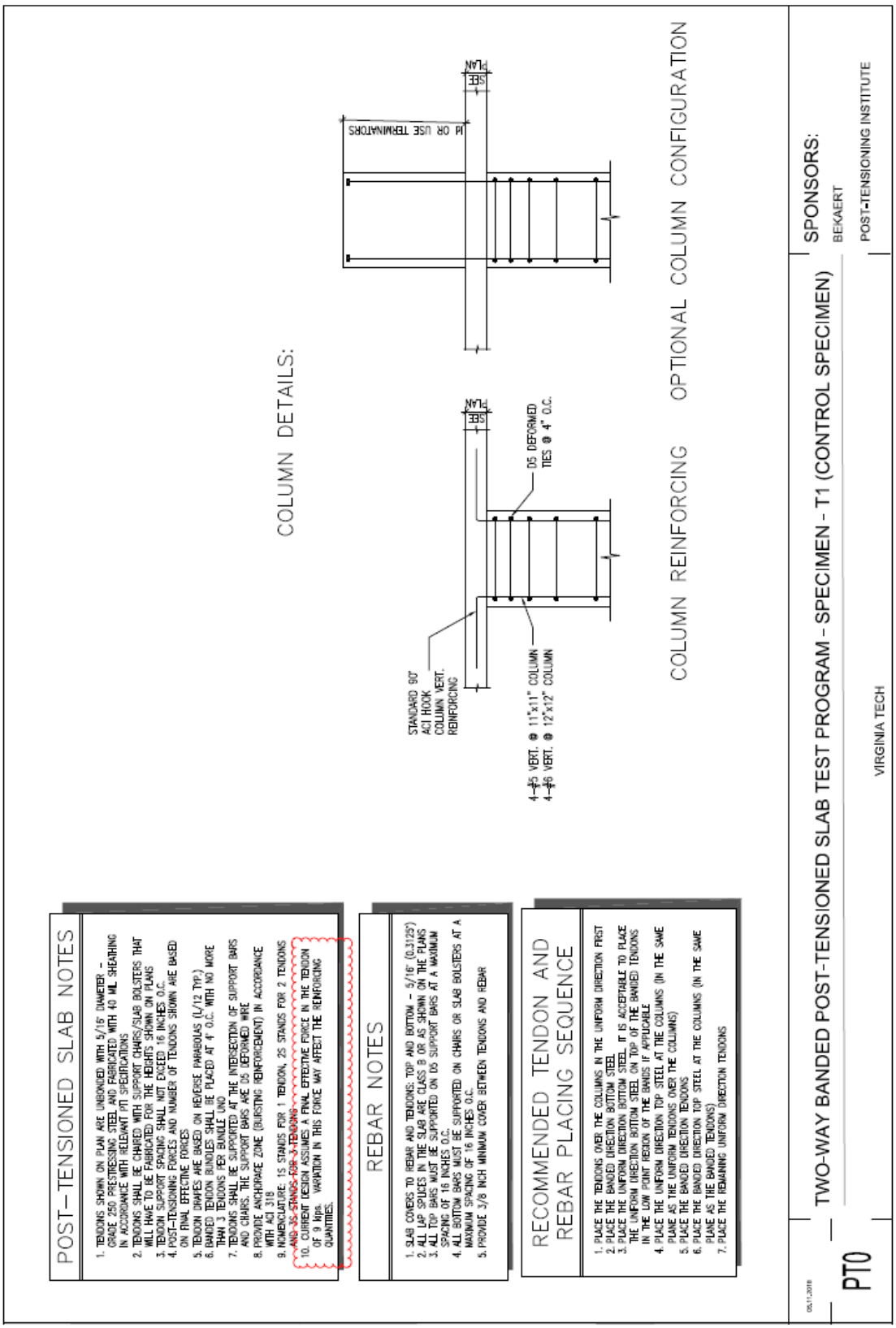

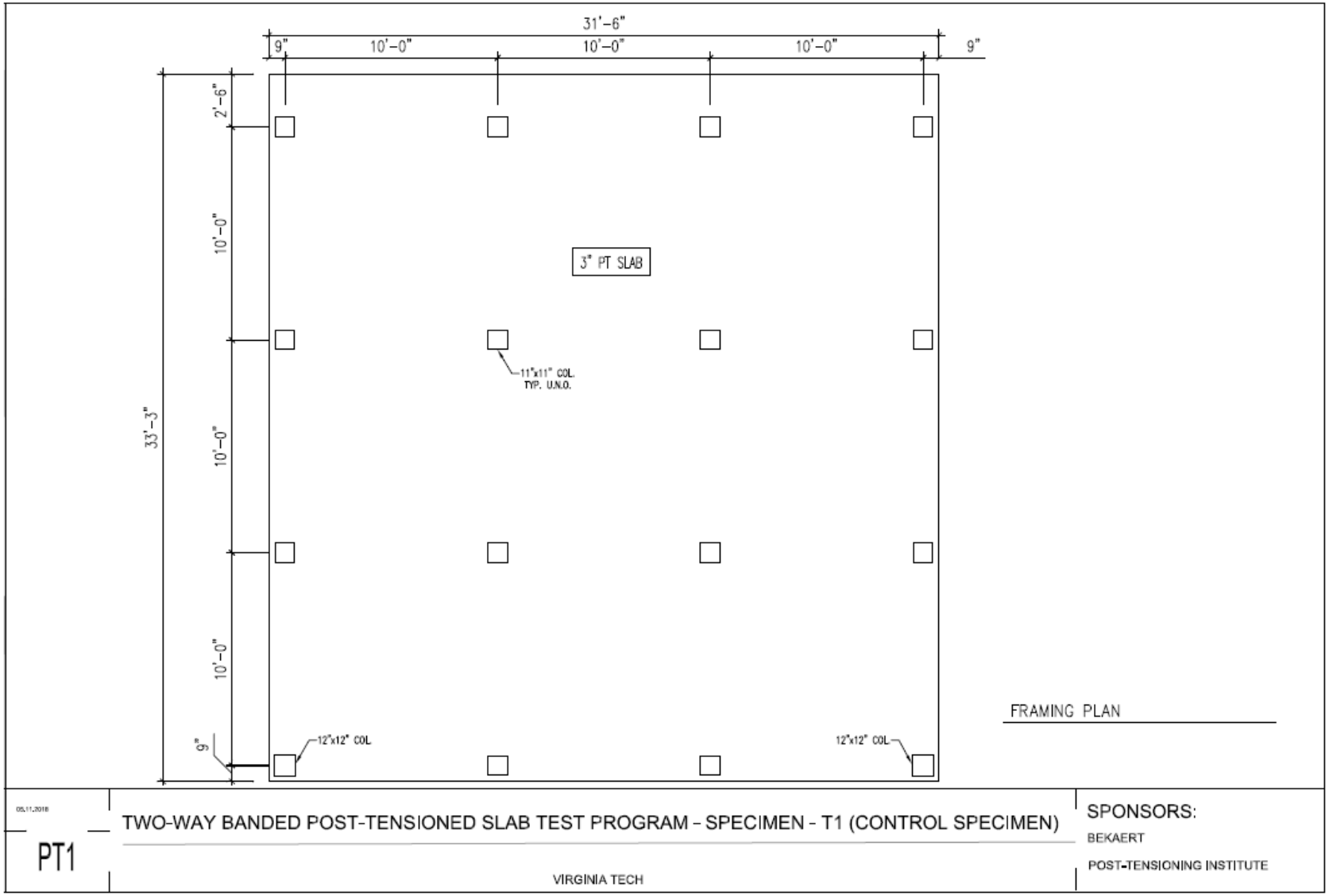
31'-6"
9"
10'-0"
10'-0"
10'-0"
9"
2'-6"
10'-0"
10'-0"
10'-0"
33'-3"
3" PT SLAB
11"x11" COL.
TYP. U.N.O.
9"
12"x12" COL
12"x12" COL
FRAMING PLAN
05.11.2018
PT1
TWO-WAY BANDED POST-TENSIONED SLAB TEST PROGRAM - SPECIMEN - T1 (CONTROL SPECIMEN)
VIRGINIA TECH
SPONSORS:
BEKAERT
POST-TENSIONING INSTITUTE

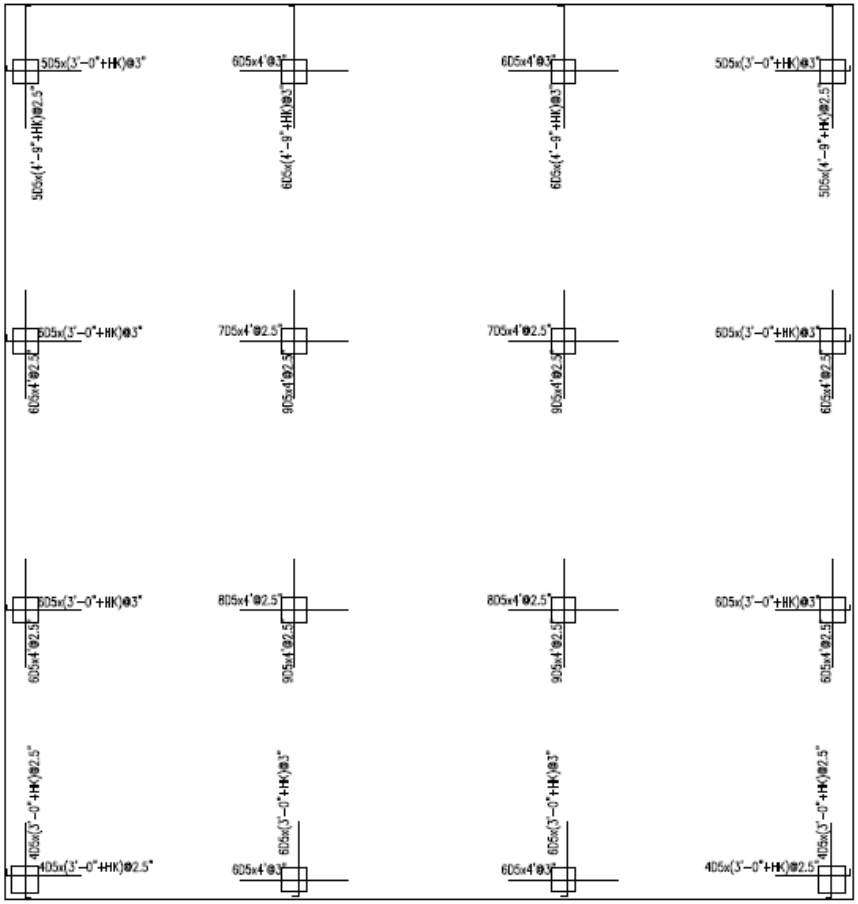

TOP REBAR PLAN

05.11.2018

PT2

TWO-WAY BANDED POST-TENSIONED SLAB TEST PROGRAM – SPECIMEN – T1 (CONTROL SPECIMEN)

VIRGINIA TECH

SPONSORS:

BEKAERT

POST-TENSIONING INSTITUTE

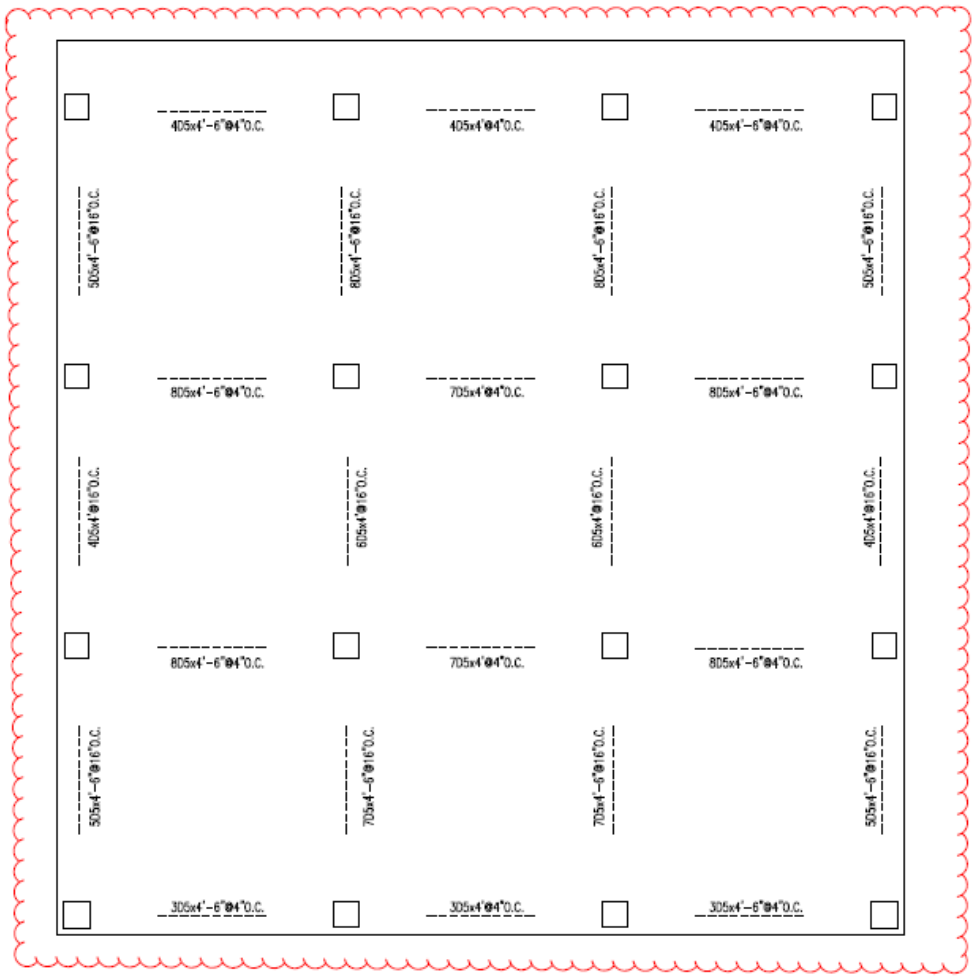

BOTTOM REBAR PLAN

05.11.2018

PT3

TWO-WAY BANDED POST-TENSIONED SLAB TEST PROGRAM – SPECIMEN - T1 (CONTROL SPECIMEN)

VIRGINIA TECH

SPONSORS:

BEKAERT

POST-TENSIONING INSTITUTE

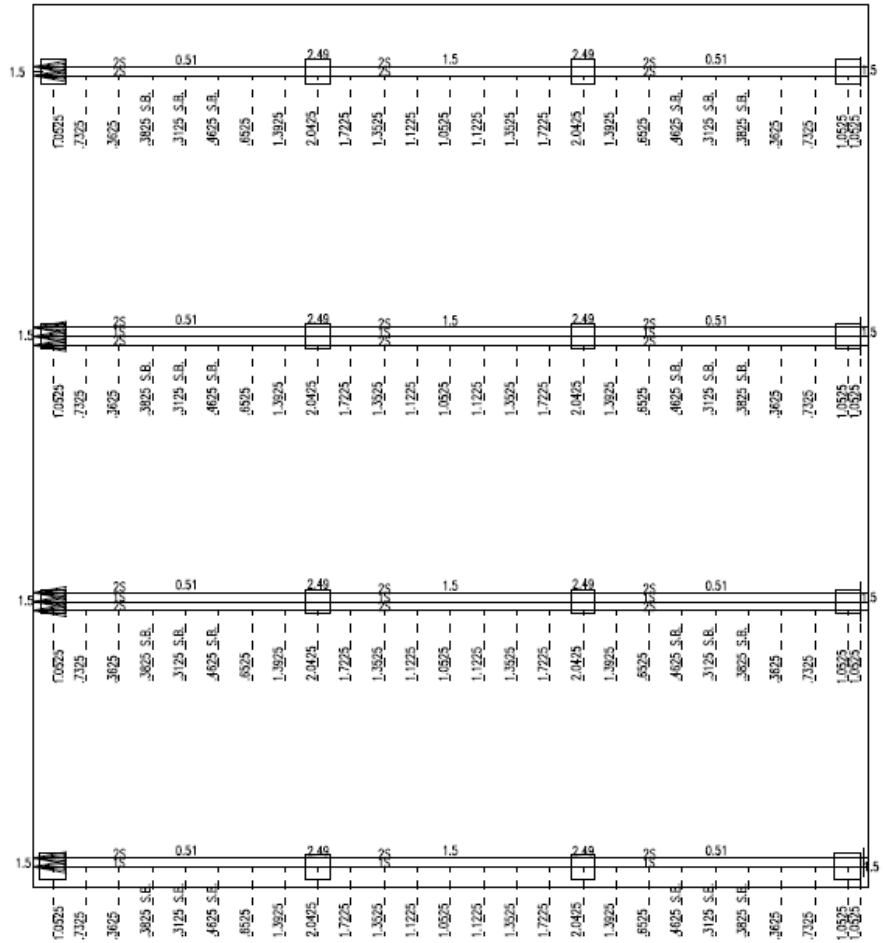

BANDED TENDON PLAN – (E–W)

NOTES: PLAN SHOWS CHAIR HEIGHTS BELOW D5 SUPPORT BAR. TENDON SITS DIRECTLY ON SLAB BOLSTER WHERE S.B. SHOWN

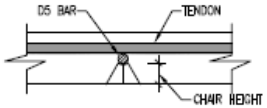

CHAIR SUPPORT

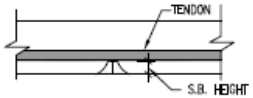

SLAB BOLSTER SUPPORT

05.11.2018

PT4

TWO-WAY BANDED POST-TENSIONED SLAB TEST PROGRAM - SPECIMEN - T1 (CONTROL SPECIMEN)

VIRGINIA TECH

SPONSORS:

BEKAERT

POST-TENSIONING INSTITUTE

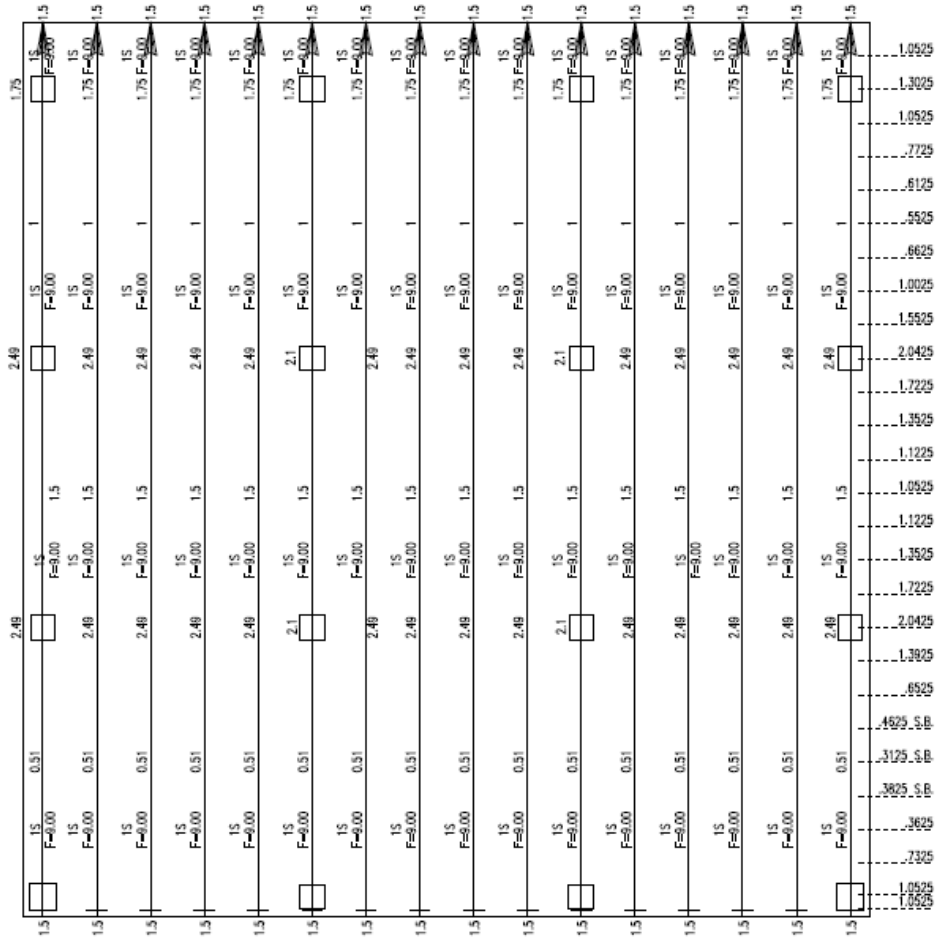

UNIFORM TENDON PLAN – (N–S)

NOTES: PLAN SHOWS CHAIR HEIGHTS BELOW 1D5 SUPPORT BAR. TENDON SITS DIRECTLY ON SLAB BOLSTER WHERE S.B. SHOWN

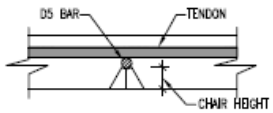

CHAIR SUPPORT

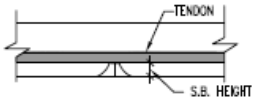

SLAB BOLSTER SUPPORT

05.11.2018

PT5

TWO-WAY BANDED POST-TENSIONED SLAB TEST PROGRAM – SPECIMEN – T1 (CONTROL SPECIMEN)

VIRGINIA TECH

SPONSORS:

BEKAERT

POST-TENSIONING INSTITUTE

Appendix C – Formwork Drawings for Specimen 2

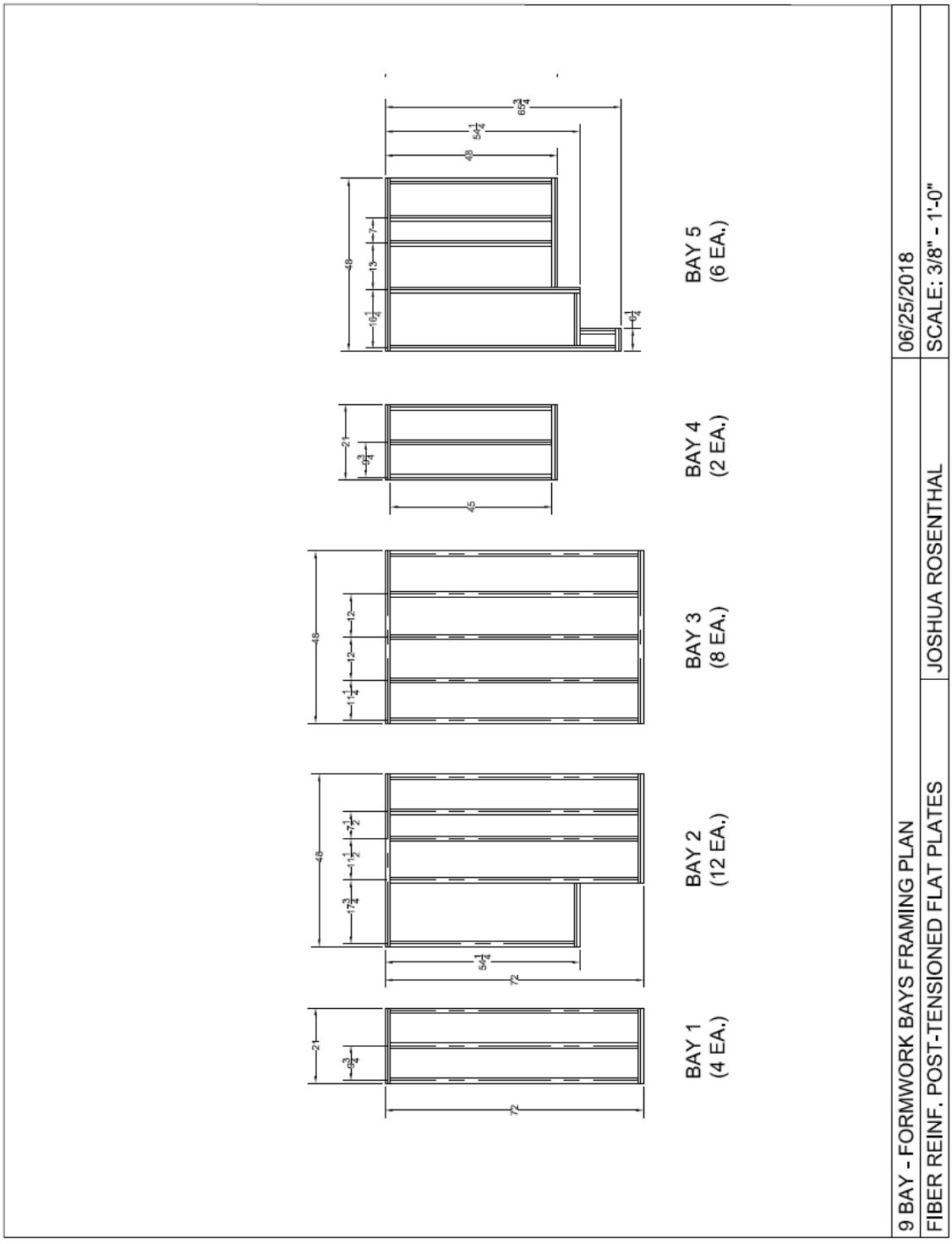

Figure C.1. Bay Dimensions

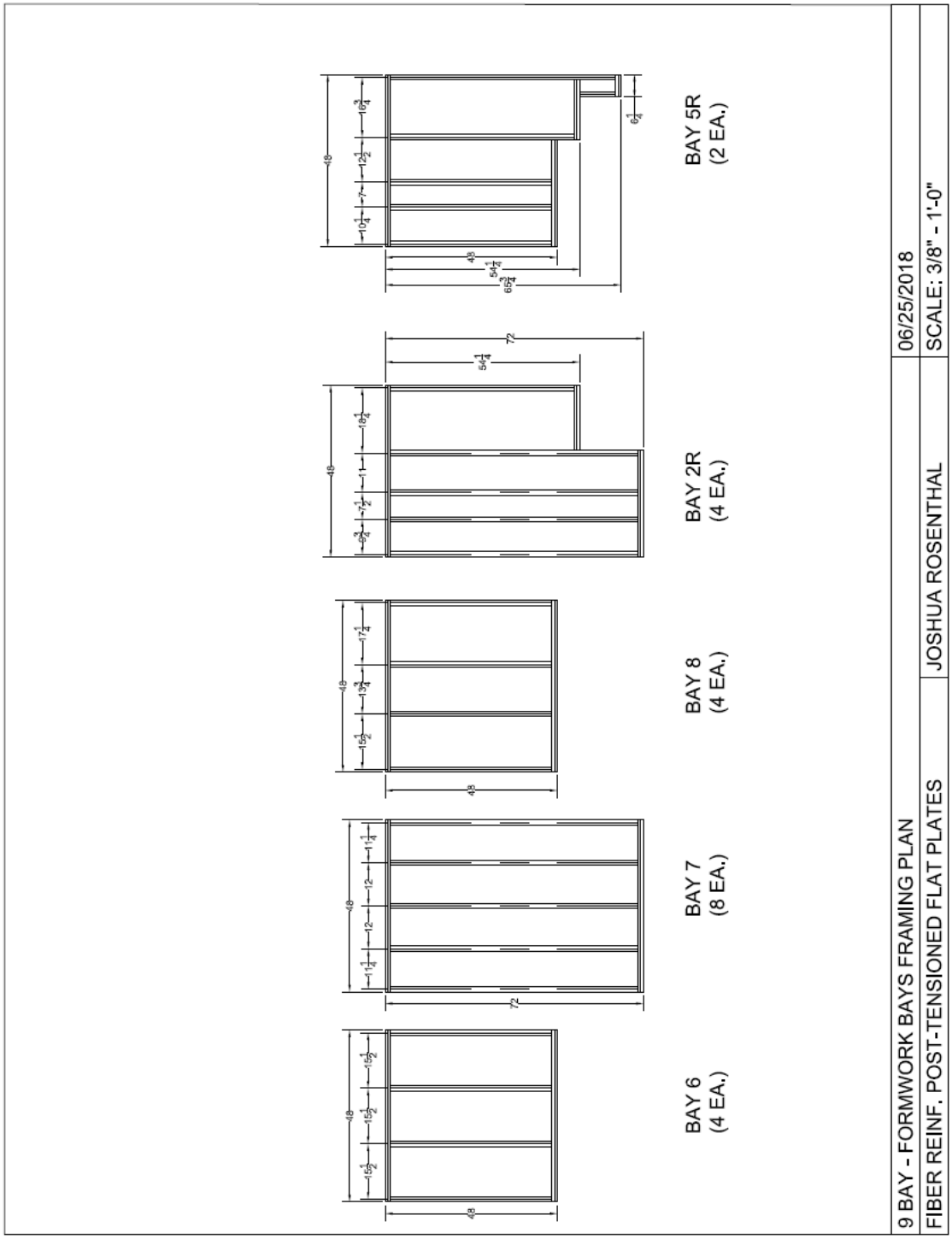

Figure C.2. Bay Dimensions

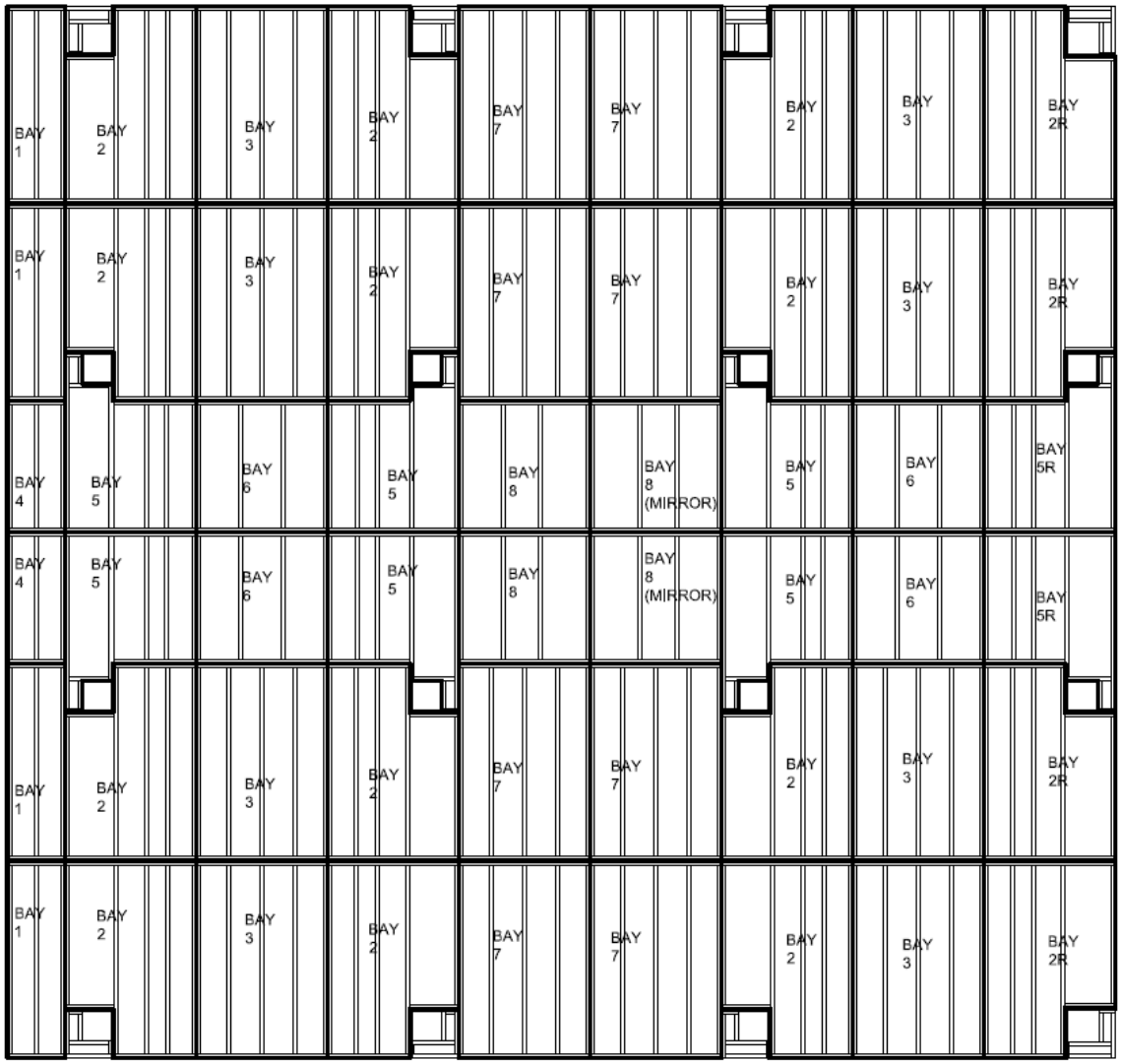

Figure C.3. Bay Layout

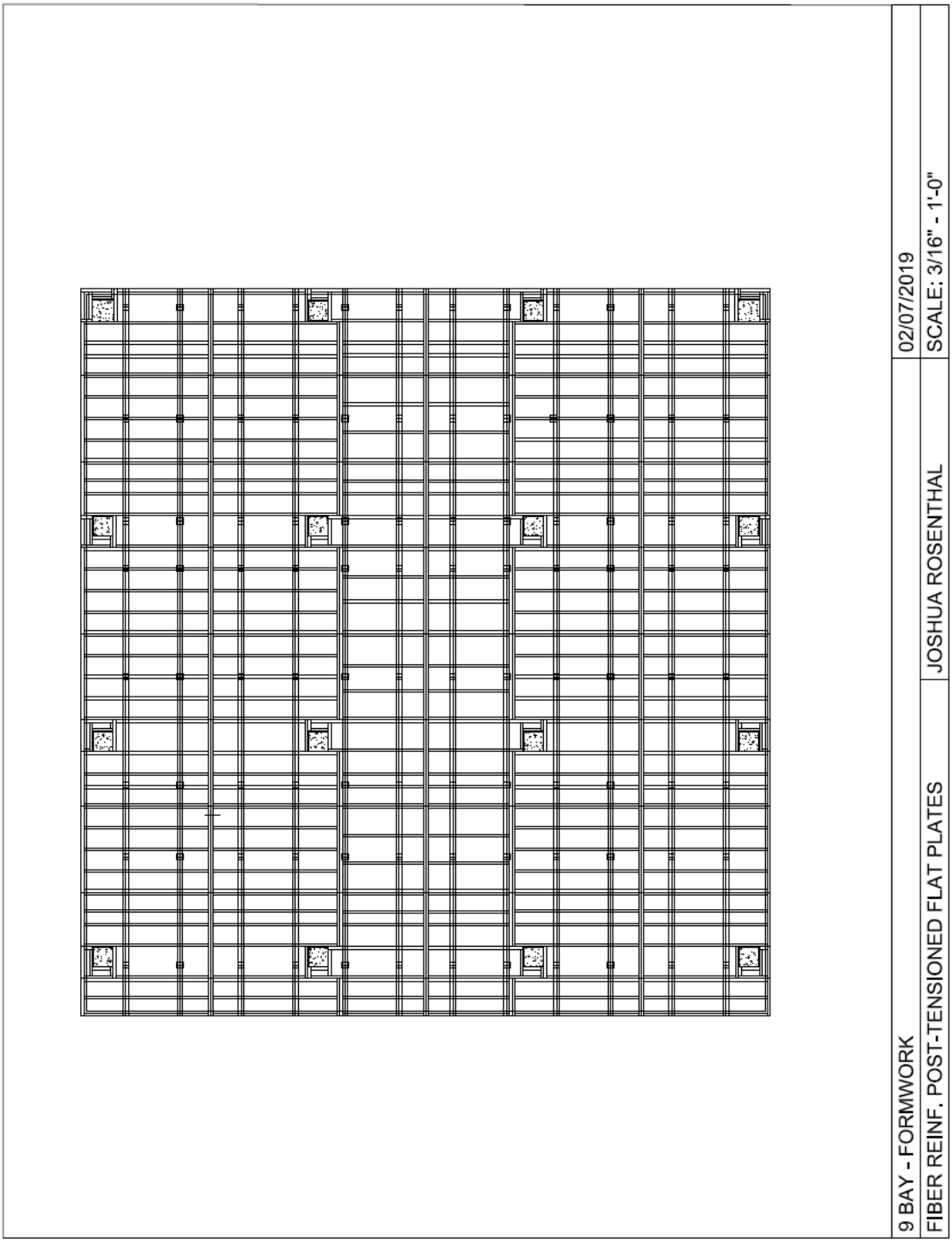

Figure C.4. Formwork Summary

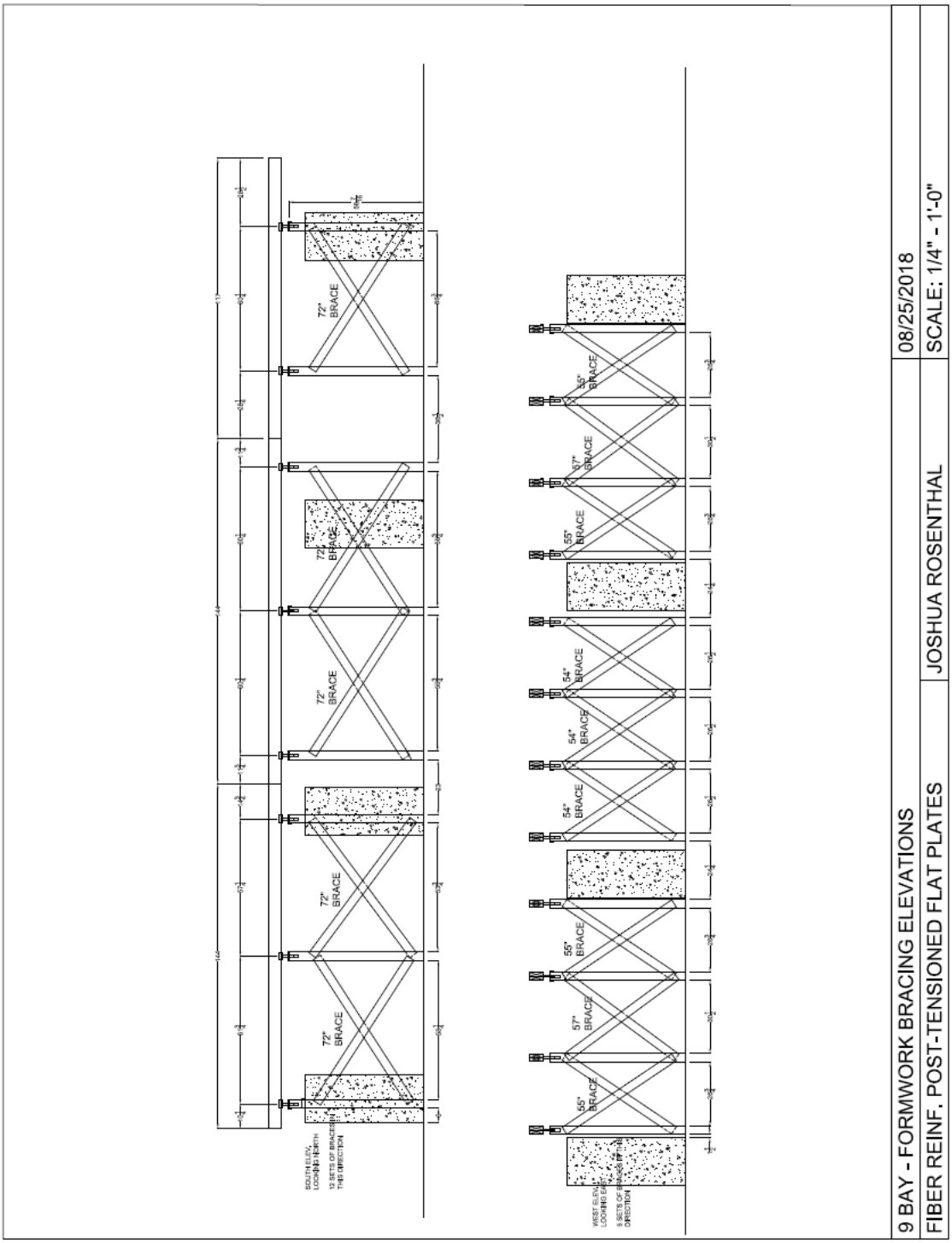

Figure C.5. Bracing Elevations

Appendix D – Data Acquisition Wiring Diagrams and Programs

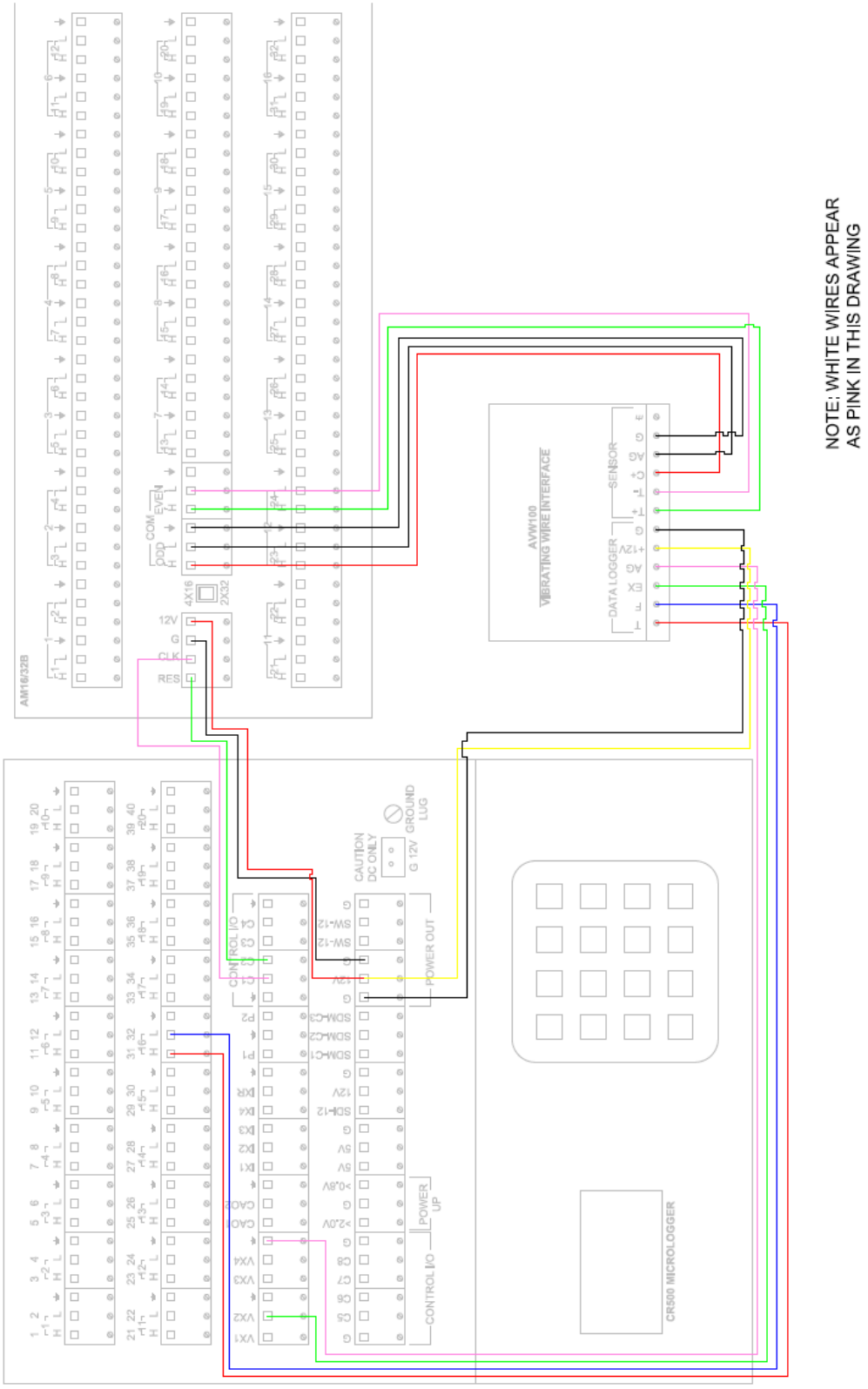

Figure D.1. Connection Between CR5000, VWG Multiplexer, and AVW100

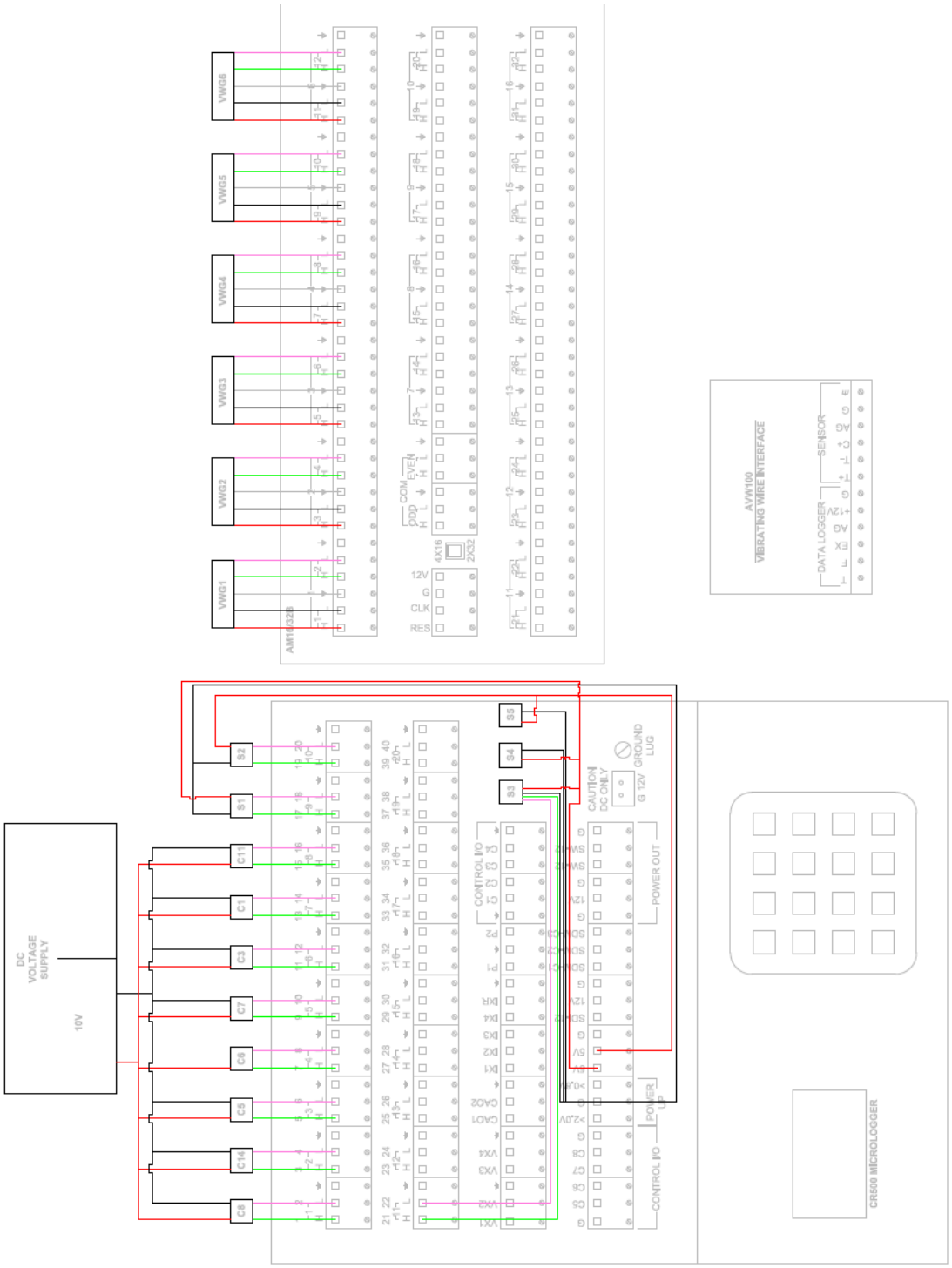

Figure D.2. Instrument Wiring to CR5000 and VWG Multiplexer

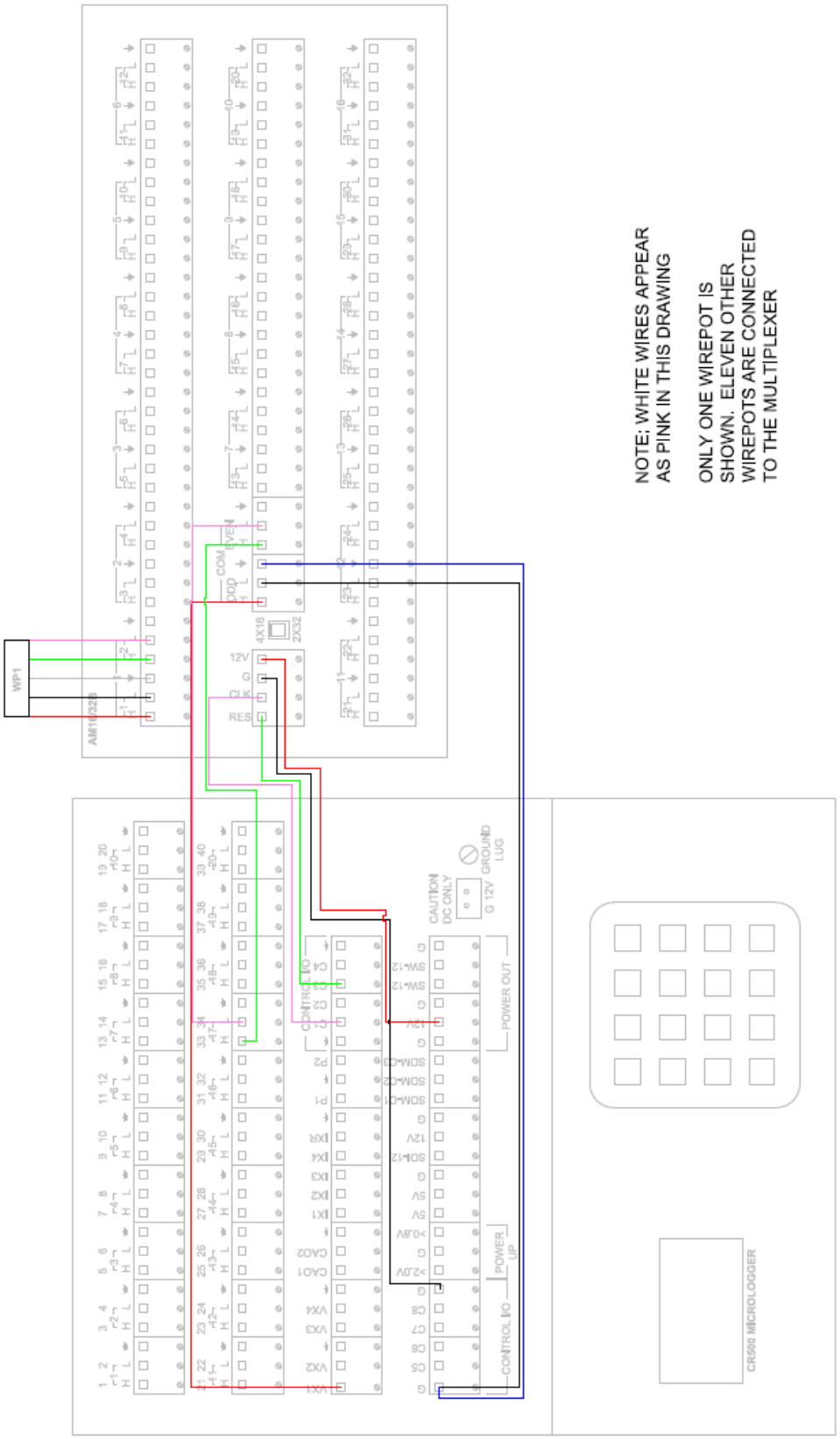

Figure D.3. Wiring for Wirepot Multiplexer

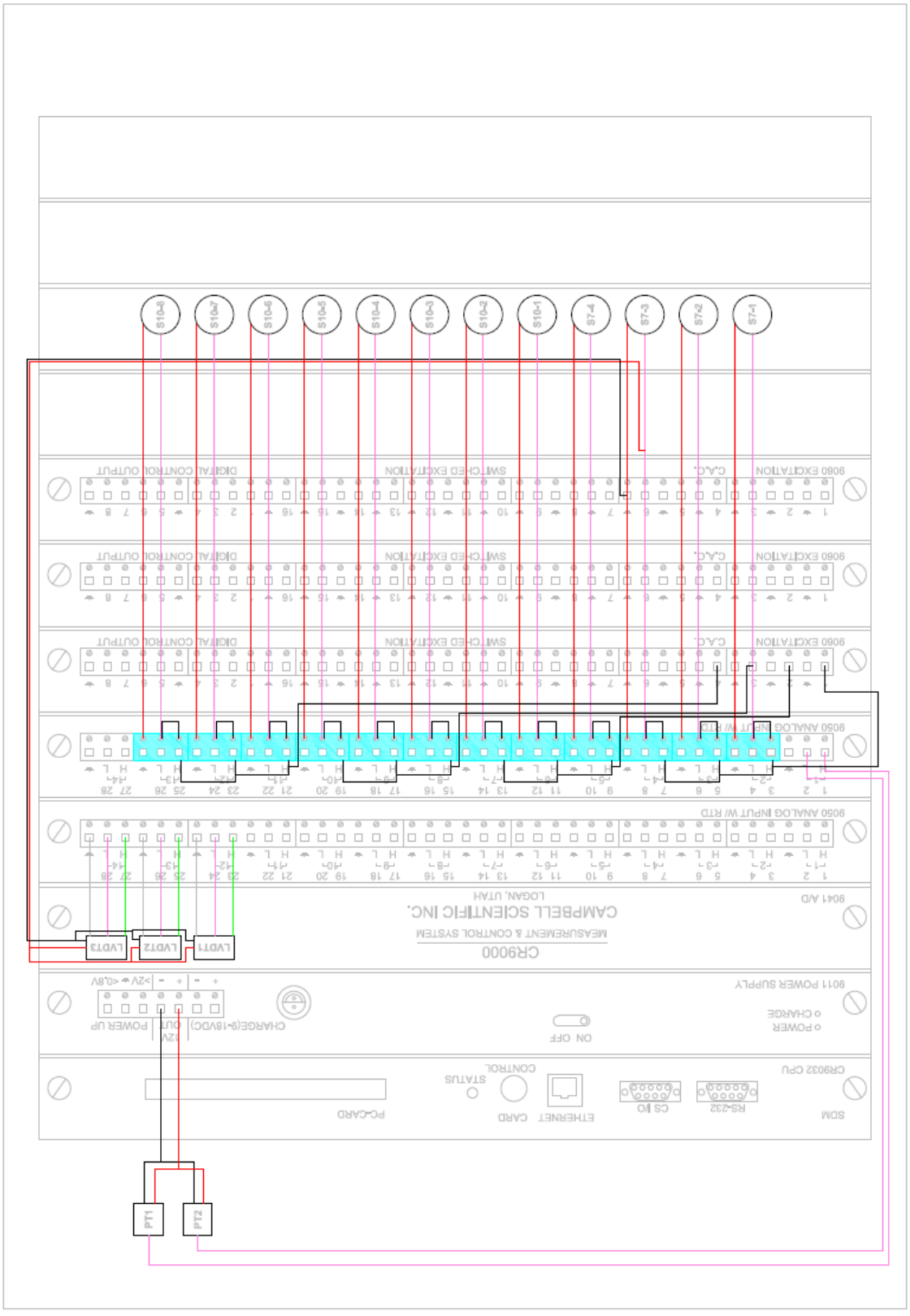

Figure D.4. Instrument Wiring to CR9000

The following program (5000-Final-3sec.CR5) was used for the CR5000 while actively stressing the tendons and lowering the formwork.

```
'                  Program name: 5000-PROGRAMGENERATOR1.CR5
'                   Written by: Name
'                   I.D. number: Number
'                  Date written: 01-11-2019
'                  Time written: 10:52:35
'                RT5GEN Version: 6.0.0066

' This program was generated using Campbell Scientific's RT5GEN
' Program Generator for the CR5000 Measurement & Control System.

'\\\\\\\\\\\\\\\\\\\\\\ TIMING CONSTANTS //////////////////////

Dim LCount_5
Const PERIOD = 3000                         'Scan interval number
Const P_UNITS = 1                           'Scan interval units (mSecs)

Const INTERVAL1 = 3000                      'Table 1 interval number
Const UNITS1 = 1                            'Table 1 interval units (mSecs)

Const INTERVAL2 = 3000                      'Table 2 interval number
Const UNITS2 = 1                            'Table 2 interval units (mSecs)

'\\\\\\\\\\\\\\\\\\\\\\ VOLTAGE CONSTANTS //////////////////////

'_____________________________ Volt Block 1 _____________________________
Const VRNG1 = 5                             'Block1 measurement range (Auto)
Const VREP1 = 8                             'Block1 repetitions
Const VSETL1 = 200                          'Block1 settling time (usecs)
Const VINT1 = 250                           'Block1 integration time (usecs)
Const VMULT1 = 1                            'Block1 default multiplier
Const VOSET1 = 0                            'Block1 default offset
Public VBlk1(VREP1)                         'Block1 dimensioned source
Public MVBlk1(VREP1)                        'Block1 dimensioned multiplier
Public OVBlk1(VREP1)                        'Block1 dimensioned offset
Public VCalMode1
Public VKnownVar1(VREP1)
Units VBlk1 = mVolts                        'Block1 default units (mVolts)
Public VCalReps1
'_____________________________ Volt Block 2 _____________________________
Const VRNG2 = 5                             'Block2 measurement range (Auto)
Const VREP2 = 7                             'Block2 repetitions
Const VSETL2 = 200                          'Block2 settling time (usecs)
Const VINT2 = 250                           'Block2 integration time (usecs)
```

```
Const VMULT2 = 1                    'Block2 default multiplier
Const VOSET2 = 0                    'Block2 default offset
Public VBlk2(VREP2)                 'Block2 dimensioned source
Public MVBlk2(VREP2)                'Block2 dimensioned multiplier
Public OVBlk2(VREP2)                'Block2 dimensioned offset
Public VCalMode2
Public VKnownVar2(VREP2)
Units VBlk2 = mVolts                'Block2 default units (mVolts)
Public VCalReps2



Public vWG(6)
Units vWG=ustrain



'\\\\\\\\\\\\\\\\\ ALIASES & OTHER VARIABLES /////////////////

Units VBlk1(1) = kips               'Assign units "kips" to VBlk1(1)
Alias MVBlk1(1) = M$VBlk1_1             'Assign alias name "M$VBlk1_1" to MVBlk1_1
Alias OVBlk1(1) = O$VBlk1_1             'Assign alias name "O$VBlk1_1" to OVBlk1_1
Units VBlk1(2) = kips               'Assign units "kips" to VBlk1(2)
Alias MVBlk1(2) = M$VBlk1_2             'Assign alias name "M$VBlk1_2" to MVBlk1_2
Alias OVBlk1(2) = O$VBlk1_2             'Assign alias name "O$VBlk1_2" to OVBlk1_2
Units VBlk1(3) = kips               'Assign units "kips" to VBlk1(3)
Alias MVBlk1(3) = M$VBlk1_3             'Assign alias name "M$VBlk1_3" to MVBlk1_3
Alias OVBlk1(3) = O$VBlk1_3             'Assign alias name "O$VBlk1_3" to OVBlk1_3
Units VBlk1(4) = kips               'Assign units "kips" to VBlk1(4)
Alias MVBlk1(4) = M$VBlk1_4             'Assign alias name "M$VBlk1_4" to MVBlk1_4
Alias OVBlk1(4) = O$VBlk1_4             'Assign alias name "O$VBlk1_4" to OVBlk1_4
Units VBlk1(5) = kips               'Assign units "kips" to VBlk1(5)
Alias MVBlk1(5) = M$VBlk1_5             'Assign alias name "M$VBlk1_5" to MVBlk1_5
Alias OVBlk1(5) = O$VBlk1_5             'Assign alias name "O$VBlk1_5" to OVBlk1_5
Units VBlk1(6) = kips               'Assign units "kips" to VBlk1(6)
Alias MVBlk1(6) = M$VBlk1_6             'Assign alias name "M$VBlk1_6" to MVBlk1_6
Alias OVBlk1(6) = O$VBlk1_6             'Assign alias name "O$VBlk1_6" to OVBlk1_6
Units VBlk1(7) = kips               'Assign units "kips" to VBlk1(7)
Alias MVBlk1(7) = M$VBlk1_7             'Assign alias name "M$VBlk1_7" to MVBlk1_7
Alias OVBlk1(7) = O$VBlk1_7             'Assign alias name "O$VBlk1_7" to OVBlk1_7
Units VBlk1(8) = kips               'Assign units "kips" to VBlk1(8)
Alias MVBlk1(8) = M$VBlk1_8             'Assign alias name "M$VBlk1_8" to MVBlk1_8
Alias OVBlk1(8) = O$VBlk1_8             'Assign alias name "O$VBlk1_8" to OVBlk1_8
Units VBlk2(1) = kips               'Assign units "kips" to VBlk2(1)
Alias MVBlk2(1) = M$VBlk2_1             'Assign alias name "M$VBlk2_1" to MVBlk2_1
Alias OVBlk2(1) = O$VBlk2_1             'Assign alias name "O$VBlk2_1" to OVBlk2_1
```

```
Units VBlk2(2) = kips                    'Assign units "kips" to VBlk2(2)
Alias MVBlk2(2) = M$VBlk2_2                  'Assign alias name "M$VBlk2_2" to MVBlk2_2
Alias OVBlk2(2) = O$VBlk2_2                  'Assign alias name "O$VBlk2_2" to OVBlk2_2
Units VBlk2(3) = kips                    'Assign units "kips" to VBlk2(3)
Alias MVBlk2(3) = M$VBlk2_3                  'Assign alias name "M$VBlk2_3" to MVBlk2_3
Alias OVBlk2(3) = O$VBlk2_3                  'Assign alias name "O$VBlk2_3" to OVBlk2_3
Units VBlk2(4) = kips                    'Assign units "kips" to VBlk2(4)
Alias MVBlk2(4) = M$VBlk2_4                  'Assign alias name "M$VBlk2_4" to MVBlk2_4
Alias OVBlk2(4) = O$VBlk2_4                  'Assign alias name "O$VBlk2_4" to OVBlk2_4
Units VBlk2(5) = kips                    'Assign units "kips" to VBlk2(5)
Alias MVBlk2(5) = M$VBlk2_5                  'Assign alias name "M$VBlk2_5" to MVBlk2_5
Alias OVBlk2(5) = O$VBlk2_5                  'Assign alias name "O$VBlk2_5" to OVBlk2_5
Units VBlk2(6) = NotWorking                 'Assign units "NotWorking" to VBlk2(6)
Alias MVBlk2(6) = M$VBlk2_6                  'Assign alias name "M$VBlk2_6" to MVBlk2_6
Alias OVBlk2(6) = O$VBlk2_6                  'Assign alias name "O$VBlk2_6" to OVBlk2_6
Units VBlk2(7) = kips                    'Assign units "kips" to VBlk2(7)
Alias MVBlk2(7) = M$VBlk2_7                  'Assign alias name "M$VBlk2_7" to MVBlk2_7
Alias OVBlk2(7) = O$VBlk2_7                  'Assign alias name "O$VBlk2_7" to OVBlk2_7
Public Flag(8)                       'General Purpose Flags
Public ScanFlg1x(8) As Boolean
Public FlagMode8
Dim I                                'Declare I as a variable
'\\\\\\\\\\\\\\ FIELD CALIBRATION GLOBAL VARIABLES ///////////////
Public CalFileLoaded As Boolean
Public CalStartIdx
Const TwoPointMultOffs = 2
Const ZeroingCalib = 0
Public FieldCalAvgs

'\\\\\\\\\\\\\\\\\\\\\\\\ OUTPUT SECTION ////////////////////////

'---------------------------- Table 1----------------------------
DataTable(TABLE1,True,-1)                'Trigger, auto size
  DataInterval(0,INTERVAL1,UNITS1,100)          '500 mSec interval, 100 lapses, autosize
  CardOut(0,-1)                      'PC card , size Auto
  '_____________________ Voltage Blocks _____________________
  Sample (VREP1,VBlk1(),FP2)                '8 Reps,Source,Res
  Sample (VREP2,VBlk2(),FP2)                '8 Reps,Source,Res
  Sample(6,vWG(),FP2)
EndTable                             'End of table TABLE1

'---------------------------- Table 2----------------------------
DataTable(Table2,True,-1)                'Trigger, auto size
  DataInterval(0,INTERVAL2,UNITS2,100)          '500 mSec interval, 100 lapses, autosize
  CardOut(0,-1)                      'PC card , size Auto
  '_____________________ Voltage Blocks _____________________
  Average(VREP1,VBlk1(),FP2,False)          '8 Reps,Source,Res,Enabled
```

```
  Average(VREP2,VBlk2(),FP2,False)                    '8 Reps,Source,Res,Enabled
  Average(6,vwG(),FP2,False)
EndTable                                    'End of table Table2

DataTable(CalHist,NewFieldCal,50)
  SampleFieldCal
EndTable
'\\\\\\\\\\\\\\\\\\\\\\\\ SUBROUTINES ////////////////////////

'\\\\\\\\\\\\\\\\\\\\\\\\\\\ PROGRAM ///////////////////////////

BeginProg                                   'Program begins here
  'MainSequence
  For I = 1 To VREP1                            'Do the following to all of VBlk1
    MVBlk1(I) = VMULT1                            'Assign default multiplier (1) to MVBlk1
    OVBlk1(I) = VOSET1                            'Assign default offset (0) to OVBlk1
  Next I                                    'Repeat above until finished
  For I = 1 To VREP2                            'Do the following to all of VBlk2
    MVBlk2(I) = VMULT2                            'Assign default multiplier (1) to MVBlk2
    OVBlk2(I) = VOSET2                            'Assign default offset (0) to OVBlk2
  Next I                                    'Repeat above until finished
  """""""""" exception multipliers and offsets """""""""
  MVBlk1(1) = 2.5049                            'Exception multiplier for VBlk1(1) alias ""
  MVBlk1(2) = 2.447                             'Exception multiplier for VBlk1(2) alias ""
  MVBlk1(3) = 2.4967                            'Exception multiplier for VBlk1(3) alias ""
  MVBlk1(4) = 2.5251                            'Exception multiplier for VBlk1(4) alias ""
  MVBlk1(5) = 3.9711                            'Exception multiplier for VBlk1(5) alias ""
  MVBlk1(6) = 2.5098                            'Exception multiplier for VBlk1(6) alias ""
  MVBlk1(7) = 2.4787                            'Exception multiplier for VBlk1(7) alias ""
  MVBlk1(8) = 2.5211                            'Exception multiplier for VBlk1(8) alias ""
  MVBlk2(1) = -3.1262                           'Exception multiplier for VBlk2(1) alias ""
  MVBlk2(2) = -3.1254                           'Exception multiplier for VBlk2(2) alias ""
  MVBlk2(3) = -3.1384                           'Exception multiplier for VBlk2(3) alias ""
  MVBlk2(4) = -3.0815                           'Exception multiplier for VBlk2(4) alias ""
  MVBlk2(5) = -3.1741                           'Exception multiplier for VBlk2(5) alias ""
  MVBlk2(6) = 0.0001                            'Exception multiplier for VBlk2(6) alias ""
  MVBlk2(7) = -3.0762                           'Exception multiplier for VBlk2(7) alias ""
  """""""""""""""""""""""""""""""""""""""""""""""""""""""""""""""
  For I = 1 To 8
    ScanFlg1x(I) = True
  Next I

  VCalReps1 = VREP1
  VCalReps2 = VREP2

  CalFileLoaded = false
  CalFileLoaded = LoadFieldCal(1)
```

```
  FieldCalAvgs = 20
  CalStartIdx = 1

  Scan(PERIOD,P_UNITS,10,0)                    'Scan once every 100 mSecs, non-burst


PortSet(2,1)
                    Delay(0,150,mSec)
                    LCount_5=1
                    SubScan(0,uSec,6)
                            'Switch to next AM16/32 Multiplexer channel
                            PortSet(1,1)
                            Delay(0,10000,uSec)
                            PortSet(1,0)
                            Delay(0,10000,uSec)
                            'Generic Full Bridge measurements FullBR() on the AM16/32 Multiplexer:
                            VibratingWire (vWG(LCount_5),1,mV1000,32,Vx2,1400,3500,150,1,20000,250,0,.373796,0)
                            LCount_5=LCount_5+1
                    NextSubScan
                    'Turn AM16/32 Multiplexer Off
                    PortSet(2,0)
                    Delay(0,150,mSec)



    If Flag(8) Then
      If ScanFlg1x(8) Then
        CalStartIdx = 1
        VCalReps1 = VREP1
        VCalReps2 = VREP2
        FlagMode8 = 1
        ScanFlg1x(8) = False
      EndIf
      If (FlagMode8 <= 0) or (FlagMode8 = 6) Then Flag(8) = 0
    Else
      ScanFlg1x(8) = True
    EndIf

    '_____________________________ Volt Blocks _____________________________
    VoltDiff(VBlk1(),VREP1,VRNG1,1,True,VSETL1,VINT1,MVBlk1(),OVBlk1())
    VoltDiff(VBlk2(),VREP2,VRNG2,9,True,VSETL2,VINT2,MVBlk2(),OVBlk2())

    FieldCal(TwoPointMultOffs,VBlk1(),1,MVBlk1(),OVBlk1(),VCalMode1,VKnownVar1(),CalStartIdx,FieldCalAvgs)
    FieldCal(ZeroingCalib,VBlk1(),VCalReps1,0,OVBlk1(),FlagMode8,0,CalStartIdx,FieldCalAvgs)
    FieldCal(TwoPointMultOffs,VBlk2(),1,MVBlk2(),OVBlk2(),VCalMode2,VKnownVar2(),CalStartIdx,FieldCalAvgs)
    FieldCal(ZeroingCalib,VBlk2(),VCalReps2,0,OVBlk2(),FlagMode8,0,CalStartIdx,FieldCalAvgs)
```

```
    CallTable(CalHist)

    '_____ Output Table Control _____
    If Flag(1) Then CallTable TABLE1
    If Flag(1) Then CallTable Table2
    'CallTable(TABLE1)
    'CallTable(Table2)
  Next Scan                          'Loop up for the next scan
EndProg                              'Program ends here

'***** Program End *****
```

The following program (5000-Final-10min.CR5) was used for the CR5000 overnight during the stressing operations and before the load testing of Specimen 2.

```
'                Program name: 5000-PROGRAMGENERATOR1.CR5
'                 Written by: Name
'                 I.D. number: Number
'                Date written: 01-11-2019
'                Time written: 10:52:35
'              RT5GEN Version: 6.0.0066

' This program was generated using Campbell Scientific's RT5GEN
' Program Generator for the CR5000 Measurement & Control System.

'\\\\\\\\\\\\\\\\\\\\\\ TIMING CONSTANTS //////////////////////

Dim LCount_5
Const PERIOD = 600000                    'Scan interval number
Const P_UNITS = 1                        'Scan interval units (mSecs)

Const INTERVAL1 = 600000                 'Table 1 interval number
Const UNITS1 = 1                         'Table 1 interval units (mSecs)

Const INTERVAL2 = 600000                 'Table 2 interval number
Const UNITS2 = 1                         'Table 2 interval units (mSecs)

'\\\\\\\\\\\\\\\\\\\\\\ VOLTAGE CONSTANTS //////////////////////

'_____ Volt Block 1 _____
Const VRNG1 = 5                          'Block1 measurement range (Auto)
Const VREP1 = 8                          'Block1 repetitions
Const VSETL1 = 200                       'Block1 settling time (usecs)
Const VINT1 = 250                        'Block1 integration time (usecs)
Const VMULT1 = 1                         'Block1 default multiplier
Const VOSET1 = 0                         'Block1 default offset
```

```
Public VBlk1(VREP1)                    'Block1 dimensioned source
Public MVBlk1(VREP1)                   'Block1 dimensioned multiplier
Public OVBlk1(VREP1)                   'Block1 dimensioned offset
Public VCalMode1
Public VKnownVar1(VREP1)
Units VBlk1 = mVolts                   'Block1 default units (mVolts)
Public VCalReps1
'_____________________ Volt Block 2 _____________________
Const VRNG2 = 5                        'Block2 measurement range (Auto)
Const VREP2 = 7                        'Block2 repetitions
Const VSETL2 = 200                     'Block2 settling time (usecs)
Const VINT2 = 250                      'Block2 integration time (usecs)
Const VMULT2 = 1                       'Block2 default multiplier
Const VOSET2 = 0                       'Block2 default offset
Public VBlk2(VREP2)                    'Block2 dimensioned source
Public MVBlk2(VREP2)                   'Block2 dimensioned multiplier
Public OVBlk2(VREP2)                   'Block2 dimensioned offset
Public VCalMode2
Public VKnownVar2(VREP2)
Units VBlk2 = mVolts                   'Block2 default units (mVolts)
Public VCalReps2




Public vWG(6)
Units vWG=ustrain



'\\\\\\\\\\\\\\\\\ ALIASES & OTHER VARIABLES /////////////////

Units VBlk1(1) = kips                  'Assign units "kips" to VBlk1(1)
Alias MVBlk1(1) = M$VBlk1_1            'Assign alias name "M$VBlk1_1" to MVBlk1_1
Alias OVBlk1(1) = O$VBlk1_1            'Assign alias name "O$VBlk1_1" to OVBlk1_1
Units VBlk1(2) = kips                  'Assign units "kips" to VBlk1(2)
Alias MVBlk1(2) = M$VBlk1_2            'Assign alias name "M$VBlk1_2" to MVBlk1_2
Alias OVBlk1(2) = O$VBlk1_2            'Assign alias name "O$VBlk1_2" to OVBlk1_2
Units VBlk1(3) = kips                  'Assign units "kips" to VBlk1(3)
Alias MVBlk1(3) = M$VBlk1_3            'Assign alias name "M$VBlk1_3" to MVBlk1_3
Alias OVBlk1(3) = O$VBlk1_3            'Assign alias name "O$VBlk1_3" to OVBlk1_3
Units VBlk1(4) = kips                  'Assign units "kips" to VBlk1(4)
Alias MVBlk1(4) = M$VBlk1_4            'Assign alias name "M$VBlk1_4" to MVBlk1_4
Alias OVBlk1(4) = O$VBlk1_4            'Assign alias name "O$VBlk1_4" to OVBlk1_4
Units VBlk1(5) = kips                  'Assign units "kips" to VBlk1(5)
Alias MVBlk1(5) = M$VBlk1_5            'Assign alias name "M$VBlk1_5" to MVBlk1_5
Alias OVBlk1(5) = O$VBlk1_5            'Assign alias name "O$VBlk1_5" to OVBlk1_5
```

```
Units VBlk1(6) = kips                    'Assign units "kips" to VBlk1(6)
Alias MVBlk1(6) = M$VBlk1_6                  'Assign alias name "M$VBlk1_6" to MVBlk1_6
Alias OVBlk1(6) = O$VBlk1_6                  'Assign alias name "O$VBlk1_6" to OVBlk1_6
Units VBlk1(7) = kips                    'Assign units "kips" to VBlk1(7)
Alias MVBlk1(7) = M$VBlk1_7                  'Assign alias name "M$VBlk1_7" to MVBlk1_7
Alias OVBlk1(7) = O$VBlk1_7                  'Assign alias name "O$VBlk1_7" to OVBlk1_7
Units VBlk1(8) = kips                    'Assign units "kips" to VBlk1(8)
Alias MVBlk1(8) = M$VBlk1_8                  'Assign alias name "M$VBlk1_8" to MVBlk1_8
Alias OVBlk1(8) = O$VBlk1_8                  'Assign alias name "O$VBlk1_8" to OVBlk1_8
Units VBlk2(1) = kips                    'Assign units "kips" to VBlk2(1)
Alias MVBlk2(1) = M$VBlk2_1                  'Assign alias name "M$VBlk2_1" to MVBlk2_1
Alias OVBlk2(1) = O$VBlk2_1                  'Assign alias name "O$VBlk2_1" to OVBlk2_1
Units VBlk2(2) = kips                    'Assign units "kips" to VBlk2(2)
Alias MVBlk2(2) = M$VBlk2_2                  'Assign alias name "M$VBlk2_2" to MVBlk2_2
Alias OVBlk2(2) = O$VBlk2_2                  'Assign alias name "O$VBlk2_2" to OVBlk2_2
Units VBlk2(3) = kips                    'Assign units "kips" to VBlk2(3)
Alias MVBlk2(3) = M$VBlk2_3                  'Assign alias name "M$VBlk2_3" to MVBlk2_3
Alias OVBlk2(3) = O$VBlk2_3                  'Assign alias name "O$VBlk2_3" to OVBlk2_3
Units VBlk2(4) = kips                    'Assign units "kips" to VBlk2(4)
Alias MVBlk2(4) = M$VBlk2_4                  'Assign alias name "M$VBlk2_4" to MVBlk2_4
Alias OVBlk2(4) = O$VBlk2_4                  'Assign alias name "O$VBlk2_4" to OVBlk2_4
Units VBlk2(5) = kips                    'Assign units "kips" to VBlk2(5)
Alias MVBlk2(5) = M$VBlk2_5                  'Assign alias name "M$VBlk2_5" to MVBlk2_5
Alias OVBlk2(5) = O$VBlk2_5                  'Assign alias name "O$VBlk2_5" to OVBlk2_5
Units VBlk2(6) = NotWorking                 'Assign units "NotWorking" to VBlk2(6)
Alias MVBlk2(6) = M$VBlk2_6                  'Assign alias name "M$VBlk2_6" to MVBlk2_6
Alias OVBlk2(6) = O$VBlk2_6                  'Assign alias name "O$VBlk2_6" to OVBlk2_6
Units VBlk2(7) = kips                    'Assign units "kips" to VBlk2(7)
Alias MVBlk2(7) = M$VBlk2_7                  'Assign alias name "M$VBlk2_7" to MVBlk2_7
Alias OVBlk2(7) = O$VBlk2_7                  'Assign alias name "O$VBlk2_7" to OVBlk2_7
Public Flag(8)                       'General Purpose Flags
Public ScanFlg1x(8) As Boolean
Public FlagMode8
Dim I                                'Declare I as a variable
'\\\\\\\\\\\\\ FIELD CALIBRATION GLOBAL VARIABLES ////////////
Public CalFileLoaded As Boolean
Public CalStartIdx
Const TwoPointMultOffs = 2
Const ZeroingCalib = 0
Public FieldCalAvgs

'\\\\\\\\\\\\\\\\\\\\\\\\ OUTPUT SECTION ////////////////////////

'---------------------------- Table 1----------------------------
DataTable(TABLE1,True,-1)                'Trigger, auto size
  DataInterval(0,INTERVAL1,UNITS1,100)          '500 mSec interval, 100 lapses, autosize
  CardOut(0,-1)                      'PC card , size Auto
```

```
  '_____ Voltage Blocks _____
  Sample (VREP1,VBlk1(),FP2)                    '8 Reps,Source,Res
  Sample (VREP2,VBlk2(),FP2)                    '8 Reps,Source,Res
  Sample(6,vWG(),FP2)
EndTable                                        'End of table TABLE1

'---------- Table 2----------
DataTable(Table2,True,-1)                       'Trigger, auto size
  DataInterval(0,INTERVAL2,UNITS2,100)          '500 mSec interval, 100 lapses, autosize
  CardOut(0,-1)                                 'PC card , size Auto
  '_____ Voltage Blocks _____
  Average(VREP1,VBlk1(),FP2,False)              '8 Reps,Source,Res,Enabled
  Average(VREP2,VBlk2(),FP2,False)              '8 Reps,Source,Res,Enabled
  Average(6,vwG(),FP2,False)
EndTable                                        'End of table Table2

DataTable(CalHist,NewFieldCal,50)
  SampleFieldCal
EndTable
'\\\\\\\\\\\\\\\\\\\\\\\\ SUBROUTINES ////////////////////////

'\\\\\\\\\\\\\\\\\\\\\\\\ PROGRAM ////////////////////////////

BeginProg                                       'Program begins here
  'MainSequence
  For I = 1 To VREP1                            'Do the following to all of VBlk1
    MVBlk1(I) = VMULT1                          'Assign default multiplier (1) to MVBlk1
    OVBlk1(I) = VOSET1                          'Assign default offset (0) to OVBlk1
  Next I                                        'Repeat above until finished
  For I = 1 To VREP2                            'Do the following to all of VBlk2
    MVBlk2(I) = VMULT2                          'Assign default multiplier (1) to MVBlk2
    OVBlk2(I) = VOSET2                          'Assign default offset (0) to OVBlk2
  Next I                                        'Repeat above until finished
  """""""""" exception multipliers and offsets """""""""
  MVBlk1(1) = 2.5049                            'Exception multiplier for VBlk1(1) alias ""
  MVBlk1(2) = 2.447                             'Exception multiplier for VBlk1(2) alias ""
  MVBlk1(3) = 2.4967                            'Exception multiplier for VBlk1(3) alias ""
  MVBlk1(4) = 2.5251                            'Exception multiplier for VBlk1(4) alias ""
  MVBlk1(5) = 3.9711                            'Exception multiplier for VBlk1(5) alias ""
  MVBlk1(6) = 2.5098                            'Exception multiplier for VBlk1(6) alias ""
  MVBlk1(7) = 2.4787                            'Exception multiplier for VBlk1(7) alias ""
  MVBlk1(8) = 2.5211                            'Exception multiplier for VBlk1(8) alias ""
  MVBlk2(1) = -3.1262                           'Exception multiplier for VBlk2(1) alias ""
  MVBlk2(2) = -3.1254                           'Exception multiplier for VBlk2(2) alias ""
  MVBlk2(3) = -3.1384                           'Exception multiplier for VBlk2(3) alias ""
  MVBlk2(4) = -3.0815                           'Exception multiplier for VBlk2(4) alias ""
  MVBlk2(5) = -3.1741                           'Exception multiplier for VBlk2(5) alias ""
```

```
MVBlk2(6) = 0.0001                          'Exception multiplier for VBlk2(6) alias ""
MVBlk2(7) = -3.0762                         'Exception multiplier for VBlk2(7) alias ""
''''''''''''''''''''''''''''''''''''''''''''''''''''''''''''
For I = 1 To 8
  ScanFlg1x(I) = True
Next I

VCalReps1 = VREP1
VCalReps2 = VREP2

CalFileLoaded = false
CalFileLoaded = LoadFieldCal(1)
FieldCalAvgs = 20
CalStartIdx = 1

Scan(PERIOD,P_UNITS,10,0)                          'Scan once every 100 mSecs, non-burst


PortSet(2,1)
            Delay(0,150,mSec)
            LCount_5=1
            SubScan(0,uSec,6)
                  'Switch to next AM16/32 Multiplexer channel
                  PortSet(1,1)
                  Delay(0,10000,uSec)
                  PortSet(1,0)
                  Delay(0,10000,uSec)
                  'Generic Full Bridge measurements FullBR() on the AM16/32 Multiplexer:
                  VibratingWire (vWG(LCount_5),1,mV1000,32,Vx2,1400,3500,150,1,20000,250,0,.373796,0)
                  LCount_5=LCount_5+1
            NextSubScan
            'Turn AM16/32 Multiplexer Off
            PortSet(2,0)
            Delay(0,150,mSec)



  If Flag(8) Then
    If ScanFlg1x(8) Then
      CalStartIdx = 1
      VCalReps1 = VREP1
      VCalReps2 = VREP2
      FlagMode8 = 1
      ScanFlg1x(8) = False
    EndIf
    If (FlagMode8 <= 0) or (FlagMode8 = 6) Then Flag(8) = 0
```

```
    Else
      ScanFlg1x(8) = True
    EndIf

    '_____________________________ Volt Blocks _____________________________
    VoltDiff(VBlk1(),VREP1,VRNG1,1,True,VSETL1,VINT1,MVBlk1(),OVBlk1())
    VoltDiff(VBlk2(),VREP2,VRNG2,9,True,VSETL2,VINT2,MVBlk2(),OVBlk2())

    FieldCal(TwoPointMultOffs,VBlk1(),1,MVBlk1(),OVBlk1(),VCalMode1,VKnownVar1(),CalStartIdx,FieldCalAvgs)
    FieldCal(ZeroingCalib,VBlk1(),VCalReps1,0,OVBlk1(),FlagMode8,0,CalStartIdx,FieldCalAvgs)
    FieldCal(TwoPointMultOffs,VBlk2(),1,MVBlk2(),OVBlk2(),VCalMode2,VKnownVar2(),CalStartIdx,FieldCalAvgs)
    FieldCal(ZeroingCalib,VBlk2(),VCalReps2,0,OVBlk2(),FlagMode8,0,CalStartIdx,FieldCalAvgs)
    CallTable(CalHist)

    '_____________________________ Output Table Control _____________________________
   If Flag(1) Then CallTable TABLE1
   If Flag(1) Then CallTable Table2
   'CallTable(TABLE1)
   'CallTable(Table2)
  Next Scan                              'Loop up for the next scan
EndProg                                  'Program ends here

'***** Program End *****
```

The following program (5000-Wirepots5.CR5) was used for the CR5000 during the load testing of Specimen 2.

```
'                Program name: 5000-PROGRAMGENERATOR1.CR5
'                  Written by: Name
'                  I.D. number: Number
'                  Date written: 01-11-2019
'                  Time written: 10:52:35
'                RT5GEN Version: 6.0.0066

' This program was generated using Campbell Scientific's RT5GEN
' Program Generator for the CR5000 Measurement & Control System.

'\\\\\\\\\\\\\\\\\\\\\\\\ TIMING CONSTANTS ////////////////////////

Dim LCount_5
Dim LCount_7
Const PERIOD = 2000                      'Scan interval number
Const P_UNITS = 1                        'Scan interval units (mSecs)

Const INTERVAL1 = 2000                   'Table 1 interval number
Const UNITS1 = 1                         'Table 1 interval units (mSecs)

Const INTERVAL2 = 2000                   'Table 2 interval number
Const UNITS2 = 1                         'Table 2 interval units (mSecs)

'\\\\\\\\\\\\\\\\\\\\\\\\ VOLTAGE CONSTANTS ////////////////////////

'_____________________________ Volt Block 1 _____________________________
Const VRNG1 = 5                          'Block1 measurement range (Auto)
Const VREP1 = 8                          'Block1 repetitions
Const VSETL1 = 200                       'Block1 settling time (usecs)
```

```
Const VINT1 = 250                       'Block1 integration time (usecs)
Const VMULT1 = 1                        'Block1 default multiplier
Const VOSET1 = 0                        'Block1 default offset
Public VBlk1(VREP1)                     'Block1 dimensioned source
Public MVBlk1(VREP1)                    'Block1 dimensioned multiplier
Public OVBlk1(VREP1)                    'Block1 dimensioned offset
Public VCalMode1
Public VKnownVar1(VREP1)
Units VBlk1 = mVolts                    'Block1 default units (mVolts)
Public VCalReps1
'_____________________ Volt Block 2 _____________________
Const VRNG2 = 5                         'Block2 measurement range (Auto)
Const VREP2 = 7                         'Block2 repetitions
Const VSETL2 = 200                      'Block2 settling time (usecs)
Const VINT2 = 250                       'Block2 integration time (usecs)
Const VMULT2 = 1                        'Block2 default multiplier
Const VOSET2 = 0                        'Block2 default offset
Public VBlk2(VREP2)                     'Block2 dimensioned source
Public MVBlk2(VREP2)                    'Block2 dimensioned multiplier
Public OVBlk2(VREP2)                    'Block2 dimensioned offset
Public VCalMode2
Public VKnownVar2(VREP2)
Units VBlk2 = mVolts                    'Block2 default units (mVolts)
Public VCalReps2



Public vWG(6)
Units vWG=ustrain

Const VREPWP = 12
Public WirePots(VREPWP)
Units WirePots=inches

Public WPMult(VREPWP)                   'Block1 dimensioned multiplier
Public WPOff(VREPWP)



'\\\\\\\\\\\\\\\\\\ ALIASES & OTHER VARIABLES //////////////////

Units VBlk1(1) = kips                   'Assign units "kips" to VBlk1(1)
Alias MVBlk1(1) = M$VBlk1_1             'Assign alias name "M$VBlk1_1" to MVBlk1_1
Alias OVBlk1(1) = O$VBlk1_1             'Assign alias name "O$VBlk1_1" to OVBlk1_1
Units VBlk1(2) = kips                   'Assign units "kips" to VBlk1(2)
Alias MVBlk1(2) = M$VBlk1_2             'Assign alias name "M$VBlk1_2" to MVBlk1_2
Alias OVBlk1(2) = O$VBlk1_2             'Assign alias name "O$VBlk1_2" to OVBlk1_2
Units VBlk1(3) = kips                   'Assign units "kips" to VBlk1(3)
Alias MVBlk1(3) = M$VBlk1_3             'Assign alias name "M$VBlk1_3" to MVBlk1_3
Alias OVBlk1(3) = O$VBlk1_3             'Assign alias name "O$VBlk1_3" to OVBlk1_3
Units VBlk1(4) = kips                   'Assign units "kips" to VBlk1(4)
Alias MVBlk1(4) = M$VBlk1_4             'Assign alias name "M$VBlk1_4" to MVBlk1_4
Alias OVBlk1(4) = O$VBlk1_4             'Assign alias name "O$VBlk1_4" to OVBlk1_4
Units VBlk1(5) = kips                   'Assign units "kips" to VBlk1(5)
Alias MVBlk1(5) = M$VBlk1_5             'Assign alias name "M$VBlk1_5" to MVBlk1_5
Alias OVBlk1(5) = O$VBlk1_5             'Assign alias name "O$VBlk1_5" to OVBlk1_5
Units VBlk1(6) = kips                   'Assign units "kips" to VBlk1(6)
Alias MVBlk1(6) = M$VBlk1_6             'Assign alias name "M$VBlk1_6" to MVBlk1_6
Alias OVBlk1(6) = O$VBlk1_6             'Assign alias name "O$VBlk1_6" to OVBlk1_6
Units VBlk1(7) = kips                   'Assign units "kips" to VBlk1(7)
Alias MVBlk1(7) = M$VBlk1_7             'Assign alias name "M$VBlk1_7" to MVBlk1_7
Alias OVBlk1(7) = O$VBlk1_7             'Assign alias name "O$VBlk1_7" to OVBlk1_7
Units VBlk1(8) = kips                   'Assign units "kips" to VBlk1(8)
Alias MVBlk1(8) = M$VBlk1_8             'Assign alias name "M$VBlk1_8" to MVBlk1_8
Alias OVBlk1(8) = O$VBlk1_8             'Assign alias name "O$VBlk1_8" to OVBlk1_8
Units VBlk2(1) = kips                   'Assign units "kips" to VBlk2(1)
Alias MVBlk2(1) = M$VBlk2_1             'Assign alias name "M$VBlk2_1" to MVBlk2_1
Alias OVBlk2(1) = O$VBlk2_1             'Assign alias name "O$VBlk2_1" to OVBlk2_1
```

```
Units VBlk2(2) = kips                    'Assign units "kips" to VBlk2(2)
Alias MVBlk2(2) = M$VBlk2_2                  'Assign alias name "M$VBlk2_2" to MVBlk2_2
Alias OVBlk2(2) = O$VBlk2_2                 'Assign alias name "O$VBlk2_2" to OVBlk2_2
Units VBlk2(3) = kips                    'Assign units "kips" to VBlk2(3)
Alias MVBlk2(3) = M$VBlk2_3                  'Assign alias name "M$VBlk2_3" to MVBlk2_3
Alias OVBlk2(3) = O$VBlk2_3                 'Assign alias name "O$VBlk2_3" to OVBlk2_3
Units VBlk2(4) = kips                    'Assign units "kips" to VBlk2(4)
Alias MVBlk2(4) = M$VBlk2_4                  'Assign alias name "M$VBlk2_4" to MVBlk2_4
Alias OVBlk2(4) = O$VBlk2_4                 'Assign alias name "O$VBlk2_4" to OVBlk2_4
Units VBlk2(5) = kips                    'Assign units "kips" to VBlk2(5)
Alias MVBlk2(5) = M$VBlk2_5                  'Assign alias name "M$VBlk2_5" to MVBlk2_5
Alias OVBlk2(5) = O$VBlk2_5                 'Assign alias name "O$VBlk2_5" to OVBlk2_5
Units VBlk2(6) = NotWorking               'Assign units "NotWorking" to VBlk2(6)
Alias MVBlk2(6) = M$VBlk2_6                  'Assign alias name "M$VBlk2_6" to MVBlk2_6
Alias OVBlk2(6) = O$VBlk2_6                 'Assign alias name "O$VBlk2_6" to OVBlk2_6
Units VBlk2(7) = kips                    'Assign units "kips" to VBlk2(7)
Alias MVBlk2(7) = M$VBlk2_7                  'Assign alias name "M$VBlk2_7" to MVBlk2_7
Alias OVBlk2(7) = O$VBlk2_7                 'Assign alias name "O$VBlk2_7" to OVBlk2_7
Public Flag(8)                         'General Purpose Flags
Public ScanFlg1x(8) As Boolean
Public FlagMode8
Dim I                                  'Declare I as a variable
'\\\\\\\\\\\\\\ FIELD CALIBRATION GLOBAL VARIABLES ///////////////
Public CalFileLoaded As Boolean
Public CalStartIdx
Const TwoPointMultOffs = 2
Const ZeroingCalib = 0
Public FieldCalAvgs

'\\\\\\\\\\\\\\\\\\\\\\\\ OUTPUT SECTION ////////////////////////

'---------------------------- Table 1----------------------------
DataTable(TABLE1,True,-1)                  'Trigger, auto size
  DataInterval(0,INTERVAL1,UNITS1,100)          '500 mSec interval, 100 lapses, autosize
  CardOut(0,-1)                        'PC card , size Auto
  '_____________________ Voltage Blocks _____________________
  Sample (VREP1,VBlk1(),FP2)                '8 Reps,Source,Res
  Sample (VREP2,VBlk2(),FP2)                '8 Reps,Source,Res
  Sample(6,vWG(),FP2)
  Sample (12,WirePots(),FP2)
EndTable                               'End of table TABLE1

'---------------------------- Table 2----------------------------
DataTable(Table2,True,-1)                  'Trigger, auto size
  DataInterval(0,INTERVAL2,UNITS2,100)          '500 mSec interval, 100 lapses, autosize
  CardOut(0,-1)                        'PC card , size Auto
  '_____________________ Voltage Blocks _____________________
  Average(VREP1,VBlk1(),FP2,False)          '8 Reps,Source,Res,Enabled
  Average(VREP2,VBlk2(),FP2,False)          '8 Reps,Source,Res,Enabled
  Average(6,vwG(),FP2,False)
  Average (12,WirePots(),FP2,False)
EndTable                               'End of table Table2

DataTable(CalHist,NewFieldCal,50)
  SampleFieldCal
EndTable
'\\\\\\\\\\\\\\\\\\\\\\\\ SUBROUTINES ////////////////////////

'\\\\\\\\\\\\\\\\\\\\\\\\\\\\ PROGRAM ////////////////////////////

BeginProg                              'Program begins here
  'MainSequence
  For I = 1 To VREP1                       'Do the following to all of VBlk1
    MVBlk1(I) = VMULT1                        'Assign default multiplier (1) to MVBlk1
    OVBlk1(I) = VOSET1                       'Assign default offset (0) to OVBlk1
  Next I                               'Repeat above until finished
  For I = 1 To VREP2                       'Do the following to all of VBlk2
    MVBlk2(I) = VMULT2                        'Assign default multiplier (1) to MVBlk2
    OVBlk2(I) = VOSET2                       'Assign default offset (0) to OVBlk2
  Next I                               'Repeat above until finished
```

```
'''''''''''' exception multipliers and offsets ''''''''''''
MVBlk1(1) = 2.5049                      'Exception multiplier for VBlk1(1) alias ""
MVBlk1(2) = 2.447                       'Exception multiplier for VBlk1(2) alias ""
MVBlk1(3) = 2.4967                      'Exception multiplier for VBlk1(3) alias ""
MVBlk1(4) = 2.5251                      'Exception multiplier for VBlk1(4) alias ""
MVBlk1(5) = 3.9711                      'Exception multiplier for VBlk1(5) alias ""
MVBlk1(6) = 2.5098                      'Exception multiplier for VBlk1(6) alias ""
MVBlk1(7) = 2.4787                      'Exception multiplier for VBlk1(7) alias ""
MVBlk1(8) = 2.5211                      'Exception multiplier for VBlk1(8) alias ""
MVBlk2(1) = -3.1262                     'Exception multiplier for VBlk2(1) alias ""
MVBlk2(2) = -3.1254                     'Exception multiplier for VBlk2(2) alias ""
MVBlk2(3) = -3.1384                     'Exception multiplier for VBlk2(3) alias ""
MVBlk2(4) = -3.0815                     'Exception multiplier for VBlk2(4) alias ""
MVBlk2(5) = -3.1741                     'Exception multiplier for VBlk2(5) alias ""
MVBlk2(6) = 0.0001                      'Exception multiplier for VBlk2(6) alias ""
MVBlk2(7) = -3.0762
WPMult(1) = 14.8859
WPMult(2) = 4.9765
WPMult(3) = -4.7852
WPMult(4) = 4.9118
WPMult(5) = 4.7673
WPMult(6) = 4.7258
WPMult(7) = 4.9063
WPMult(8) = 4.953
WPMult(9) = 4.8341
WPMult(10) = 4.9391
WPMult(11) = 4.881
WPMult(12) = 4.8285
WPOff(1) = 0.256
WPOff(2) = 0.282
WPOff(3) = -2.958
WPOff(4) = -1.326
WPOff(5) = 0.595
WPOff(6) = -2.648
WPOff(7) = -1.62
WPOff(8) = -0.742
WPOff(9) = -0.003
WPOff(10) = -0.82
WPOff(11) = -0.735
WPOff(12) = -1.792                      'Exception multiplier for VBlk2(7) alias ""
''''''''''''''''''''''''''''''''''''''''''''''''''''''''''''''''
For I = 1 To 8
  ScanFlg1x(I) = True
Next I

VCalReps1 = VREP1
VCalReps2 = VREP2

CalFileLoaded = false
CalFileLoaded = LoadFieldCal(1)
FieldCalAvgs = 20
CalStartIdx = 1

Scan(PERIOD,P_UNITS,10,0)                       'Scan once every 100 mSecs, non-burst


'PortSet(2,1)
          '         Delay(0,150,mSec)
                    'LCount_7=1
'                   'SubScan(0,uSec,6)
                            'Switch to next AM16/32 Multiplexer channel
'                           PortSet(1,1)
'                           Delay(0,10000,uSec)
'                           PortSet(1,0)
'                           Delay(0,10000,uSec)
                            'Generic Full Bridge measurements FullBR() on the AM16/32 Multiplexer:
'                           VibratingWire (vWG(LCount_7),1,mV1000,32,Vx2,1400,3500,150,1,20000,250,0,.373796,0)
'                           LCount_7=LCount_7+1
'                   NextSubScan
                    'Turn AM16/32 Multiplexer Off
```

```
'                       PortSet(2,0)
'                       Delay(0,150,mSec)



PortSet(3,1)
                        Delay(0,150,mSec)
                        LCount_5=1
                        SubScan(0,uSec,12)
                                'Switch to next AM16/32 Multiplexer channel
                                PortSet(1,1)
                                Delay(0,10000,uSec)
                                PortSet(1,0)
                                Delay(0,10000,uSec)
                                'Generic Full Bridge measurements FullBR() on the AM16/32 Multiplexer:
                                BrFull (WirePots(LCount_5),1,mV200,17,Vx1,1,5000,True
,True,0,_60Hz,WPMult(LCount_5),WPOff(LCount_5))
                                LCount_5=LCount_5+1
                        NextSubScan
                        'Turn AM16/32 Multiplexer Off
                        PortSet(3,0)
                        Delay(0,150,mSec)


    If Flag(8) Then
      If ScanFlg1x(8) Then
        CalStartIdx = 1
        VCalReps1 = VREP1
        VCalReps2 = VREP2
        FlagMode8 = 1
        ScanFlg1x(8) = False
      EndIf
      If (FlagMode8 <= 0) or (FlagMode8 = 6) Then Flag(8) = 0
    Else
      ScanFlg1x(8) = True
    EndIf

    '_____________________________ Volt Blocks _____________________________
    VoltDiff(VBlk1(),VREP1,VRNG1,1,True,VSETL1,VINT1,MVBlk1(),OVBlk1())
    VoltDiff(VBlk2(),VREP2,VRNG2,9,True,VSETL2,VINT2,MVBlk2(),OVBlk2())

    FieldCal(TwoPointMultOffs,VBlk1(),1,MVBlk1(),OVBlk1(),VCalMode1,VKnownVar1(),CalStartIdx,FieldCalAvgs)
    FieldCal(ZeroingCalib,VBlk1(),VCalReps1,0,OVBlk1(),FlagMode8,0,CalStartIdx,FieldCalAvgs)
    FieldCal(TwoPointMultOffs,VBlk2(),1,MVBlk2(),OVBlk2(),VCalMode2,VKnownVar2(),CalStartIdx,FieldCalAvgs)
    FieldCal(ZeroingCalib,VBlk2(),VCalReps2,0,OVBlk2(),FlagMode8,0,CalStartIdx,FieldCalAvgs)
    CallTable(CalHist)

    '_____________________ Output Table Control _____________________
   If Flag(1) Then CallTable TABLE1
   If Flag(1) Then CallTable Table2
   'CallTable(TABLE1)
   'CallTable(Table2)
  Next Scan                             'Loop up for the next scan
EndProg                                 'Program ends here

'***** Program End *****
```

The following program (FinalTest_3.C9X) was used for the CR9000 during the load testing of Specimen 2.

```
'                 Program name: WIREPOT-TEST2.C9X
'                   Written by: Name
'                  I.D. number: Number
'                 Date written: 05-09-2019
'                 Time written: 11:16:51
'               RT9GEN Version: 6.0.0066
```

```
' This program was generated using Campbell Scientific's RT9GEN
' Program Generator for the CR9000 Measurement & Control System.

'        _____________ Logger CONFIGURATION _____________
'        Slot 1 = 9011    Slot 5 = 9050/51  Slot  9 = None
'        Slot 2 = 9032    Slot 6 = 9060     Slot 10 = None
'        Slot 3 = 9041    Slot 7 = 9060     Slot 11 = None
'        Slot 4 = 9050/51  Slot 8 = 9060    Slot 12 = None

'\\\\\\\\\\\\\\\\\\\\\\\\ SlotConfigure ////////////////////////
SlotConfigure(9050,9050,9060,9060,9060)

'\\\\\\\\\\\\\\\\\\\\\\\\ TIMING CONSTANTS ////////////////////////

Const PERIOD = 250                              'Scan interval number
Const P_UNITS = 1                               'Scan interval units (mSecs)

Const INTERVAL1 = 250                           'Table 1 interval number
Const UNITS1 = 1                                'Table 1 interval units (mSecs)

Const INTERVAL2 = 1                             'Table 2 interval number
Const UNITS2 = 2                                'Table 2 interval units (Secs)

Const INTERVAL3 = 3                             'Table 3 interval number
Const UNITS3 = 2                                'Table 3 interval units (Secs)

'\\\\\\\\\\\\\\\\\\\\\\\\ VOLTAGE CONSTANTS ////////////////////////

'_____________________________ Volt Block 1 _____________________________
Const VRNG1 = 1                                 'Block1 measurement range (5000 mV)
Const VREP1 = 11                                'Block1 repetitions
Const VSETL1 = 200                              'Block1 settling time (usecs)
Const VINT1 = 200                               'Block1 integration time (usecs)
Const VMULT1 = 1                                'Block1 default multiplier
Const VOSET1 = 0                                'Block1 default offset

Public VBlk1(VREP1)
Public MVBlk1(VREP1)                            'Block1 dimensioned multiplier
Public OVBlk1(VREP1)                            'Block1 dimensioned offset
Units VBlk1 = mVolts                            'Block1 default units (mVolts)
Public VCalReps1
'_____________________________ Volt Block 2 _____________________________
Const VRNG2 = 0                                 'Block2 measurement range (5000 mV)
Const VREP2 = 3                                 'Block2 repetitions
Const VSETL2 = 30                               'Block2 settling time (usecs)
Const VINT2 = 40                                'Block2 integration time (usecs)
Const VMULT2 = 1                                'Block2 default multiplier
Const VOSET2 = 0                                'Block2 default offset
Public VBlk2(VREP2)                             'Block2 dimensioned source
Public OVBlk2(VREP2)                            'Block2 dimensioned offset
Public MVBlk2(VREP2)
Units VBlk2 = mVolts                            'Block2 default units (mVolts)
Public VCalReps2
'_____________________________ Volt Block 3 _____________________________
Const VRNG3 = 0                                 'Block3 measurement range (5000 mV)
Const VREP3 = 2                                 'Block3 repetitions
Const VSETL3 = 30                               'Block3 settling time (usecs)
Const VINT3 = 40                                'Block3 integration time (usecs)
Const VMULT3 = 1                                'Block3 default multiplier
Const VOSET3 = 0                                'Block3 default offset

Public VBlk3(VREP3)
Public MVBlk3(VREP3)                            'Block3 dimensioned multiplier
Public OVBlk3(VREP3)                            'Block3 dimensioned offset
Units VBlk3 = mVolts                            'Block3 default units (mVolts)
Public VCalReps3

'\\\\\\\\\\\\\\\\\\\\\\\\ BRIDGE CONSTANTS ////////////////////////

'_____________________________ Bridge Block 1 _____________________________
```

```
Const BRNG1 = 16                                'Block1 measurement range (Secs)
Const BREP1 = 12                                'Block1 repetitions
Const BEXCIT1 = 5000                            'Block1 excitation mVolts
Const BSETL1 = 30                               'Block1 settling time (usecs)
Const BINT1 = 40                                'Block1 integration time (usecs)
Const BGF1 = 2.12                               'Block1 gauge factor
Const BCODE1 = -1                               'Block1 gauge code for 1/4 bridge strain
Const BMULT1 = 1                                'Block1 default multiplier
Const BOSET1 = 0                                'Block1 default offset
Public BBlk1(BREP1)                             'Block1 dimensioned source
Public BBlk1mV_V(BREP1)
Public GBBlk1Raw(BREP1)
Public GBBlk1(BREP1)                            'Block1 dimensioned gauge factor
Public BBlk1ZeroMv(BREP1)                       'Block1 zero mV variable
Public BCalMode1
Public BKnownVar1(BREP1)
Public BCalReps1
Units BBlk1ZeroMv = mVperV                      'Block1 default units (mVperV)
Units BBlk1 = uStrain                           'Block1 default units (uStrain)

'\\\\\\\\\\\\\\\\\ ALIASES & OTHER VARIABLES ////////////////

Alias VBlk1(1) = Bay7                           'Assign alias name "Bay7" to VBlk1(1)
Units Bay7 = inches                             'Assign units "inches" to Bay7
Alias VBlk1(2) = Bay8                           'Assign alias name "Bay8" to VBlk1(2)
Units Bay8 = inches                             'Assign units "inches" to Bay8
Alias VBlk1(3) = Bay12                          'Assign alias name "Bay12" to VBlk1(3)
Units Bay12 = inches                            'Assign units "inches" to Bay12
Alias VBlk1(4) = Bay11                          'Assign alias name "Bay11" to VBlk1(4)
Units Bay11 = inches                            'Assign units "inches" to Bay11
Alias VBlk1(5) = Bay4                           'Assign alias name "Bay4" to VBlk1(5)
Units Bay4 = inches                             'Assign units "inches" to Bay4
Alias VBlk1(6) = Bay3                           'Assign alias name "Bay3" to VBlk1(6)
Units Bay3 = inches                             'Assign units "inches" to Bay3
Alias VBlk1(7) = Bay9                           'Assign alias name "Bay9" to VBlk1(7)
Units Bay9 = inches                             'Assign units "inches" to Bay9
Alias VBlk1(8) = Bay2                           'Assign alias name "Bay2" to VBlk1(8)
Units Bay2 = inches                             'Assign units "inches" to Bay2
Alias VBlk1(9) = Bay6                           'Assign alias name "Bay6" to VBlk1(9)
Units Bay6 = inches                             'Assign units "inches" to Bay6
Alias VBlk1(10) = Bay1                          'Assign alias name "Bay1" to VBlk1(10)
Units Bay1 = inches                             'Assign units "inches" to Bay1
Alias VBlk1(11) = Bay10                         'Assign alias name "Bay10" to VBlk1(11)
Units Bay10 = inches                            'Assign units "inches" to Bay10
Alias VBlk3(1) = OverhangLoad                   'Assign alias name "OverhangLoad" to VBlk3(1)
Units OverhangLoad = lbs                        'Assign units "lbs" to OverhangLoad
Alias VBlk3(2) = MainBayLoad                    'Assign alias name "MainBayLoad" to VBlk3(2)
Units MainBayLoad = lbs                         'Assign units "lbs" to MainBayLoad
Public Flag(8)                                  'General Purpose Flags
Public ScanFlg1x(8) As Boolean
Public FlagMode8
Dim I                                           'Declare I as a variable
'\\\\\\\\\\\\\ FIELD CALIBRATION GLOBAL VARIABLES //////////////
Public CalFileLoaded As Boolean
Public CalStartIdx
Const ZeroingCalib = 0
Const CalStrainZero = 10
Const Strain1_4Shunt = 13
Public FieldCalAvgs

'\\\\\\\\\\\\\\\\\\\\\\ OUTPUT SECTION ////////////////////////

'---------------------------- Table 1----------------------------
DataTable(Table1,True,-1)                       'Trigger, auto size
  DataInterval(0,INTERVAL1,UNITS1,100)          '250 mSec interval, 100 lapses, autosize
  CardOut(0,-1)                                 'PC card , size Auto
  '_____________________ Voltage Blocks _____________________
  Sample (VREP1,VBlk1(),FP2)                    '12 Reps,Source,Res
  Sample (VREP2,VBlk2(),FP2)                    '2 Reps,Source,Res
  Sample (VREP3,VBlk3(),FP2)                    '2 Reps,Source,Res
```

```
  '_____________________________ Bridge Blocks _____________________________
  Sample (BREP1,BBlk1(),IEEE4)                    '12 Reps,Source,Res
EndTable                                          'End of table Table1

'---------------------------- Table 2----------------------------
DataTable(TABLE2,True,-1)                         'Trigger, auto size
  DataInterval(0,INTERVAL2,UNITS2,100)            '1 Sec interval, 100 lapses, autosize
  CardOut(0,-1)                                   'PC card , size Auto
  '_____________________________ Voltage Blocks _____________________________
  Average(VREP1,VBlk1(),FP2,False)                '12 Reps,Source,Res,Enabled
  Average(VREP2,VBlk2(),FP2,False)                '2 Reps,Source,Res,Enabled
  Average(VREP3,VBlk3(),FP2,False)                '2 Reps,Source,Res,Enabled
  '_____________________________ Bridge Blocks _____________________________
  Average(BREP1,BBlk1(),IEEE4,False)              '12 Reps,Source,Res,Enabled
EndTable                                          'End of table TABLE2

'---------------------------- Table 3----------------------------
DataTable(Table3,True,-1)                         'Trigger, auto size
  DataInterval(0,INTERVAL3,UNITS3,100)            '3 Sec interval, 100 lapses, autosize
  CardOut(0,-1)                                   'PC card , size Auto
  '_____________________________ Voltage Blocks _____________________________
  Average(VREP3,VBlk3(),FP2,False)                '2 Reps,Source,Res,Enabled
EndTable                                          'End of table Table3

DataTable(CalHist,NewFieldCal,50)
  SampleFieldCal
EndTable
'\\\\\\\\\\\\\\\\\\\\\\\\\ SUBROUTINES ////////////////////////////

'\\\\\\\\\\\\\\\\\\\\\\\\\\\\\ PROGRAM ////////////////////////////

BeginProg                                         'Program begins here
  'MainSequence
  For I = 1 To VREP1                              'Do the following to all of VBlk1
    MVBlk1(I) = VMULT1                            'Assign default multiplier (1) to MVBlk1
    OVBlk1(I) = VOSET1                            'Assign default offset (0) to OVBlk1
  Next I                                          'Repeat above until finished
  For I = 1 To VREP2                              'Do the following to all of VBlk2
    OVBlk2(I) = VOSET2                            'Assign default offset (0) to OVBlk2
  Next I                                          'Repeat above until finished
  For I = 1 To VREP3                              'Do the following to all of VBlk3
    MVBlk3(I) = VMULT3                            'Assign default multiplier (1) to MVBlk3
    OVBlk3(I) = VOSET3                            'Assign default offset (0) to OVBlk3
  Next I                                          'Repeat above until finished
  For I = 1 To BREP1                              'Do the following to all of BBlk1
    GBBlk1(I) = BGF1                              'Assign default gauge factor (2.12) to GBBlk1
  Next I                                          'Repeat above until finished
  """""""""" exception multipliers and offsets """""""""
  MVBlk1(1) = 0.9665                              'Exception multiplier for VBlk1(1) alias "Bay7"
  MVBlk1(2) = 0.9631                              'Exception multiplier for VBlk1(2) alias "Bay8"
  MVBlk1(3) = -0.9391                             'Exception multiplier for VBlk1(3) alias "Bay12"
  MVBlk1(4) = 0.9705                              'Exception multiplier for VBlk1(4) alias "Bay11"
  MVBlk1(5) = 0.9416                              'Exception multiplier for VBlk1(5) alias "Bay4"
  MVBlk1(6) = 0.9526                              'Exception multiplier for VBlk1(6) alias "Bay3"
  MVBlk1(7) = 1.0296                              'Exception multiplier for VBlk1(7) alias "Bay9"
  MVBlk1(8) = 0.9823                              'Exception multiplier for VBlk1(8) alias "Bay2"
  MVBlk1(9) = 0.9603                              'Exception multiplier for VBlk1(9) alias "Bay6"
  MVBlk1(10) = 0.9791                             'Exception multiplier for VBlk1(10) alias "Bay1"
  MVBlk1(11) = 0.9645                             'Exception multiplier for VBlk1(11) alias "Bay10"
  MVBlk2(1) = 0.0004825
  MVBlk2(2) = 0.0004898
  MVBlk2(3) = 0.0005870
  MVBlk3(1) = 10.3846                             'Exception multiplier for VBlk3(1) alias "OverhangLoad"
  MVBlk3(2) = 1.03806                             'Exception multiplier for VBlk3(2) alias "MainBayLoad"
  OVBlk3(1) = 403.2                               'Exception offset for VBlk3(1) alias "OverhangLoad"
  OVBlk3(2) = 255                                 'Exception offset for VBlk3(2) alias "MainBayLoad"
  """""""""""""""""""""""""""""""""""""""""""""""""""""""""""""""""""""""
  For I = 1 To 8
    ScanFlg1x(I) = True
  Next I
```

```
VCalReps1 = VREP1
VCalReps2 = VREP2
VCalReps3 = VREP3
For I = 1 To BREP1
  GBBlk1Raw(I) = GBBlk1(I)
Next I

CalFileLoaded = false
CalFileLoaded = LoadFieldCal(1)
FieldCalAvgs = 1
CalStartIdx = 1

Scan(PERIOD,P_UNITS,10,0)                    'Scan once every 250 mSecs, non-burst
  '_____________________________ Excitation Control _____________________________
  Excite(8,1,5000,0)                         'Set excitation channel
  """""""""""""
  Excite(8,6,2000,0)                         'Set excitation channel
  """""""""""""
  If Flag(8) Then
    If ScanFlg1x(8) Then
      CalStartIdx = 1
      VCalReps1 = VREP1
      VCalReps2 = VREP2
      VCalReps3 = VREP3
      BCalReps1 = BREP1
      FlagMode8 = 1
      ScanFlg1x(8) = False
    EndIf
    If (FlagMode8 <= 0) or (FlagMode8 = 6) Then Flag(8) = 0
  Else
    ScanFlg1x(8) = True
  EndIf

  '_____________________________ Volt Blocks _____________________________
  VoltDiff(VBlk1(),VREP1,VRNG1,4,1,True,VSETL1,VINT1,MVBlk1(),OVBlk1())
  VoltDiff(VBlk2(),VREP2,VRNG2,4,12,True,VSETL2,VINT2,MVBlk2(),OVBlk2())
  VoltSE(VBlk3(),VREP3,VRNG3,5,1,VSETL3,VINT3,MVBlk3(),OVBlk3())
  '_____________________________ Bridge Blocks _____________________________
  BrFull(BBlk1mV_V(),BREP1,mV200,5,2,6,1,1,BEXCIT1,False,True,BSETL1,BINT1,1,BOSET1) 'Strain
  StrainCalc(BBlk1(),BREP1,BBlk1mV_V(),BBlk1ZeroMv(),BCODE1,GBBlk1(),0) 'Strain calculation


  FieldCal(ZeroingCalib,VBlk1(),VCalReps1,0,OVBlk1(),FlagMode8,0,CalStartIdx,FieldCalAvgs)
  FieldCal(ZeroingCalib,VBlk2(),VCalReps2,0,OVBlk2(),FlagMode8,0,CalStartIdx,FieldCalAvgs)
  FieldCal(ZeroingCalib,VBlk3(),VCalReps3,0,OVBlk3(),FlagMode8,0,CalStartIdx,FieldCalAvgs)
  FieldCalStrain(Strain1_4Shunt,BBlk1(),1,GBBlk1(),0,BCalMode1,BKnownVar1(),CalStartIdx,FieldCalAvgs,GBBlk1Raw(),0)
  FieldCalStrain(CalStrainZero,BBlk1mV_V(),BCalReps1,0,BBlk1ZeroMv(),FlagMode8,0,CalStartIdx,FieldCalAvgs,0,BBlk1())
  CallTable(CalHist)
  '_____________________________ Output Table Control _____________________________
  If Flag(1) Then CallTable Table1
  If Flag(1) Then CallTable TABLE2
  If Flag(1) Then CallTable Table3
Next Scan                                    'Loop up for the next scan

'\\\\\\\\\\\\\\\\\\\\\\\\ LOW PRIORITY ////////////////////////

'BackgroundSequence
SlowSequence                                 'Used for slow measurements

Dim CountSlow                                'Dimension CountSlow
Dim TripVolt                                 'Dimension TripVolt
Dim CountAvg                                 'Dimension CountAvg
'SlowSequence Scan
'-----------------------------------------------------------------
Scan(1,Sec,0,0)                              'Scan once every 1 second
  Calibrate                                  'Corrects ADC offset and gain
  BiasComp                                   'Corrects ADC bias current
  Battery(TripVolt,0)                        'Battery voltage measurement
  CountSlow = CountSlow + 1                  'Increment counter
```

```
    If CountSlow >= 60 Then                         'Test counter
      CountSlow = 0                                 'Reset counter
      '_____________________ Battery Saver _____________________
      AvgRun(TripVolt,1,TripVolt,10)                'Running average (10 mins) of TripVolt
      CountAvg = CountAvg + 1                       'Increment CountAvg
      If CountAvg > 9 Then                          'Test TripVolt after 10 AvgRun inputs
        CountAvg = 0                                'Reset AvgCount after it equals 10
        If TripVolt < 11.5 Then                     'Test for less than 11.5 volts
          PowerOff(0,1,Hr)                          'Kill the Logger
        End If                                      'End of If TripVolt
      End If                                        'End of If CountAvg
    End If                                          'End of If
  Next Scan                                         'Loop up for the next scan
EndProg                                             'Program ends here

'***** Program End *****
```

Appendix E – Stressing Calculation Sheets

This appendix contains the stressing calculation sheets for each tendon that was stressed. These calculations sheets use a friction coefficient of 0.12 and a wobble coefficient of 0.0009/ft to calculate the predicted elongation. These values were obtained from the trial slab stressing operation. Figure E.1 contains the location of each tendon (U represents uniform-direction tendons, and B represents banded-direction tendons). Tables A6.1-A6.33 provide the calculation sheets for each tendon.

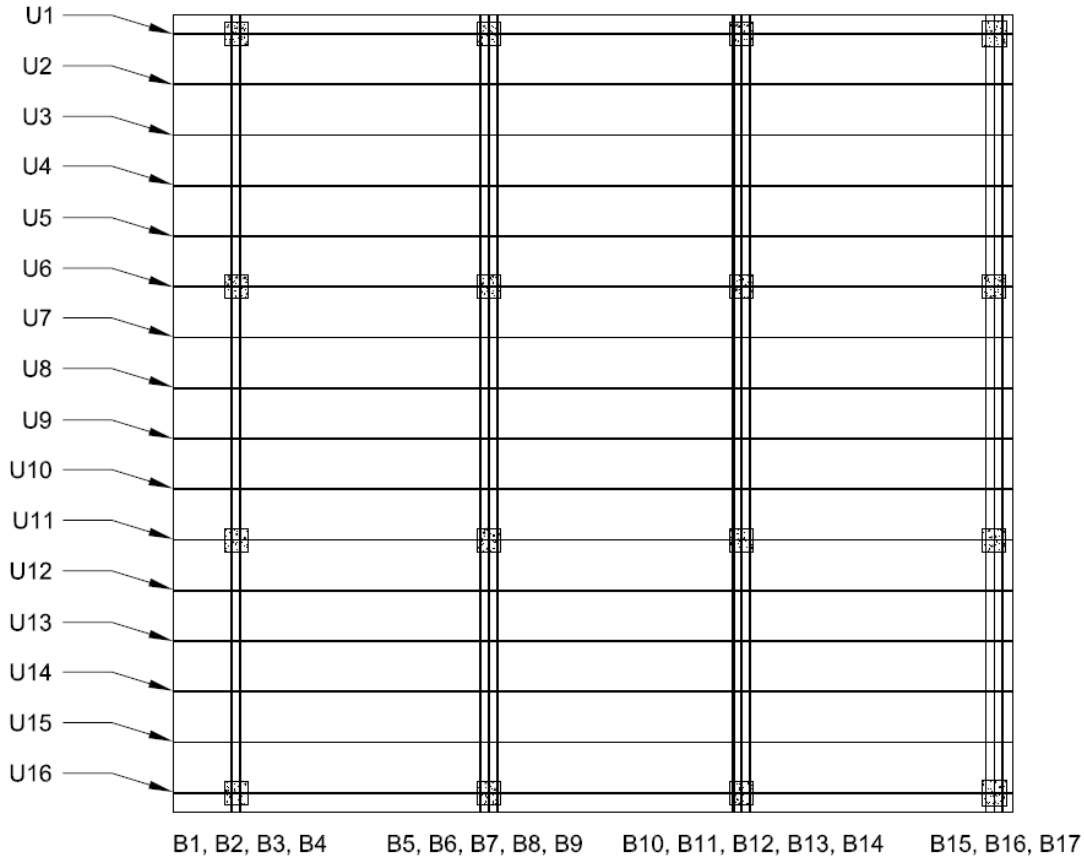

Figure E.1. Tendon Identifiers

Table E.1. Stressing Sheet for Uniform Tendon 1

Uniform Tendon 1				
Loading				
	Load Cell	**Readout**	**Load (kip)**	**Readout Aim**
Init	S8	-153	**1.687**	-135
5kip	S8	-478	**5.002**	-478
8kip	S8	-775	**8.032**	-772
10.904kip	S8	-1058	**10.918**	-1057
Measured Elongation				
Piston Extension (in)	**Fact. Piston Extension (in)**	**Dead End Seating (in)**	**Live End Seating (in)**	**Strand Elongation (in)**
0.25		1.4375	1.6875	
1.0625	1.2260	1.40625	1.6875	1.19478
1.8125	1.9780	1.40625	1.6875	1.94677
2.5	2.6612	1.375	1.65625	2.56749
Expected Elongation				
Ram Elongation (in)	**In-Slab Elongation (in)**	**Predicted Elongation (in)**	**Percent Difference**	
0.1082	1.15068	1.25887	-5.1%	
0.1737	1.84755	2.02125	-3.7%	
0.2361	2.51157	2.74770	-6.6%	
Seating Loss				
Ram Length @ Low Force (<1kip)	**Calculated Seating Loss (in.)**	**Measured Seating Loss (in.)**		**L_ram (in)**
2.25	0.0139	3/32		35.75

Table E.2. Stressing Sheet for Uniform Tendon 2

Uniform Tendon 2				
Loading				
	Load Cell	**Readout**	**Load (kip)**	**Readout Aim**
Init	S8	-140	**1.555**	-135
5kip	S8	-478	**5.002**	-478
8kip	S8	-772	**8.001**	-772
10.904kip	S8	-1058	**10.918**	-1057
Measured Elongation				
Piston Extension (in)	**Fact. Piston Extension (in)**	**Dead End Seating (in)**	**Live End Seating (in)**	**Strand Elongation (in)**
0.1875		1.4375	1.9375	
0.9375	1.0882	1.375	1.9375	1.02569
1.625	1.7842	1.34375	1.9375	1.69041
2.3125	2.4778	1.34375	1.9375	2.38406
Expected Elongation				
Ram Elongation (in)	**In-Slab Elongation (in)**	**Predicted Elongation (in)**	**Percent Difference**	
0.1105	1.15068	1.26114	-18.7%	
0.1767	1.84051	2.01718	-16.2%	
0.2411	2.51157	2.75266	-13.4%	
Seating Loss				
Ram Length @ Low Force (<1kip)	**Calculated Seating Loss (in.)**	**Measured Seating Loss (in.)**		**L_ram (in)**
2.03125	0.0402	1/16		36.5

Table E.3. Stressing Sheet for Uniform Tendon 3

Uniform Tendon 3 Loading				
	Load Cell	**Readout**	**Load (kip)**	**Readout Aim**
Init	S8	-136	**1.514**	-135
5kip	S8	-478	**5.002**	-478
8kip	S8	-773	**8.011**	-772
10.904kip	S8	-1059	**10.928**	-1057
Measured Elongation				
Piston Extension (in)	**Fact. Piston Extension (in)**	**Dead End Seating (in)**	**Live End Seating (in)**	**Strand Elongation (in)**
0.21875		1	1.0625	
1.125	1.2995	1	1.0625	1.29952
1.90625	2.0807	0.96875	1.0625	2.04941
2.625	2.7932	0.96875	1	2.69941
Expected Elongation				
Ram Elongation (in)	**In-Slab Elongation (in)**	**Predicted Elongation (in)**	**Percent Difference**	
0.1086	1.15068	1.25925	3.2%	
0.1739	1.84286	2.01673	1.6%	
0.2372	2.51392	2.75110	-1.9%	
Seating Loss				
Ram Length @ Low Force (<1kip)	**Calculated Seating Loss (in.)**	**Measured Seating Loss (in.)**		**L_ram (in)**
2.34375	0.0441	1/16		35.875

Table E.4. Stressing Sheet for Uniform Tendon 4

Uniform Tendon 4 Loading				
	Load Cell	**Readout**	**Load (kip)**	**Readout Aim**
Init	S8	-141	**1.565**	-135
5kip	S8	-479	**5.012**	-478
8kip	S8	-772	**8.001**	-772
10.904kip	S8	-1057	**10.908**	-1057
Measured Elongation				
Piston Extension (in)	**Fact. Piston Extension (in)**	**Dead End Seating (in)**	**Live End Seating (in)**	**Strand Elongation (in)**
0.25		1	1.125	
1.125	1.2721	0.96875	1.125	1.24090
1.84375	1.9812	0.96875	1.125	1.94998
2.5625	2.6998	0.9375	1.125	2.63730
Expected Elongation				
Ram Elongation (in)	**In-Slab Elongation (in)**	**Predicted Elongation (in)**	**Percent Difference**	
0.1082	1.15303	1.26124	-1.6%	
0.1727	1.84051	2.01325	-3.1%	
0.2355	2.50923	2.74472	-3.9%	
Seating Loss				
Ram Length @ Low Force (<1kip)	**Calculated Seating Loss (in.)**	**Measured Seating Loss (in.)**		**L_ram (in)**
2.25	0.0770	3/32		35.6875

Table E.5. Stressing Sheet for Uniform Tendon 5

Uniform Tendon 5 Loading				
	Load Cell	**Readout**	**Load (kip)**	**Readout Aim**
Init	S8	-150	**1.657**	-135
5kip	S8	-478	**5.002**	-478
8kip	S8	-773	**8.011**	-772
10.904kip	S8	-1058	**10.918**	-1057
Measured Elongation				
Piston Extension (in)	**Fact. Piston Extension (in)**	**Dead End Seating (in)**	**Live End Seating (in)**	**Strand Elongation (in)**
0.28125		1	2.25	
1.0625	1.1681	0.96875	2.25	1.13684
1.75	1.8516	0.96875	2.1875	1.75789
2.4375	2.5419	0.96875	2.1875	2.44818
Expected Elongation				
Ram Elongation (in)	**In-Slab Elongation (in)**	**Predicted Elongation (in)**	**Percent Difference**	
0.1080	1.15068	1.25868	-9.7%	
0.1730	1.84286	2.01582	-12.8%	
0.2357	2.51157	2.74729	-10.9%	
Seating Loss				
Ram Length @ Low Force (<1kip)	**Calculated Seating Loss (in.)**	**Measured Seating Loss (in.)**		**L_ram (in)**
2.1875	0.0143	1/16		35.6875

Table E.6. Stressing Sheet for Uniform Tendon 6

Uniform Tendon 6 Loading				
	Load Cell	**Readout**	**Load (kip)**	**Readout Aim**
Init	S8	-137	**1.524**	-135
5kip	S8	-481	**5.033**	-478
8kip	S8	-772	**8.001**	-772
10.904kip	S8	-1058	**10.918**	-1057
Measured Elongation				
Piston Extension (in)	**Fact. Piston Extension (in)**	**Dead End Seating (in)**	**Live End Seating (in)**	**Strand Elongation (in)**
0.28125		1	1.90625	
1.15625	1.2550	0.96875	1.875	1.19254
1.90625	2.0074	0.96875	1.875	1.94485
2.625	2.7240	0.9375	1.8125	2.56772
Expected Elongation				
Ram Elongation (in)	**In-Slab Elongation (in)**	**Predicted Elongation (in)**	**Percent Difference**	
0.1088	1.15772	1.26657	-5.8%	
0.1730	1.84051	2.01355	-3.4%	
0.2361	2.51157	2.74770	-6.6%	
Seating Loss				
Ram Length @ Low Force (<1kip)	**Calculated Seating Loss (in.)**	**Measured Seating Loss (in.)**		**L_ram (in)**
2.34375	0.0451	1/16		35.75

Table E.7. Stressing Sheet for Uniform Tendon 7

Uniform Tendon 7				
Loading				
	Load Cell	**Readout**	**Load (kip)**	**Readout Aim**
Init	S8	-136	**1.514**	-135
5kip	S8	-478	**5.002**	-478
8kip	S8	-776	**8.042**	-772
10.904kip	S8	-1058	**10.918**	-1057
Measured Elongation				
Piston Extension (in)	**Fact. Piston Extension (in)**	**Dead End Seating (in)**	**Live End Seating (in)**	**Strand Elongation (in)**
0.3125		1	0.6875	
1.28125	1.3891	1	0.6875	1.38914
1.96875	2.0403	0.96875	0.6875	2.00907
2.75	2.8299	0.96875	0.65625	2.76736
Expected Elongation				
Ram Elongation (in)	**In-Slab Elongation (in)**	**Predicted Elongation (in)**	**Percent Difference**	
0.1052	1.15068	1.25584	10.6%	
0.1691	1.84990	2.01896	-0.5%	
0.2295	2.51157	2.74110	1.0%	
Seating Loss				
Ram Length @ Low Force (<1kip)	**Calculated Seating Loss (in.)**	**Measured Seating Loss (in.)**		**L_ram (in)**
2.40625	0.1142	3/32		34.75

Table E.8. Stressing Sheet for Uniform Tendon 8

Uniform Tendon 8				
Loading				
	Load Cell	**Readout**	**Load (kip)**	**Readout Aim**
Init	S8	-141	**1.565**	-135
5kip	S8	-480	**5.023**	-478
8kip	S8	-772	**8.001**	-772
10.904kip	S8	-1057	**10.908**	-1057
Measured Elongation				
Piston Extension (in)	**Fact. Piston Extension (in)**	**Dead End Seating (in)**	**Live End Seating (in)**	**Strand Elongation (in)**
0.25		1.4375	1.125	
1.03125	1.1348	1.4375	1.09375	1.10355
1.71875	1.8258	1.40625	1.09375	1.76334
2.375	2.4809	1.375	1.0625	2.35590
Expected Elongation				
Ram Elongation (in)	**In-Slab Elongation (in)**	**Predicted Elongation (in)**	**Percent Difference**	
0.1022	1.15538	1.25754	-12.2%	
0.1628	1.84051	2.00327	-12.0%	
0.2219	2.50923	2.73111	-13.7%	
Seating Loss				
Ram Length @ Low Force (<1kip)	**Calculated Seating Loss (in.)**	**Measured Seating Loss (in.)**		**L_ram (in)**
2.125	0.0281	1/16		33.625

Table E.9. Stressing Sheet for Uniform Tendon 9

Uniform Tendon 9				
Loading				
	Load Cell	**Readout**	**Load (kip)**	**Readout Aim**
Init	S8	-139	**1.544**	-135
5kip	S8	-478	**5.002**	-478
8kip	S8	-772	**8.001**	-772
10.904kip	S8	-1058	**10.918**	-1057
Measured Elongation				
Piston Extension (in)	**Fact. Piston Extension (in)**	**Dead End Seating (in)**	**Live End Seating (in)**	**Strand Elongation (in)**
0.3125		1.4375	2	
1.25	1.3562	1.375	1.9375	1.23123
2.0625	2.1686	1.375	1.9375	2.04359
2.875	2.9847	1.34375	1.875	2.76594
Expected Elongation				
Ram Elongation (in)	**In-Slab Elongation (in)**	**Predicted Elongation (in)**	**Percent Difference**	
0.1080	1.15068	1.25868	-2.2%	
0.1727	1.84051	2.01325	1.5%	
0.2357	2.51157	2.74729	0.7%	
Seating Loss				
Ram Length @ Low Force (<1kip)	**Calculated Seating Loss (in.)**	**Measured Seating Loss (in.)**		**L_ram (in)**
2.5625	0.0768	1/16		35.6875

Table E.10. Stressing Sheet for Uniform Tendon 10

Uniform Tendon 10				
Loading				
	Load Cell	**Readout**	**Load (kip)**	**Readout Aim**
Init	S8	-137	**1.524**	-135
5kip	S8	-479	**5.012**	-478
8kip	S8	-775	**8.032**	-772
10.904kip	S8	-1059	**10.928**	-1057
Measured Elongation				
Piston Extension (in)	**Fact. Piston Extension (in)**	**Dead End Seating (in)**	**Live End Seating (in)**	**Strand Elongation (in)**
0.1875		1	0.6875	
1.0625	1.2573	0.96875	0.6875	1.22602
1.78125	1.9670	0.96875	0.65625	1.90449
2.5	2.6872	0.9375	0.65625	2.59349
Expected Elongation				
Ram Elongation (in)	**In-Slab Elongation (in)**	**Predicted Elongation (in)**	**Percent Difference**	
0.1050	1.15303	1.25802	-2.5%	
0.1682	1.84755	2.01579	-5.5%	
0.2289	2.51392	2.74283	-5.4%	
Seating Loss				
Ram Length @ Low Force (<1kip)	**Calculated Seating Loss (in.)**	**Measured Seating Loss (in.)**		**L_ram (in)**
2.25	0.0211	1/16		34.625

Table E.11. Stressing Sheet for Uniform Tendon 11

Uniform Tendon 11 Loading				
	Load Cell	**Readout**	**Load (kip)**	**Readout Aim**
Init	S8	-143	**1.585**	-135
5kip	S8	-481	**5.033**	-478
8kip	S8	-774	**8.021**	-772
10.904kip	S8	-1058	**10.918**	-1057
Measured Elongation				
Piston Extension (in)	**Fact. Piston Extension (in)**	**Dead End Seating (in)**	**Live End Seating (in)**	**Strand Elongation (in)**
0.1875		1	1.4375	
1.09375	1.3229	0.96875	1.40625	1.26044
1.875	2.1031	0.9375	1.375	1.97812
2.625	2.8515	0.9375	1.375	2.72651
Expected Elongation				
Ram Elongation (in)	**In-Slab Elongation (in)**	**Predicted Elongation (in)**	**Percent Difference**	
0.1115	1.15772	1.26923	-0.7%	
0.1777	1.84521	2.02293	-2.2%	
0.2419	2.51157	2.75348	-1.0%	
Seating Loss				
Ram Length @ Low Force (<1kip)	**Calculated Seating Loss (in.)**	**Measured Seating Loss (in.)**		**L_ram (in)**
2.34375	0.0393	1/16		36.625

Table E.12. Stressing Sheet for Uniform Tendon 12

Uniform Tendon 12 Loading				
	Load Cell	**Readout**	**Load (kip)**	**Readout Aim**
Init	S8	-140	**1.555**	-135
5kip	S8	-479	**5.012**	-478
8kip	S8	-772	**8.001**	-772
10.904kip	S8	-1060	**10.939**	-1057
Measured Elongation				
Piston Extension (in)	**Fact. Piston Extension (in)**	**Dead End Seating (in)**	**Live End Seating (in)**	**Strand Elongation (in)**
0.1875		1	1.125	
1	1.1778	0.96875	1.125	1.14654
1.6875	1.8617	0.96875	1.09375	1.79924
2.34375	2.5135	0.9375	1.09375	2.41972
Expected Elongation				
Ram Elongation (in)	**In-Slab Elongation (in)**	**Predicted Elongation (in)**	**Percent Difference**	
0.1080	1.15303	1.26105	-9.1%	
0.1724	1.84051	2.01295	-10.6%	
0.2357	2.51626	2.75201	-12.1%	
Seating Loss				
Ram Length @ Low Force (<1kip)	**Calculated Seating Loss (in.)**	**Measured Seating Loss (in.)**		**L_ram (in)**
2.09375	0.0143	1/16		35.625

Table E.13. Stressing Sheet for Uniform Tendon 13

Uniform Tendon 13 Loading				
	Load Cell	**Readout**	**Load (kip)**	**Readout Aim**
Init	S8	-142	**1.575**	-135
5kip	S8	-479	**5.012**	-478
8kip	S8	-773	**8.011**	-772
10.904kip	S8	-1058	**10.918**	-1057
Measured Elongation				
Piston Extension (in)	**Fact. Piston Extension (in)**	**Dead End Seating (in)**	**Live End Seating (in)**	**Strand Elongation (in)**
0.21875		1	2.3125	
1.03125	1.1848	0.96875	2.25	1.09103
1.6875	1.8282	0.96875	2.25	1.73442
2.375	2.5197	0.9375	2.25	2.39473
Expected Elongation				
Ram Elongation (in)	**In-Slab Elongation (in)**	**Predicted Elongation (in)**	**Percent Difference**	
0.1109	1.15303	1.26390	-13.7%	
0.1772	1.84286	2.02006	-14.1%	
0.2415	2.51157	2.75307	-13.0%	
Seating Loss				
Ram Length @ Low Force (<1kip)	**Calculated Seating Loss (in.)**	**Measured Seating Loss (in.)**		**L_ram (in)**
2.125	0.0085	1/16		36.5625

Table E.14. Stressing Sheet for Uniform Tendon 14

Uniform Tendon 14 Loading				
	Load Cell	**Readout**	**Load (kip)**	**Readout Aim**
Init	S8	-137	**1.524**	-135
5kip	S8	-479	**5.012**	-478
8kip	S8	-772	**8.001**	-772
10.904kip	S8	-1058	**10.918**	-1057
Measured Elongation				
Piston Extension (in)	**Fact. Piston Extension (in)**	**Dead End Seating (in)**	**Live End Seating (in)**	**Strand Elongation (in)**
0.21875		1	0.9375	
1	1.1226	1	0.90625	1.09131
1.71875	1.8529	0.96875	0.875	1.75919
2.40625	2.5424	0.9375	0.875	2.41737
Expected Elongation				
Ram Elongation (in)	**In-Slab Elongation (in)**	**Predicted Elongation (in)**	**Percent Difference**	
0.1092	1.15303	1.26219	-13.5%	
0.1743	1.84051	2.01476	-12.7%	
0.2378	2.51157	2.74935	-12.1%	
Seating Loss				
Ram Length @ Low Force (<1kip)	**Calculated Seating Loss (in.)**	**Measured Seating Loss (in.)**		**L_ram (in)**
2.125	0.0435	3/32		36

Table E.15. Stressing Sheet for Uniform Tendon 15

Uniform Tendon 15				
Loading				
	Load Cell	**Readout**	**Load (kip)**	**Readout Aim**
Init	S8	-140	**1.555**	-135
5kip	S8	-479	**5.012**	-478
8kip	S8	-773	**8.011**	-772
10.904kip	S8	-1057	**10.908**	-1057
Measured Elongation				
Piston Extension (in)	**Fact. Piston Extension (in)**	**Dead End Seating (in)**	**Live End Seating (in)**	**Strand Elongation (in)**
0.28125		1	1.625	
1.0625	1.1325	1	1.5625	1.06999
1.75	1.8224	0.96875	1.5	1.66614
2.40625	2.4782	0.96875	1.5	2.32194
Expected Elongation				
Ram Elongation (in)	**In-Slab Elongation (in)**	**Predicted Elongation (in)**	**Percent Difference**	
0.1114	1.15303	1.26447	-15.4%	
0.1781	1.84286	2.02097	-17.6%	
0.2425	2.50923	2.75174	-15.6%	
Seating Loss				
Ram Length @ Low Force (<1kip)	**Calculated Seating Loss (in.)**	**Measured Seating Loss (in.)**		**L_ram (in)**
2.125	0.0387	1/16		36.75

Table E.16. Stressing Sheet for Uniform Tendon 16

Uniform Tendon 16				
Loading				
	Load Cell	**Readout**	**Load (kip)**	**Readout Aim**
Init	S8	-140	**1.555**	-135
5kip	S8	-479	**5.012**	-478
8kip	S8	-772	**8.001**	-772
10.904kip	S8	-1057	**10.908**	-1057
Measured Elongation				
Piston Extension (in)	**Fact. Piston Extension (in)**	**Dead End Seating (in)**	**Live End Seating (in)**	**Strand Elongation (in)**
0.21875		1.40625	2.25	
0.96875	1.0872	1.375	2.25	1.05594
1.65625	1.7842	1.375	2.1875	1.69041
2.375	2.5146	1.34375	2.1875	2.38963
Expected Elongation				
Ram Elongation (in)	**In-Slab Elongation (in)**	**Predicted Elongation (in)**	**Percent Difference**	
0.1111	1.15303	1.26409	-16.5%	
0.1773	1.84051	2.01779	-16.2%	
0.2417	2.50923	2.75091	-13.1%	
Seating Loss				
Ram Length @ Low Force (<1kip)	**Calculated Seating Loss (in.)**	**Measured Seating Loss (in.)**		**L_ram (in)**
2.125	0.0083	1/16		36.625

Table E.17. Stressing Sheet for Banded Tendon 1

Banded Tendon 1 Loading				
	Load Cell	**Readout**	**Load (kip)**	**Readout Aim**
Init	S8	-137	**1.524**	-135
5kip	S8	-478	**5.002**	-478
8kip	S8	-772	**8.001**	-772
10.904kip	S8	-1015	**10.480**	-1045
Measured Elongation				
Piston Extension (in)	**Fact. Piston Extension (in)**	**Dead End Seating (in)**	**Live End Seating (in)**	**Strand Elongation (in)**
0.375		1.4375	1.75	
1.40625	1.4831	1.40625	1.6875	1.38935
2.25	2.3162	1.375	1.6875	2.19118
3	3.0717	1.34375	1.625	2.85295
Expected Elongation				
Ram Elongation (in)	**In-Slab Elongation (in)**	**Predicted Elongation (in)**	**Percent Difference**	
0.1122	1.10150	1.21365	14.5%	
0.1794	1.76184	1.94123	12.9%	
0.2350	2.30763	2.54260	12.2%	
Seating Loss				
Ram Length @ Low Force (<1kip)	**Calculated Seating Loss (in.)**	**Measured Seating Loss (in.)**		**L_ram (in)**
2.65625	0.1088	1/16		37.0625

Table E.18. Stressing Sheet for Banded Tendon 2

Banded Tendon 2 Loading				
	Load Cell	**Readout**	**Load (kip)**	**Readout Aim**
Init	S8	-140	**1.555**	-135
5kip	S8	-480	**5.023**	-478
8kip	S8	-772	**8.001**	-772
10.904kip	S8	-1045	**10.786**	-1045
Measured Elongation				
Piston Extension (in)	**Fact. Piston Extension (in)**	**Dead End Seating (in)**	**Live End Seating (in)**	**Strand Elongation (in)**
0.28125		N/A	1.375	
1.1875	1.3125	1.4375	1.375	1.31249
2	2.1332	1.40625	1.375	2.10199
2.75	2.8845	1.40625	1.3125	2.79076
Expected Elongation				
Ram Elongation (in)	**In-Slab Elongation (in)**	**Predicted Elongation (in)**	**Percent Difference**	
0.1136	1.10599	1.21955	7.6%	
0.1809	1.76184	1.94274	8.2%	
0.2439	2.37501	2.61888	6.6%	
Seating Loss				
Ram Length @ Low Force (<1kip)	**Calculated Seating Loss (in.)**	**Measured Seating Loss (in.)**		**L_ram (in)**
2.4375	0.0686	1/16		37.375

Table E.19. Stressing Sheet for Banded Tendon 3

Banded Tendon 3 Loading				
	Load Cell	**Readout**	**Load (kip)**	**Readout Aim**
Init	S8	-143	**1.585**	-135
5kip	S8	-478	**5.002**	-478
8kip	S8	-772	**8.001**	-772
10.904kip	S8	-1045	**10.786**	-1045
Measured Elongation				
Piston Extension (in)	**Fact. Piston Extension (in)**	**Dead End Seating (in)**	**Live End Seating (in)**	**Strand Elongation (in)**
0.3125		1.4375	1.9375	
1.09375	1.1437	1.40625	1.9375	1.11243
1.78125	1.8316	1.375	1.875	1.70665
2.40625	2.4545	1.375	1.875	2.32950
Expected Elongation				
Ram Elongation (in)	**In-Slab Elongation (in)**	**Predicted Elongation (in)**	**Percent Difference**	
0.1112	1.10150	1.21271	-8.3%	
0.1779	1.76184	1.93972	-12.0%	
0.2398	2.37501	2.61480	-10.9%	
Seating Loss				
Ram Length @ Low Force (<1kip)	**Calculated Seating Loss (in.)**	**Measured Seating Loss (in.)**		**L_ram (in)**
2.125	0.0415	1/16		36.75

Table E.20. Stressing Sheet for Banded Tendon 4

Banded Tendon 4 Loading				
	Load Cell	**Readout**	**Load (kip)**	**Readout Aim**
Init	S8	-135	**1.504**	-135
5kip	S8	-478	**5.002**	-478
8kip	S8	-772	**8.001**	-772
10.904kip	S8	-1045	**10.786**	-1045
Measured Elongation				
Piston Extension (in)	**Fact. Piston Extension (in)**	**Dead End Seating (in)**	**Live End Seating (in)**	**Strand Elongation (in)**
0.28125		1.4375	2.125	
1.25	1.3851	1.40625	2.125	1.35384
2.03125	2.1550	1.375	2.125	2.09248
2.75	2.8687	1.375	2.0625	2.74367
Expected Elongation				
Ram Elongation (in)	**In-Slab Elongation (in)**	**Predicted Elongation (in)**	**Percent Difference**	
0.1135	1.10150	1.21498	11.4%	
0.1815	1.76184	1.94335	7.7%	
0.2447	2.37501	2.61970	4.7%	
Seating Loss				
Ram Length @ Low Force (<1kip)	**Calculated Seating Loss (in.)**	**Measured Seating Loss (in.)**		**L_ram (in)**
2.4375	0.0678	3/32		37.5

Table E.21. Stressing Sheet for Banded Tendon 5

Banded Tendon 5				
Loading				
	Load Cell	**Readout**	**Load (kip)**	**Readout Aim**
Init	S8	-137	**1.524**	-135
5kip	S8	-475	**4.972**	-478
8kip	S8	-772	**8.001**	-772
10.904kip	S8	-1045	**10.786**	-1045
Measured Elongation				
Piston Extension (in)	**Fact. Piston Extension (in)**	**Dead End Seating (in)**	**Live End Seating (in)**	**Strand Elongation (in)**
0.25		N/A	N/A	
1.125	1.2618	N/A	N/A	1.26179
1.875	2.0074	N/A	N/A	2.00735
2.5625	2.6930	N/A	N/A	2.69302
Expected Elongation				
Ram Elongation (in)	**In-Slab Elongation (in)**	**Predicted Elongation (in)**	**Percent Difference**	
0.1105	1.09476	1.20529	4.7%	
0.1779	1.76184	1.93972	3.5%	
0.2398	2.37501	2.61480	3.0%	
Seating Loss				
Ram Length @ Low Force (<1kip)	**Calculated Seating Loss (in.)**	**Measured Seating Loss (in.)**		**L_ram (in)**
2.25	0.0727	Not Measured		36.75

Table E.22. Stressing Sheet for Banded Tendon 6

Banded Tendon 6				
Loading				
	Load Cell	**Readout**	**Load (kip)**	**Readout Aim**
Init	S8	-153	**1.687**	-135
5kip	S8	-477	**4.992**	-478
8kip	S8	-774	**8.021**	-772
10.904kip	S8	-1046	**10.796**	-1045
Measured Elongation				
Piston Extension (in)	**Fact. Piston Extension (in)**	**Dead End Seating (in)**	**Live End Seating (in)**	**Strand Elongation (in)**
0.25		N/A	N/A	
1.0625	1.2273	N/A	N/A	1.22731
1.6875	1.8204	N/A	N/A	1.82040
2.3125	2.4445	N/A	N/A	2.44454
Expected Elongation				
Ram Elongation (in)	**In-Slab Elongation (in)**	**Predicted Elongation (in)**	**Percent Difference**	
0.1114	1.09925	1.21061	1.4%	
0.1789	1.76633	1.94527	-6.4%	
0.2408	2.37726	2.61809	-6.6%	
Seating Loss				
Ram Length @ Low Force (<1kip)	**Calculated Seating Loss (in.)**	**Measured Seating Loss (in.)**		**L_ram (in)**
2.0625	0.0092	Not Measured		36.875

Table E.23. Stressing Sheet for Banded Tendon 7

Banded Tendon 7 Loading				
	Load Cell	**Readout**	**Load (kip)**	**Readout Aim**
Init	S8	-142	**1.575**	-135
5kip	S8	-474	**4.961**	-478
8kip	S8	-776	**8.042**	-772
10.904kip	S8	-967	**9.990**	-1045
Measured Elongation				
Piston Extension (in)	**Fact. Piston Extension (in)**	**Dead End Seating (in)**	**Live End Seating (in)**	**Strand Elongation (in)**
0.875		N/A	N/A	
1.6875	1.1904	N/A	N/A	1.19039
2.5	2.0208	N/A	N/A	2.02077
3	2.5227	N/A	N/A	2.52273
Expected Elongation				
Ram Elongation (in)	**In-Slab Elongation (in)**	**Predicted Elongation (in)**	**Percent Difference**	
0.1146	1.09251	1.20713	-1.4%	
0.1858	1.77082	1.95660	3.3%	
0.2308	2.19982	2.43061	3.8%	
Seating Loss				
Ram Length @ Low Force (<1kip)	**Calculated Seating Loss (in.)**	**Measured Seating Loss (in.)**		**L_ram (in)**
2.75	0.0192	Not Measured		38.1875

Table E.24. Stressing Sheet for Banded Tendon 8

Banded Tendon 8 Loading				
	Load Cell	**Readout**	**Load (kip)**	**Readout Aim**
Init	S8	-176	**1.922**	-135
5kip	S8	-473	**4.951**	-478
8kip	S8	-773	**8.011**	-772
10.904kip	S8	-1045	**10.786**	-1045
Measured Elongation				
Piston Extension (in)	**Fact. Piston Extension (in)**	**Dead End Seating (in)**	**Live End Seating (in)**	**Strand Elongation (in)**
0.375		N/A	N/A	
1	1.0215	N/A	N/A	1.02149
1.6875	1.7267	N/A	N/A	1.72672
2.25	2.2815	N/A	N/A	2.28153
Expected Elongation				
Ram Elongation (in)	**In-Slab Elongation (in)**	**Predicted Elongation (in)**	**Percent Difference**	
0.1144	1.09027	1.20465	-15.2%	
0.1851	1.76408	1.94916	-11.4%	
0.2492	2.37501	2.62418	-13.1%	
Seating Loss				
Ram Length @ Low Force (<1kip)	**Calculated Seating Loss (in.)**	**Measured Seating Loss (in.)**		**L_ram (in)**
2	0.0008	Not Measured		38.1875

Table E.25. Stressing Sheet for Banded Tendon 9

Banded Tendon 9				
Loading				
	Load Cell	**Readout**	**Load (kip)**	**Readout Aim**
Init	S8	-137	**1.524**	-135
5kip	S8	-478	**5.002**	-478
8kip	S8	-781	**8.093**	-772
10.904kip	S8	-1045	**10.786**	-1045
Measured Elongation				
Piston Extension (in)	**Fact. Piston Extension (in)**	**Dead End Seating (in)**	**Live End Seating (in)**	**Strand Elongation (in)**
0.3125		N/A	N/A	
1.125	1.1685	N/A	N/A	1.16850
1.875	1.9250	N/A	N/A	1.92501
2.5625	2.6202	N/A	N/A	2.62024
Expected Elongation				
Ram Elongation (in)	**In-Slab Elongation (in)**	**Predicted Elongation (in)**	**Percent Difference**	
0.1120	1.10150	1.21346	-3.7%	
0.1811	1.78205	1.96320	-1.9%	
0.2414	2.37501	2.61643	0.1%	
Seating Loss				
Ram Length @ Low Force (<1kip)	**Calculated Seating Loss (in.)**	**Measured Seating Loss (in.)**		**L_ram (in)**
2.25	0.0711	1/16		37

Table E.26. Stressing Sheet for Banded Tendon 10

Banded Tendon 10				
Loading				
	Load Cell	**Readout**	**Load (kip)**	**Readout Aim**
Init	S8	-134	**1.493**	-135
5kip	S8	-478	**5.002**	-478
8kip	S8	-770	**7.981**	-772
10.904kip	S8	-1045	**10.786**	-1045
Measured Elongation				
Piston Extension (in)	**Fact. Piston Extension (in)**	**Dead End Seating (in)**	**Live End Seating (in)**	**Strand Elongation (in)**
0.25		1.4375	2.125	
1.125	1.2474	1.40625	2.125	1.21616
1.75	1.8453	1.375	2.125	1.78281
2.4375	2.5391	1.375	2.125	2.47657
Expected Elongation				
Ram Elongation (in)	**In-Slab Elongation (in)**	**Predicted Elongation (in)**	**Percent Difference**	
0.1123	1.10150	1.21384	0.2%	
0.1792	1.75735	1.93658	-7.9%	
0.2422	2.37501	2.61725	-5.4%	
Seating Loss				
Ram Length @ Low Force (<1kip)	**Calculated Seating Loss (in.)**	**Measured Seating Loss (in.)**		**L_ram (in)**
2.125	0.0703	1/16		37.125

Table E.27. Stressing Sheet for Banded Tendon 11

Banded Tendon 11 Loading				
	Load Cell	**Readout**	**Load (kip)**	**Readout Aim**
Init	S8	-141	**1.565**	-135
5kip	S8	-478	**5.002**	-478
8kip	S8	-772	**8.001**	-772
10.904kip	S8	-1046	**10.796**	-1045
Measured Elongation				
Piston Extension (in)	**Fact. Piston Extension (in)**	**Dead End Seating (in)**	**Live End Seating (in)**	**Strand Elongation (in)**
0.25		1.4375	2	
1.0625	1.1824	1.375	1.9375	1.05737
1.6875	1.7870	1.34375	1.9375	1.63074
2.3125	2.4121	1.34375	1.9375	2.25588
Expected Elongation				
Ram Elongation (in)	**In-Slab Elongation (in)**	**Predicted Elongation (in)**	**Percent Difference**	
0.1127	1.10150	1.21422	-12.9%	
0.1803	1.76184	1.94214	-16.0%	
0.2433	2.37726	2.62054	-13.9%	
Seating Loss				
Ram Length @ Low Force (<1kip)	**Calculated Seating Loss (in.)**	**Measured Seating Loss (in.)**		**L_ram (in)**
2	0.0692	1/16		37.25

Table E.28. Stressing Sheet for Banded Tendon 12

Banded Tendon 12 Loading				
	Load Cell	**Readout**	**Load (kip)**	**Readout Aim**
Init	S8	-135	**1.504**	-135
5kip	S8	-478	**5.002**	-478
8kip	S8	-770	**7.981**	-772
10.904kip	S8	-1044	**10.775**	-1045
Measured Elongation				
Piston Extension (in)	**Fact. Piston Extension (in)**	**Dead End Seating (in)**	**Live End Seating (in)**	**Strand Elongation (in)**
0.3125		N/A	N/A	
1.25	1.3404	N/A	N/A	1.34041
2	2.0792	N/A	N/A	2.07924
2.75	2.8328	N/A	N/A	2.83279
Expected Elongation				
Ram Elongation (in)	**In-Slab Elongation (in)**	**Predicted Elongation (in)**	**Percent Difference**	
0.1127	1.10150	1.21422	10.4%	
0.1798	1.75735	1.93719	7.3%	
0.2428	2.37277	2.61559	8.3%	
Seating Loss				
Ram Length @ Low Force (<1kip)	**Calculated Seating Loss (in.)**	**Measured Seating Loss (in.)**		**L_ram (in)**
2.5	0.0072	1/16		37.25

Table E.29. Stressing Sheet for Banded Tendon 13

Banded Tendon 13				
Loading				
	Load Cell	**Readout**	**Load (kip)**	**Readout Aim**
Init	S8	-139	**1.544**	-135
5kip	S8	-482	**5.043**	-478
8kip	S8	-772	**8.001**	-772
10.904kip	S8	-1045	**10.786**	-1045
Measured Elongation				
Piston Extension (in)	**Fact. Piston Extension (in)**	**Dead End Seating (in)**	**Live End Seating (in)**	**Strand Elongation (in)**
0.3125		1.4375	2	
1.1875	1.2613	1.375	2	1.19875
1.9375	2.0137	N/A	2	2.01370
2.6875	2.7719	1.375	1.9375	2.64691
Expected Elongation				
Ram Elongation (in)	**In-Slab Elongation (in)**	**Predicted Elongation (in)**	**Percent Difference**	
0.1138	1.11048	1.22431	-2.1%	
0.1806	1.76184	1.94244	3.7%	
0.2435	2.37501	2.61847	1.1%	
Seating Loss				
Ram Length @ Low Force (<1kip)	**Calculated Seating Loss (in.)**	**Measured Seating Loss (in.)**		**L_ram (in)**
2.3125	0.1315	1/16		37.3125

Table E.30. Stressing Sheet for Banded Tendon 14

Banded Tendon 14				
Loading				
	Load Cell	**Readout**	**Load (kip)**	**Readout Aim**
Init	S8	-135	**1.504**	-135
5kip	S8	-478	**5.002**	-478
8kip	S8	-774	**8.021**	-772
10.904kip	S8	-1047	**10.806**	-1045
Measured Elongation				
Piston Extension (in)	**Fact. Piston Extension (in)**	**Dead End Seating (in)**	**Live End Seating (in)**	**Strand Elongation (in)**
0.375		1.40625	1.625	
1.1875	1.1617	1.375	1.625	1.13044
1.9375	1.9230	1.375	1.5625	1.82921
2.5625	2.5411	1.34375	1.5625	2.41608
Expected Elongation				
Ram Elongation (in)	**In-Slab Elongation (in)**	**Predicted Elongation (in)**	**Percent Difference**	
0.1095	1.10150	1.21100	-6.7%	
0.1756	1.76633	1.94193	-5.8%	
0.2366	2.37950	2.61607	-7.6%	
Seating Loss				
Ram Length @ Low Force (<1kip)	**Calculated Seating Loss (in.)**	**Measured Seating Loss (in.)**		**L_ram (in)**
2.25	0.0759	3/32		36.1875

Table E.31. Stressing Sheet for Banded Tendon 15

Banded Tendon 15				
Loading				
	Load Cell	**Readout**	**Load (kip)**	**Readout Aim**
Init	S8	-139	**1.544**	-135
5kip	S8	-478	**5.002**	-478
8kip	S8	-773	**8.011**	-772
10.904kip	S8	-1045	**10.786**	-1045
Measured Elongation				
Piston Extension (in)	**Fact. Piston Extension (in)**	**Dead End Seating (in)**	**Live End Seating (in)**	**Strand Elongation (in)**
0.25		1.4375	2.125	
1.25	1.4466	1.375	2.125	1.38414
2.03125	2.2066	1.34375	2.125	2.11290
2.75	2.9178	1.34375	2.125	2.82405
Expected Elongation				
Ram Elongation (in)	**In-Slab Elongation (in)**	**Predicted Elongation (in)**	**Percent Difference**	
0.1112	1.10150	1.21271	14.1%	
0.1781	1.76408	1.94219	8.8%	
0.2398	2.37501	2.61480	8.0%	
Seating Loss				
Ram Length @ Low Force (<1kip)	**Calculated Seating Loss (in.)**	**Measured Seating Loss (in.)**		**L_ram (in)**
2.4375	0.0727	1/16		36.75

Table E.32. Stressing Sheet for Banded Tendon 16

Banded Tendon 16				
Loading				
	Load Cell	**Readout**	**Load (kip)**	**Readout Aim**
Init	S8	-135	**1.504**	-135
5kip	S8	-480	**5.023**	-478
8kip	S8	-772	**8.001**	-772
10.904kip	S8	-1045	**10.786**	-1045
Measured Elongation				
Piston Extension (in)	**Fact. Piston Extension (in)**	**Dead End Seating (in)**	**Live End Seating (in)**	**Strand Elongation (in)**
0.3125		1.4375	2.125	
1.125	1.1597	1.375	2.125	1.09717
1.8125	1.8471	1.375	2.125	1.78462
2.5	2.5419	1.375	2.125	2.47936
Expected Elongation				
Ram Elongation (in)	**In-Slab Elongation (in)**	**Predicted Elongation (in)**	**Percent Difference**	
0.1120	1.10599	1.21803	-9.9%	
0.1785	1.76184	1.94032	-8.0%	
0.2406	2.37501	2.61562	-5.2%	
Seating Loss				
Ram Length @ Low Force (<1kip)	**Calculated Seating Loss (in.)**	**Measured Seating Loss (in.)**		**L_ram (in)**
2.25	0.0094	1/16		36.875

Table E.33. Stressing Sheet for Banded Tendon 17

Banded Tendon 17				
Loading				
	Load Cell	**Readout**	**Load (kip)**	**Readout Aim**
Init	S8	-143	**1.585**	-135
5kip	S8	-478	**5.002**	-478
8kip	S8	-773	**8.011**	-772
10.904kip	S8	-1045	**10.786**	-1045
Measured Elongation				
Piston Extension (in)	**Fact. Piston Extension (in)**	**Dead End Seating (in)**	**Live End Seating (in)**	**Strand Elongation (in)**
0.1875		1.40625	2.3125	
0.9375	1.0979	1.375	2.3125	1.12919
1.625	1.7921	1.375	2.3125	1.82336
2.1875	2.3446	1.34375	2.3125	2.40709
Expected Elongation				
Ram Elongation (in)	**In-Slab Elongation (in)**	**Predicted Elongation (in)**	**Percent Difference**	
0.1116	1.10150	1.21308	-6.9%	
0.1787	1.76408	1.94280	-6.1%	
0.2406	2.37501	2.61562	-8.0%	
Seating Loss				
Ram Length @ Low Force (<1kip)	**Calculated Seating Loss (in.)**	**Measured Seating Loss (in.)**		**L_ram (in)**
1.9375	0.0094	1/16		36.875

The calculations for the determination of the measured elongations are provided below:

Δ_{piston} : Factored Piston Extension (in.)

Δ_{Dead} : Dead End Seating (in.)

Δ_{Live} : Live End Seating (in.)

$Extension$: Measured Piston Extension (in.)

s_{Dead} : Dead End Wedge Seating Distance (in.)

s_{Live} : Live End Wedge Seating Distance (in.)

P_f, P_i : Ram Force (kip)

$\Delta L_{measured}$: Measured Strand Elongation (in.)

$$\Delta_{piston} = \frac{Extension_f - Extension_i}{P_f - P_i} * P_f$$

$$\Delta_{Dead} = s_{Dead,i} - s_{Dead,f}$$

$$\Delta_{Live} = s_{Live,i} - s_{Live,f}$$

$$\Delta L_{measured} = \Delta_{piston} - \Delta_{Dead} - \Delta_{Live}$$

The calculations for the determination of the expected elongations are provided below:

$\Delta L_{predicted}$: Predicted Strand Elongation (in.)

ΔL_{ram} : Elongation of Strand Outside of Slab (in.)

ΔL_{slab} : Elongation of Strand Inside of Slab (in.)

L_{ram} : Length of Tendon From Slab Edge to Actuator Chuck (in.)

A_{ps} : Area of Strand (in^2)

E_p : Modulus of Elasticity of Strand (ksi)

L_{slab} : Length of Slab (in.)

P_{strand} : Force in Strand at a Given Location in Slab, Considering Both Friction and Wobble (kip)

$$\Delta L_{ram} = \frac{P_f L_{ram}}{A_{ps} E_p}$$

$$\Delta L_{ram} = \frac{1}{E_p} * \int_0^{L_{slab}} \frac{P_{strand}}{A_{ps}}$$

$$\Delta L_{predicted} = \Delta L_{ram} + \Delta L_{slab}$$

The calculations for the determination of the actual seating loss for a given tendon are provided below:

Δ_s : Seating Losses (in.)

$Extension_f$: Measured Piston Extension at Ultimate Strand Load (in.)

$Extension_{release}$: Measured Piston Extension After Releasing Majority of the Ram's Load* (in.)

* = Approximately 1 kip of load remains in the ram

$$\Delta_s = Extension_f - Extension_{release} - \Delta L_{ram}$$

Appendix F – Equivalent Frame Method

The following figures (Figures A6.1 through A6.5) are plots of the five slab strips for the equivalent frame method analysis of the post-tensioned flat plate after stressing (including form removal and the self-weight of the whiffle tree).

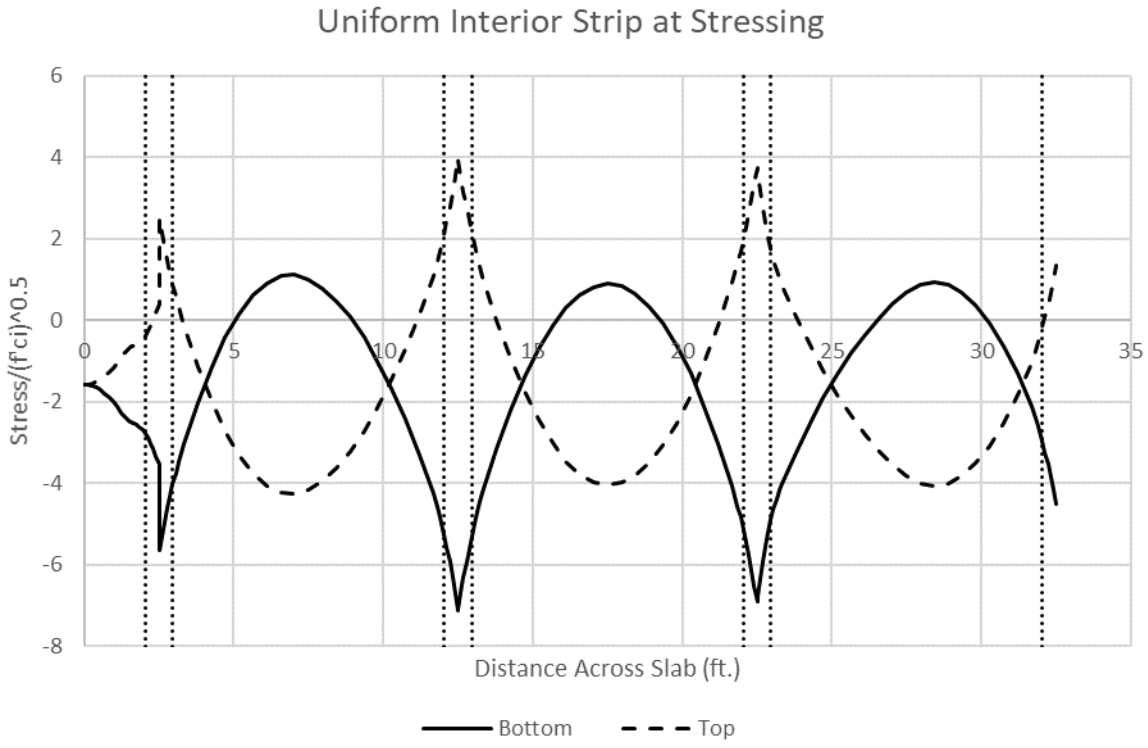

Figure F.1. Uniform Interior Strip at Stressing

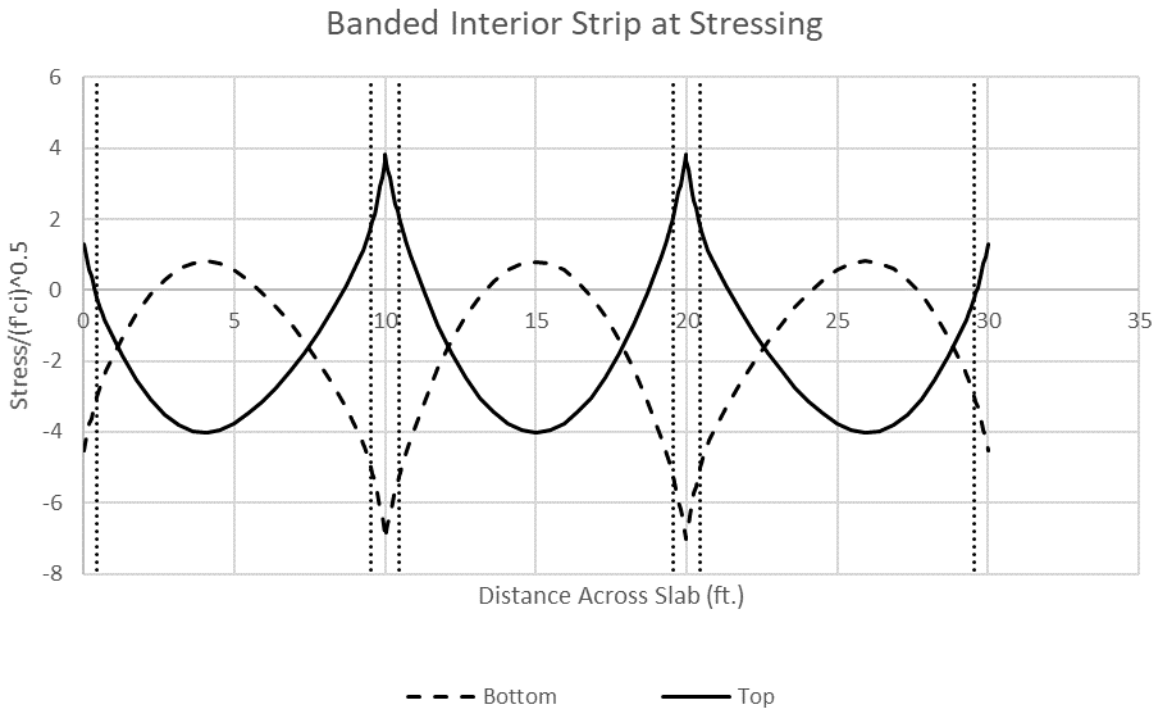

Figure F.2. Banded Interior Strip at Stressing

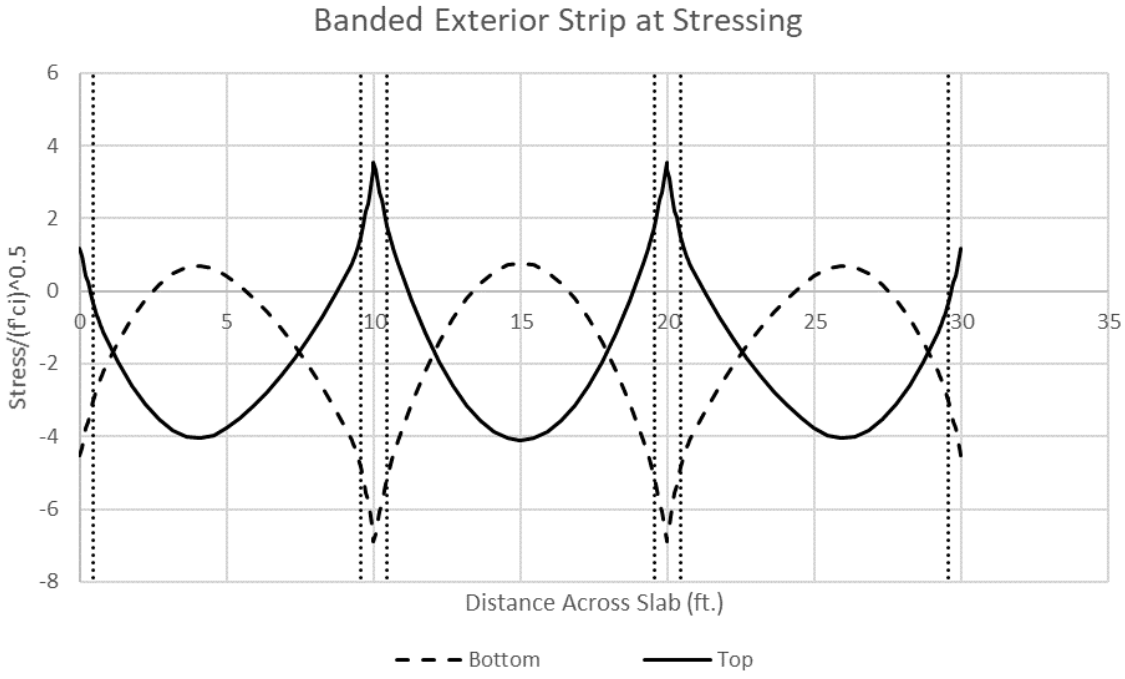

Figure F.3. Banded Exterior Strip at Stressing

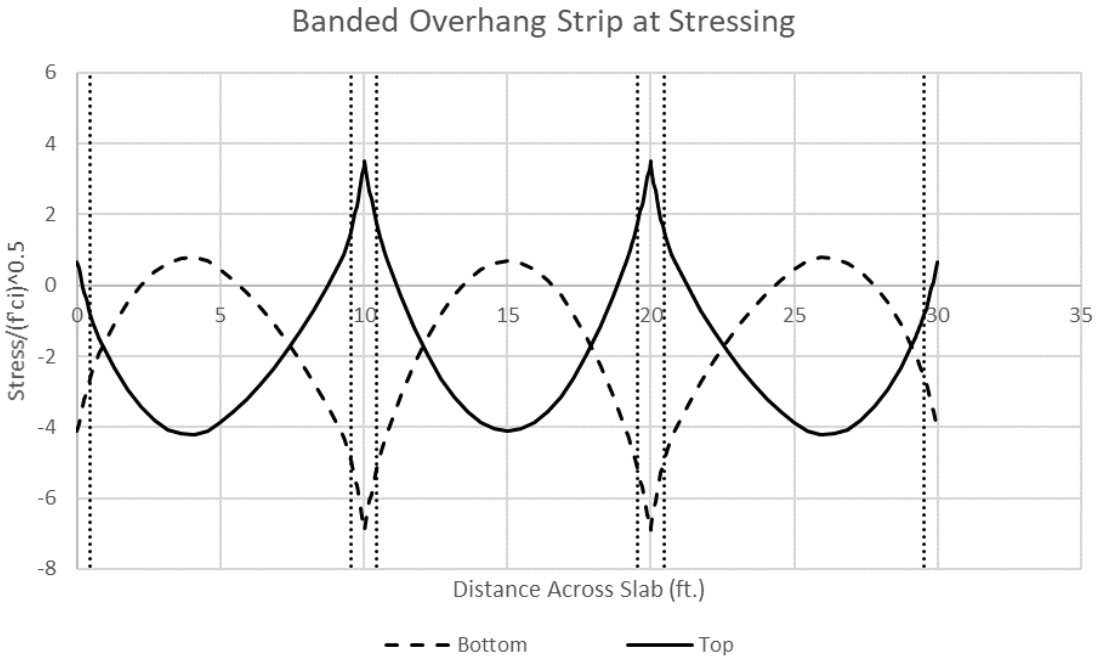

Figure F.4. Banded Overhang Strip at Stressing

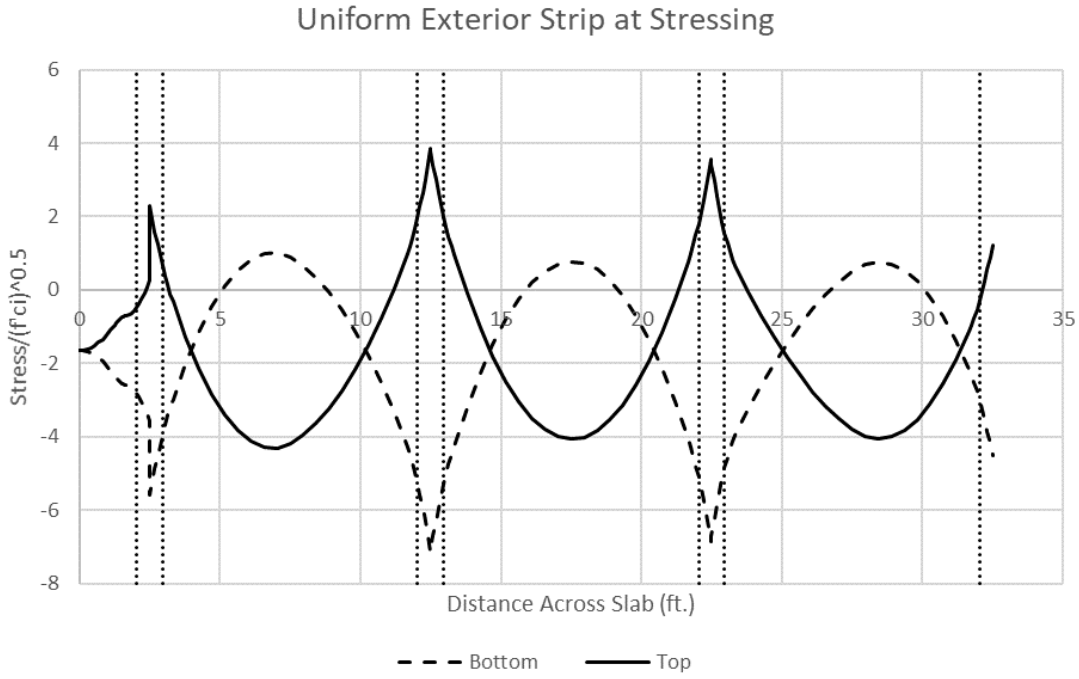

Figure F.5. Uniform Exterior Strip at Stressing

The following figures (Figures A6.6 through A6.10) are plots of the five slab strips for the equivalent frame method analysis of the post-tensioned flat plate at the updated service-level loads.

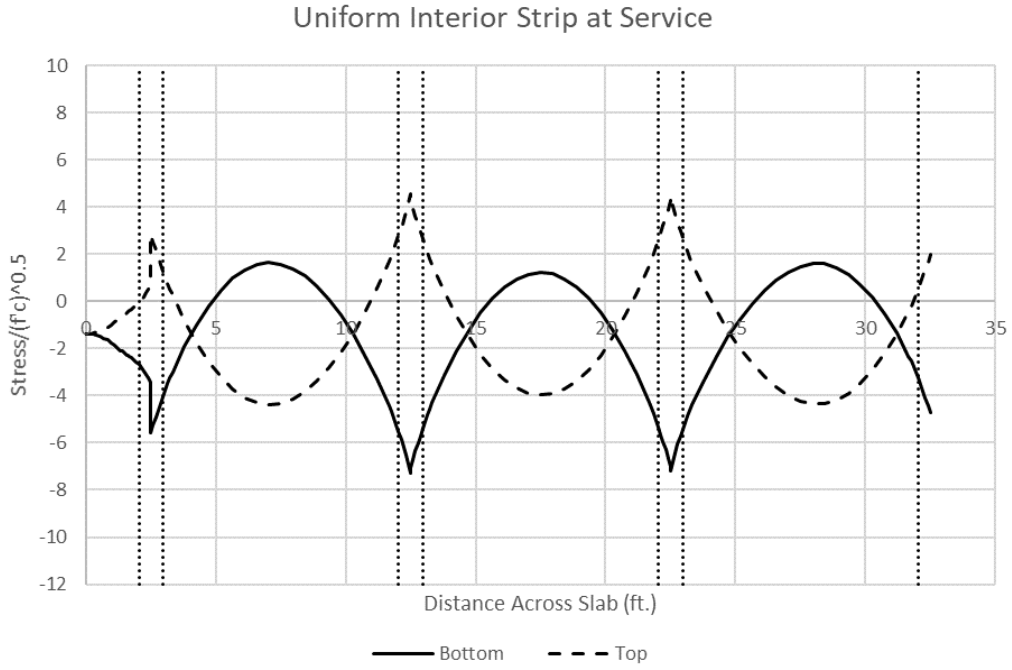

Figure F.6. Uniform Interior Strip at Service-Level Loads

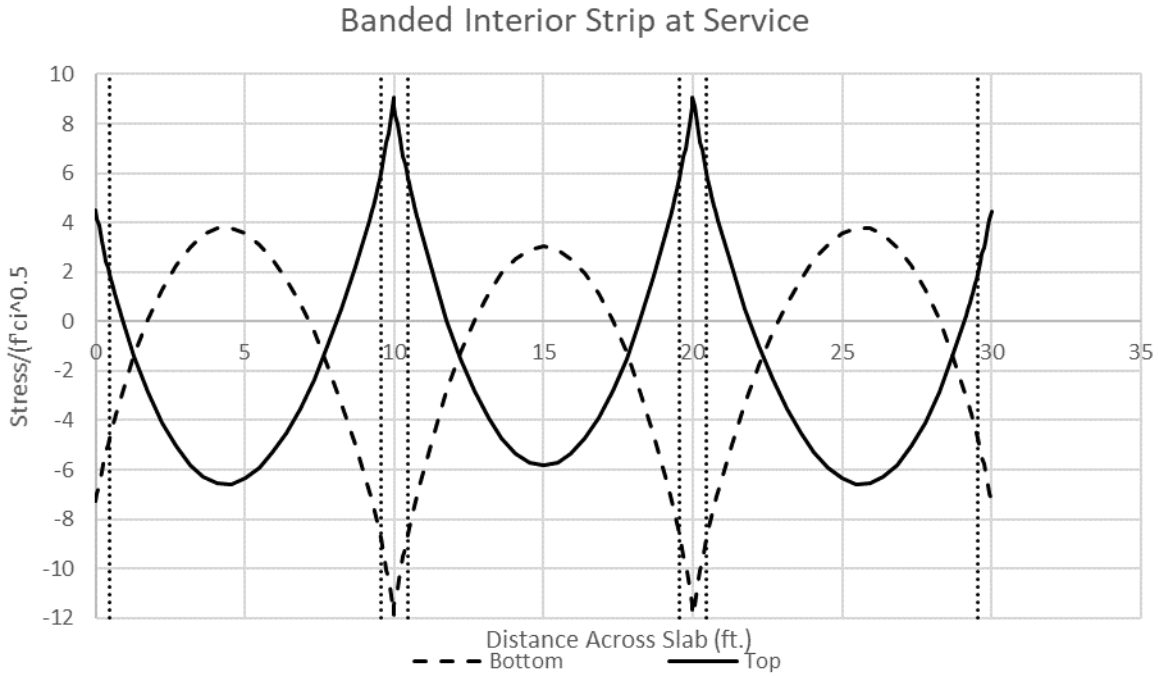

Figure F.7. Banded Interior Strip at Service-Level Loads

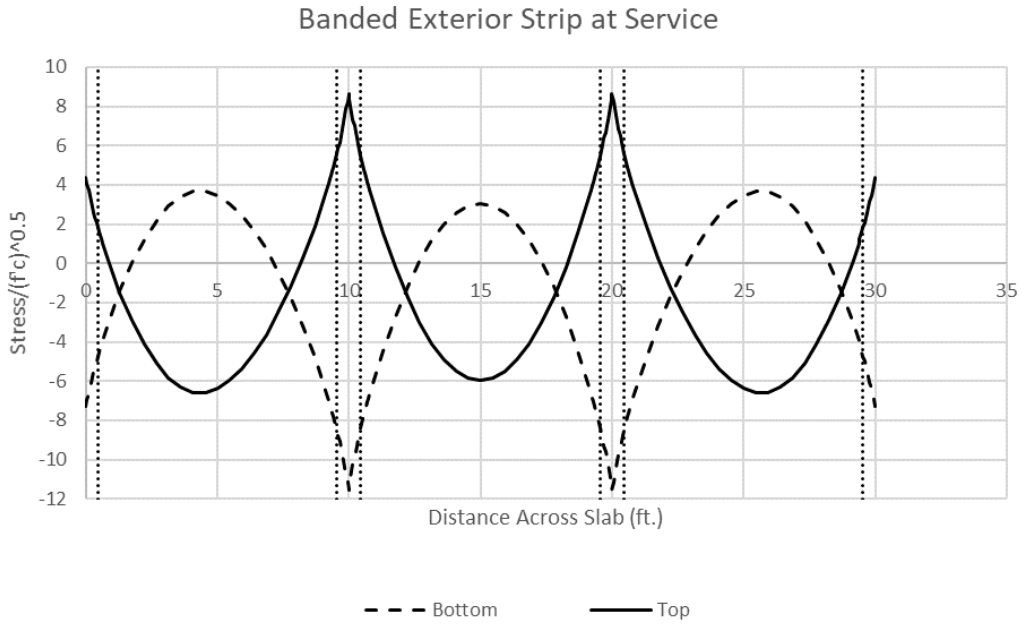

Figure F.8. Banded Exterior Strip at Service-Level Loads

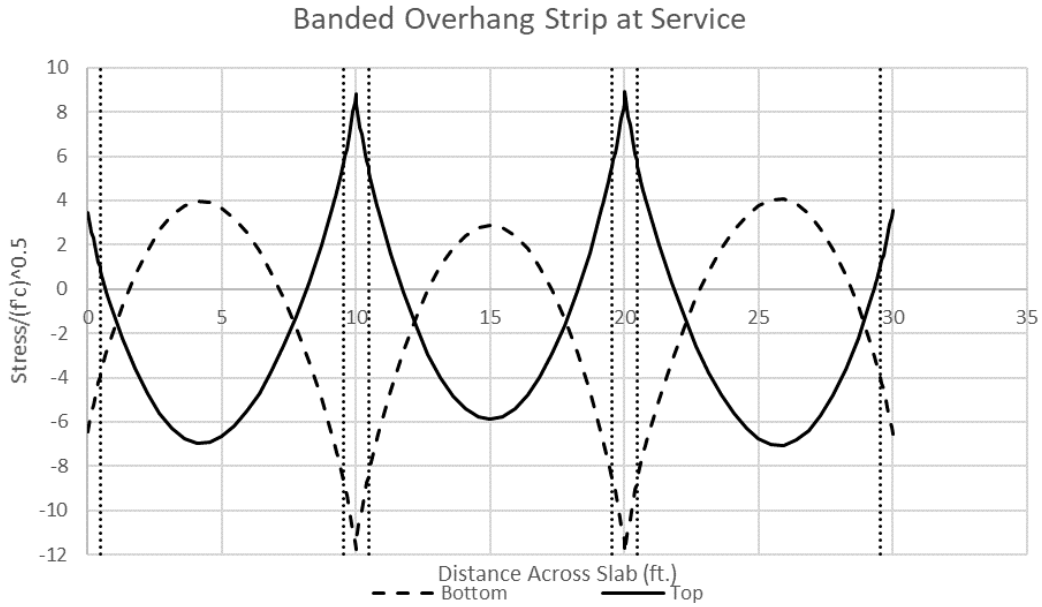

Figure F.9. Banded Overhang Strip at Service-Level Loads

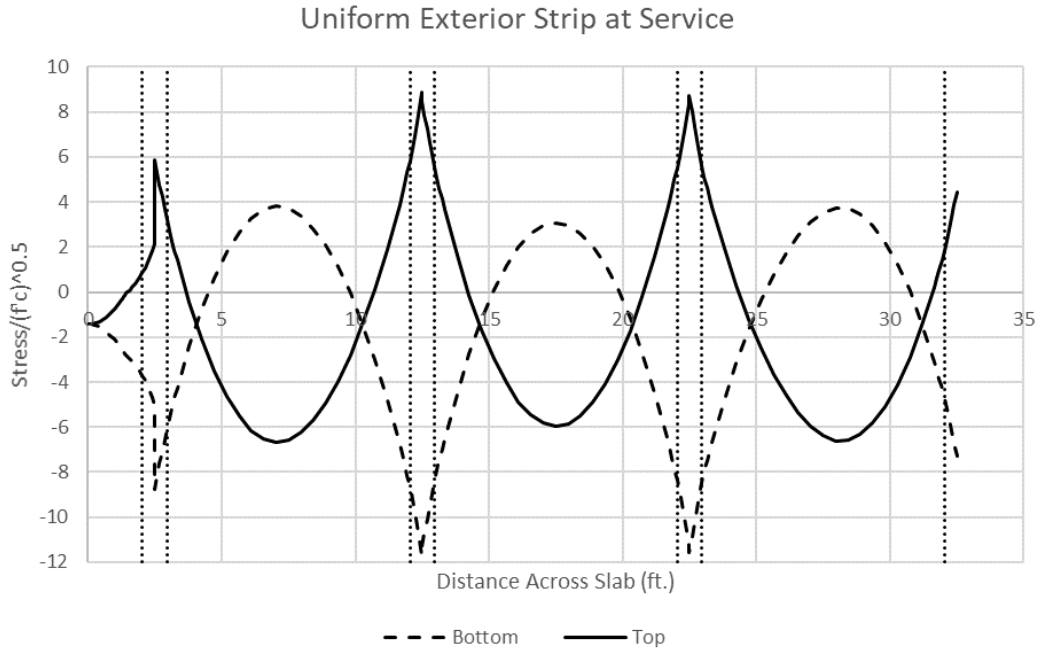

Figure F.10. Uniform Exterior Strip at Service-Level Loads

Appendix G – Concrete Properties for Specimen 2

Table G.1 and Table G.2 provide the concrete mix properties for both concrete mixes. For Truck 2, one-half gallon of superplasticizer was added to increase the original slump of 5.00in.

Table G.1. Concrete Mixture for Truck 1

Truck 1 Mixture	
Material	**Quantity (lbs)**
Type I/II Cement	714
Natural Sand	1285
Crushed Limestone (#9)	1571
Water	371
Fibers (Bekaert RC-80/30-BP)	84
Other Properties:	
Slump (in.)	6.50
Air Content (%)	3.1

Table G.2. Concrete Mixture for Truck 2

Truck 2 Mixture	
Material	**Quantity (lbs)**
Type I/II Cement	714
Natural Sand	1285
Crushed Limestone (#9)	1571
Water	371
Fibers (Bekaert RC-80/30-BP)	84
Other Properties:	
Slump (in.)	7.00
Air Content (%)	3.4

Table G.3 contains the concrete compressive strengths at stressing (9 days), at twenty-eight days, and at Specimen 2's load testing (44 days).

Table G.3. Concrete Compressive Strengths

Compressive Strengths (From 6x12 Cylinders)			
Time (Days)	**Truck 1 Strength (psi)**	**Truck 2 Strength (psi)**	**Average Strength (psi)**
9	6932	6572	6752
28	7774	7444	7609
44	7709	7617	7663

The results for the shrinkage testing and creep testing for the shrinkage prisms and creep cylinders, respectively, are shown below in Figures A7.1 and A7.2.

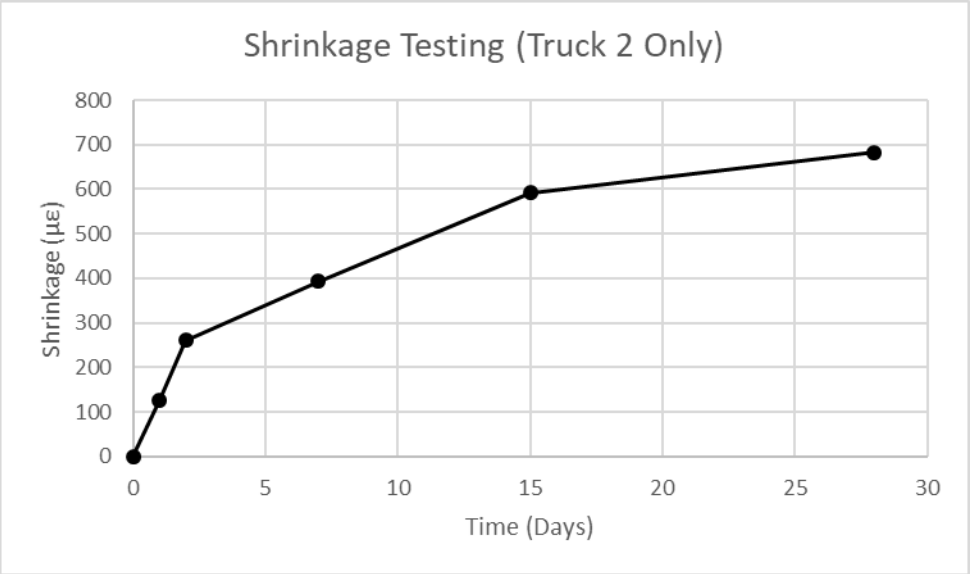

Figure G.1. Shrinkage Testing for Truck 2

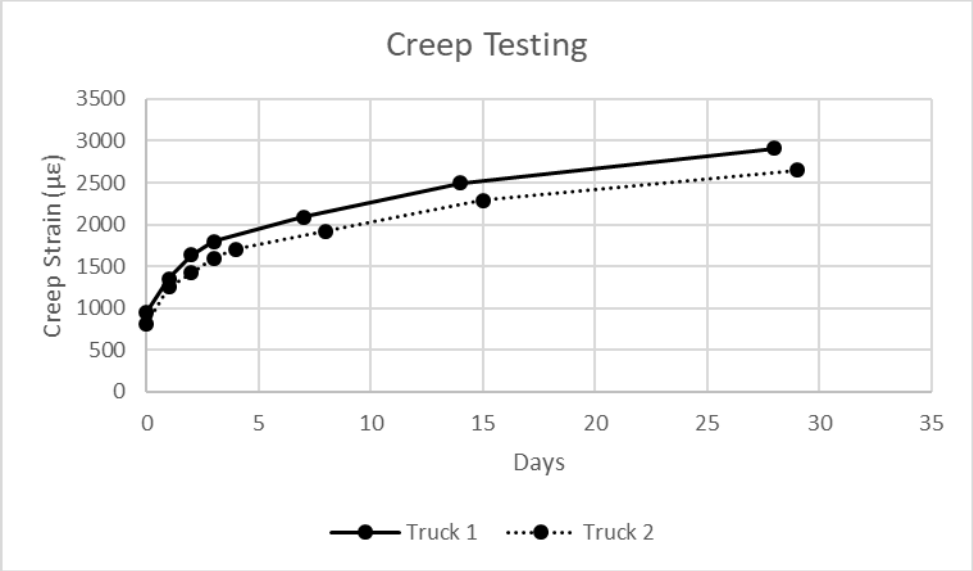

Figure G.2. Creep Testing Results

The results of splitting tensile tests and modulus of elasticity tests are shown below in Tables A7.4 and A7.5.

Table G.4. Splitting Tensile Testing

Specimen	Time (Days)	Ultimate Stress (psi)
Truck 1	47	1150
Truck 2	47	1215
Average:	47	1183

Table G.5. Modulus of Elasticity Results

Truck 1		Truck 2		Average
Time (Days)	Modulus (psi)	Time (Days)	Modulus (psi)	Modulus (psi)
9	3464600	9	3405300	3434950
47	3990950	47	3522950	3756950

Flexural beams were sent for testing by TEC Services. A summary of the test results for the beams from both concrete trucks is provided below in Table G.6 (TEC Services, 2019a), (TEC Services, 2019b).

Table G.6. Flexural Beam Testing Results

Concrete Mix:	Truck 1	Truck 2	Average
Deflection at First Crack (in.)	0.0026	0.0026	0.0026
Deflection at Peak Load (in.)	0.0029	0.0039	0.0034
First Crack Load (lbs)	12231	11254	11743
Ultimate Load (lbs)	13074	11874	12474
First Crack Stress (psi)	1020	990	1005
Toughness (lbs-in.)	980	983	982
Load at CMOD1 (lbs)	6125	4999	5562
Stress at CMOD1 (psi)	1265	1035	1150

Appendix H – Crack Photographs During Testing

Figure H.1. Column D1 at 0psf

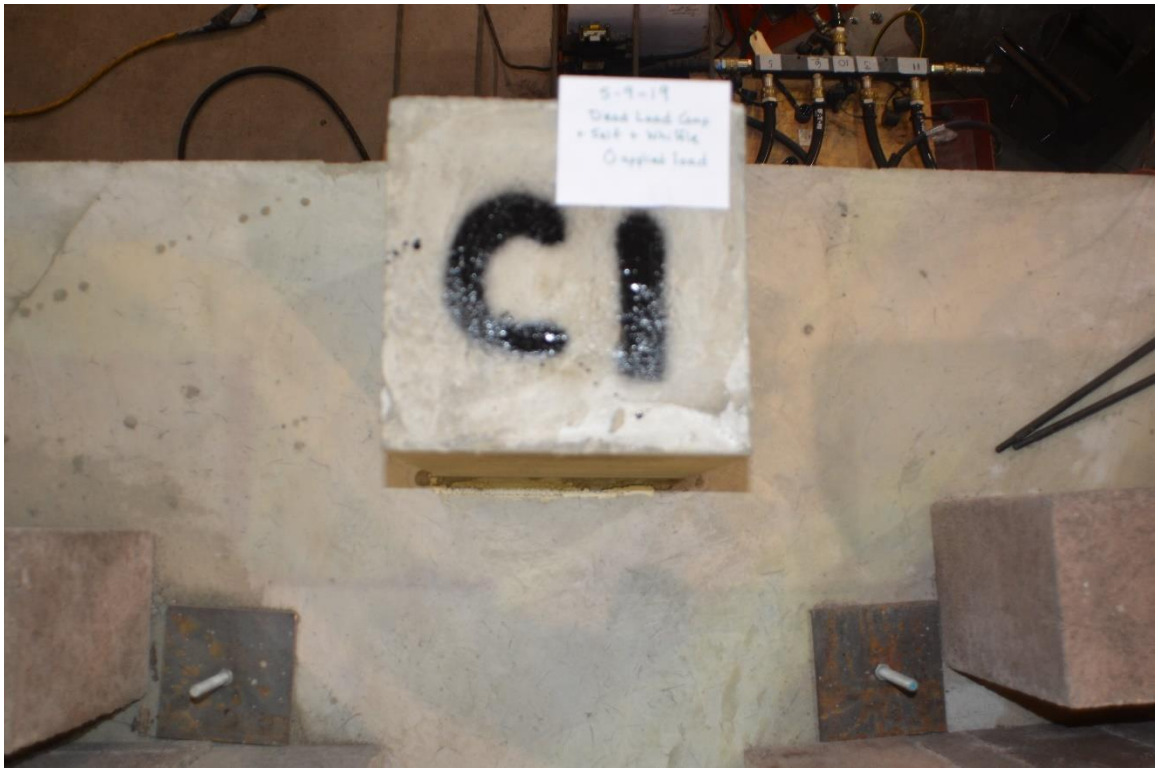

Figure H.2. Column C1 at 0psf

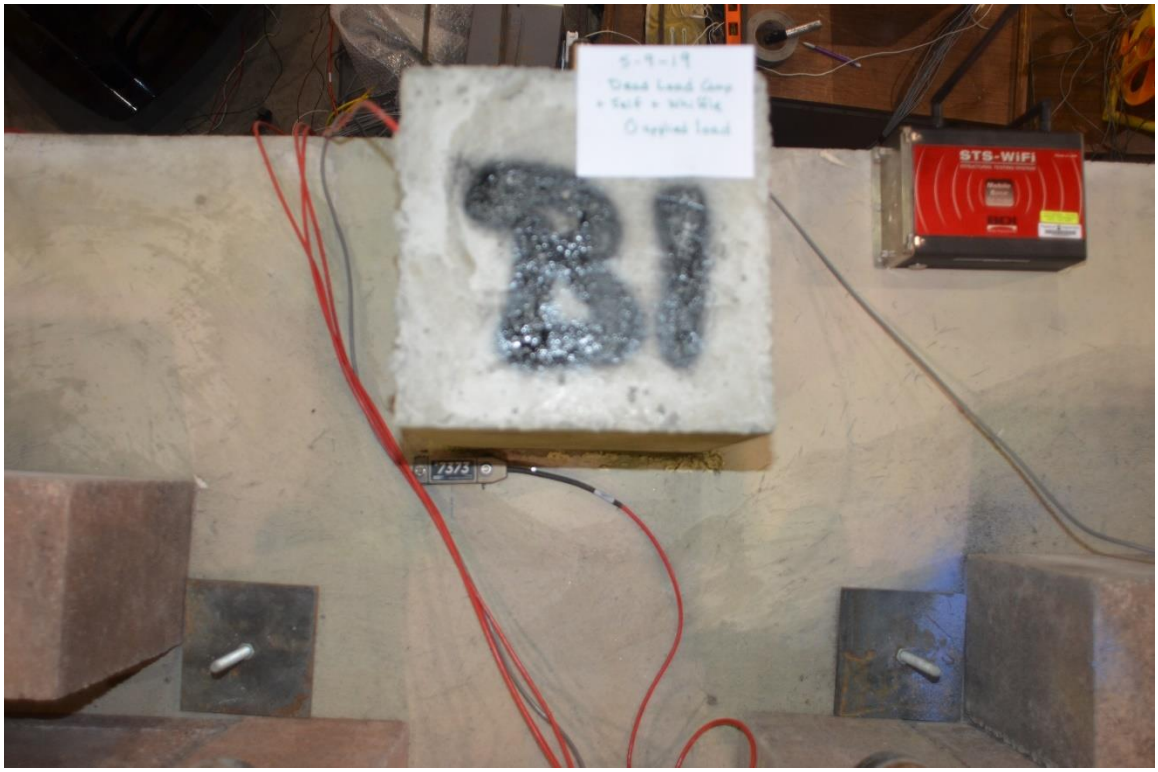

Figure H.3. Column B1 at 0psf

Figure H.4. Column A1 at 0psf

Figure H.5. Column D2 at 0psf

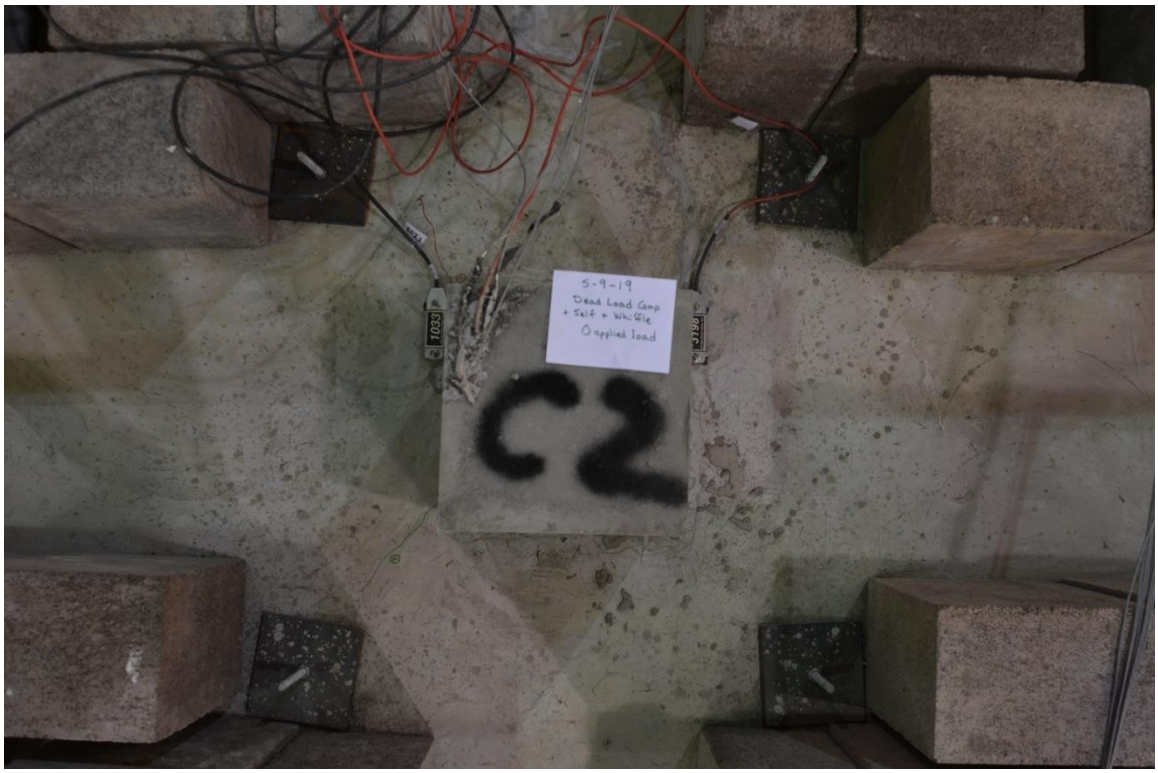

Figure H.6. Column C2 at 0psf

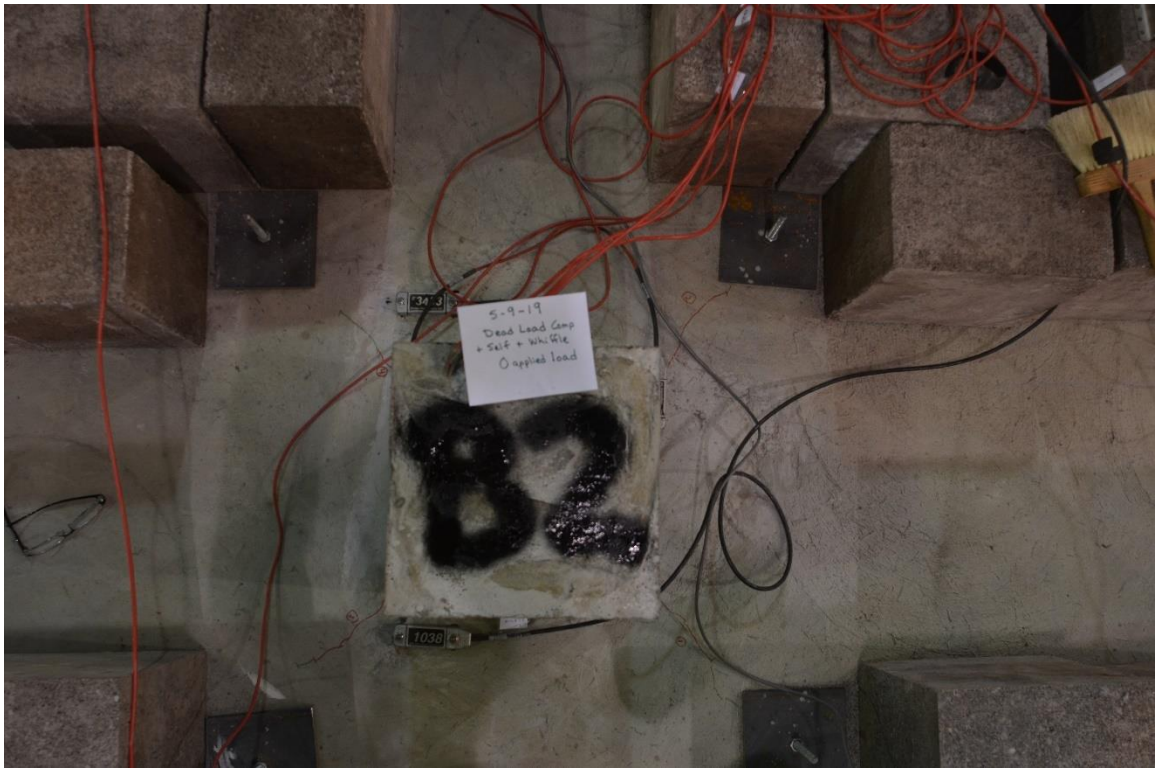

Figure H.7. Column B2 at 0psf

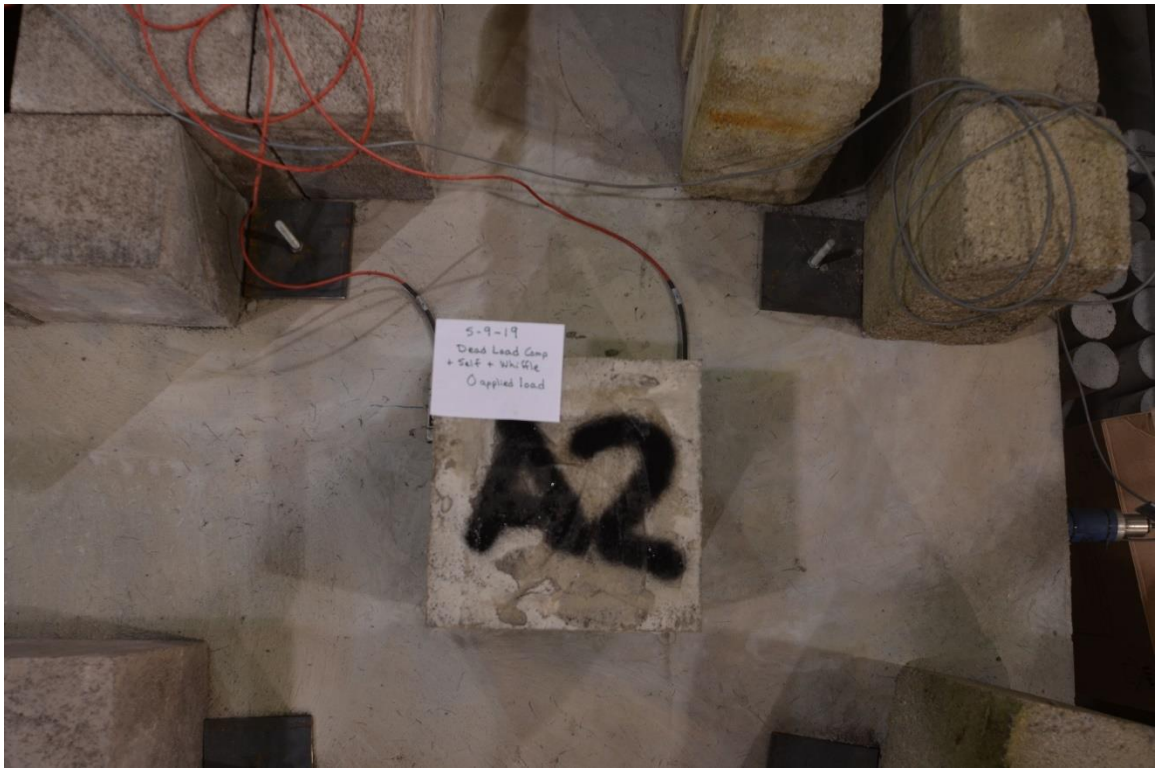

Figure H.8. Column A2 at 0psf

Figure H.9. Column D3 at 0psf

Figure H.10. Column C3 at 0psf

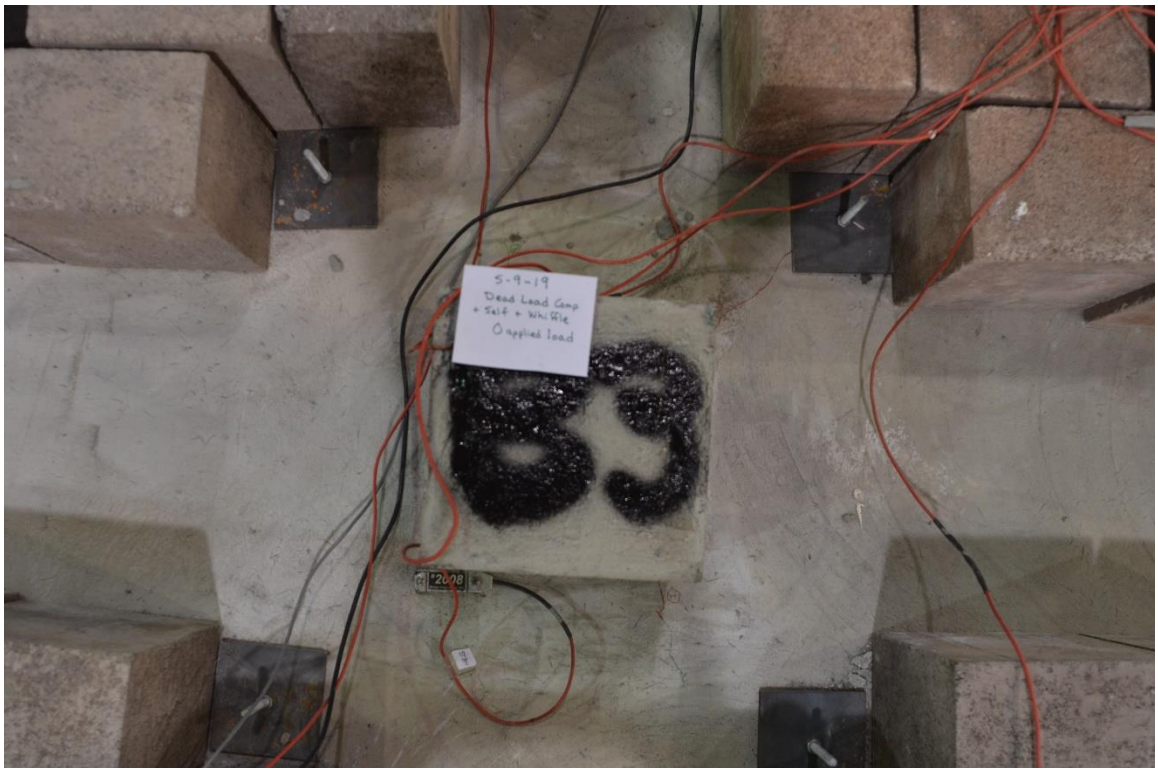

Figure H.11. Column B3 at 0psf

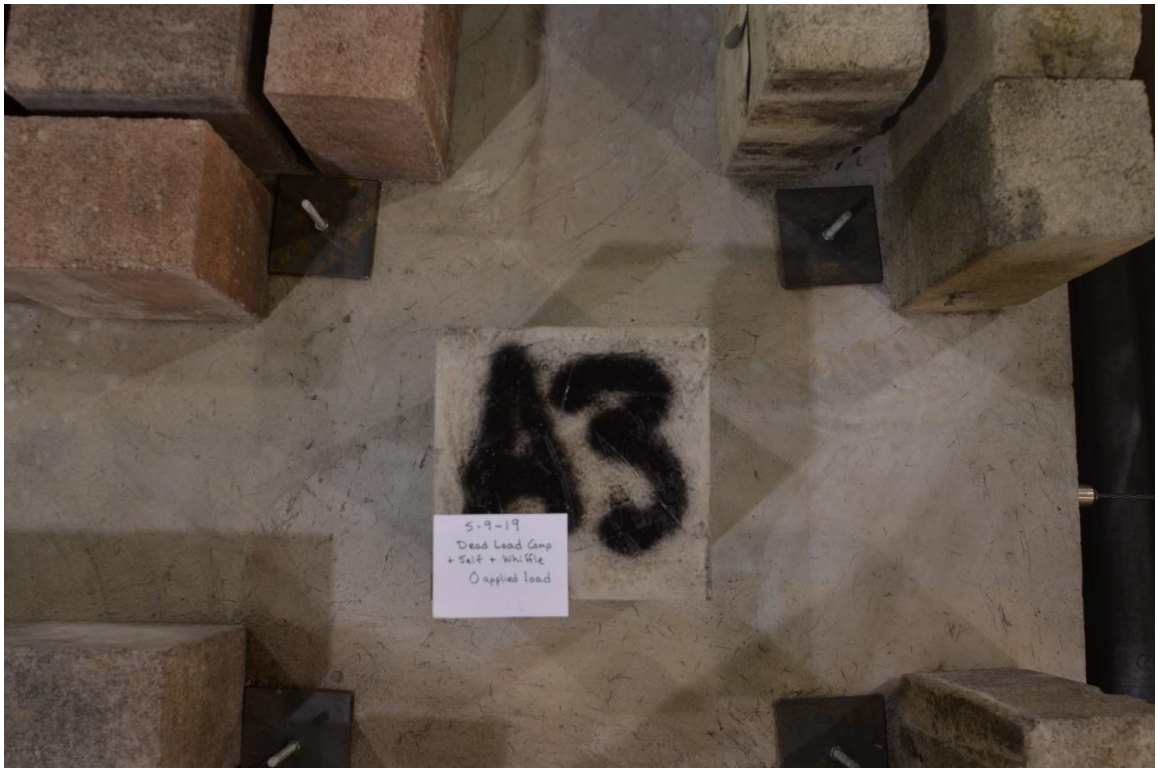

Figure H.12. Column A3 at 0psf

Figure H.13. Column D4 at 0psf

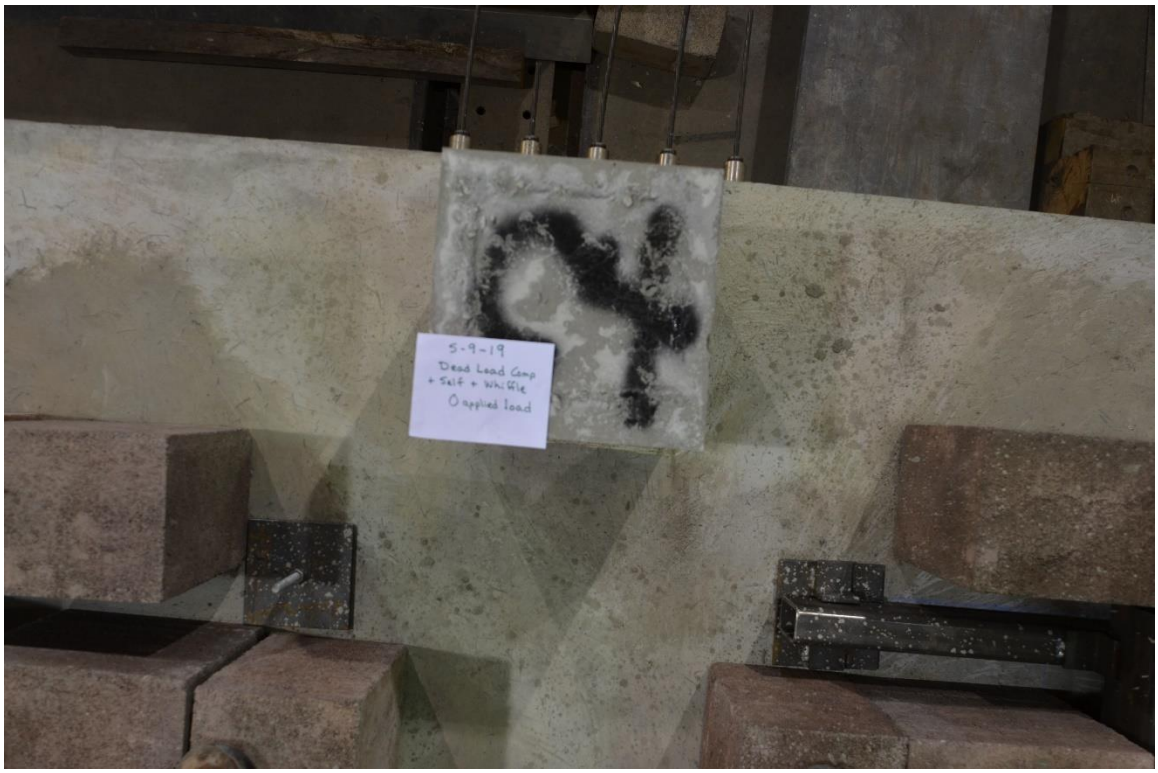

Figure H.14. Column C4 at 0psf

Figure H.15. Column B4 at 0psf

Figure H.16. Column A4 at 0psf

Figure H.17. Column D1 at Service-Level Loading

Figure H.18. Column C1 at Service-Level Loading

Figure H.19. Column B1 at Service-Level Loading

Figure H.20. Column A1 at Service-Level Loading

Figure H.21. Column D2 at Service-Level Loading

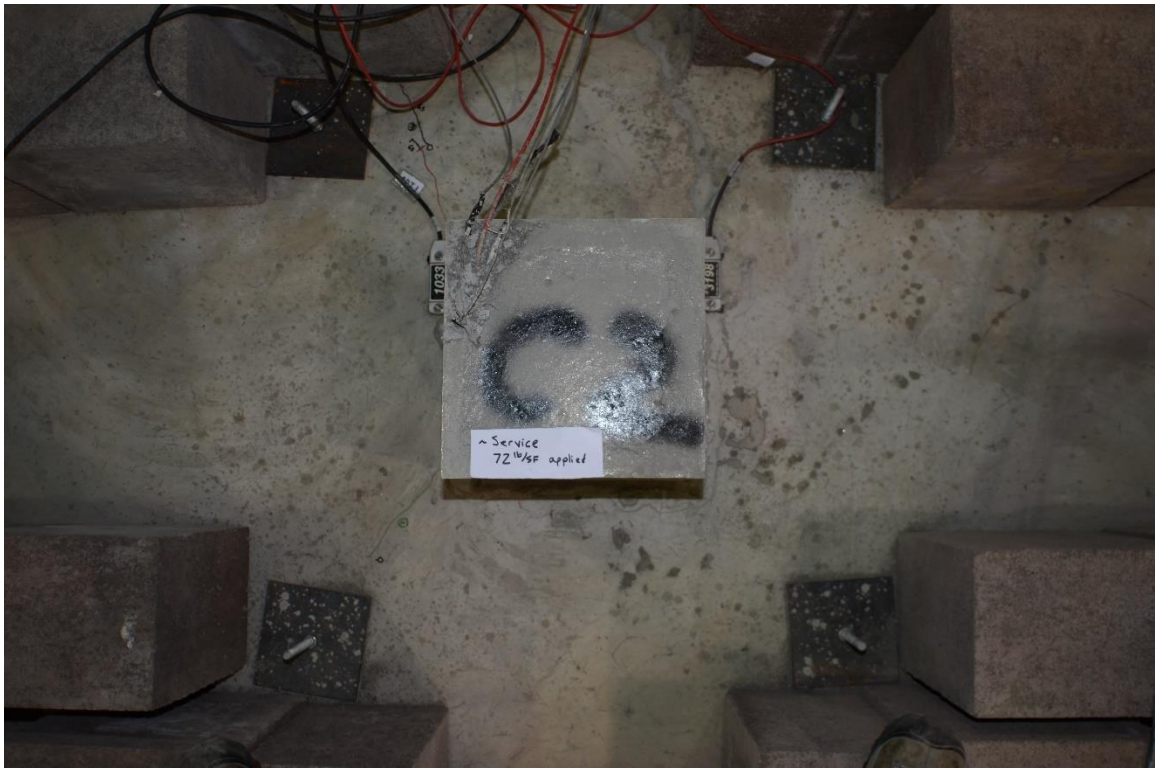

Figure H.22. Column C2 at Service-Level Loading

Figure H.23. Column B2 at Service-Level Loading

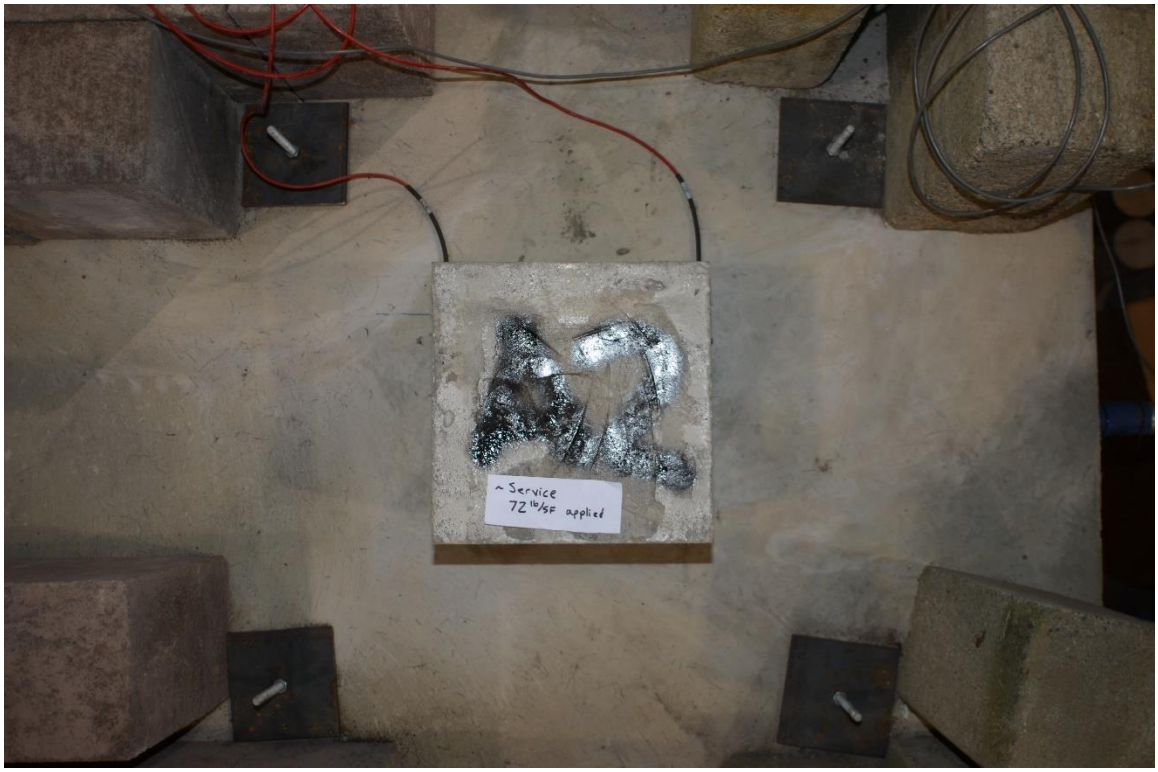

Figure H.24. Column A2 at Service-Level Loading

Figure H.25. Column D3 at Service-Level Loading

Figure H.26. Column C3 at Service-Level Loading

Figure H.27. Column B3 at Service-Level Loading

Figure H.28. Column A3 at Service-Level Loading

Figure H.29. Column D4 at Service-Level Loading

Figure H.30. Column C4 at Service-Level Loading

Figure H.31. Column B4 at Service-Level Loading

Figure H.32. Column A4 at Service-Level Loading

Figure H.33. Column C3 at 135psf

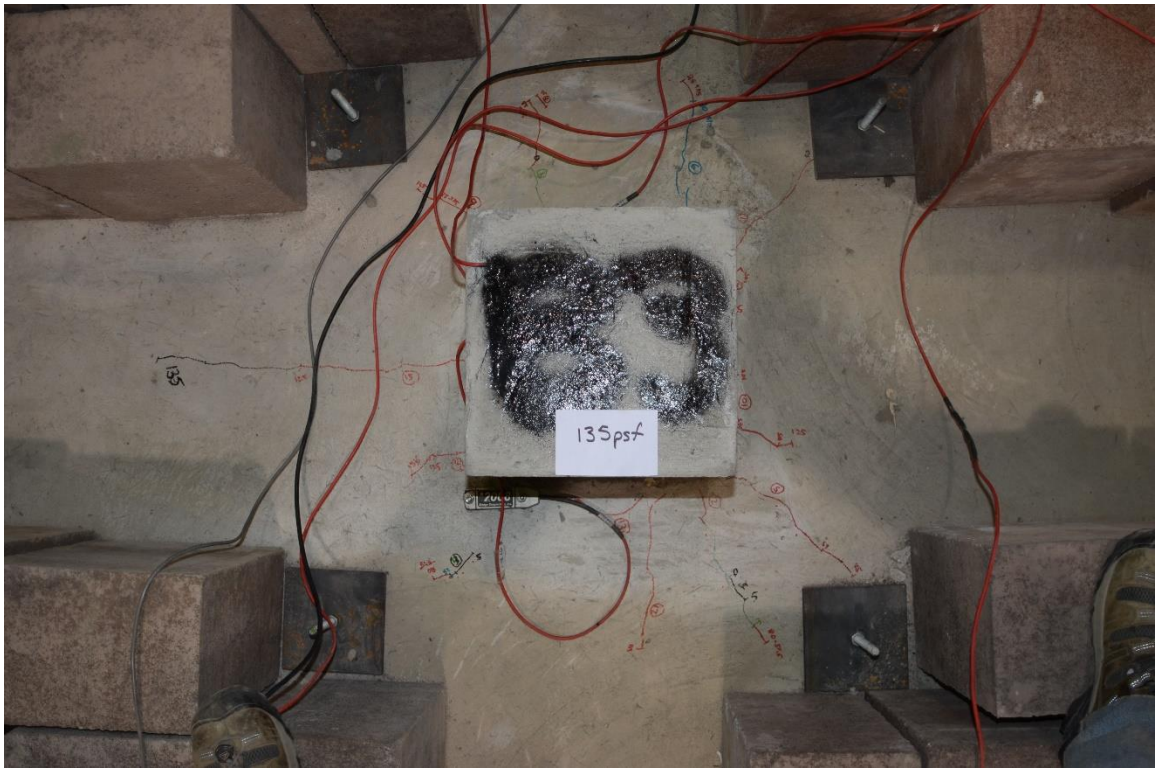

Figure H.34. Column B3 at 135psf

Figure H.35. Column A3 at 135psf

Figure H.36. Column C2 at 135psf

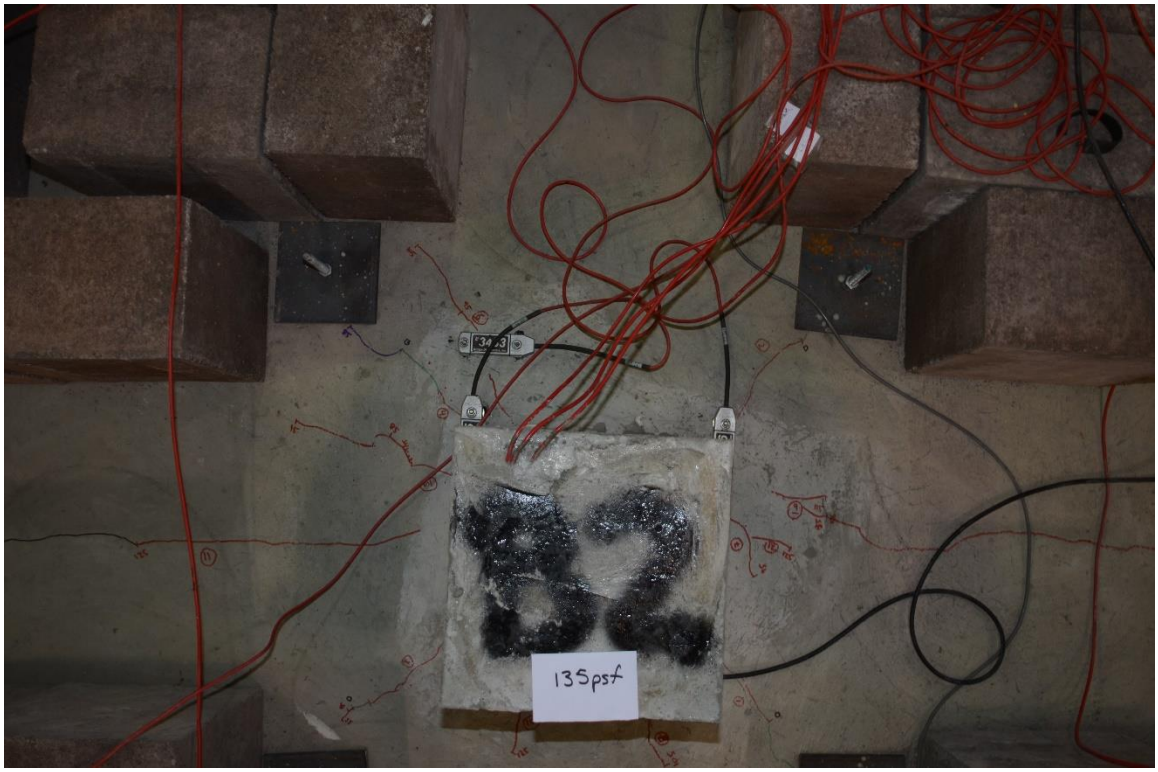

Figure H.37. Column B2 at 135psf

Figure H.38. Column A2 at 135psf

Figure H.39. Column D1 after Testing

Figure H.40. Column C1 after Testing

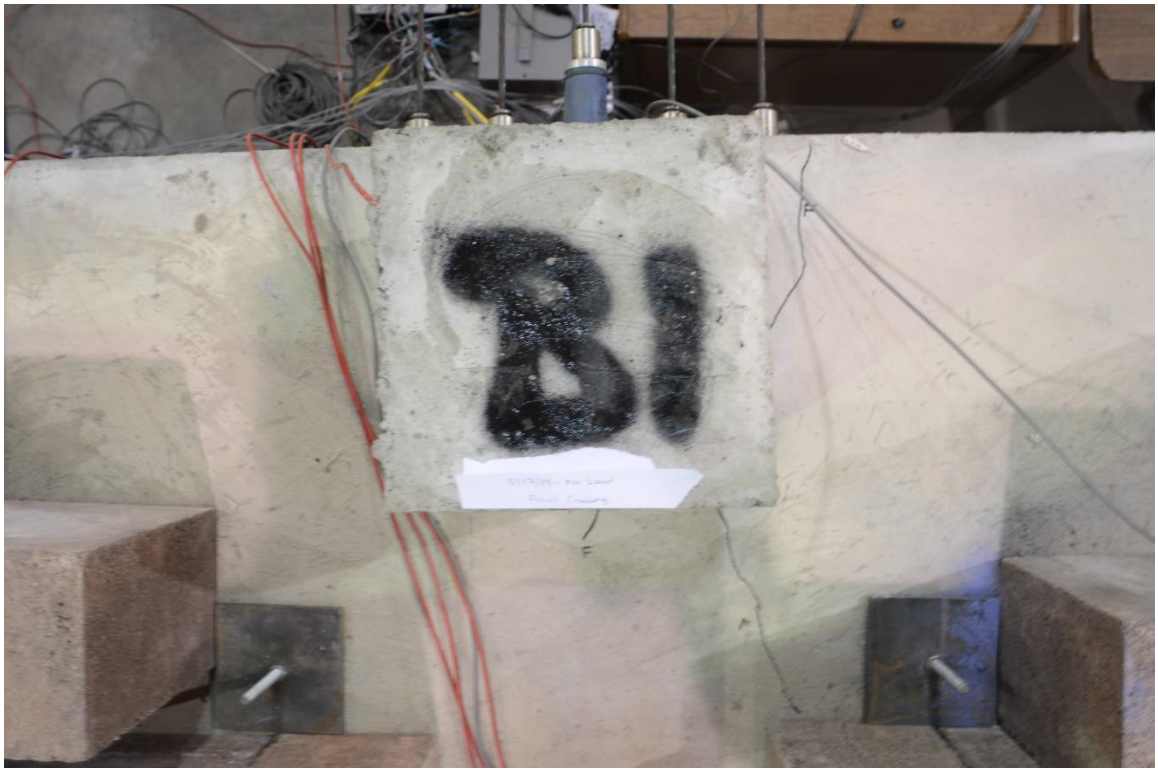

Figure H.41. Column B1 after Testing

Figure H.42. Column A1 after Testing

Figure H.43. Column D2 after Testing

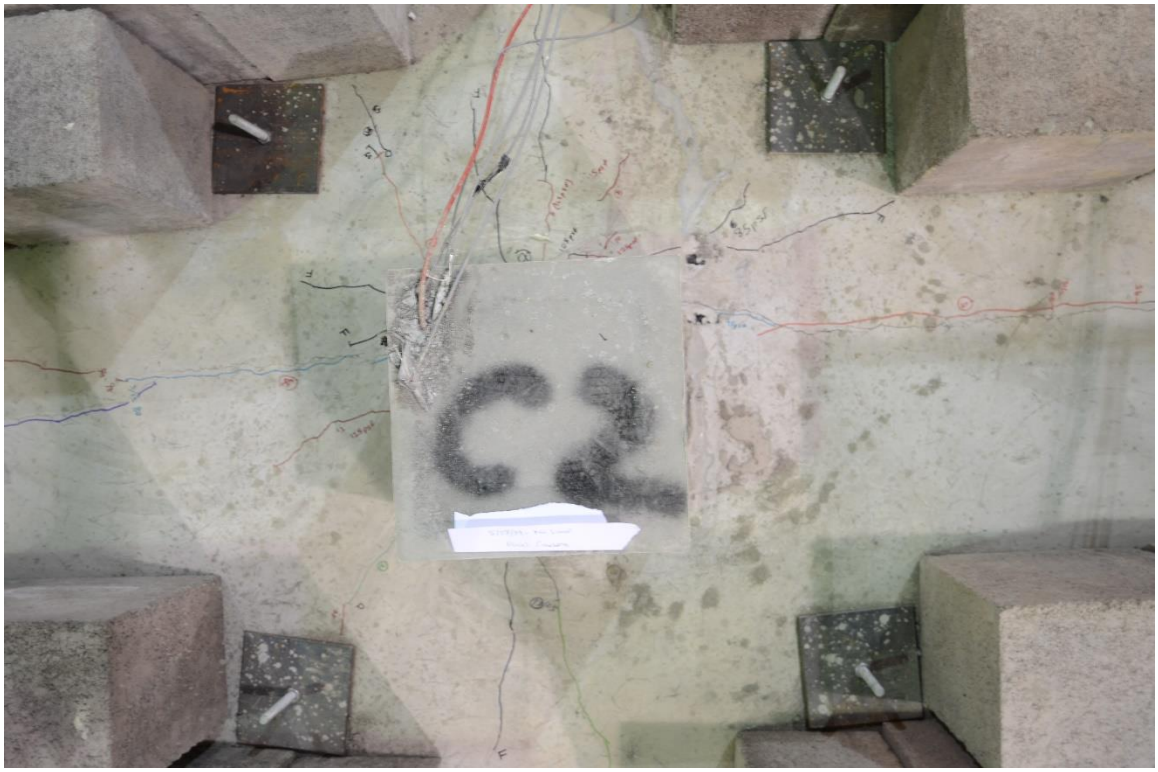

Figure H.44. Column C2 after Testing

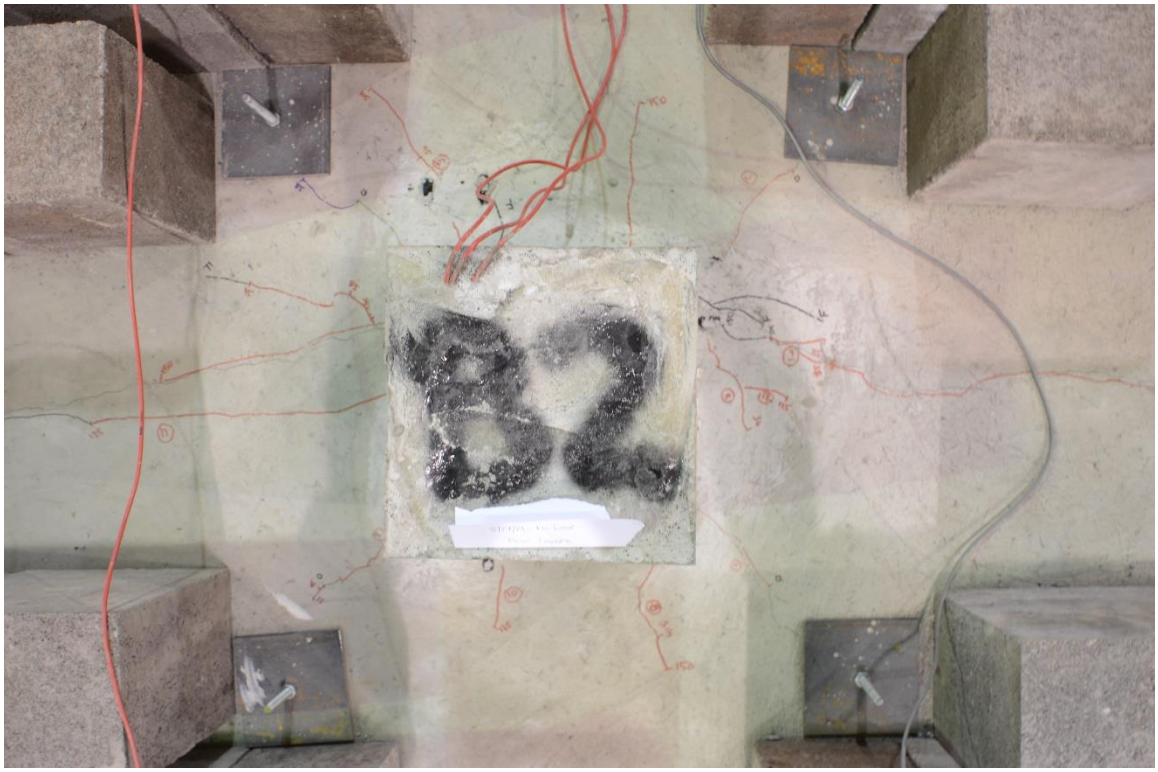

Figure H.45. Column B2 after Testing

Figure H.46. Column A2 after Testing

Figure H.47. Column D3 after Testing

Figure H.48. Column C3 after Testing

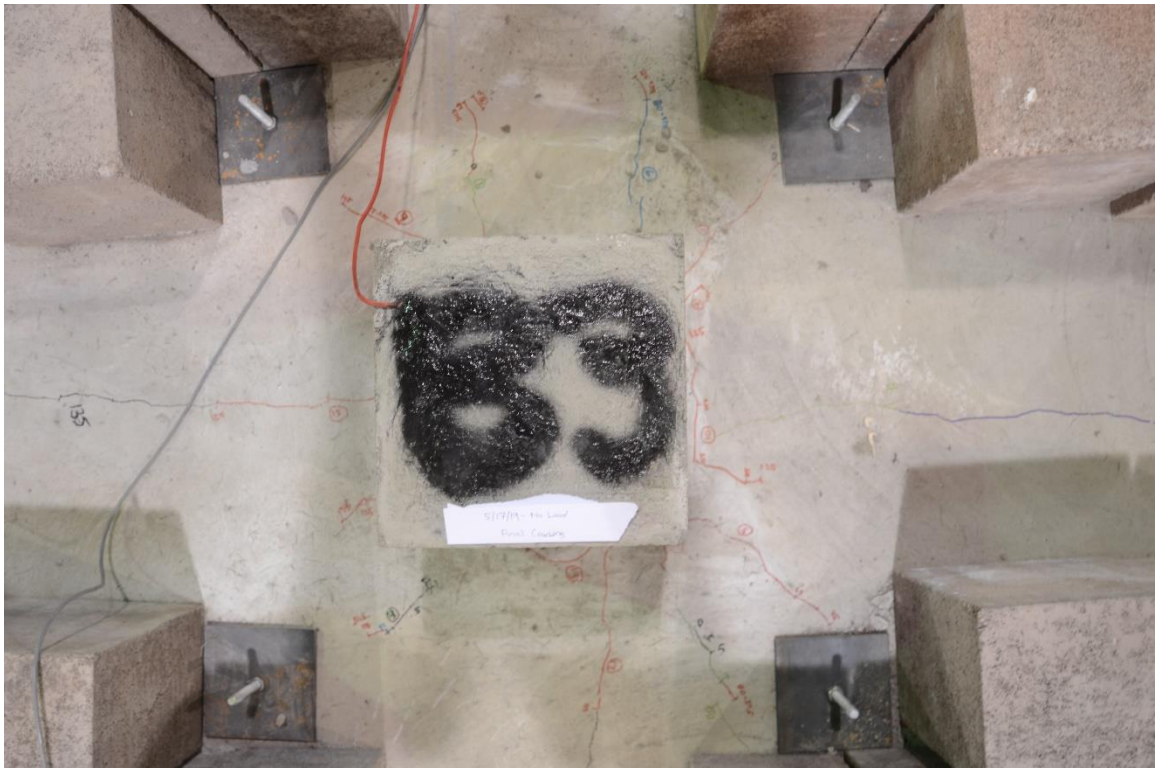

Figure H.49. Column B3 after Testing

Figure H.50. Column A3 after Testing

Figure H.51. Column D4 after Testing

Figure H.52. Column C4 after Testing

Figure H.53. Column B4 after Testing

Figure H.54. Column A4 after Testing

Appendix I – Yield Line Analysis for Specimen 2

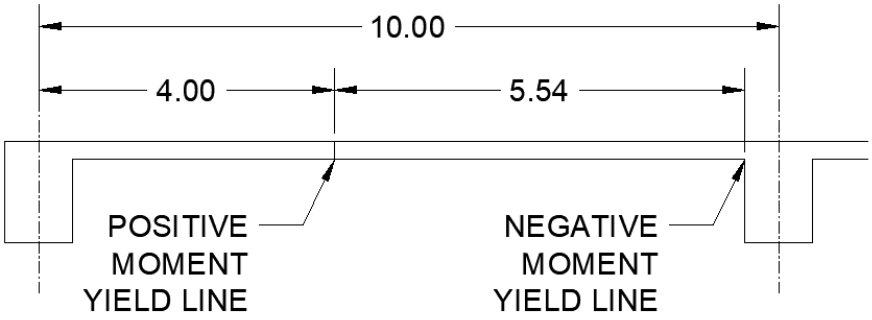

The first step in the yield line analysis was to calculate the internal work:

$$\text{Internal Work} = \sum M_i \alpha_i$$

$$\alpha_1 = \frac{\Delta}{5.54\text{ft}}$$

$$\alpha_2 = \frac{\Delta}{5.54\text{ft}} + \frac{\Delta}{4\text{ft}}$$

The strength of the post-tensioned flat plate with steel fibers was expected to be 1.9k-ft/ft, as determined by the oversight committee.

$$\text{Internal Work} = 1.9\frac{\text{k}-\text{ft}}{\text{ft}} + \alpha_1 + \alpha_2 = 1.161\Delta\frac{\text{k}-\text{ft}}{\text{ft}}$$

The next step in the analysis was to calculate the external work:

$$\text{External Work} = w\int_{x=0}^{x=9.54\text{ft}} \Delta(x)dx$$

$$\text{External Work} = w * \frac{1}{2}(9.54ft) * \Delta = 4.77 * w * \Delta\ ft$$

If the external work and internal work are set equal to each other, the uniform load leading to collapse can be determined:

$$\text{External Work} = \text{Internal Work}$$

$$w = 243\text{ psf}$$

This uniform load corresponds to 135psf of applied load.

Appendix J – Trial Slab Stressing Data

The following figures are provided to give a summary of the stressing data obtained from the trial slab. The calculations for friction and wobble were performed by Kshitij Inerkar in his report on the early stages of this project (Inerkar, 2018).

		Alpha	0	L_Chuck 4	L_Chuck5	L_Chuck6	L_Slab	L_elong		X-int					
		Straight		8.6875	28.03125	4	128	160.03125		1.0993271					
	Load Cell	Readout	Load		Piston Elongation (in	Wedge Seating (in)	P_Dead (lb)	P_Live (lbs)	P (lbs)	k	Predicted Δ	Δdead	Δlive	Actual Δ	Predicted P
	LC 5	30	313	191.5	1.15625	0.359375	313	313	313	0.0002445	0.0302934				
Init	LC 6	30	313	399		0.34375									
	LC 4		0	607											
	LC 5	202	2101	817.5	1.3125	0.359375	2096	2101	2099	0.0002359	0.2031675	0	0	0.2132	2202
2000	LC 6	202	2096	1015.5		0.34375									-4.69%
	LC 4		0												
	LC 5	399	4000		1.46875	0.359375	3995	4000	3998	0.0001125	0.3870183	0	0	0.3694	3816
4000	LC 6	400	3995			0.34375									4.76%
	LC 4		0												
	LC 5	607	6000		1.625	0.359375	5971	6000	5986	0.0004507	0.5794827	0	0	0.5257	5430
6000	LC 6	606	5971			0.34375									10.24%
	LC 4		0												
	LC 5	817	7995		1.875	0.359375	7956	7995	7976	0.000459	0.772151	0	0	0.7757	8012
8000	LC 6	810	7956			0.34375									-0.45%
	LC 4		0												
	LC 5	1015	9995		2.0625	0.359375	9773	9995	9884	0.0021048	0.9568958	0	0	0.9632	9949
10000	LC 6	1002	9773			0.34375									-0.65%
	LC 4		0		Before release -->	10	mm								
	LC 5		0				8231	8345	8288	0.001296	0.5974003				
Seat	LC 6	851	8345			0.34375									
	LC 4	831	8231			8	mm								

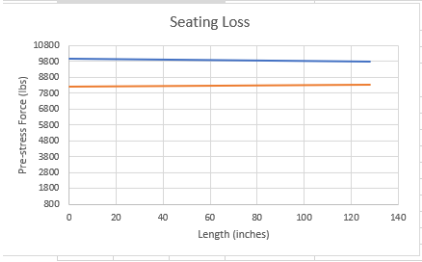

Avg Wobble coefficient 0.0006726

	Before release	After Release
0	9995	8231
128	9773	8345

Seating loss = 0.1324675 in Value from graph
0.0787402 in Measured value from tests

Figure J1. Straight Tendon Test 1

		Alpha	0.19882	L_Chuck 4	L_Chuck5	L_Chuck6	L_Slab	L_elong		X-int					
		Straight		8.71875	28.0625	4	128	160.0625		1.1884286					
	Load Cell	Readout	Load		Piston Elongation (in	Wedge Seating (in)	P_Dead (lb)	P_Live (lbs)	P (lbs)	k	Predicted Δ	Δdead	Δlive	Actual Δ	Predicted P
	LC 5	63	658	191.5	1.21875	0.359375	656	658	657	0.0002445	0.0636286				
Init	LC 6	63	656	399		0.34375									
	LC 4		0	607											
	LC 5	200	2082	817.5	1.4375	0.359375	2067	2082	2075	0.000668	0.2008806	0	0	0.2491	2572
2000	LC 6	199	2067	1015.5		0.34375									-19.35%
	LC 4		0												
	LC 5	399	4000		1.625	0.359375	3966	4000	3983	0.0007902	0.3857006	0	0	0.4366	4509
4000	LC 6	397	3966			0.34375									-11.65%
	LC 4		0												
	LC 5	607	6000		1.8125	0.359375	5914	6000	5957	0.0013587	0.5768093	0	0	0.6241	6445
6000	LC 6	600	5914			0.34375									-7.57%
	LC 4		0												
	LC 5	820	8025		2.0625	0.359375	7956	8025	7991	0.0008101	0.7737544	0	0	0.8741	9027
8000	LC 6	810	7956			0.34375									-11.48%
	LC 4		0												
	LC 5	1015	9995		2.1875	0.359375	9877	9995	9936	0.0011123	0.9621188	0	0	0.9991	10318
10000	LC 6	1013	9877			0.34375									-3.70%
	LC 4		0		Before release -->	11	mm								
	LC 5		0				8635	8714	8675	0.00085	0.6253999				
Seat	LC 6	890	8714			0.34375									
	LC 4	874	8635			9	mm								

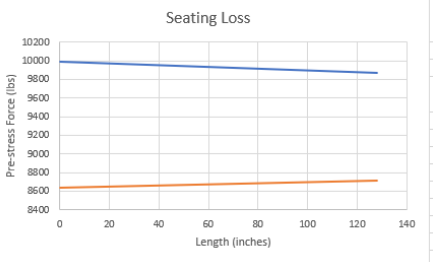

Avg Wobble coefficient 0.0009479

	Before release	After Release
0	9995	8635
128	9877	8714

Seating loss = 0.1037661 in Value from graph
0.0787402 in Measured value from tests

Figure J2. Straight Tendon Test 2

		Alpha	0.19882	L_Chuck 4	L_Chuck5	L_Chuck6	L_Slab	L_elong		X-int					
Straight				8.6875	28.09375	4	128	160.09375		1.2574184					
	Load Cell	Readout	Load		Piston Elongation (in	Wedge Seating (in)	P_Dead (lb)	P_Live (lbs)	P (lbs)	k	Predicted Δ	Δdead	Δlive	Actual Δ	Predicted P
	LC 5	103	1076	191.5	1.375	0.34375	1073	1076	1074	0.0002445	0.1040481				
Init	LC 6	103	1073	399		0.34375									
	LC 4		0	607											
	LC 5	195	2034	817.5	1.4375	0.34375	2019	2034	2026	0.0006731	0.1962635	0	0	0.1801	1859
2000	LC 6	194	2019	1015.5		0.34375									8.99%
	LC 4		0												
	LC 5	399	4000		1.625	0.34375	3880	4000	3940	0.0028532	0.3815953	0	0	0.3676	3795
4000	LC 6	388	3880			0.34375									3.81%
	LC 4		0												
	LC 5	608	6010		1.78125	0.34375	5866	6010	5938	0.0022705	0.5750595	0	0	0.5238	5409
6000	LC 6	595	5866			0.34375									9.78%
	LC 4		0												
	LC 5	817	7995		2	0.34375	7937	7995	7966	0.0006886	0.7715099	0	0	0.7426	7667
8000	LC 6	808	7937			0.34375									3.90%
	LC 4		0												
	LC 5	1013	9975		2.1875	0.34375	9868	9975	9921	0.0010124	0.9608705	0	0	0.9301	9603
10000	LC 6	1012	9868			0.34375									3.31%
	LC 4		0		Before release -->	10	mm								
	LC 5		0				8325	8449	8387	0.0013913	0.6047774				
Seat	LC 6	862	8449			0.34375									
	LC 4	841	8325			8	mm								

Avg Wobble coefficient 0.0014996

	Before release	After Release
0	9975	8325
128	9868	8449

Seating loss = 0.1284419 in Value from graph

0.0787402 in Measured value from tests

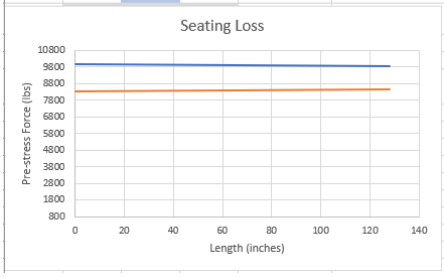

Figure J3. Straight Tendon Test 3

		Alpha	0.19882	L_Chuck 4	L_Chuck5	L_Chuck6	L_Slab	L_elong		X-int					
Straight				8.6875	27.96875	4	128	159.96875		1.2204783					
	Load Cell	Readout	Load		Piston Elongation (in	Wedge Seating (in)	P_Dead (lb)	P_Live (lbs)	P (lbs)	k	Predicted Δ	Δdead	Δlive	Actual Δ	Predicted P
	LC 5	66	689	191.5	1.3125	0.359375	729	689	709	-0.005272	0.0686357				
Init	LC 6	70	729	399		0.34375									
	LC 4		0	607											
	LC 5	192	2005	817.5	1.40625	0.34375	1990	2005	1997	0.0007152	0.1932788	0	0.01563	0.1701	1758
2000	LC 6	191	1990	1015.5		0.34375									13.60%
	LC 4		0												
	LC 5	399	4000		1.5625	0.34375	3966	4000	3983	0.0007902	0.3854747	0	0	0.3420	3534
4000	LC 6	397	3966			0.34375									12.70%
	LC 4		0												
	LC 5	609	6019		1.75	0.34375	5990	6019	6005	0.0004464	0.5811041	0	0	0.5295	5472
6000	LC 6	608	5990			0.34375									9.74%
	LC 4		0												
	LC 5	816	7986		1.96875	0.34375	8014	7986	8000	-0.000333	0.7741952	0	0	0.7483	7732
8000	LC 6	816	8014			0.34375									3.46%
	LC 4		0												
	LC 5	1017	10014		2.15625	0.34375	9981	10014	9998	0.0003119	0.9675275	0	0	0.9358	9670
10000	LC 6	1024	9981			0.34375									3.39%
	LC 4		0		Before release -->	12	mm								
	LC 5		0				7604	7723	7663	0.0014524	0.5521626				
Seat	LC 6	786	7723			0.34375									
	LC 4	766	7604			8	mm								

Avg Wobble coefficient 0.0003861

	Before release	After Release
0	10014	7604
128	9981	7723

Seating loss = 0.1899609 in Value from graph

0.1574803 in Measured value from tests

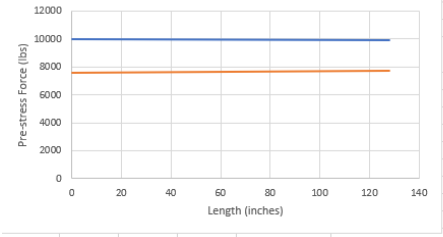

Figure J4. Straight Tendon Test 4

		Alpha	0.19882	L_Chuck 6	L_Chuck5	L_Chuck6	L_Slab	L_elong		X-int					
	Draped 2			5.5	30.40625	4	128	162.40625		0.72682072					
	Load Cell	Readout	Load		Piston Elongation (in	Wedge Seating (in)	P_Dead (lb)	P_Live (lbs)	P (lbs)	μ	Predicted Δ	Δdead	Δlive	Actual Δ	Predicted P
	LC 5	11	**115**	191.5	0.75	0.359375	73	115	94	2.23940258	0.0092256				
Init	LC 6	7	**73**	399		0.34375									
	LC 4		**0**	607											
	LC 5	195	**2034**	817.5	0.90625	0.375	1969	2034	2001	0.11628852	0.1966209	-0.03125	-0.01563	0.2263	**2303**
2000	LC 6	189	**1969**	1015.5		0.375									**-13.12%**
	LC 4		**0**												
	LC 5	397	**3981**		1.09375	0.375	3842	3981	3911	0.1317114	0.3842755	0.03125	0	0.3357	**3417**
4000	LC 6	384	**3842**			0.34375									**14.48%**
	LC 4		**0**												
	LC 5	624	**6162**		1.28125	0.34375	5971	6162	6066	0.11073884	0.5960173	0	0.03125	0.5232	**5325**
6000	LC 6	606	**5971**			0.34375									**13.92%**
	LC 4		**0**												
	LC 5	814	**7967**		1.5	0.34375	7762	7967	7864	0.08418902	0.7726481	0	0	0.7732	**7870**
8000	LC 6	790	**7762**			0.34375									**-0.07%**
	LC 4		**0**												
	LC 5	990	**9742**		1.625	0.34375	9414	9742	9578	0.12558098	0.9410394	0	0	0.8982	**9142**
10000	LC 6	964	**9414**			0.34375									**4.77%**
	LC 4		**0**		Before release -->	0.40625									
	LC 5		**0**				8513	8563	8538	-0.0177684	0.6245484				
Seat	LC 6	874	**8563**			0.34375									
	LC 4	861	**8513**			0.34375									

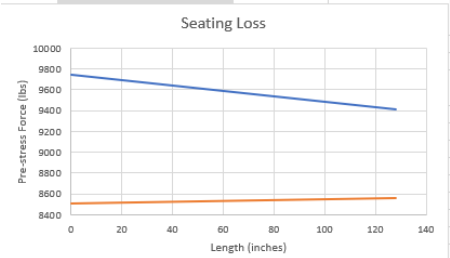

Average coefficient of friction		0.11370175

	Before release	After Release
0	9742	8513
128	9414	8563

Seating loss	=	0.0844026	in	Value from graph
		0.0625	in	Measured value from tests

Figure J5. Draped Tendon Test 1

		Alpha	0.19882	L_Chuck 4	L_Chuck5	L_Chuck6	L_Slab	L_elong		X-int					
	Draped 2			8.65625	29.625	4	128	161.625		0.4474036					
	Load Cell	Readout	Load		Piston Elongation (in	Wedge Seating (in)	P_Dead (lb)	P_Live (lbs)	P (lbs)	μ	Predicted Δ	Δdead	Δlive	Actual Δ	Predicted P
	LC 5	52	**543**	191.5	0.34375	0.375	542	543	542	-0.033936	0.05303156				
Init	LC 6	52	**542**	399		0.344									
	LC 4		**0**	607											
	LC 5	188	**1963**	817.5	0.96875	0.375	1917	1963	1940	0.0742335	0.18969246	0	0	0.5213	**5332**
2000	LC 6	184	**1917**	1015.5		0.34375									**-63.61%**
	LC 4		**0**												
	LC 5	396	**3971**		1.125	0.375	3813	3971	3892	0.1573355	0.38054885	0	0	0.6776	**6930**
4000	LC 6	381	**3813**			0.34375									**-43.84%**
	LC 4		**0**												
	LC 5	605	**5981**		1.34375	0.375	5751	5981	5866	0.1503391	0.57352767	0	0	0.8963	**9167**
6000	LC 6	583	**5751**			0.34375									**-36.01%**
	LC 4		**0**												
	LC 5	814	**7967**		1.53125	0.375	7723	7967	7845	0.1094797	0.76702813	0	0	1.0838	**11085**
8000	LC 6	786	**7723**			0.34375									**-29.23%**
	LC 4		**0**												
	LC 5	1019	**10033**		1.71875	0.375	9565	10033	9799	0.1934527	0.95813924	0	0	1.2713	**13003**
10000	LC 6	980	**9565**			0.34375									**-24.64%**
	LC 4		**0**		Before release -->	0.4375									
	LC 5		**0**				8551	8629	8590	-0.00123	0.62532382				
Seat	LC 6	881	**8629**			0.34375									
	LC 4	865	**8551**			0.375									

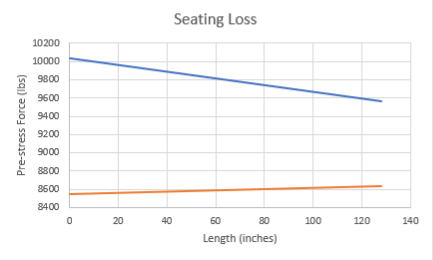

Average coefficient of friction		0.1369681

	Before release	After Release
0	10033	8551
128	9565	8629

Seating loss	=	0.09972	in	Value from graph
		0.0625	in	Measured value from tests

Figure J6. Draped Tendon Test 2

		Alpha	0.19882	L_Chuck 4	L_Chuck5	L_Chuck6	L_Slab	L_elong		X-int					
	Draped 2			8.71875	27.75	4	128	159.75		0.7870565					
	Load Cell	Readout	Load		Piston Elongation (in	Wedge Seating (in)	P_Dead (lb)	P_Live (lbs)	P (lbs)	μ	Predicted Δ	Δdead	Δlive	Actual Δ	Predicted P
	LC 5	13	**136**	191.5	0.8125	0.34375	94	136	115	1.8156004	0.0110907				
Init	LC 6	9	**94**	399		0.375									
	LC 4		**0**	607											
	LC 5	190	**1984**	817.5	0.96875	0.34375	1875	1984	1930	0.2380048	0.1864878	0	0	0.1817	**1880**
2000	LC 6	180	**1875**	1015.5		0.375									**2.64%**
	LC 4		**0**												
	LC 5	400	**4010**		1.1875	0.34375	3842	4010	3926	0.1680855	0.3793865	0.01563	0	0.3848	**3982**
4000	LC 6	384	**3842**			0.359375									**-1.41%**
	LC 4		**0**												
	LC 5	606	**5990**		1.375	0.34375	5770	5990	5880	0.1416672	0.5682659	0	0	0.5879	**6084**
6000	LC 6	585	**5770**			0.359375									**-3.35%**
	LC 4		**0**												
	LC 5	815	**7976**		1.59375	0.34375	7752	7976	7864	0.0964946	0.7599998	0	0	0.8067	**8347**
8000	LC 6	789	**7752**			0.359375									**-5.79%**
	LC 4		**0**												
	LC 5	1012	**9965**		1.78125	0.34375	9574	9965	9770	0.1538519	0.9441541	0	0	0.9942	**10287**
10000	LC 6	981	**9574**			0.359375									**-5.03%**
	LC 4		**0**		Before release -->	11									
	LC 5		**0**				8419	8525	8472	0.015881	0.6095866				
Seat	LC 6	870	**8525**			0.359375									
	LC 4	851	**8419**			9									

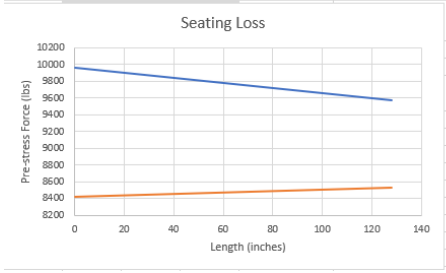

Average coefficient of friction 0.1596208

	Before release	After Release
0	9965	8419
128	9574	8525

Seating loss = 0.108698 in Value from graph
0.0787402 in Measured value from tests

Figure J7. Draped Tendon Test 3

		Alpha	0.19882	L_Chuck 4	L_Chuck5	L_Chuck6	L_Slab	L_elong		X-int					
	Draped 2			8.6875	27.6875	4	128	159.6875		0.8120669					
	Load Cell	Readout	Load		Piston Elongation (in	Wedge Seating (in)	P_Dead (lb)	P_Live (lbs)	P (lbs)	μ	Predicted Δ	Δdead	Δlive	Actual Δ	Predicted P
	LC 5	13	**136**	191.5	0.8125	0.375	94	136	115	1.8156004	0.0110864				
Init	LC 6	9	**94**	399		0.375									
	LC 4		**0**	607											
	LC 5	202	**2101**	817.5	1.03125	0.375	2029	2101	2065	0.1293788	0.1994877	0	0	0.2192	**2269**
2000	LC 6	195	**2029**	1015.5		0.375									**-8.99%**
	LC 4		**0**												
	LC 5	401	**4019**		1.21875	0.375	3909	4019	3964	0.0929826	0.3829459	0	0	0.4067	**4210**
4000	LC 6	391	**3909**			0.375									**-5.84%**
	LC 4		**0**												
	LC 5	609	**6019**		1.4375	0.375	5856	6019	5938	0.0909387	0.5735958	0	0	0.6254	**6474**
6000	LC 6	594	**5856**			0.375									**-8.29%**
	LC 4		**0**												
	LC 5	814	**7967**		1.59375	0.375	7810	7967	7888	0.0527534	0.7620641	0	0	0.7817	**8092**
8000	LC 6	795	**7810**			0.375									**-2.51%**
	LC 4		**0**												
	LC 5	1012	**9965**		1.8125	0.375	9641	9965	9803	0.1191985	0.9469821	0	0	1.0004	**10356**
10000	LC 6	988	**9641**			0.375									**-5.34%**
	LC 4		**0**		Before release -->	11	mm								
	LC 5		**0**				8504	8572	8538	-0.006653	0.6140948				
Seat	LC 6	875	**8572**			0.359375									
	LC 4	860	**8504**			9	mm								

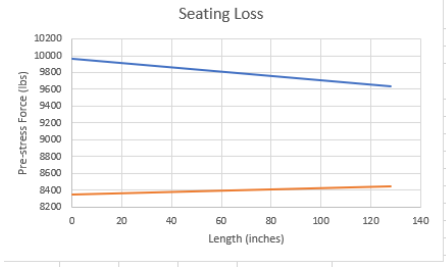

Average coefficient of friction 0.0970504

	Before release	After Release
0	9965	8504
128	9641	8572

Seating loss = 0.1032527 in Value from graph
0.0787402 in Measured value from tests

Figure J8. Draped Tendon Test 4

		Alpha	0.19882	L_Chuck 4	L_Chuck5	L_Chuck6	L_Slab	L_elong		X-int					
	Draped 2			8.71875	27.75	4	128	159.75		0.8463334					
	Load Cell	Readout	Load		Piston Elongation (in	Wedge Seating (in)	P_Dead (lb)	P_Live (lbs)	P (lbs)	μ	Predicted Δ	Δdead	Δlive	Actual Δ	Predicted P
	LC 5	22	**230**	191.5	0.875	0.375	188	230	209	0.9753727	0.0201628				
Init	LC 6	18	**188**	399		0.375									
	LC 4		**0**	607											
	LC 5	185	**1932**	817.5	1.03125	0.375	1885	1932	1909	0.0760069	0.1844678	0	0	0.1849	**1913**
2000	LC 6	181	**1885**	1015.5		0.375									**-0.24%**
	LC 4		**0**												
	LC 5	397	**3981**		1.21875	0.359375	3851	3981	3916	0.1191686	0.3784539	0	0.01563	0.3568	**3692**
4000	LC 6	385	**3851**			0.375									**6.07%**
	LC 4		**0**												
	LC 5	605	**5981**		1.40625	0.359375	5799	5981	5890	0.1085641	0.5691918	0	0	0.5599	**5794**
6000	LC 6	588	**5799**			0.375									**1.66%**
	LC 4		**0**												
	LC 5	815	**7976**		1.65625	0.359375	7791	7976	7884	0.071299	0.761881	0	0	0.8099	**8381**
8000	LC 6	793	**7791**			0.375									**-5.93%**
	LC 4		**0**												
	LC 5	1015	**9995**		1.78125	0.359375	9593	9995	9794	0.1591988	0.9465323	0	0	0.9349	**9674**
10000	LC 6	983	**9593**			0.375									**1.24%**
	LC 4		**0**		Before release -->	9	mm								
	LC 5		**0**				8353	8449	8401	0.010563	0.6044947				
Seat	LC 6	862	**8449**			0.375									
	LC 4	844	**8353**			7	mm								

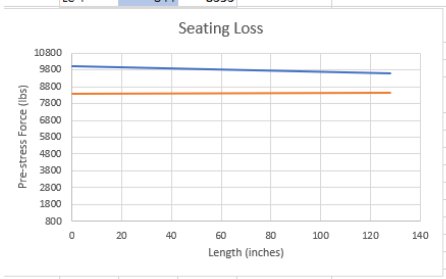

Average coefficient of friction		0.1068475	

	Before release	After Release
0	9995	8353
128	9593	8449

Seating loss	=	0.115327	in	Value from graph
		0.0787402	in	Measured value from tests

Figure J9. Draped Tendon Test 5